Diffusion d'ozone par contacteur membranaire pour l'élimination de micropolluants

Alice Schmitt

THÈSE POUR OBTENIR LE GRADE DE DOCTEUR DE L'UNIVERSITÉ DE MONTPELLIER

En Génie des Procédés

École doctorale GAIA (n°584)

Unité de recherche Institut Européen des Membranes, UMR 5635
(CNRS – ENSCM – UM)

Diffusion d'ozone par contacteur membranaire pour l'élimination de micropolluants

Présentée par Alice SCHMITT
Le 9 décembre 2021

Sous la direction de Julie MENDRET
et Stéphan BROSILLON

Devant le jury composé de

Gaël PLANTARD, Professeur, PROMES, Université de Perpignan Via Domitia	Président du jury
Marie-Hélène MANERO, Professeur, LGC, Université Toulouse III Paul Sabatier	Rapporteur et examinatrice
Éric FAVRE, Professeur, LRGP, Université de Lorraine	Rapporteur et examinateur
Denis BOUYER, Professeur, IEM, Université de Montpellier	Examinateur
Julie MENDRET, Maître de conférences-HDR, IEM, Université de Montpellier	Directrice de thèse
Stéphan BROSILLON, Professeur, IEM, Université de Montpellier	Co-directeur de thèse

UNIVERSITÉ DE MONTPELLIER

Remerciements

« … Au moment où j'avais réussi à trouver toutes les réponses, toutes les questions ont changé. »

Paulo Coelho

Parce que la recherche, c'est se poser des questions, démêler un fil, trouver une réponse, apportant ensuite de nouvelles questions. De cette aventure, de laquelle il ne me restera que de bons souvenirs, je voudrais remercier les personnes qui m'ont aidée et encouragée dans ce projet, chacune à sa manière.

Je commence en remerciant tout particulièrement celles qui sont là dans les bons comme dans les mauvais moments depuis maintenant plusieurs années : la Biquette, pour sa participation active à cette thèse in english et sa fraîcheur de vivre ; et Popo, toujours présente également, surtout lorsqu'il s'agit de bien manger ou danser. Une même formation, plusieurs voies, et surtout une amitié solide.

Merci aux doctorants de l'IEM pour leur amitié, leur soutien, et tous ces bons moments partagés : Julien, pour la découverte d'un nouveau moyen de transport, le coaching en escalade, et sa complicité ; Marianne, pour ses nombreuses conversations plantes et couture ; Louis, seul survivant 0.10, les vrais savent ; Azariel, pour son aide lors de mon arrivée au labo ; Cyril, pour ses vins alsaciens et ses soirées planchas ; Carole, toujours partante pour un footing ou un tacos ; Raph, pour son calme et ses conseils musique ; Marine, pour la découverte de Bayonne ; Lucie, pour sa bonne humeur quotidienne et ses conseils, et tous les autres que je ne citerai pas mais qui ont fait partie de cette belle aventure.

Merci beaucoup à Christophe et Loubna pour toute l'aide apportée au cours de ces trois ans : les modifications, encore et encore, la plomberie, la mécanique. Parce que c'est aussi ça, une thèse en génie des procédés…

Merci à mes encadrants, Julie et Stéphan, pour avoir su me laisser autonome tout en étant présents pour répondre à mes questions de façon réactive. Merci à l'équipe GPM pour son accueil, Christelle pour sa gentillesse et ses conversations annéciennes, Eddy pour son aide et son professionnalisme, mes stagiaires pour leur participation active à ce travail, ainsi qu'à tout le personnel de l'IEM.

Je n'oublie pas non plus ma famille qui m'a encouragée à me lancer dans ce deuxième projet « de haut-niveau », et qui m'a soutenue ensuite.

Et pour finir, un merci très spécial à Florian, qui a rendu cette fameuse 3ème année très belle : j'espère que tu m'accompagneras encore longtemps et j'ai hâte de commencer de nouveaux projets avec toi.

Résumé

L'utilisation de l'ozone pour le traitement des eaux usées est de plus en plus répandue, en particulier pour les traitements d'affinage en réutilisation des eaux usées. Habituellement, l'ozone est injecté sous forme de bulles, avec comme inconvénients des coûts opératoires importants, la possibilité de stripage de composés organiques volatils, la difficulté de maîtriser l'hydrodynamique des colonnes à bulles et la formation de mousse. Les contacteurs membranaires permettent de pallier ces faiblesses en permettant la diffusion d'un composé en phase gaz vers une phase liquide sans formation de bulles et avec une aire interfaciale élevée. En outre, les contacteurs membranaires présentent une géométrie modulable qui peut être facilement transposée à l'échelle de production requise. Ainsi, l'objectif global de cette thèse était d'évaluer la faisabilité de l'utilisation de contacteurs membranaires en lieu et place des réacteurs d'ozonation traditionnels, en traitement tertiaire d'affinage, pour la dégradation de molécules réfractaires lors du traitement des eaux usées. Après une analyse bibliographique des travaux publiés sur le sujet, il s'agissait d'effectuer une caractérisation complète du procédé et des phénomènes de transfert mis en jeu. Une maîtrise fine des pressions de part et d'autre de la membrane est nécessaire pour assurer un bon transfert du gaz vers le liquide. La résistance majoritaire au transfert ainsi que les principaux paramètres impactant le transfert ont été identifiés. L'application de ce procédé pour l'élimination de molécules organiques et la minimisation de bromates a été évaluée expérimentalement dans la configuration in/out. Le procédé s'est révélé efficace pour un temps de séjour très court sur les composés organiques d'origine pharmaceutique sélectionnés comme modèles, atteignant jusqu'à 59% et 50% d'abattement respectivement pour la carbamazépine et le sulfaméthoxazole. Ce procédé semble également être une solution intéressante pour limiter la formation de bromates grâce à un temps de séjour très court, le tout en produisant une quantité de radicaux hydroxyles importante, utile pour une élimination efficace des micropolluants organiques. Afin de permettre une meilleure compréhension des phénomènes limitants et à des fins d'optimisation du procédé, une démarche de modélisation du réacteur en trois dimensions a été associée à ce travail, via l'utilisation du logiciel Comsol Multiphysics. Les profils de concentration obtenus ont mis en évidence l'importance de l'hydrodynamique dans le carter lorsque le liquide circule dans celui-ci afin d'assurer une bonne distribution de l'ozone et ainsi un bon abattement des polluants ciblés. L'étude du vieillissement des contacteurs membranaires après ozonation a montré l'importance des matériaux utilisés, qui doivent être résistants à l'ozonation à long terme afin qu'une application à l'échelle de la station d'épuration puisse être envisagée.

Abstract

The use of ozone to disinfect sewage has significantly increased, especially when a high degree of treatment is required for water reuse. Ozone in water treatment is usually injected in the form of bubbles, with disadvantages such as operational costs, stripping of volatile organic compounds, the difficulty of control of bubble column hydrodynamics and foam generation. By using a bubbleless operation for gas transfer to liquid phase, membrane contactor can overcome these weaknesses with a high interfacial area. Furthermore, membrane contactors are modular and can thus be easily scaled up to the required production scale. The global objective of this thesis was to evaluate the feasibility of using membrane contactors as an alternative to chamber reactors in tertiary treatment for the removal of refractive pollutants in waste water treatment. After a state-of-the-art analysis, the complete characterization of ozone transfer through membrane contactors as well as the transfer phenomena involved was carried out. Precise control of the transmembrane pressures was necessary to ensure good transfer from gas to liquid. The major resistance to the transfer and the main parameters impacting the transfer were identified. The application of this process for the degradation of organic compounds and the minimization of bromates was experimentally evaluated with a in/out configuration. The process has proved to be effective for a very short residence time on organic pharmaceuticals selected as models, achieving up to 59% and 50% abatement for carbamazepine and sulfamethoxazole, respectively. Besides, this process seems to be an advantageous solution to limit the formation of bromates thanks to a very short residence time, while producing a large amount of hydroxyl radicals which are useful for an effective elimination of organic micropollutants. In order to allow a better understanding of the limiting phenomena along with process optimization purposes, a three-dimensional modeling approach of the reactor was associated with this work, through the use of the Comsol Multiphysics software. The concentration profiles obtained highlighted the importance of hydrodynamics in the shell when the liquid circulates in it in order to ensure a good distribution of ozone and thus a good removal of the targeted pollutants. The study of membrane contactors aging process after ozonation pointed out the importance of the materials used, which must be resistant to long-term ozonation so that a wastewater treatment plant scale application can be considered.

Productions scientifiques

Publications

[1] Schmitt, A., Mendret, J., Roustan, M., Brosillon, S., 2020. Ozonation using hollow fiber contactor technology and its perspectives for micropollutants removal in water: A review. *Sci. Total Environ. 729, 138664*. https://doi.org/10.1016/J.SCITOTENV.2020.138664

[2] Schmitt, A., Mendret, J., Brosillon, S., 2021. Evaluation of an ozone diffusion process using a hollow fiber membrane contactor. *Chemical Engineering Research and Design.* https://doi.org/10.1016/j.cherd.2021.11.002

[3] Schmitt, A., Mendret, J., Brosillon, S., 2022. Diffusion of ozone through a hollow fiber membrane contactor for pharmaceuticals removal and bromate minimization. *En préparation*

[4] Schmitt, A., Chevarin, C., Bouyer, D., Mendret, J., Brosillon, S., 2022. Computational fluid dynamics modeling of ozonation using a hollow fiber membrane contactor. *En préparation*

Communications orales

[1] A. Schmitt, S. Brosillon, J. Mendret, Ozonation using hollow fiber contactor technology for the elimination of pharmaceuticals: state of the art, 24th IOA World Congress & Exhibition, 20 - 25 October 2019, Nice, France

[2] A. Schmitt, S. Brosillon, J. Mendret, Diffusion of ozone for the removal of micropollutants using a hollow fibers membrane contactor, Journée des Doctorants Filière APAB de l'Ecole Doctorale GAIA, 18 juin 2021, en ligne

Table des matières

Liste des figures

Liste des tableaux

Liste des tables

Introduction générale

Les ressources en eau, ainsi que la qualité de celles-ci, ne cessent de diminuer. En parallèle, la population humaine augmente de façon exponentielle. Selon l'Organisation des Nations Unis, le stress hydrique, qui représente par définition le cas où la demande en eau est supérieure à la ressource, devrait toucher presque 3 milliards de personnes d'ici 2025 (WWAP, 2019). L'eau douce non polluée est ainsi une ressource de plus en plus rare et devient l'or bleu. En France, 90% des départements ont fait face à des cours d'eau en situation d'assèchement entre fin mai et fin septembre 2019 (Antoni et al., 2020).

Par conséquent, il est non seulement nécessaire de traiter au mieux l'eau afin de protéger l'écosystème et la santé humaine mais également de la recycler afin de protéger l'environnement de la pollution liée aux rejets, de conserver la quantité et la qualité des ressources et d'économiser de l'énergie grâce à la mise en place d'un circuit de traitement adapté à l'application visée. La REUSE (issue de l'expression anglaise wastewater reuse ou REUT, Réutilisation des Eaux Usées Traitées) prend ainsi tout son sens.

Si les traitements conventionnels permettent d'atteindre une très bonne qualité globale de l'eau traitée, ces dernières décennies ont vu apparaître de nouveaux polluants aquatiques appelés micropolluants. Ces polluants émergents nécessitent la mise en place de nouveaux traitements spécifiques et font ainsi l'objet d'études intensives depuis une vingtaine d'année. Les micropolluants sont présents partout dans notre quotidien. Au niveau européen, on en recense plus de 110 000 à ce jour. Ils sont générés par les activités industrielles (industries chimiques, papeteries, etc), agricoles (pesticides), urbaines (rejets domestiques, entretien des rues, etc), les hôpitaux, ou encore directement les stations d'épuration via les effluents ou les boues. Ils peuvent être classés en plusieurs catégories : médicaments, perturbateurs endocriniens, métaux, hydrocarbures, pesticides, cosmétiques, détergents, plastifiants, etc. Par définition dans le « Plan micropolluants 2016-2021 pour préserver la qualité des eaux et la biodiversité » de l'État français, un micropolluant est une *« substance indésirable détectable dans l'environnement à très faible concentration (microgramme par litre voire nanogramme par litre). Sa présence est, au moins en partie, due à l'activité humaine (procédés industriels, pratiques agricoles ou activités quotidiennes) et peut à ces très faibles concentrations engendrer des effets négatifs sur les organismes vivants en raison de sa toxicité, de sa persistance et de sa bioaccumulation. »*

Si la première station d'épuration est née en 1914 en Angleterre et était constituée d'un bassin dans lequel les eaux usées étaient aérées et purifiées par les microorganismes, il n'était alors pas encore question de micropolluants mais uniquement de macropolluants tels que l'azote, les nitrates, ou le

phosphore, composés toxiques pour l'homme ayant une concentration supérieure au $mg.L^{-1}$ (Barrault and Dumas, 2016).

En 1962, la biologiste américaine Rachel Carson publie « Printemps silencieux », un livre dans lequel elle alerte sur l'impact négatif des pesticides, notamment du dichlorodiphényltrichloroéthane (qui sera interdit dix ans plus tard aux Etats-Unis), sur l'environnement et plus spécifiquement sur les oiseaux (Carson, 1962). Elle y affirme que les pesticides devraient être appelés biocides en raison de leur action négative voire létale sur d'autres organismes que ceux visés.

Il faudra attendre les années 70 et l'évolution de la chimie analytique, notamment avec le développement de la chromatographie gazeuse utilisée pour la quantification des macropolluants, pour révéler au grand jour l'existence des micropolluants. Ces composés n'étant pas visibles et leur concentration étant extrêmement faible ($mg.L^{-1}$ voire $ng.L^{-1}$), l'amélioration des limites de détection des appareils d'analyse entraîne la détection de plus en plus de substances au fur et à mesure des années. Pour autant, cela ne signifie pas qu'ils n'étaient pas présents auparavant.

Les sources des micropolluants étant diverses, cette pollution peut être diffuse (eaux de ruissellement, épandage, etc) ou localisée (effluents urbains, effluents industriels). S'ajoutant à leur présence invisible, leurs effets sont également très peu connus, une exposition chronique même à très faible concentration pouvant être responsable d'effets négatifs sur l'écosystème et la santé humaine sur le long terme. Une étude réalisée en France et basée sur l'Analyse du Cycle de Vie à partir des flux vers l'environnement (calculés grâce à la littérature scientifique ainsi qu'aux rapport nationaux de surveillance des effluents de station d'épuration) a prouvé que les micropolluants avaient un impact potentiel significatif (Aemig et al., 2021). Plus particulièrement, les auteurs ont démontré que les micropolluants organiques, qui seront ciblés dans ce manuscrit de thèse, avaient un impact significatif sur le milieu aquatique. Dans cette même étude, l'impact sur la santé humaine était plus difficile à déterminer et potentiellement sous-estimé du fait d'un manque de données permettant de faire le lien entre la santé humaine et les micropolluants en sortie de station d'épuration, l'exposition directe à ces substances étant faible grâce aux traitements de potabilisation. De ce fait, l'impact possible sur la santé humaine dû à l'exposition à ces substances à long terme malgré leurs très faibles doses ainsi qu'à certains phénomènes comme par exemple le développement d'antibiorésistance n'ont ainsi pas été pris en compte dans l'étude mentionnée.

De plus, plusieurs études expérimentales ont démontré la présence d'un effet cocktail lié à l'exposition simultanée de l'organisme à plusieurs substances toxiques (Cizmas et al., 2015; Hayes et al., 2006; Thrupp et al., 2018). Cependant, ces travaux étaient réalisés en laboratoire et avec des concentrations généralement plus élevées que dans l'environnement. Hayes et al. ont par exemple démontré que le

S-métolachlore (un herbicide) n'avait pas d'effet sur les amphibiens lorsqu'il était utilisé seul, mais associé à l'atrazine, il en multipliait les effets nocifs (Hayes et al., 2006). A l'inverse, Altenburger et al. ont montré à partir de bioessais que l'effet total correspondait à l'addition de l'effet de chaque micropolluant individuellement dans la majeure partie de leurs résultats, malgré quelques exceptions explicables par des facteurs expérimentaux (Altenburger et al., 2018). Plus récemment, des modèles mathématiques ont été développés afin d'évaluer le risque lié à l'effet cocktail (D'Almeida et al., 2020; Gosset et al., 2020). Cependant, ces modèles sont encore très peu nombreux et présentent plusieurs verrous. Ainsi, l'effet cocktail est encore très difficilement quantifiable et méconnu (Aemig et al., 2021).

En France, deux tiers des micropolluants quantifiés dans les cours d'eau sont des hydrocarbures aromatiques polycycliques (HAP) (Antoni et al., 2020). Ces composés proviennent de la combustion domestique de charbon, de bois, de carburants automobiles, des feux de forêts, ou encore de l'incinération de déchets. Concernant les pesticides, ils ont diminué d'environ 20% depuis 2008 dans les cours d'eau, notamment grâce à une baisse de l'utilisation de certains herbicides dont l'acétochlore et l'amitrole, interdits respectivement depuis 2013 et 2017. Cependant, certains autres composés de la même catégorie sont eux en augmentation comme par exemple la cyperméthrine qui est un insecticide. Au niveau des eaux souterraines, en 2018, 46% des 760 composés phytopharmaceutiques recherchés dans le cadre du suivi de l'état chimique des eaux en France ont été quantifiés, contre 40% des 660 ciblés en 2010. Parmi eux, 53 % sont des substances autorisées ou leurs produits de dégradation (métabolites), et 46 % sont des substances interdites ou leurs métabolites. D'autre part, plus d'un pesticide a été détecté dans presque 80% des points de mesure des réseaux de surveillance de la qualité des eaux souterraines (2 340 points au total). 80% des micropolluants quantifiés dans les eaux souterraines proviennent de produits du quotidien (médicaments, solvants, détergents, etc) (Antoni et al., 2020). Parmi eux, on retrouve en grande quantité la carbamazépine et le sulfaméthoxazole qui sont les composés ciblés durant cette thèse.

Depuis 2000, la réglementation européenne, avec notamment la Directive Cadre sur l'Eau (DCE - 23 octobre 2000/directive 2000/60), encadre le rejet de certains micropolluants présents dans l'environnement aquatique. La liste des substances réglementées augmente petit à petit et les concentrations limites de rejet diminuent parallèlement à l'amélioration des limites de détection des appareils d'analyse. En outre, entre 2006 et 2018, le nombre d'échantillons prélevés pour l'analyse de micropolluants dans le cadre du suivi de l'état chimique des eaux de surface en France a été multiplié par 8 (Antoni et al., 2020). Cette réglementation s'étoffe progressivement via la mise en place de diverses actions publiques. Ainsi, depuis 2002, l'action nationale de recherche et de réduction des

rejets de substances dangereuses dans les eaux (RSDE), mise en place au niveau national suite à la DCE, a pour objectif de réduire puis supprimer les rejets, pertes et émissions de substances dangereuses prioritaires dans le milieu aquatique (listées sur l'annexe X de la DCE).

Afin de réduire la quantité de micropolluants rejetée dans l'environnement, plusieurs solutions sont envisageables. Premièrement, un traitement pourrait être ajouté au niveau des stations d'épuration, celles-ci n'ayant initialement pas été conçues pour traiter ces composés, elles les rejettent donc partiellement ou totalement en sortie. Deuxièmement, le traitement à la source permettrait de limiter la mise en place de traitement complémentaire au niveau des stations d'épuration, et d'éviter la dilution de ces substances parmi de grands volumes potentiellement moins pollués, facilitant ainsi le traitement. Cependant ce type de traitement n'est pas efficace sur la pollution diffuse et n'éliminerait donc pas tous les micropolluants. Enfin, la réduction (voire l'interdiction) à la source de l'utilisation de certaines substances, qui implique la mise en place de pratiques quotidiennes différentes et d'un changement des habitudes des usagers (par exemple avec l'utilisation de produits d'entretien naturels pour les ménages) (Heitz et al., 2017), diminuerait considérablement la quantité de micropolluants arrivant en entrée des stations d'épuration, les rejets domestiques étant responsables en grande partie de la présence de ces substances (Bergé, 2012; Paxéus et al., 1992). La présence dans l'environnement aquatique de substances toxiques pourtant interdites depuis plusieurs années à cause de leur très longue persistance, tels que les polychlorobiphényles (PCB), souligne l'intérêt de coupler une action de réduction à la source avec un procédé spécifique lors du traitement des eaux usées.

Au niveau des stations d'épuration, l'utilisation de l'ozone est de plus en plus répandue, en particulier lors les traitements d'affinage dans un objectif de réutilisation des eaux usées traitées. Le traitement des micropolluants par ozonation se révèle être une solution efficace pour traiter une large gamme de ces substances avec plus de 70% d'abattement (Choubert et al., 2012). Habituellement, l'ozone est injecté sous forme de bulles, avec comme inconvénients des coûts opératoires importants, la possibilité de stripage de composés organiques volatils, des limitations au transfert (entrainant des coûts énergétiques élevés), la formation de mousse, et la production de sous-produits issus des réactions d'oxydation et potentiellement plus toxiques que les produits initialement traités. Parmi ces sous-produits, une des grandes problématiques du traitement par ozonation est la production de bromates, formés lors de l'ozonation d'eau contenant des bromures réagissant avec l'ozone résiduel présent en excès (Pinkernell and Von Gunten, 2001). Ce composé, potentiellement cancérigène, est encadré par la réglementation européenne dans les eaux potables avec une limite fixée à 10 $\mu g.L^{-1}$, l'ozone étant souvent employé dans les traitements de potabilisation.

Les contacteurs membranaires sont une alternative intéressante pour pallier ces faiblesses en assurant une diffusion de l'ozone sans formation de bulles. En effet, un contacteur membranaire diffuse l'ozone du gaz vers le liquide de manière homogène grâce aux multiples points de dosage créés par la membrane et ses pores, le tout avec une aire interfaciale élevée (Merle et al., 2017). Plus particulièrement, une géométrie de membrane sous forme de fibres creuses offre une surface d'échange pouvant atteindre 10 000 $m^2.m^{-3}$, tandis que celle-ci varie entre 3 et 600 $m^2.m^{-3}$ dans des réacteurs à bulles (Chabanon and Favre, 2017; Reed et al., 1995). Grâce à un dosage plus précis, la quantité d'ozone résiduel serait alors inférieure à celle émise dans les procédés conventionnels, ce qui permettrait de limiter la formation de sous-produits tout en économisant les coûts liés notamment à la production et à la destruction d'ozone in-situ. En outre, les contacteurs membranaires présentent une géométrie modulable, qui peut être facilement transposée à l'échelle de production requise.

Ainsi, l'objectif global de cette thèse est d'évaluer la faisabilité de l'utilisation de contacteurs membranaires en lieu et place des réacteurs d'ozonation traditionnels, en traitement tertiaire d'affinage, pour la dégradation de molécules réfractaires lors du traitement des eaux usées. Plus particulièrement, il s'agit d'effectuer une caractérisation complète du procédé et des phénomènes de transfert mis en jeu, puis d'étudier son application pour l'élimination de molécules organiques et la minimisation de bromates. Ce travail concerne plus spécifiquement des composés organiques d'origine pharmaceutique (la carbamazépine et le sulfaméthoxazole). De nombreuses études ont en effet démontré une quantité importante de ces composés dans les effluents de stations d'épuration (Bolong et al., 2009), mais également dans les eaux de surface (Björlenius et al., 2018; Kolpin et al., 2002; Ternes, 1998; Valdés et al., 2016), ces médicaments étant excrétés via les urines et les fèces sans avoir été complètement assimilés par l'organisme.

Ainsi, les verrous scientifiques abordés durant ces travaux de thèse sont les suivants :

- Lors de l'ozonation par contacteur membranaire, où se situe la principale résistance au transfert ?
- Quels sont les paramètres du procédé influençant le transfert de l'ozone (pH, température, vitesse de circulation des fluides, etc) ?
- Quel est l'effet de la présence de réaction chimique sur le transfert ?
- Comment vieillissent les membranes au contact de l'ozone ?
- Le procédé d'ozonation par contacteur membranaire est-il efficace sur les micropolluants organiques d'origine pharmaceutique ciblés ?

- Le procédé d'ozonation par contacteur membranaire permet-il de limiter la formation de bromates par rapport à un procédé d'ozonation conventionnel ?
- Est-il possible de prévoir les profils de concentration de l'ozone dans un contacteur à géométrie fibre creuse, en monofibre et en multifibres, à partir de la simulation numérique ? De cette façon, est-il possible de mieux comprendre les phénomènes locaux limitants grâce à la modélisation et ainsi d'optimiser le procédé ?

Afin de répondre à ces différentes questions, ces travaux de thèse ont associé une démarche expérimentale et numérique. Ces recherches ont consisté en en i) une analyse bibliographique des travaux publiés sur le sujet, ii) un travail expérimental de caractérisation du transfert d'ozone à travers un contacteur membranaire, iii) un travail expérimental d'évaluation de l'efficacité du procédé sur la dégradation des micropolluants sélectionnés et sur la minimisation des bromates formés, et iv) un travail numérique de simulation du procédé. Les résultats du travail réalisé sont synthétisés dans ce manuscrit de thèse, articulé en cinq chapitres.

Le premier chapitre est un état de l'art des travaux publiés sur l'ozonation par contacteur membranaire et plus spécifiquement des premières études réalisées au sujet de l'utilisation des contacteurs membranaires pour une application d'élimination des micropolluants. Il décrit les mécanismes réactionnels ayant lieu lors de l'ozonation de polluants organiques et aborde les difficultés expérimentales rencontrées sur ce sujet telles que les limitations dues aux pressions transmembranaires ainsi que les matériaux compatibles. Ce chapitre fait également un bilan des principaux paramètres du procédé ayant un impact sur le transfert.

Le second chapitre présente les matériels et méthodes employés au cours de ces recherches.

Le troisième chapitre consiste en la caractérisation du transfert d'ozone via un pilote expérimental comprenant un contacteur membranaire possédant des fibres creuses en polytétrafluoroéthylène, dans une matrice composée d'eau pure puis de colorant (Acide Orange 7). Dans ce même chapitre, le vieillissement du contacteur membranaire utilisé au cours du temps est analysé.

Le quatrième chapitre est consacré à l'évaluation de l'efficacité du procédé sur l'élimination de deux médicaments sélectionnés dans le cadre de cette thèse (la carbamazépine et le sulfaméthoxazole), ainsi qu'à la détermination de la quantité de bromates formés lors de l'ozonation d'une eau concentrée en bromures par rapport ceux formés lors de l'utilisation d'un procédé d'ozonation conventionnel de type réacteur à bulles.

Enfin, le dernier chapitre correspond à la création d'un modèle validé expérimentalement et réalisé à l'aide du logiciel Comsol Multiphysics (logiciel de simulation multi-physique) couplé à un module de calcul de dynamique des fluides (CFD). Ainsi, à partir du modèle établi, ce chapitre expose les résultats de simulation du procédé d'ozonation par contacteur membranaire dans différentes conditions dans le but de mieux comprendre les phénomènes physiques et chimiques ayant lieu localement. De cette manière, le modèle présenté constitue une base pour l'optimisation de la géométrie des contacteurs membranaires et des paramètres du procédé.

Bibliographie de l'Introduction Générale

Aemig, Q., Hélias, A., Patureau, D., 2021. Impact assessment of a large panel of organic and inorganic micropollutants released by wastewater treatment plants at the scale of France. Water Res. 188, 116524. https://doi.org/10.1016/j.watres.2020.116524

Altenburger, R., Scholze, M., Busch, W., Escher, B.I., Jakobs, G., Krauss, M., Krüger, J., Neale, P.A., Ait-Aissa, S., Almeida, A.C., Seiler, T.-B., Brion, F., Hilscherová, K., Hollert, H., Novák, J., Schlichting, R., Serra, H., Shao, Y., Tindall, A., Tollefsen, K.E., Umbuzeiro, G., Williams, T.D., Kortenkamp, A., 2018. Mixture effects in samples of multiple contaminants – An inter-laboratory study with manifold bioassays. Environ. Int. 114, 95–106. https://doi.org/https://doi.org/10.1016/j.envint.2018.02.013

Antoni, V., Cerisier-Auger, A., Dossa-Thauvin, V., Eumont, D., Guilhen, J.-M., Guzmova, L., Lamprea, K., Larrieu, C., Nauroy, F., Parisse, S., 2020. Eau et milieux aquatiques. Les chiffres clés. Edition 2020.

Barrault, J., Dumas, L., 2016. Projet REGARD - Livrable de la tâche 1.2.1 - Les enjeux globaux des micropolluants. Bordeaux.

Bergé, A., 2012. Identification des sources d'alkylphénols et de phtalates en milieu urbain: comparaison des rejets à dominante urbaine (domestique) par rapport à des rejets purement industriels. Thèse de doctorat. Université Paris-Est. Français.

Björlenius, B., Ripszám, M., Haglund, P., Lindberg, R.H., Tysklind, M., Fick, J., 2018. Pharmaceutical residues are widespread in Baltic Sea coastal and offshore waters – Screening for pharmaceuticals and modelling of environmental concentrations of carbamazepine. Sci. Total Environ. 633, 1496–1509. https://doi.org/10.1016/j.scitotenv.2018.03.276

Bolong, N., Ismail, A.F., Salim, M.R., Matsuura, T., 2009. A review of the effects of emerging contaminants in wastewater and options for their removal. Desalination 239, 229–246. https://doi.org/10.1016/j.desal.2008.03.020

Carson, R., 1962. Silent Spring, Greenwich, Fawcett. Traduction française : Printemps silencieux, Paris, Plon, 1968.

Chabanon, E., Favre, E., 2017. 3.9 Membranes Contactors for Intensified Gas–Liquid Absorption Processes. Compr. Membr. Sci. Eng., Elsevier, pp.249-281. https://doi.org/10.1016/B978-0-12-409547-2.12250-4 ⟨hal-02055331⟩

Choubert, J.-M., Pomies, M., Miege, C., Coquery, M., Martin-Ruel, S., Budzinski, H., Wisniewski, C., 2012. Élimination Des Micropolluants Par Les Stations D'Épuration Domestiques. Sci. Eaux Territ. Numéro 9, 6. https://doi.org/10.3917/set.009.0003

Cizmas, L., Sharma, V.K., Gray, C.M., McDonald, T.J., 2015. Pharmaceuticals and personal care products in waters: occurrence, toxicity, and risk. Environ. Chem. Lett. 13, 381–394. https://doi.org/10.1007/s10311-015-0524-4

D'Almeida, M., Sire, O., Lardjane, S., Duval, H., 2020. Development of a new approach using mathematical modeling to predict cocktail effects of micropollutants of diverse origins. Environ. Res. 188. https://doi.org/10.1016/j.envres.2020.109897

Gosset, A., Polomé, P., Perrodin, Y., 2020. Ecotoxicological risk assessment of micropollutants from treated urban wastewater effluents for watercourses at a territorial scale: Application and comparison of two approaches. Int. J. Hyg. Environ. Health 224, 113437.

https://doi.org/10.1016/j.ijheh.2019.113437

Hayes, T.B., Case, P., Chui, S., Chung, D., Haeffele, C., Haston, K., Lee, M., Mai, V.P., Marjuoa, Y., Parker, J., Tsui, M., 2006. Pesticide mixtures, endocrine disruption, and amphibian declines: Are we underestimating the impact? Environ. Health Perspect. 114, 40–50. https://doi.org/10.1289/ehp.8051

Heitz, C., Pierrette, M., Barbier, R., 2017. Les micropolluants d'origine domestique dans l'eau: enquête sur la représentation d'une nouvelle menace. VertigO la Rev. électronique en Sci. l'environnement, volume 17, no 3.

Kolpin, D.W., Furlong, E.T., Meyer, M.T., Thurman, E.M., Zaugg, S.D., Barber, L.B., Buxton, H.T., 2002. Pharmaceuticals, hormones, and other organic wastewater contaminants in U.S. streams, 1999-2000: a national reconnaissance. Environ. Sci. Technol. 36, 1202–1211. https://doi.org/10.1021/es0200903

Merle, T., Pronk, W., Von Gunten, U., Eawag, †, 2017. MEMBRO 3 X, a Novel Combination of a Membrane Contactor with Advanced Oxidation (O 3 /H 2 O 2) for Simultaneous Micropollutant Abatement and Bromate Minimization. Environ. Sci. Technol. Lett 4, 13. https://doi.org/10.1021/acs.estlett.7b00061

Paxéus, N., Robinson, P., Balmer, P., 1992. Study of organic pollutants in municipal wastewater in Göteborg, Sweden. Water Sci. Technol. 25, 249–256.

Pinkernell, U., Von Gunten, U., 2001. Bromate minimization during ozonation: Mechanistic considerations. Environ. Sci. Technol. 35, 2525–2531. https://doi.org/10.1021/es001502f

Reed, B.W., Semmens, M.J., Cussler, E.L., 1995. Chapter 10 Membrane contactors. Membr. Sci. Technol. 2, 467–498. https://doi.org/10.1016/S0927-5193(06)80012-4

Ternes, T.A., 1998. Occurrence of drugs in German sewage treatment plants and rivers. Water Res. 32, 3245–3260. https://doi.org/10.1016/S0043-1354(98)00099-2

Thrupp, T.J., Runnalls, T.J., Scholze, M., Kugathas, S., Kortenkamp, A., Sumpter, J.P., 2018. The consequences of exposure to mixtures of chemicals: Something from 'nothing' and 'a lot from a little' when fish are exposed to steroid hormones. Sci. Total Environ. 619–620, 1482–1492. https://doi.org/https://doi.org/10.1016/j.scitotenv.2017.11.081

Valdés, M.E., Huerta, B., Wunderlin, D.A., Bistoni, M.A., Barceló, D., Rodriguez-Mozaz, S., 2016. Bioaccumulation and bioconcentration of carbamazepine and other pharmaceuticals in fish under field and controlled laboratory experiments. Evidences of carbamazepine metabolization by fish. Sci. Total Environ. 557–558, 58–67. https://doi.org/10.1016/j.scitotenv.2016.03.045

WWAP, Programme mondial de l'UNESCO pour l'évaluation des ressources en eau, 2019. Rapport mondial des Nations Unies sur la mise en valeur des ressources en eau 2019 : Ne laisser personne pour compte. Paris, UNESCO.

Chapitre I

Ozonation using hollow fiber contactor technology ant its perspectives for micropollutants removal in water: A review

Liste des symboles et abréviations du Chapitre I

ε_m	Membrane porosity	-
τ_m	Membrane tortuosity	-
$[O_3], [M], [OH^\circ]$	Respectively the concentration of molecular ozone, micropollutant, and hydroxyl radicals	mol.m^{-3}
A_{outer}, A_{lm}, A_{inner}	Respectively the outer, logarithmic mean, and inner surface area of the membrane	m^2
a	Surface area of membrane per volume of liquid	m^2.m^{-3}
$C_{i,liquid,interface}$, $C_{i,gas,interface}$, $C_{i,gas,membrane}$	Respectively the concentration of the compound of interest at the interface on the liquid side, at the interface on the gas side, and at the gas-membrane interface	mol.m^{-3}
$C_{i,liquid}$, $C_{i,gas}$:	Respectively the concentration of the compound of interest in the liquid bulk and in the gas bulk	mol.m^{-3}
C_i	Dissolved gases concentrations	mol/L or mol.m^{-3}
C_f	Solute concentration at the tube outlet	mol.m^{-3}
C_{eq}	Solubility of ozone in the liquid	mol.m^{-3}
C_0	Feed ozone concentration	mol.m^{-3}
d_i, d_{ln}, d_o	Respectively the inner, logarithmic mean, and outer diameters of the fibers or the tube	m
D_g, D_L	Diffusion coefficient respectively in the gas phase and in the liquid phase	m^2.s^{-1}
E	Enhancement factor	-
Ha	Hatta's number	-
H	Partition coefficient of the gas in the liquid (Henry's law constant)	-
J_i	Molar flux of the compound of interest across the membrane	mol.m^2.s^{-1}
$K_{H,i}$	Dissolution constant of the gas (Henry's law constant)	mol.kg^{-1}.hPa^{-1} or mol.L^{-1}.hPa^{-1}

k_g, k_m, k_L	Respectively the mass transfer coefficient in the gas, in the membrane, and in the liquid	$m.s^{-1}$
K_L	Overall mass transfer coefficient	$m.s^{-1}$
$k^0_{L,O3}, k^r_{L,O3}$	Ozone mass transfer coefficient in the liquid phase respectively without and with reaction	$m.s^{-1}$
k_{O3}, k_{OH}	Second-order reaction rate constant for the reaction of micropollutant (M) (or another compound of interest) respectively with O_3 and with OH°	$m^3.\ mol^{-1}.s^{-1}$
Lc	Hydraulic diameter of the liquid phase	m
l_m	Membrane thickness	m
L	Total tube length	m
n	Order of the reaction	-
p_i	Partial pressure of the gas in the air	hPa
R	Elovitz constant	-
Re	Reynolds number	-
r_M	Reaction rate	$mol.m^{-3}.s^{-1}$
$S_{g,m}$	Solubility of the gas in the membrane	-
Sc	Schmidt number	-
Sh	Sherwood number	-
$u_{L,mean}$	Mean liquid velocity	$m.s^{-1}$
x	Direction of the flow	m
x_{O3}	Fraction of ozone in the gas	-

Objectifs et approche du Chapitre I

Ce premier chapitre est un état de l'art de la technologie du contacteur membranaire appliquée au transfert d'ozone d'une phase gaz vers une phase liquide (absorption). Plus particulièrement, il cible les premiers travaux réalisés concernant l'utilisation des contacteurs membranaires afin d'éliminer les micropolluants dans l'eau, qui constituent l'objet central de ce manuscrit de thèse.

Diverses études ont démontré l'efficacité de l'ozonation sur l'élimination des micropolluants organiques. Cependant, les procédés d'ozonation conventionnels comme les chambres d'ozonation, dans lesquelles l'ozone est diffusé sous forme de bulles, possèdent plusieurs inconvénients comme par exemple un risque de moussage ou encore un dosage difficile de l'ozone transféré, provoquant la formation de sous-produits issus des réactions d'oxydation et parfois plus toxiques que les produits initialement traités. D'après la littérature, le contacteur membranaire serait une solution efficace pour pallier ces inconvénients (Bamperng et al., 2010; Berry et al., 2017; Jansen, 2005; Merle et al., 2017; Stylianou et al., 2015; Wenten et al., 2012).

En effet, dans un contacteur membranaire, le transfert de matière a lieu par diffusion, et non par dispersion comme dans les procédés conventionnels. Il n'y a donc pas de risque de moussage ou de noyage. La membrane agit comme une barrière entre la phase liquide et la phase gazeuse, la matière étant transférée grâce à un gradient de concentration. Contrairement à d'autres procédés membranaires, il s'agit d'un procédé basse pression pour lequel l'application d'un gradient de pression n'est pas nécessaire.

Le transfert est ainsi effectué uniformément via de très multiples points de dosage créés par les pores de la membrane (dans le cas des membranes poreuses), cette dernière offrant d'autre part une très large surface d'échange. Son utilisation pourrait permettre de doser plus précisément l'ozone nécessaire pour éliminer les composés ciblés et ainsi éviterait d'avoir un excès en ozone dissous, appelé ozone résiduel, qui serait responsable de la formation de certains sous-produits toxiques. Par exemple, son utilisation pourrait permettre de limiter la formation des bromates, apparaissant lors de l'ozonation d'eau contenant des bromures.

Sa géométrie rend cette technologie particulièrement compacte et modulable par rapport à un procédé conventionnel, notamment dans le cas de fibres creuses. L'aire interfaciale d'un contacteur membranaire peut atteindre 10 000 $m^2.m^{-3}$ de liquide, tandis qu'elle varie entre 3 et 600 $m^2.m^{-3}$ dans le cas de réacteurs d'ozonation traditionnels (Chabanon and Favre, 2017; Reed et al., 1995). De plus, un recyclage du gaz est envisageable en sortie du contacteur, entraînant ainsi l'économie du coût lié à la production et destruction de l'ozone en excès.

Ainsi, la revue bibliographique réalisée dans ce premier chapitre décrit le processus d'ozonation et les mécanismes réactionnels associés, explicite le principe de la diffusion d'ozone par contacteur membranaire et permet d'appréhender les travaux ayant d'ores-et-déjà été réalisés avec succès sur le sujet, notamment à des fins d'abattement des micropolluants. Les verrous rencontrés lors de ces recherches sont présentés, notamment les limites du procédé dues aux pressions transmembranaires maximum applicables. Enfin, l'importance du matériau membranaire employé est abordé.

Ozonation using hollow fiber contactor technology and its perspectives for micropollutants removal in water: a review

Alice Schmitt[a], Julie Mendret[a], Michel Roustan[b], Stephan Brosillon[a]

[a] IEM, University of Montpellier, CNRS, ENSCM, Montpellier, France

[b] TBI, Université de Toulouse, CNRS, INRA, INSA, Toulouse, France

Published in Science of the Total Environment 729 (2020) 138664

Abstract

Membrane contactor is a device generally used for the removal or the absorption of a gas into another fluid. The membrane acts as a barrier between the two phases and mass transfer occurs by diffusion and not by dispersion. This article is a review of the application of membrane contactor technology for ozonation applied to water treatment. The challenge of removing micropollutants is also discussed. In the first part, the ozonation process is mentioned, in particular chemical reactions induced by ozone and its advantages and disadvantages. In the second part, generalities on membrane contactor technology using hollow fibers are presented. Then, the benefit of using a membrane contactor for the elimination of micropollutants is shown through a critical analysis of the influence of several parameters on the ozonation efficiency. The impact of the membrane material is also highlighted. Finally, several modeling approaches are presented as a tool for a better understanding of the phenomena occurring in the contactor and a possible optimization of this process.

Graphical abstract

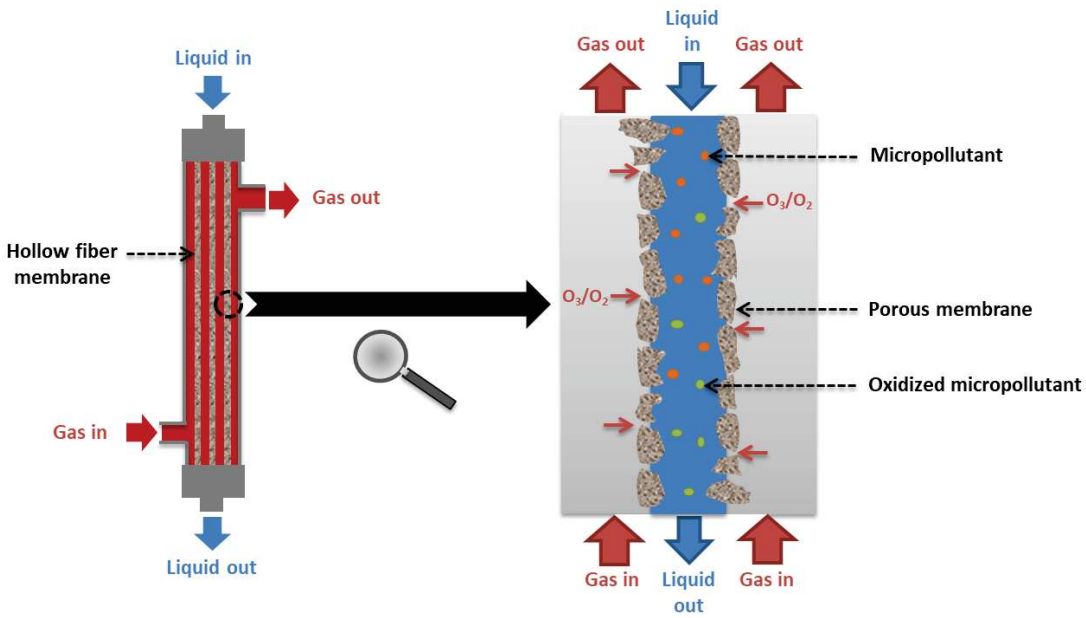

1. Introduction

To protect the ecosystem and drinking water resources, requirements on water treatment will become increasingly stricter. It is only a matter of time before treatment plants will be required to incorporate treatment steps to ensure that micropollutants (i.e. harmful substances, detectable in the environment at very low concentrations (ng/L up to µg/L)) are eliminated and do not enter the water bodies. For instance, in Switzerland, a new Swiss water protection act entered into force in 2016 aiming to reduce the discharge of micropollutants from wastewater treatment plants (WWTPs) (Office fédéral de l'environnement, 2014). As a consequence, selected WWTPs must be upgraded by an advanced treatment for micropollutants abatement with suitable and economic options such as ozonation. Ozone treatment is easy to automate and clean to handle. It provides a chemical-free means of removing 90 percent of emerging contaminants (Prieto-Rodríguez et al., 2013; Snyder et al., 2006). It can be quite simply incorporated into existing and new applications and is a reliable and control-supported process. Another advantage of ozonation is the direct oxidation, breaking the molecule which is destroyed and not only absorbed. Ozonation is thus an interesting technology for water reuse since it can both disinfect and oxidize, or be used with other technologies in a multiple-barrier concept.

The conventional reactors used during the ozonation processes are presented in Table 1. A schematic drawing of each reactor is exposed in Figure 1. Depending on the application (i.e. the objectives of the ozonation), the reactor is chosen according to its contact time (especially for slow reactions), its hydrodynamics (especially for fast and moderately fast reaction, where a plug flow is preferable), and its ozone transfer (especially for very fast reaction, where a high interfacial area is preferable). Generally, ozone in water treatment is injected in the form of bubbles, with disadvantages such as operational costs, stripping of volatile organic compounds, high footprint of the reactor, mass transfer limitations (leading to high energetic costs) and foam generation. Moreover, in some cases, these processes do not ensure a controlled dosage, and can lead to the production of by-products sometimes more dangerous than the original products (Gao et al., 2016; Gogoi et al., 2018; Schlüter-Vorberg et al., 2015).

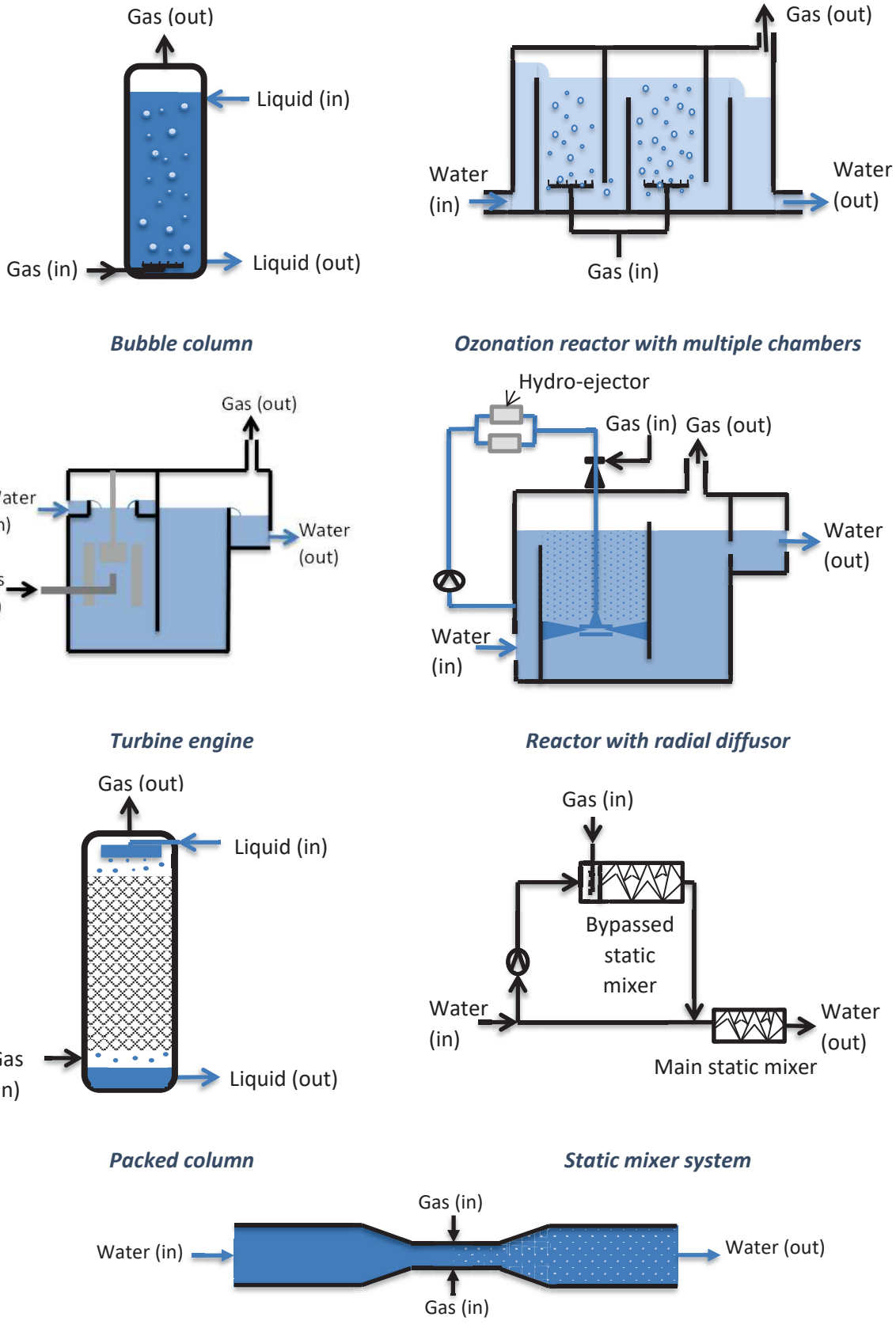

Figure 1. Schemes of conventional reactors used for ozonation.

Table 1. Conventional reactors used for ozonation, adapted from Suez, 2007.

Type of reactor	Dispersed phase	Value range of kLa according to the literature (s^{-1})	Value range of gas retention Ɛg	Value range of power consumption ($kW.m^{-3}$ of reactor)	Advantages	Disadvantages	Application fields
Bubble column with porous diffusers	Gas	0.0001-0.1 (K_La between 0.005 and 0.12 (Chabanon and Favre, 2017))	< 0,2	0.01 - 1	Smooth operation Low maintenance cost	Risk of clogging Complex hydrodynamics	Drinking water (Low ozone dose transferred and slow reaction)
Turbine engine or with radial diffuser	Gas	0.01-0.2	< 0.1	0.5 - 4	Gas/Liquid mix and contact Flexible to the variation in the liquid flow	High energy consumption Mechanical equipment maintenance	Drinking water and wastewater (High ozone dose transferred, moderately fast reaction)
Packed column	Liquid	0.005-0.02 K_La between 0.0004 and 0.07 (Chabanon and Favre, 2017))	> 0.3	0.01 - 0.2	Transfer and plug flow Low maintenance cost	Risk of fouling of the lining	Gas washing, production of ozonated water (Fast reaction)
Static mixer	Gas	0.1-10	Around 0.5	10 - 200	Mix and transfer Low maintenance cost Low size of installation	High energy consumption Short contact time Risk of clogging	Drinking water and wastewater (Very fast reaction)
Venturi injector	Gas	0.06-0.21 (Roustan, 2003)	1-10 (Roustan, 2003)	N.A.	High mass transfer (Cachon et al., 2019; Ozkan et al., 2006) High gas-liquid interfacial area High energy efficiency Applicable to short contact time (Briens et al., 1992) No additional equipment needed (i.e. located directly in the process stream) (Bauer et al., 1963) Minimal maintenance (Cachon et al., 2019)	Power from a recirculating pump required, or pressurized water supply (Cachon et al., 2019)	Petroleum refining, Hydrogenation, Fermentation, Waste-water treatment (Briens et al., 1992)

The use of membrane contactors for ozone diffusion in water treatment recently emerged as a very interesting option. Indeed, by using a bubbleless operation, membrane contactors can overcome these challenges. Indeed, membrane contactors have been pointed out as a good alternative for the transfer of gas to the liquid phase (Alves dos Santos et al., 2015; Berry et al., 2017; Pabby and Sastre, 2013; Stylianou et al., 2016), and to control the dosage of ozone during ozonation processes (Atchariyawut et al., 2009; Bamperng et al., 2010; Berry et al., 2017; Janknecht et al., 2001; Jansen et al., 2005; Leiknes et al., 2005; Merle et al., 2017; Picard et al., 2001; Pines et al., 2005; Shanbhag et al., 1998, 1995; Stylianou et al., 2018, 2016; Wenten et al., 2012; Zoumpouli et al., 2018). The following list describes the major advantages of a membrane contactor technology:

- This process has a smaller foot print than conventional reactor, thanks to its large interfacial area. Since treatment of wastewater are targeted, very fast reaction will occur and thus the transfer will be accelerated by the reaction, as a consequence it is interesting to develop high interfacial area in the reactors. According to Reed et al., membrane contactors have an interfacial area between 1640 and 6562 m^2/m^3. According to Chabanon et al., membrane contactors have a surface area/volume ratio around 1,000-10,000 m^2/m^3, whereas this ratio is between 50 and 600 m^2/m^3 for a bubble column and between 10 and 500 m^2/m^3 for a packed column. (Chabanon and Favre, 2017). In contrast, conventional contactors have an interfacial area between 3 and 492 m^2/m^3.(Reed et al., 1995). Pines et al (2005) have carried out calculations, an hypothetical case of 167 m^3/h flow rate and 2 mg/L transferred ozone dose was used in order to compare the volume required for hollow fiber membrane contactors (PVDF) configurations compared to a fine-bubble diffuser contactor. The assumptions were a gas O_3 concentration of about 6%, no chemical reaction and a system mass transfer limited. Stylianou et al (2016) have carried out the same calculations based on their experimental results obtained with ceramic tubular membrane. The volume of each reactor was 12 m^3, 1.9 m^3 and 0.15 m^3 respectively for bubble column; ceramic tubular membrane contactor and PVDF hollow fiber membrane. This first approach demonstrates the real interest of membrane contactor to increase the compactness of the unit operation.

- The mass transfer (i.e. the K_La) obtained with a membrane contactor is significantly higher than with other conventional reactors. For a membrane contactor, the mass transfer is estimated between 0.05 and 0.50 s^{-1}, whereas it is between 0.005 and 0.12 s^{-1} for a bubble column and between 0.0004 and 0.07 s^{-1} for a packed column. The difference is mainly due to a surface area/volume ratio particularly interesting with the membranes.

- The compound of interest (i.e. here the ozone molecule) has a uniform distribution, thanks to the large exchange surface (i.e. interfacial area) offered by the hollow fiber membranes.

- The risk of flooding and of entrainment of the dispersed phase is avoided thanks to a bubbleless process.

- Increasing the production capacity of a membrane contactor is easy by adding more membrane modules (i.e. this process is especially modular).

- The exchange surface is independent of the flow rates. The process can work efficiently at different gas/liquid ratios, and therefore has a wide range of capacities for the same number of modules.

- Operations are performed under low pressures because transfer is driven by the concentration gradient and not by the pressure gradient. Therefore, energy requirement by this process can be lower (depending on pressure drop).

- A gas stream recycling can be implemented, and thus energy and reagent savings can be made.

- Thanks to the independent flow adjustment for gas and liquid phases, an optimization of applied reagent dosage (i.e. here ozone) also allows to save reagent.

- All the ozone diffused through the membrane is transferred into the liquid phase (reacting or not in this phase), due to the bubbleless process. The rest (in the gas phase) can be recycled to the ozone generator thanks to a lower moisture content than in conventional processes (Phattaranawik et al., 2005; Stylianou et al., 2016). In comparison to bubble column where 25% of ozone is not transferred in the liquid phase, fewer reagents are needed for the same oxidation.

- Less by-products (e.g. bromates) could be produced than in conventional ozonation processes thanks to the minimization of the dissolved ozone concentration ((Heeb et al., 2014; Merle et al., 2017).

On the contrary, according to several studies, the main disadvantages of the membrane contactor process are the following (Gabelman and Hwang, 1999; Mulder, 1996).

- The risk of wetting is important and depends on the transmembrane pressure. Its consequence is a lower ozone transfer.

- A risk of bubbling is common and also depends on the transmembrane pressure. Ozone which is diffused by bubbles through the membrane may not be completely transferred into the liquid phase, and thus stays in gaseous form.

- The liquid can cause the fouling of the fibers. Fouling is one of the main problems in the application of porous membrane for water treatment (Van Geluwe et al., 2011). Gas/liquid contactors are less sensitive to fouling than filtration membranes) because no flow circulates through the membrane pores (Van Geluwe et al., 2011; Yu et al., 2015). However, membrane contactors have generally a small diameter, and therefore suspended particles in the gas phase or in the liquid phase can cause plugging (Van Geluwe et al., 2011). When the gas circulates in the lumen and the liquid in the shell side, this phenomenon is limited. There is little available literature on ozone transfer into water with membranes, and to date no literature concerning the fouling during such a process. Most studies focus on ozone as a pretreatment (i.e. as a supplementary agent) within hybrid treatment processes, leading to the reduction of fouling or the increase of the biodegradation of contaminants in membrane bioreactor, and therefore to better membrane performances (Kim et al., 2008; Laera et al., 2012; Van Geluwe et al., 2011; Zoumpouli et al., 2018).

- The overall resistance to transfer is increased due to the addition of a new phase (i.e. the membrane).

- A bypass may be created into the shell side. If the liquid is in the shell side, a part of the water could not be treated. If the gas is in the shell side, a part of the oxidizing compound could not be transferred in the other phase.

In recent years, very interesting reviews on advanced oxidation processes for water treatment were generated, but none concerning the ozonation with membrane contactors (Von Gunten, 2018). In this context, this review focuses on the ozonation of water using membrane contactors, that had not yet been previously reviewed in detail. Hollow fibers and tubular technologies for the elimination of micropollutants in water are described more specifically. The significance of the membrane material is highlighted, as well as the importance of the modeling in order to optimize the transfer. Conversely, processes like ozonation on catalytic membranes, or ozonation for cleaning, are not covered.

2. General principles of ozonation

2.1. Ozonation reaction

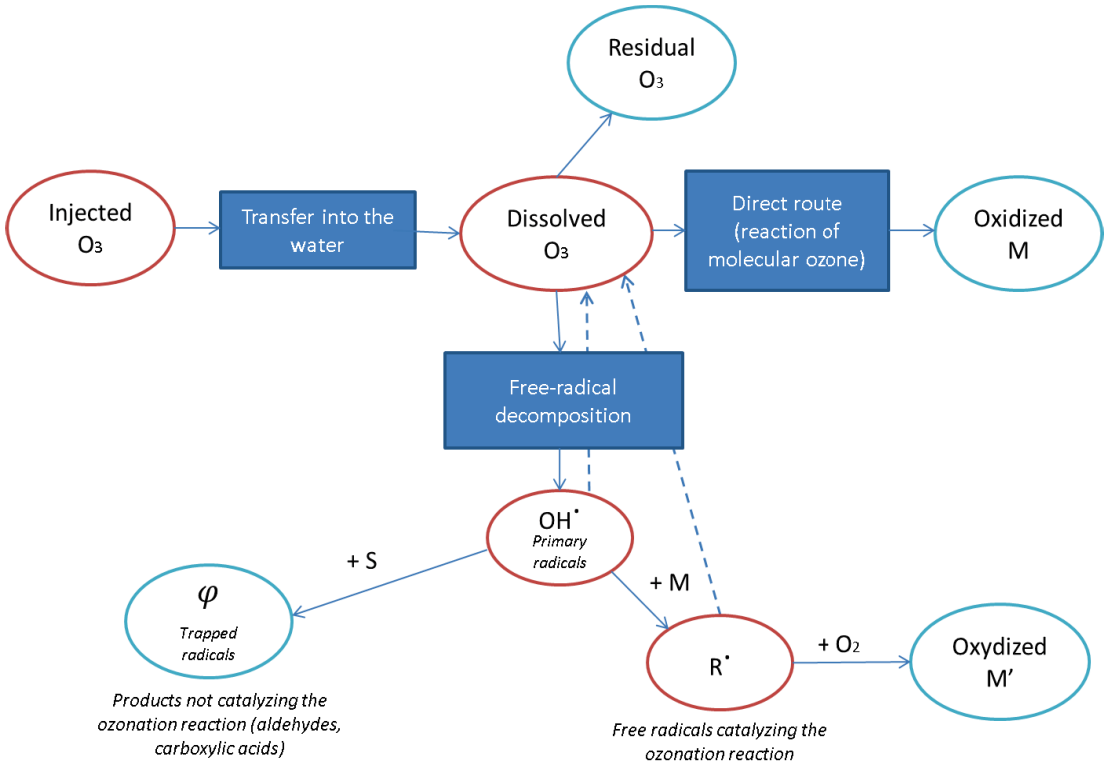

Figure 2. Ozonation reaction in water during oxidation of a pollutant M.

The ozonation reaction is described in Figure 2 (Nawrocki and Kasprzyk-Hordern, 2010). Several mechanisms occur simultaneously and by chain reactions during degradation of an organic substance M. In the first case, molecular ozone can directly oxidize the polluting substance. In the second case, ozone can decompose into hydroxyl radicals. This way leads to a succession of radical reactions, initiated by the interaction between hydroxyl radicals and ozone (Gordon, 1995; Westerhoff et al., 1997). Hydroxyl radicals are non-selective and have strong oxidation properties (Kanakaraju et al., 2018).

These mechanisms coexist and the kinetic expression of the reaction can be described by equation 1:

$$r_M = k_{O3}[O_3][M] + k_{OH}[OH^\circ][M]$$

$$= [O_3][M][k_{O3} + k_{OH}R], \quad [1]$$

Where:

- r_M: reaction rate (mol.L^{-1}.s^{-1})
- [HO°]: concentration of hydroxyl radicals (mol.L^{-1})

- $[O_3]$: concentration of molecular ozone (mol.L^{-1})
- k_{O3} , $k_{HO°}$: second-order rate constant for the reaction of micropollutant (M) with O_3 and HO° (L. $mol^{-1}s^{-1}$)
- $R=[HO°]/[O_3]$: ratio between the concentration of hydroxyl radicals and the concentration of molecular ozone, varying between 10^{-9} and 10^{-7} and depending on the water type (according to Elovitz et al., 2000)

The mechanism favoring the oxidation efficiency depends on the k_{O3} value, which is a second order rate constant. When k_{O3} < 100 mol.L^{-1}.s^{-1}, the main way of degradation is the radical mechanisms. When k_{O3} is between 100 and 10,000 mol.L^{-1}.s^{-1}, both radical and molecular mechanisms occur simultaneously with the same order of magnitude. When k_{O3} > 10,000 mol.L^{-1}.s^{-1}, molecular mechanisms are promoted. (Bourgin et al., 2017)

2.2. Ozonation efficiency for the elimination of micropollutants in water

Advanced treatment technologies remove MP more efficiently than primary and secondary treatments (Luo et al., 2014). Several studies about the application of ozonation for MP elimination have been carried out (Behera et al., 2011; Huber et al., 2003; Lishman et al., 2006; Paxéus, 2004; Santos et al., 2007). Ozone eliminates a wide range of MP in WWTP, with a dose of dissolved ozone around 3-8 mgO_3/L (Gomes et al., 2017; Hollender et al., 2009; Margot et al., 2013; Nakada et al., 2007; Reungoat et al., 2012, 2010; Rosal et al., 2010). This process is also efficient on several pharmaceuticals often detected in surface waters (Tootchi et al., 2013). The degradation efficiency of MP depends on several parameters (see 2.3. Influential parameters), in particular their reaction rates with O_3 and HO°, which involve different mechanisms of MP removal (see 2.3.2. Influence of the reaction rate of the compound with O_3 and HO°).

From equation 1, a chemical kinetic model can be deducted for the prediction of micropollutants abatement by ozonation (Elovitz and Von Gunten, 1999; Guo et al., 2018; Lee et al., 2014, 2013; Lee and von Gunten, 2016; Wang et al., 2018) :

$$-\boldsymbol{ln}\left(\frac{\boldsymbol{M}}{\boldsymbol{M_0}}\right) = \boldsymbol{k_{O_3}} \int [\boldsymbol{O_3}]\boldsymbol{dt} + \boldsymbol{k_{HO^\circ}} \int \left[\boldsymbol{OH^\circ}\right]\boldsymbol{dt}, \quad [2]$$

Where:

- k_{O3} , $k_{HO°}$: second-order rate constant for the reaction of micropollutant (M) with O_3 and HO°
- $\int[O_3]dt$ and $\int[HO°]dt$: O_3 and HO° exposures, which are defined as the time-integrated concentration of O_3 and HO° over a given reaction period

Other species than molecular ozone and hydroxyl radicals play an important role in the mechanisms of ozone consumption (Westerhoff et al., 1997). As shown in Figure 2, a part of hydroxyl radicals does not react with micropollutants but with scavengers. The presence of scavengers depends on the matrix to treat (e.g. natural water, drinking water, and wastewater) (Buffle et al., 2006). It corresponds to some background water constituents, for instance carbonates (Yao et al., 2018). By scavenging hydroxyl radicals, some compounds can inhibit the ozone decomposition without producing hydrogen peroxide or superoxide radical ions. Other compounds can promote ozone decomposition by forming superoxide radical ions. Water with natural organic matter will be consequently complex to model because of its heterogeneity (Westerhoff et al., 1997) (see *2.2.1.*) .

2.3. Influential parameters

2.3.1. Effect of matrix

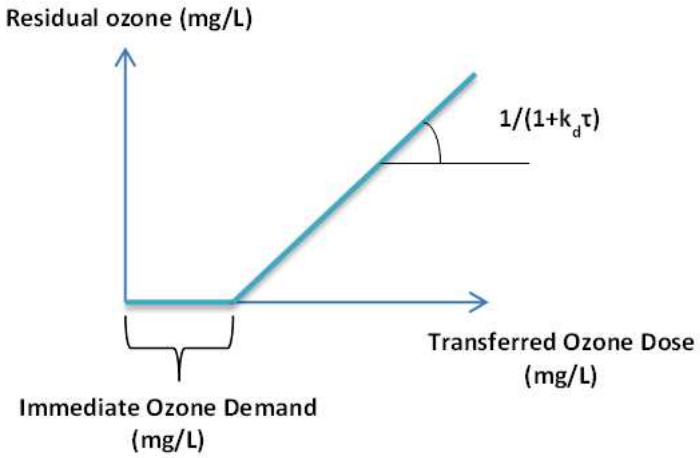

Figure 3. Determination of Immediate Ozone demand (mg/L) and kd (min^{-1}), in a G/L contactor operating continuously for the 2 phases, adapted from Roustan et al., 2003.

The efficiency of ozonation process depends on the matrix to treat. For instance, water is a complex mixture with a lot of different compounds, both organic and inorganic. They react simultaneously, with molecular and free-radical mechanisms. Therefore, it is possible to formulate the overall ozone consumption of water using two criteria. The first one is the Immediate Ozone Demand (IOD), which represents the amount of ozone to apply before detecting a measurable residue of ozone. It reflects very fast reactions of the natural organic matter of the water with ozone. The higher the pH and the temperature of the water are, the faster the ozone self-destructs. The second criterion is the slow consumption velocity. This is defined by k_d, which is in this case a first order rate constant. In order to determine these two characteristics, a graph (see Figure 3) can be drawn, representing the residual ozone in function of the transferred ozone dose. The intercept of the straight line with the horizontal

axis gives the IOD, and the slope allows calculating $k_d\tau$, which is the Damköhler number (Roustan et al., 1998) .

For instance, for a surface water at 18°C, the IOD is about 0.4 gO_3/m^3 and the k_d about 0.18 min^{-1} (Roustan, 2003). Another example is provided by the works of Cruz-Alcalde et al., 2019. The authors measured an average IOD of 16 mgO_3/L at the outlet of the biological treatment of 5 different WWTP.

Antoniou et al. predicted the ozone dose to be transferred to remove 42 pharmaceuticals. They found that the sensitivity of pharmaceuticals to degradation with ozone differs, depending on the target compound, but mostly on the matrix (i.e. the type of water) (Antoniou et al., 2013). Specifically, most of the difference is explained by the Dissolved Organic Carbon (DOC) of the water to be treated (Antoniou et al., 2013; Hansen et al., 2016). Antoniou et al. correlated the specific dose of ozone required to achieve reduction by one decade of each investigated pharmaceutical with the DOC of the effluent, which consumes a part of the dissolved ozone available by reacting with it.

2.3.2. Influence of the reaction rate of the compound with O_3 and HO°

As seen previously, the rate constant k_{O3} is a significant parameter for the ozonation efficiency. This parameter depends on the compound. A high second order reaction rate with O_3 leads to a good elimination of the pollutant. Yue et al. showed that compounds with a high k_{O3} were effectively removed with a rate superior to 95% with an ozone dose transferred varying between 0.3 and 1.5 mg/L, and a contact time of 8.6 min during pilot-scale experiments using a conventional ozonator (Yue et al., 2009). Bourgin et al. came to the same conclusions during conventional ozonation of surface water (i.e. Lake Zürich water, Switzerland). For instance, diclofenac and carbamazepine, with a k_{O3} superior to $10^4\ M^{-1}.s^{-1}$, were removed at more than 90% even for the lowest ozone dose transferred of 0.5 $mg.L^{-1}$ (Bourgin et al., 2017). Zimmermann et al. showed the same results within a gas bubble column. For substances reacting fast with ozone (e.g. diclofenac and carbamazepine, $k_{O3}=10^4\ M^{-1}.s^{-1}$), they observed a good elimination for an ozone dosage transferred between 0.21 to 1.24 $g_{O3}.g_{Dissolved\ Organic\ Carbon}^{-1}$, except for the lowest dose (Zimmermann et al., 2011).

For compounds with a low to moderate reaction rate with O_3 (i.e. ozone resistant compounds with k_{O3} up to $10^1\ M^{-1}.s^{-1}$, and moderately ozone-resistant compounds with k_{O3} between 10^2 and $10^3\ M^{-1}.s^{-1}$), generally, oxidation increases with increasing ozone exposure and is influenced by the quality of the water matrix (Bourgin et al., 2017; Yue et al., 2009; Zimmermann et al., 2011). Yue et al. showed variable results. For instance, ibuprofen and clorfibric acid were removed between 3 and 62%. The same phenomena was observed for bezafibrate, which was removed between 28 and 99% under the same ozone exposure (Yue et al., 2009). Bourgin et al. found that sucralose (i.e. compound which only

react with HO° and have a low reaction rate with O_3) was removed between 19 and 90%. The author also found that during conventional ozonation of resistant compounds, the abatement was moderate, even with a high ozone dose transferred of 3 $mg0_3.L^{-1}$ (Bourgin et al., 2017). In their work about transformation by-products of pharmaceutically compounds during drinking water ozonation, Tootchi et al. selected carbamazepine as pharmaceutical with a fast reaction rate with ozone and bezafibrate as pharmaceutical with a slow to moderate reaction rate with ozone (i.e. respectively over and under 10^4 $M^{-1}.s^{-1}$). The authors found that the major oxidation pathway for carbamazepine was the direct route (i.e. reaction with molecular ozone), while for bezafibrate it was both radical and molecular reactions (Tootchi et al., 2013).

2.3.3. Influence of operating parameters

Other parameters have an influence on the ozonation efficiency. For example, a higher pH promotes free radical mechanisms and causes a faster ozone decomposition because of the presence of hydroxide anions (Buffle et al., 2006; Mecha et al., 2016). A higher temperature leads to a better mobility of the water molecules and thus to a lower water viscosity and a higher water diffusivity. A higher ionic strength decreases the solubility of ozone and thus makes ozonation processes more difficult. The influence of these parameters is discussed later with more details in the specific case of membrane contactors (section 5).

2.3.4. Ozonation by-products

During the ozonation reaction, a low mineralization can occur (i.e. the oxidation could be incomplete). It conducts to the accumulation of intermediates, which are degradation by-products. These by-products in some cases, but not systematically, could be potentially more toxic than the initial contaminants (Gao et al., 2016; Gomes et al., 2017; Luo et al., 2014; Margot et al., 2013; Petala et al., 2008, 2006; Stalter et al., 2010a, 2010b; von Gunten, 2003a).

Several by-products can be cited as examples, like the NDMA (i.e. N-Nitrosodimethylamine), or the formaldehydes, which are produced by the reaction between ozone and natural organic matter (Hollender et al., 2009; Richardson, 2003; Samadi et al., 2015; Wert et al., 2007).

According to Gao et al., the products of parabens after reaction with hydroxyl radicals have a higher toxicity to green algae than the original paraben. They showed that when the alkyl-chain length of the parabens increases, the ecotoxicity of the degradation products also increases (Gao et al., 2016).

Bromates are other degradation by-products. They are formed during the ozonation of bromide-containing waters, such as river waters (Nobukawa and Sanukida, 2000; von Gunten, 2003a). Bromates

are potentially carcinogenic and are not removed in biological filtration processes. Moreover, it is the only ozonation by-product regulated in drinking water (Merle et al., 2017; von Gunten, 2003a). Therefore, a lot of studies about water ozonation focus on this compound. A limit was established by the European Union at 10 µg/L in drinking water, but with the recommendation for the member states of having a lower value if possible (AIDA, 1998).

The bromate-forming mechanism is described in the Figure 4. In order to minimize bromates' formation, several solutions can be considered.

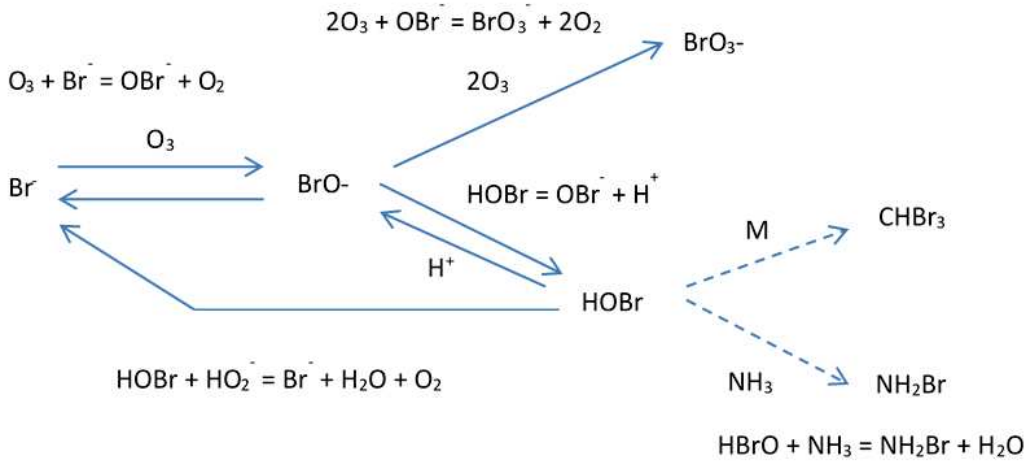

Figure 4. Bromate formation – chemical pathway, adapted from von Gunten, 2003b.

The first one is an ammonia (NH_3) addition. NH_3 does not alter the ozone stability, and therefore does not interfere with oxidation processes. NH_3 reacts with HOBr, which is an important intermediate of the bromates' formation. Adding NH_3 leads to a lower bromates' formation up to a certain concentration of ammonia (except during the initial phase of ozonation in which it has no influence). No improvement is noticed beyond this limit. A balance between HOBr and NH_3 is established, which always leaves a fraction of HOBr, transformed then into BrO_3^- (i.e. bromates). This method is therefore not efficient with waters that already have a medium or high level of ammonia (von Gunten, 2003b) .

A second solution to minimize bromates' formation is a pH depression. This method influences bromates' formation by shifting the balance between HOBr and OBr^- toward HOBr. When the pH decreases, hydroxyl radicals' exposure decreases as well, leading to a smaller overall oxidant exposure (i.e. ozone and hydroxyl radicals' exposure) and a lower bromates' formation. In the same way as the solution of ammonia addition, this solution does not reduce the initial fast bromates' formation, which is almost independent of the pH (von Gunten, 2003b).

3. Generalities on membrane contactors with hollow fibers

3.1. Principle of a G/L membrane contactor with hollow fibers

In gas/liquid membrane contactors, the membrane acts as an interface between two phases. In contrast with membranes used for filtration, membrane contactors are non-selective (i.e. they don't offer any preference between compounds). The phases could be liquid/liquid or gas/liquid. The phases are keeping separated. The operation is bubbleless, thus the transfer takes place mainly by diffusion and not by dispersion of one phase into another. The driving force of the transfer is the concentration gradient. However, the pressure gradient have to be taken carefully to keep the interface at the entrance of the pores (Gabelman and Hwang, 1999) and thus avoid some problems with the membrane.

Depending on the membrane material, the fluids, and the operational conditions, the interface could be on one side or the other of the membrane, and sometimes inside. For a gas/liquid system and a hydrophobic membrane, the phase that fills the pores is the gas one. For a hydrophilic membrane, the liquid phase fills the pores. The best configuration for the diffusion of ozone is described in a next part.

Membranes could be made with organic (polymers) or inorganic (ceramic) materials. The selection of the material is made according to the future use of the membrane contactor, the fluids to keep in contact, the desired fluxes, etc.

According to several sources about gas absorption membrane contactor (Al-Saffar et al., 1995; deMontigny et al., 2006; Dindore et al., 2005; Li et al., 2010), counter-current mode performs better than co-current mode. According to DeMontigny (deMontigny et al., 2006), counter-current mode can be up to 20% more efficient than co-current mode.

3.2. Mass transfer using membrane contactors

As described by Bamperng et al. (see Figure 5), the absorption of a gas into the liquid phase is broken down into several parts (Bamperng et al., 2010). The first is a transport of the interested gas from the bulk of gas to the interface, between gas phase and a membrane. The second is the transport of gas through the membrane pores. The last part is the dissolution of a gas component into a liquid, eventually with a chemical reaction in addition which accelerates the transfer.

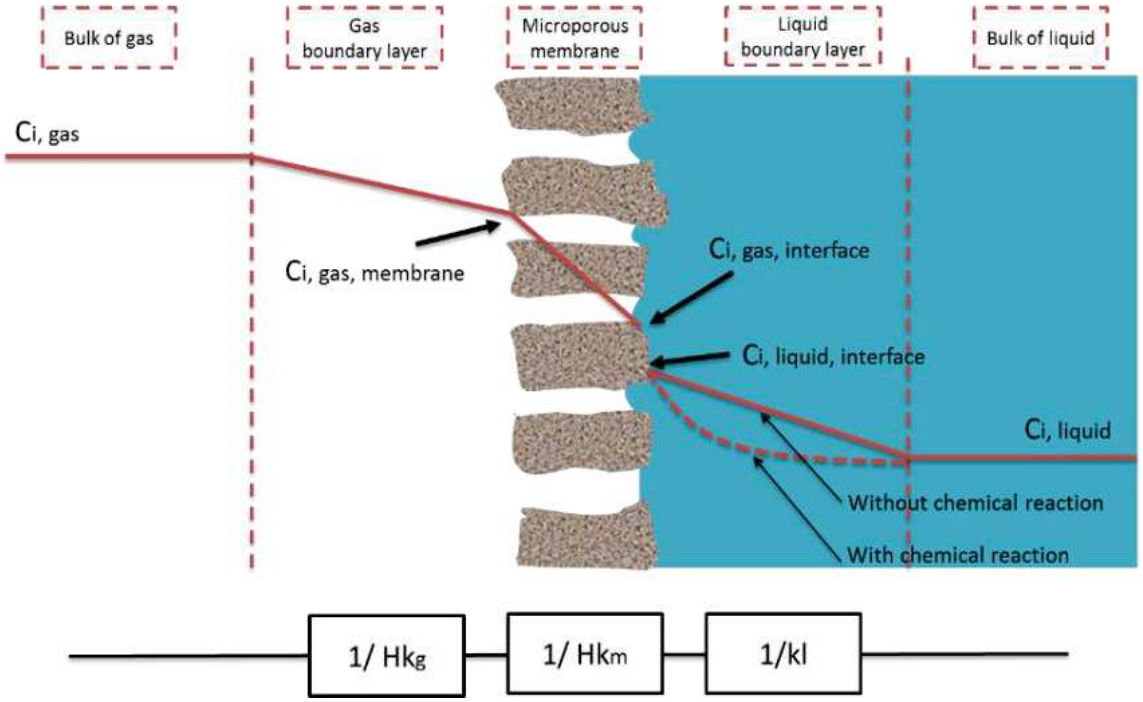

Figure 5. Mass transfer regions and resistance-in-series in non-wetted membrane contactor, adapted from Atchariyawut et al., 2007.

3.2.1. Henry's law

At the interface between the 2 phases, the Henry's law is applicable if the following assumptions are respected. The solute (i.e. here the ozone) has to be slightly soluble in the solvent ($x_{O3} < 0.05$) and the gas phase is assumed to be perfect (moderate pressure and a temperature far from the condensation temperature) (Roustan, 2003).

$$C_i = K_{H,i} \cdot p_i \,, \quad [3]$$

According to this law, dissolved gases concentrations (C_i in mol/L) are proportional to the partial pressure of the gas in the air (p_i in hPa), depending on the dissolution constant of the gas ($K_{H,i}$ in mol.kg^{-1}.hPa^{-1} or mol.L^{-1}.hPa^{-1}). Henry's law constant depends on the compound and can be expressed in several ways, and thus in several units.

3.2.2. The membrane mass transfer coefficient

The membrane mass transfer coefficient k_m is defined by the following relation, using the membrane structure properties:

$$k_m = \frac{D_g \times \varepsilon_m}{\tau_m \times l_m} \,, \quad \text{(Mavroudi et al., 2006) [4]}$$

Where:

- k_m : Mass transfer coefficient in the membrane ($m.s^{-1}$).
- D_g : Diffusion coefficient in the gas phase ($m^2.s^{-1}$)
- ε_m: Membrane porosity (dimensionless)
- τ_m : Membrane tortuosity (dimensionless)
- l_m : Membrane thickness (m)

3.2.3. Molar flux

The molar flux of the compound of interest (i.e. here the ozone) at the gas side can be expressed by:

$$\boldsymbol{J_i = k_g \times \left(C_{i,gas} - C_{i,gas,interface}\right)}, \quad \text{(Berry et al., 2017) [5]}$$

Where:

- J_i : Molar flux of the compound of interest across the membrane ($mol.m^{-2}.s^{-1}$)
- k_g: Mass transfer coefficient in the gas ($m.s^{-1}$).
- $C_{i,gas,interface}$: Concentration of the compound of interest at the interface on the gas side ($mol.m^{-3}$)
- $C_{i,gas}$: Concentration of the compound of interest in the gas bulk ($mol.m^{-3}$)

The molar flux across the membrane can be described by:

$$\boldsymbol{J_i = k_m \times \left(C_{i,gas,membrane} - C_{i,gas,interface}\right)}, \quad \text{(Berry et al., 2017) [6]}$$

Where:

- $C_{i,gas,membrane}$: Concentration at the gas-membrane interface ($mol.m^{-3}$), which can described by $C_{i,gas,membrane} = C_{,I,gas,interface}/S$, where S is the solubility of the gas in the membrane. Some studies assumed that $C_{i,gas,membrane}=C_{i,gas}$ (i.e. the concentration at the gas-membrane interface) is continuous (Pines et al., 2005; Shen et al., 1990).
- $C_{i,gas,interface}$: Concentration at the membrane-liquid interface on the membrane side ($mol.m^{-3}$), which can described by $C_{i,gas,interface}=C_{i,liquid,interface}$ x He, where He is the Henry's law constant (dimensionless, as described in [7]) and $C_{i,liquid,interface}$ is the concentration at the membrane-liquid interface on the liquid side.

The molar flux at the liquid phase side is described in the following equation.

$$\boldsymbol{J_i = k_L \times \left(C_{i,liquid,interface} - C_{i,liquid}\right)}, \quad \text{(Berry et al., 2017) [8]}$$

Where:

- k_L: Mass transfer coefficient in the liquid ($m.s^{-1}$)
- $C_{i,liquid,interface}$: Concentration of the compound of interest at the interface on the liquid side ($mol.m^{-3}$)
- $C_{i,liquid}$: Concentration of the compound of interest in the liquid bulk ($mol.m^{-3}$)

Therefore, thanks to the previous equations, the following formula can be used to express the molar flux from the overall mass transfer coefficient (Berry et al., 2017).

$$\boldsymbol{J_i = K_L \times \left(\frac{C_{i,gas}}{S_{g,m}} - H \times C_{i,liquid}\right)}, \text{ [9]}$$

Where K_L is the overall mass transfer coefficient ($m.s^{-1}$) described in the following section (see 3.2.4), H is the partition coefficient of the gas in the liquid (dimensionless), and $S_{g,m}$ is the solubility of the gas in the membrane (dimensionless).

The mass balance on the liquid phase for steady state conditions can be described by:

$$\boldsymbol{\frac{dC_{i,liquid}}{dx} = \frac{1}{u_{L,mean}} K_L a \times \left(\frac{C_{i,gas}}{S_{g,m}} - H \times C_{i,liquid}\right)}, \text{ (Berry et al., 2017) [10]}$$

Where:

- a : Surface area of membrane per volume of liquid ($m^2.m^{-3}$)
- x : Direction of the flow (m)
- $u_{L,mean}$: Mean liquid velocity ($m.s^{-1}$)

Integrating the previous equation leads to the following relation, allowing the calculation of the theoretical K_La. The boundary conditions are such that the concentration of the compound of interest (i.e. the ozone) at the liquid inlet (i.e. x=0) is zero, and is equal to $C_{i,liquid,out}$ at the liquid outlet (i.e. x=L, representing the membrane length):

$$\boldsymbol{\frac{K_L a.L}{u_{L,mean}} = \frac{1}{H} ln\left(\frac{\frac{C_{i,gas}}{S}}{C_{i,gas} - H \times C_{i,liquid,out}}\right)}, \text{ [11]}$$

3.2.4. The overall mass transfer coefficient

The total resistance can be described by the resistance in series model, by analogy to Ohm's Law:

$$\boldsymbol{\frac{1}{K_L \times A_{outer}} = \frac{1}{S_{g,m} \times k_g \times A_{inner}} + \frac{1}{k_m \times A_m} + \frac{H}{k_L \times A_{outer}}}, \text{ (Berry et al., 2017) [12]}$$

Where:

- K_L : Overall mass transfer coefficient ($m.s^{-1}$)
- k_m, k_g, k_L: Mass transfer coefficient, respectively in the membrane, in the gas, and in the liquid ($m.s^{-1}$). When a chemical reaction occurs in the liquid, k_L can be replaced with $k_L = \frac{k_L^r}{E}$ such as $E = \frac{J_{O3} \text{ with reaction}}{J_{O3} \text{ without reaction}}$. E is called the enhancement factor and takes into account the effect of the reaction, which increases the concentration gradient and therefore the transfer speed at the interface (see Figure 5) (Nguyen, 2018). E can also be described in terms of Hatta number and instantaneous enhancement factor.
- A_{outer}, A_m, A_{inner}: Respectively the outer, logarithmic mean, and inner surface of the membrane (m^2)
- S: Solubility (e.g. of ozone) in the membrane material (dimensionless)
- H: Partition coefficient (e.g. of ozone) in water (dimensionless). He can be described by the following equation.

$$\boldsymbol{H} = \frac{\mathbf{1}}{\boldsymbol{\alpha}} = \left(\frac{C_{O3,G}}{C_{O3,L}}\right)_{eq}, \text{ (Roustan, 2003) [13]}$$

This equation is one form of the Henry's law. For the dissolution of ozone in water at 295K, the Henry's constant is 3.823 (mg/L)/(mg/L) (Atchariyawut et al., 2009). At 293K, this same constant is reduced to 2.907 (Roustan, 2003).

For hollow fibers membranes where the gas flows inside the fibers and the liquid outside, the previous equation becomes $\frac{1}{K_L} = \frac{d_o}{S_{g,m} \times k_g \times d_i} + \frac{d_o}{k_m \times d_{ln}} + \frac{H}{k_L}$, where d_i, d_{ln}, d_o are respectively the inner, logarithmic mean, and outer diameters of the fibers (m).

4. Membrane materials

4.1. Membrane materials for gas/liquid membrane contactors

4.1.1. Microporous/dense membrane

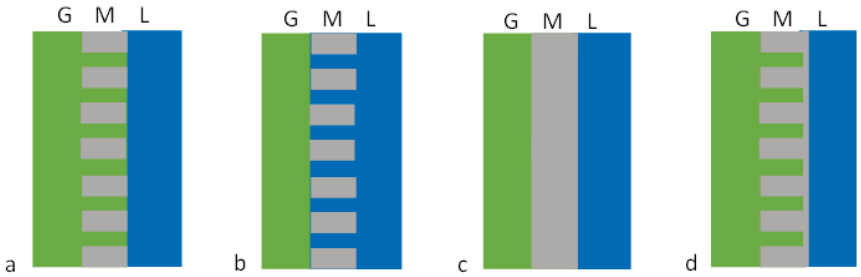

Figure 6. Membrane configurations (a. non-wetted porous membrane, b. wetted porous membrane, c. dense membrane, d. composite membrane), adapted from Nguyen et al., 2011.

The material of the membrane affects its performance and has to be chosen according to its application. Properties of the membrane, especially the pore size and the surface porosity, influence the transfer rate. Membranes can be classified in 3 categories: dense, porous, or composite (see Figure 6). According to Bakeri et al., the higher the pore size is, the higher the membrane mass transfer coefficient is (i.e. resistance within membrane is higher in dense membrane than in microporous) (Bakeri et al., 2012). Yet, higher pores increase the risk of wetting, which reduces the transfer quickly (Bakeri et al., 2012). Therefore, the operating pressure can be higher with dense membrane than with microporous because no bubbles are formed (i.e. no risk of bubbling). However, during their experiments, Pines et al. found a global mass transfer coefficient comparable between a Teflon nonporous membrane (i.e. a dense membrane) and different porous membranes (see Figure 7). The porous membranes used in this work were made with Teflon, PVDF, or PTFE. The pore volume was from 45 up to 55%. The pore size was from 0.5 up to 5 µm, and membrane thickness from 0.102 to 0.254 mm. (Pines et al., 2005)

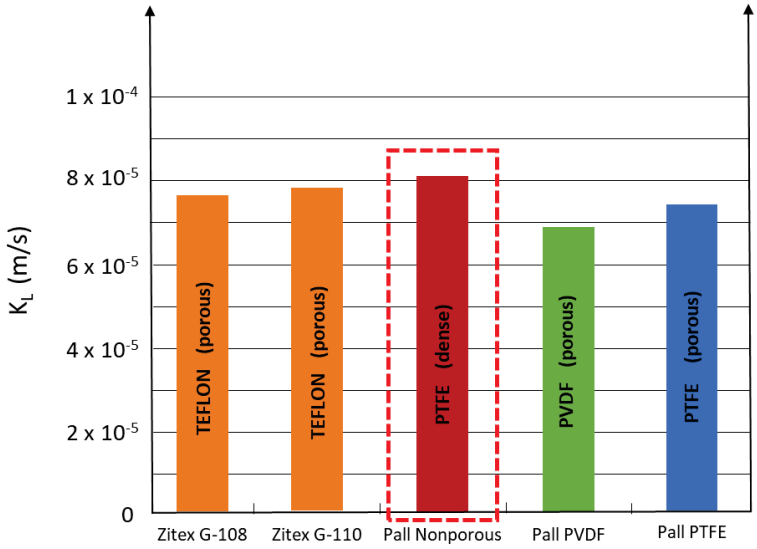

Figure 7. Global mass transfer coefficient at liquid side Reynolds number of 2000 for different materials, adapted from Pines et al., 2005.

According to Nguyen et al., a dense material can compete with classical porous membrane contactors materials, depending on the dense skin thickness (i.e. it can have the same mass transfer coefficient in the membrane) (see Figure 8). In their work, the authors highlighted the interest of composite fibers for the CO_2 absorption. The fibers were fabricated from porous polymers as supports and coated with dense permeable (here to CO_2) materials. The use of a dense or a composite membrane seems therefore to be a possible solution to avoid bubbling and wetting problems (i.e. transmembrane pressure limitations), without minimizing the global mass transfer. (Chabanon and Favre, 2017; Nguyen et al., 2011)

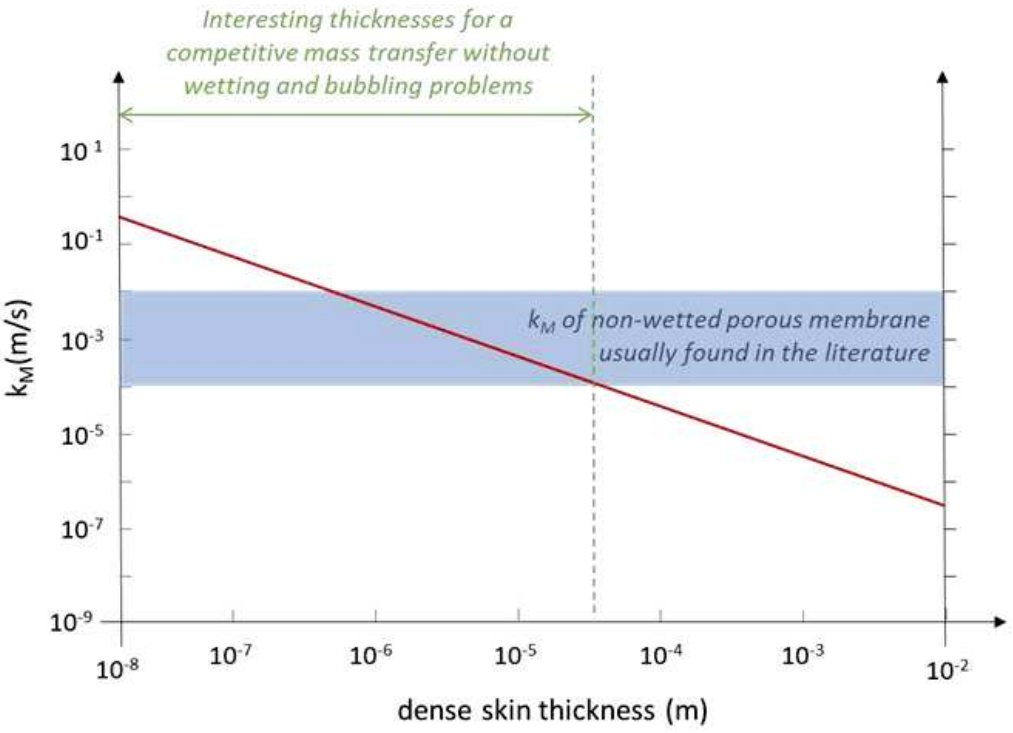

Figure 8. Effective mass transfer coefficient of a dense skin layer versus the layer thickness for a polymer permeability of 500 Barrer, adapted from Nguyen et al., 2011.

4.1.2. Advantages and disadvantages of organic membranes used in membrane contactor

Table 2 summarizes the advantages and disadvantages of various organic materials which can be used for membrane contactor.

Table 2. Synthesis of the different organic materials used in membrane contactors (* Material resistant towards ozone).

Family	*Material (Abbreviation)*	*Characteristics*	*Advantages*	*Disadvantages*	*Sources*
Polyolefins and fluoropolymers	Polyvinylidene fluoride **(PVDF*)**	Hydrophobic. Semi-crystalline (4 different crystalline forms with for each different mechanical and chemical resistances). Less hydrophobic than PTFE, but more hydrophobic than the other materials presented here. Degradation temperature between 375 and 400°C, and thus appropriate for water treatment.	Thermal stability, resistant to most of the corrosive chemicals and organic compounds. More resistant to ozone than PP. Better ozone flux than with PTFE for a same Reynolds number (liquid), but lower flux at long-term (after a couple of hours).	Sensitive to adsorption	(Bamperng et al., 2010; Khaisri et al., 2009; Khayet and Matsuura, 2001; Mori et al., 1998)
	Polytetrafluoroethylene **(PTFE*)**	Hydrophobic (contact angle between water and membrane at 110° for a PTFE dense film). More hydrophobic than PVDF.	High thermal and chemical stability (resistant to solvents and oxidizers). More resistant to ozone than PVDF.		(Khaisri et al., 2009; Mori et al., 1998)
	Polyethylene **(PE)**	Hydrophobic	High thermal and chemical stability (resistant to solvents and oxidizers)		(deMontigny et al., 2006; Drioli et al., 2006)
	Polypropylene **(PP)**				
Polysulfones	Polyether sulfone **(PES)**	Less hydrophilic than cellulose acetate Contact angle between water and membrane at 73°	High thermal and chemical stability, stable at a wide range of pH values, resistant to chlorine.	Risk of fouling by adsorption	(Drioli et al., 2006)
	Polysulfone **(PSu)**				(Zhang et al., 1989)
Cellulose and its chemical derivatives	Cellulose acetate (di or tri) **(CA)**	Hydrophilic	Low fouling, high permeability to water, good selectivity.	Low thermal and chemical stability	(Mark, 1999; Zhang et al., 1989)

4.2. Membrane materials used for ozonation with membrane contactors

4.2.1. Organic/inorganic membrane

Organic membranes are made with polymers. They are often used because of the possibility to modulate their intrinsic properties (e.g. mechanical, thermal, selectivity, etc). These membranes can be prepared by sintering, stretching, track-etching, phase inversion, or other ways. A material often used with ozone is for instance the PVDF (i.e. polyvinylidene fluoride) (Atchariyawut et al., 2007; Bamperng et al., 2010; Jansen et al., 2005; Khaisri et al., 2009; Leiknes et al., 2005; Pines et al., 2005).

Inorganic membranes are made with ceramic, metals, glass, or zeolite. They can be porous (e.g. ceramic) or dense (e.g. made with metals or glass). Ceramics are the major class of inorganic membranes. These membranes are prepared by mixing a metal (e.g. aluminium, titanium, silicium, zirconium) with a non-metal (i.e. nitride, oxide, or carbide). They are prepared by sintering or sol-gel processes, and have a great thermal, chemical, and mechanical stability (Mulder, 1996). Membranes can also be hybrid (i.e. composed with both organic and inorganic materials).

Ceramic membranes could be a good alternative for membrane contactors in comparison to organic membranes because of their chemical, thermal, and mechanical stabilities. They seem therefore to be an appropriate material for the use of ozone, which is a strong oxidant. However, those membranes have hydrophilic properties due to the presence of hydroxyl groups on their surface, and thus water is able to penetrate in their pores resulting in a higher mass transfer resistance (Bamperng et al., 2010; Stylianou et al., 2016). Consequently, ceramic membranes have a lower mass transfer coefficient compared to hydrophobic organic membranes. The surface of ceramic membranes can be modified by grafting hydrophobic compounds in order to solve this problem. The ozone mass transfer of such membranes may be 5 times higher than non-grafted ceramic membranes (Picard et al., 2001). In the experiments of Kukuzaki et al., the authors used shirasu porous glass (i.e. as membrane), coated with nonafluorohexyltrichlorosilane (i.e. a highly hydrophobic compound). The ozone mass transfer coefficient of these membranes was higher than the one of non-coated membranes (i.e. the overall mass transfer coefficient was about 10^{-6} m/s for the hydrophilic non-coated membranes and about 10^{-5} m/s for the hydrophobic coated membranes) (Kukuzaki et al., 2010).

Other disadvantages of ceramic membranes have to be considered. Ceramic membranes have a higher cost than polymeric counterparts (i.e. ≥ \$1,000 /m² versus \$100/m², respectively for the ceramic versus the polymeric membrane material), due to higher production costs and expensive starting materials (Amin et al., 2016; Ciora and Liu, 2003). However, the membrane performance stability can be assured because of a higher cleaning efficiency with harsh chemical if necessary (thanks to better chemical and

thermal resistances). Therefore, ceramic membranes have less fouling propensity, and thus a longer operational life, making the cost of ceramic membranes more competitive (Ciora and Liu, 2003; Guerra and Pellegrino, 2013).

Moreover, another drawback is the higher inner diameter of the ceramic in comparison to polymeric membranes, leading to a lower surface area per unit volume. Tubular membranes (i.e. internal diameter between 5 mm and 15 mm) and capillary membranes (i.e. internal diameter between 0.5 mm and 5 mm) can be produced with ceramic materials, but hollow fibers (i.e. internal diameter < 0.5 mm) are tougher to obtain, unlike with polymeric materials (Amin et al., 2016).

4.2.2. Hydrophobic/hydrophilic membrane

As explained before, pores are filled with liquid in hydrophilic membranes while they are filled with gas using a hydrophobic membrane. Ozone and oxygen diffusion are higher in gas than in water, thus the membrane resistance is lower with a hydrophobic membrane. However, wetting and condensation problems may occur, unlike with hydrophilic membrane.

4.2.3. Sustainability

The sustainability of membrane material under highly reactive character of ozone is one of the main challenges of using a membrane contactor for ozonation.

Bamperng et al. compared a membrane contactor with PVDF material to a membrane contactor with PTFE material, for the ozonation of dye wastewater. They found that PTFE has a better sustainability because its performance was barely reduced, while PVDF lost 30% of its initial performance within a few hours (Bamperng et al., 2010). Dos Santos et al. investigated the resistance to ozone oxidation of organic (i.e. polymeric) membranes in order to select the best material to use in ozonation process for water treatment. The authors showed that materials with electrophilic atoms attached to the carbon in the polymer backbone (e.g. PVDF and PTFE) have a good resistance to ozone. They observed that membranes with single C-C or Si-C bonds (e.g. PP and PDMS) also have a good resistance to ozone but showed structural modifications after a long period of use. Lastly, materials with carbon-carbon double bonds (e.g. PEI and PES) were highly degraded (Alves dos Santos et al., 2015).

5. Ozonation using membrane contactors

In this review, experiments using oxygen as gas (instead of ozone) have also been taken into account as oxygen and ozone are oxidizing gas, and have a relatively similar behavior.

5.1. Transmembrane operating pressure (TMP) using membrane as gas/liquid contactor

If the pressure of the liquid is too high, membrane could be wetted (i.e. the liquid phase penetrates into the membrane pores and the membrane loses its hydrophobicity), creating a stagnant film which interferes with the transfer. The transfer is therefore better when the gas/liquid interface is kept at the membrane surface. Moreover, ozone diffusivity is better inside the gas than inside the liquid, and thus ozone transfer is promoted when the interface is located on the liquid side of the membrane. It highlights the importance of the material used, especially its hydrophobicity (Goh et al., 2019; Picard et al., 2001; Xu et al., 2019).

Picard et al. quantified the influence of the membrane's humidity. The authors studied the drying time of wet membranes before an experiment, and made a correlation with the transfer rates obtained. They concluded that water inside the membrane pores is a major limiting factor to the transfer (Picard et al., 2001). The maximum pressure to avoid this phenomenon is called the breakthrough transmembrane pressure, or the liquid entry pressure of water (LEPw), or the wetting pressure (Khayet and Matsuura, 2001; Smolders and Franken, 1989). It is defined by Laplace equation such as $LEPw = -\frac{B\gamma_L}{d_{pore,max}}$, with $d_{pore,max}$ the diameter of the largest pore, B the form factor of the pore, and γ_L the superficial tension of the liquid (Xu et al., 2019). In order to determine the LEPw of a membrane, the method described by Smolders and Franken can be used (Smolders and Franken, 1989; Khayet and Matsuura, 2001). This consists of applying a slight pressure in the liquid phase of about 0.3 x 10^5 Pa, during at least 10min. Then, the pressure is increased by step of 0.68 x 10^3 Pa. The LEPw is reached when a continuous flow is observed in the permeate side (i.e. in the gas phase).

The liquid pressure has to be higher than the gas pressure, in order to avoid bubbling (i.e. cross of bubbles in the liquid side), but lower than the breakthrough transmembrane pressure. This TMP depends on the membrane pore size: small pores allow higher pressure. For instance, microporous membranes have a breakthrough transmembrane pressure of about 20 kPa. (Fang et al., 2004)

5.2. Effect of several parameters on mass transfer

5.2.1. Effect of liquid velocity

Ozone flux increases with increasing liquid velocity (Atchariyawut et al., 2009; Bamperng et al., 2010; Pines et al., 2005; Stylianou et al., 2016; Zoumpouli et al., 2018). In the experiments of Atchariyawut et al., Bamperng et al., Pines et al., Stylianou et al., and Zoumpouli et al., ozone flowed through the shell side and the liquid through the tube side (i.e. inside the fibers). Ozone flux was calculated from a mass balance in the gas phase or in the liquid phase. Concentration gradient is the driving force for the ozone transfer into the membrane. When the liquid flow velocity increased, the resistance to ozone transfer at the interface between the gas and liquid phases decreased (i.e. the liquid mass transfer coefficient kL increases). The concentration difference was maintained high and thus higher ozone flux could be transferred. This trend was demonstrated for both porous and non-porous membranes. According to Zoumpouli et al., liquid flow velocity is the dominant parameter for ozone transfer, followed by membrane thickness and ozone gas concentration (Zoumpouli et al., 2018). However, it must be noticed that in these experiments, the impact of other parameters (e.g. the pH) was not investigated.

For practical applications, it seems interesting to keep a high liquid velocity to have a high mass transfer and to keep important shear forces at the surface of the membrane that could decrease a possible fouling. However, higher liquid velocity implies lower residence time. For many applications, it is important to reach a given value of dissolved ozone concentration in order to get sufficient kinetic reaction or good disinfection level. As a consequence, a compromise between high liquid velocity (i.e. high transfer) and high dissolved ozone concentration should be found.

5.2.2. Effect of gas

5.2.2.1. Gas velocity

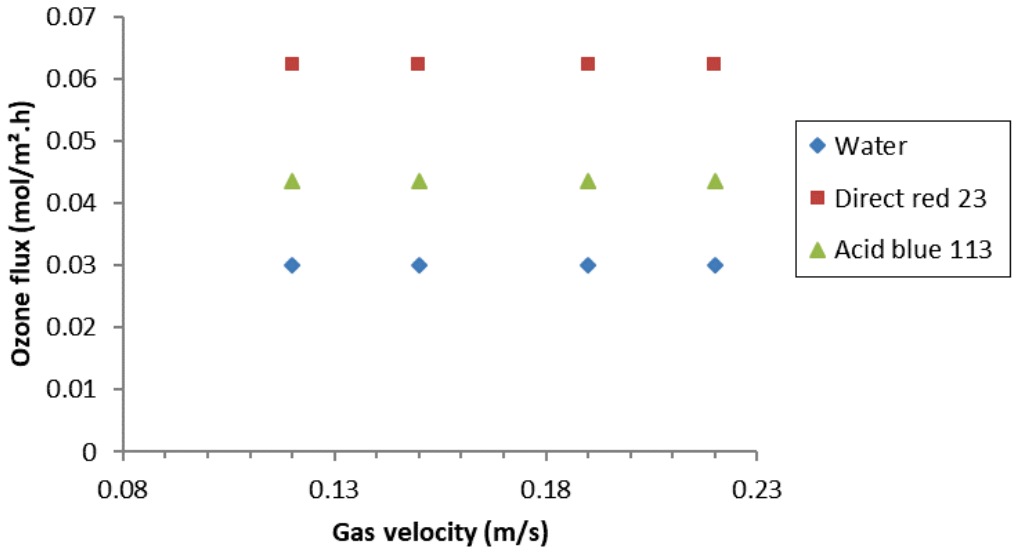

Figure 9: Ozone molar transfer flux as function of gas flow velocities with PVDF membrane at T=28°C, liquid phase velocity = 0,46 m/s, and initial dye concentration = 100 mg/L, adapted from Bamperng et al., 2010

Ozone flux is not influenced by gas velocity. The work of Bamperng et al (see Figure 9) showed that when gas velocity increases, ozone flux is not impacted (Bamperng et al., 2010). These experiments were made using water, direct red 23, and acid blue 113 (i.e. two dyes) and with a hollow fiber polyvinylidenefluoride (PVDF) membrane module. The ozone was produced with ozone generator by pure oxygen. The gas velocity varied between 0.12 and 0.22 m/s, and the ozone concentration was 40 mg/L. The liquid phase velocity was set at 0.46 m/s and the initial dye concentration was set as 100 mg/L. The ozone fluxes for pure water were determined by mass balance in the liquid phase, and the ozone fluxes for dye solution by mass balance in the gas phase. Results showed that for both water and dye solution (i.e. the liquid phase), the ozone flux did not evolve with an increasing gas velocity.

As seen previously (5.2), ozone flux is influenced by liquid velocity, therefore the mass transfer resistance is in the liquid phase, and not in the gas phase (Atchariyawut et al., 2009, 2007; Bamperng et al., 2010; Berry et al., 2017; Khaisri et al., 2009). In addition, Pines et al. found that the resistance is higher in the liquid film than in the membrane (Pines et al., 2005).

5.2.2.2. Nature of the gas

According to Berry et al., unlike ozone, the mass transfer resistance of oxygen is located in the membrane (Schwarzenbach et al., 2006). Côté et al. showed that oxygen mass transfer coefficient was better with pure oxygen than with air (Côté et al., 1989). According to the authors, this difference in transfer comes from the formation of nitrogen bubbles (i.e. with air), which strip the oxygen. The bubbles are formed against the fibers, and then escape to the liquid side and its outside in the form of gas, since the water is initially saturated with nitrogen at atmospheric pressure. Thus, the mass transfer in a membrane contactor depends on the nature of the gas. These results were obtained with gas inside the fibers and liquid in the shell.

5.2.2.3. Concentration in the gas

When the concentration of ozone in the gas increases, the dissolved ozone concentration measured at the outlet of the contactor in the liquid phase also increases. Stylaniou et al. obtained the results represented in the Figure 10, at a liquid temperature of 20°C, with a hydrophobically modified α-Al_2O_3 ceramic membrane (Stylianou et al., 2016). It is important to note that the membrane used was tubular, which implies a larger diameter than with hollow fibers (see 4.2.1). The ozone concentration was measured with potassium iodide method. The authors made the same experiments for different temperatures (i.e. 15, 25, 30 and 30°C), with different concentrations (i.e. 20, 40 and 60 mg/L). All the plots present the same trend as seen in the Figure 10.

The concentration of a compound (e.g. ozone or oxygen) at the interface between gas and liquid is linked to its partial pressure by Henry's law (see 3.2.1) with respect to its concentration in the gas phase (i.e., $C_{interface} = \frac{C_{O3,gas}}{H}$ where H is the dimensionless partition coefficient for ozone (Stylianou et al., 2016)). Therefore, when the concentration in the inlet gas increases, partial pressure also increases. According to the results of Stylaniou presented previously, the increase of partial pressure should raise the same way.

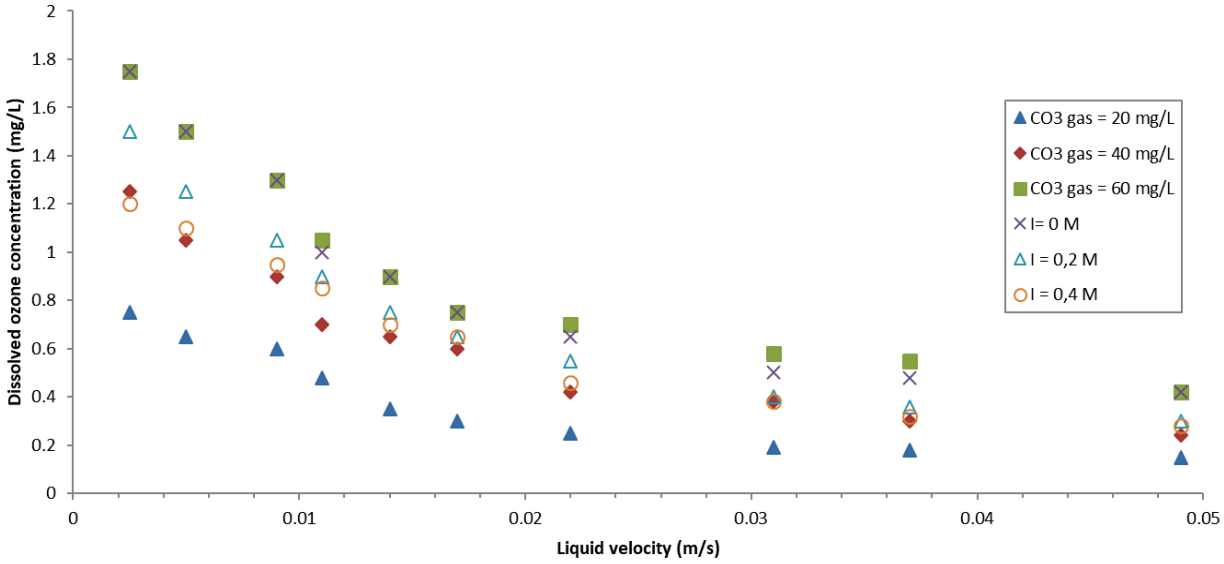

Figure 10. Dissolved ozone concentration at the outlet of the contactor for different ozone concentration in gas phase and for several ionic strengths, in function of liquid velocity, at 20°C, adapted from Stylianou et al., 2016.

5.2.2.4. Operating gas pressure and oxidant partial pressure

In the experiments of Côté et al. with dense hollow fiber membranes, the global mass coefficient K is independent of oxygen partial pressure up to 3 bar (K=28.3 x 10^{-6} m.s^{-1}) (Côté et al., 1989). However, at higher pressure, K dropped to 23.3 x 10^{-6} m.s^{-1}. Côté explained this drop with the apparition of micro-bubbles on the surface of the fibers. This phenomenon could be avoided with a higher water velocity, preventing the partial pressure from exceeding the saturation point. In contrast, Ahmed et al. showed in their studies that the mass transfer coefficient K increases with increasing operating pressure (Ahmed et al., 2004). The same result was obtained in previous studies (Ahmed and Semmens, 1992a, 1992b; Li et al., 2010). Li et al. found that, for hydrophilic treated polypropylene hollow fiber membranes, when the operating pressures increases from 20 to 100 kPa, the membrane resistance decreased almost linearly from 8.8 x 10^{-4} to 4.6 x 10^{-4} s.m^{-1}(i.d 1/K), giving a higher oxygen flux due to the higher partial pressure of oxygen (Li et al., 2010). These results go against Côté's conclusions. However, the same ultimate pressure beyond which bubbles appear was mentioned. It represents one of the limits of this process.

5.2.3. Effect of temperature

The experiments of Stylaniou et al. showed that temperature has a very little impact on the dissolved ozone concentration, compared to the influence of liquid velocity, pH, and ozone concentration values in the gas phase (Stylianou et al., 2016). However, temperature affects ozone diffusivity, decomposition rate constant, and ozone solubility in the water. At the interface, Henry's law is applicable (see 3.2.1), which depends on the temperature (Sotelo et al., 1989). When the temperature increases, water molecules have a greater mobility, and thus the viscosity of water decreases and its diffusivity increases (by around 1.2 times every 5°C according to Stylaniou et al.). As a consequence, the mass transfer coefficient in the liquid phase raises. In the same way, when the temperature increases, lower energy is required for the reaction between ozone and hydroxyl ions, and thus the ozone decomposition rate increases (by around 1.5 times every 5°C). Conversely, ozone equilibrium concentration decreases (by around 1.15 times) due to the decrease of gas solubility. Therefore, it seems important to take this factor into account.

5.2.4. Effect of transfer direction

The majority of the studies about ozonation using a membrane contactor use the gas in the shell side and the liquid inside the fibers. The main advantage of this configuration is a good distribution of the dissolved ozone in the liquid, thus allowing a good treatment of the pollutants. However, this configuration is more favorable to clogging. The circulation of the liquid in the shell side greatly reduces this risk. Nevertheless, a risk of short circuit in the shell appears, and therefore this configuration promotes the formation of areas without dissolved ozone, in which the pollutants are not treated (i.e. there is a risk of mal-distribution of the dissolved ozone and of channeling of the water in the carter (Dindore et al., 2005). According to Wenten et al., the best configuration for iodide ozonation with a membrane contactor is the one illustrated in the Figure 11 where the gas (ozone) passes through the tube side (i.e. inside the fibers) and the liquid (acidic iodide) solution passes through the shell side (Wenten et al., 2012). It corresponds to the configuration where the higher iodine concentration is obtained at the outside of the system (i.e. the objective was to oxidize iodide into iodine). In their study and for this configuration, the highest iodine concentration reached 300 mg/L, after a contact time of 720s. For the other configuration, where the ozone was flowing in the shell side, the highest concentration reached 35 mg/L, after a contact time of 1800s. According to the authors, the difference between the two results can be explained by the reaction of the ozone with the membrane material when the gas was running in the shell side. It causes the transformation of the ozone into oxygen, which reacts very slowly with iodide.

Figure 11. Configuration of membrane contactor with internal/external ozone transfer.

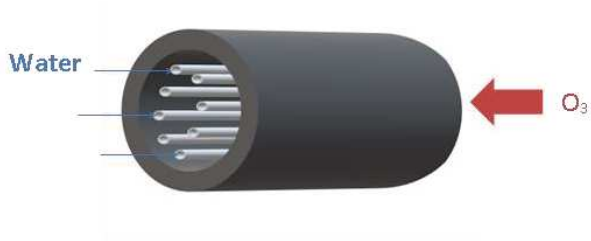

Figure 12. Configuration of membrane contactor with external/internal ozone transfer.

5.2.5. Effect of chemical reaction

When the liquid used in the contactor is pure water, no chemical reaction takes place. In the experiments of Stylaniou et al., ozone flux is lower with pure water than with surface water (Stylianou et al., 2016). It can be explained by the concentration gradient, which is maintained higher when ozone reacts with surface water, and in this case with micropollutants. According to Roustan et al., with hollow fiber organic membrane, the mass transfer coefficient of oxygen K_La is 6 times higher with fast reaction time in the liquid than without (i.e. 0.240 s^{-1} for 0.040 s^{-1} without) (Roustan, 2003). Therefore, the oxygen mass transfer is also 6 times higher with fast reaction than without. This is reflected in the mass transfer model with the several dimensionless numbers. The first one is the Hatta's number. It gives information on the competition between reaction and diffusion speed, inside the liquid film. It also indicates where the chemical reaction takes place. For a second order reaction (see 2.1, this number is defined by $\boldsymbol{Ha} = \frac{\sqrt{\boldsymbol{k_{O3} C_{i,liquid} D_{O3,L}}}}{\boldsymbol{k_L}}$, where $D_{O3,L}$ is the diffusivity of ozone in liquid phase ($m^2.s^{-1}$), $C_{i,liquid}$ is the concentration of the targeted compound in the liquid phase ($mol.m^{-3}$), k_L is the transfer coefficient in liquid phase ($m.s^{-1}$), and k_{O3} is the 2nd order reaction rate constant of ozone with the compound of interest ($m^3.\ mol^{-1}s^{-1}$). If Ha is small (i.e. Ha<0.3), the reaction is slow compared to the diffusion. If Ha is high (i.e. Ha>3), the reaction is fast compared to the diffusion.

The enhancement factor ($\boldsymbol{E} = \frac{\boldsymbol{Flux\ at\ the\ interface\ with\ chemical\ reaction}}{\boldsymbol{Flux\ at\ the\ interface\ without\ chemical\ reaction}}$) describes the importance of the chemical reaction on the mass transfer at the interface between the gas and liquid phase. If E=1, the reaction does not accelerate the transfer. If E>1, the reaction accelerates the transfer.

Another number is helpful to characterize the transfer, and to determine the material which reacted in the liquid film: the M criterion, such as: $M = \frac{Flux\ between\ liquid\ film\ and\ bulk\ of\ liquid}{Flux\ at\ the\ interface\ between\ gas\ and\ liquid}$. When M=1, all the compound quantity transferred from the gas phase to the liquid phase is also transferred to the bulk of liquid. Therefore, the chemical reaction only takes place in the bulk of liquid and the reaction does not accelerate the mass transfer (i.e. E=1 and Ha<0.3). The concentration profile of the compound in the liquid film is linear. When M<1, the reaction takes place in both liquid film and bulk of liquid, and thus reaction accelerates the transfer (i.e. E>1 and Ha between 0.3 and 3). When M=0, all the compound in the liquid phase reacts in the film. No molecule reaches the bulk of liquid. The reaction accelerates the transfer (i.e. E>1 and Ha>3).

5.2.6. Effect of pH

According to Wenten et al., pH of the liquid phase does not have a significant impact on the ozonation of iodide into iodine (Wenten et al., 2012). However, several studies revealed the opposite (Bamperng et al., 2010; Stylianou et al., 2016). Free radicals mechanisms are promoted with increasing pH and ozone decomposition is faster due to the presence of hydroxide anions. Therefore, ozone resistant compounds may react by indirect reaction thanks to the formation of hydroxyl radicals, which are non-selective oxidants. Simultaneously, ozone decomposition at higher pH keeps the ozone concentration gradient higher, and thus promotes the flux through the membrane. In their experiments on dye solutions, Bamperng et al. showed that the higher the pH solution was, the higher the ozone flux was (Bamperng et al., 2010). In the study of Stylaniou et al., the reaction rate constant increased with the pH increase (see Table 3) (Stylianou et al., 2016).

Table 3. Influence of pH on reaction order and rate constant of ozone decomposition at 20°C, adapted from Stylianou et al., 2016.

pH	Reaction order n	Rate constant of ozone decomposition K' ($1.s^{-1}\cdot(L/mg)^{(n-1)}$) (±5%)
4	2	0,0017
6	2	0,0049
9	1	0,624

5.2.7. Effect of ionic strength

Stylaniou et al. investigated the effect of ionic strength on ozone flux (Stylianou et al., 2016). Ionic strength was adjusted by the addition of NaCl solution. The authors made the same experiments for

different temperatures (i.e. 15, 25, 30 and 30°C), with different concentrations (i.e. 0, 0.2 and 0.4 M). All the plots present the same trend as in the Figure 10, where the dissolved ozone concentration at the outlet of the contactor decreases when the liquid velocity increases. Zero ionic strength corresponds to the use of deionized water without the addition of NaCl.

An increase of ionic strength decreases the solubility of ozone and thus also decreases the equilibrium concentration of ozone at the interface between gas and liquid, as described by Henry's law (see 3.2.1). The ionic strength has also an impact on the surface tension, and thus on the allowable transmembrane pressure. Indeed, dissolved salts increase the surface tension, and in the same way the breakthrough pressure.

5.2.8. Effect of surfactant

Côté et al. studied the impact of surfactant in liquid phase on the oxygen flux (Côté et al., 1989). For these experiments, commercial soap containing 3.2% by weight of anionic surfactant was added to the initial deoxygenated water. It appeared that the addition of soap increased the mass transfer coefficient (i.e. 7% for a liquid velocity of 2.28 cm/s and 20% for a velocity of 7.71 cm/s). According to the authors, it is a significant parameter because the amount added (i.e. 190.5 mg/L) is equivalent to approximately 6 mg/L of surfactant (i.e. lauryl sulphate), which is a concentration often observed in wastewater (Boon, 1980).Surfactants have an impact on the surface tension, and thus on the allowable transmembrane pressure. Indeed, surfactants decrease the surface tension, and in the same way the breakthrough pressure. Therefore, the risk of wetting is higher.

5.2.9. Effect of membrane material

The membrane material has a significant role in the mass transfer efficiency. As mentioned above (see 3.1), membranes have to be porous in order to facilitate the transfer, and hydrophobic to avoid the wetting phenomenon, which leads to the formation of a stagnant film inside the membrane and thus to a reduced mass transfer. Ozone is a very strong oxidant, and thus can attack the membrane material if this one is not sufficiently resistant. For an application of ozonation with a membrane contactor, two materials stand out: the PVDF and the PTFE which are the only organic membranes that can be used with ozone. According to Bamperng et al., PTFE leads to a more stable and higher flux than PVDF for a long operation period (i.e. few hours of use) (Bamperng et al., 2010).

5.2.10. Summary table of the effect of parameters on mass transfer

Table 4. Effect of parameters on mass transfer.

Parameters	Range in literature	Influence on the ozone transfer when the parameter increases	Sources
Liquid velocity	0.002 - 0.9 m/s	+	(Atchariyawut et al., 2009; Bamperng et al., 2010; Pines et al., 2005; Stylianou et al., 2016; Zoumpouli et al., 2018)
Gas velocity	0.003 - 0.22 m/s	=	(Atchariyawut et al., 2009, 2007; Bamperng et al., 2010; Berry et al., 2017; Khaisri et al., 2009)
Concentration of O_3 in the gas	20 - 60 mg/L	+	(Stylianou et al., 2016)
Operating gas pressure	6.9 - 413.7 kPa	+	(Ahmed et al., 2004; Ahmed and Semmens, 1992a, 1992b; Li et al., 2010)
Temperature	15 - 50°C	+	(Stylianou et al., 2016)
pH	4 - 9	+	(Bamperng et al., 2010; Stylianou et al., 2016)
Ionic strength	0 - 0.4 mol/L	-	(Stylianou et al., 2016)
Surfactant	0 - 6 mg/L	+	(Côté et al., 1989)
Chemical reaction	With or Without (pure water)	+ (With)	(Stylianou et al., 2016)
Transfer direction	In/Out or Out/In	+ (In/Out)	(Wenten et al., 2012)

5.3. First results on micropollutants

During their experiments, Stylaniou et al. showed the technical feasibility of a membrane contactor for the removal of various micropollutants in surface waters with diffusion of ozone and peroxone (Stylianou et al., 2018). They studied the transformation of carbamazepine (CBZ), benzotriazole (BZT), p-chlorobenzoic acid (pCBA), atrazine (ATZ), and the formation of bromates in a ceramic tubular membrane contactor, where the gas was in the shell side. The CBZ was removed at more than 90%, with a diminution of its concentration below 0.1 µM at 0.4mgO_3/mgDOC. BTZ, pCBA, and ATZ was removed respectively at 70, 57, and 49%. The removal efficiency followed the reactivity order of the

compounds with O_3. The addition of peroxone reduced the elimination of CBZ by 8%, but increased the elimination of ozone-resistant compounds (i.e. pCBA and ATZ) by about 5-10%.

In order to make a comparison between the different contacting ozonation processes, batch experiments (i.e. conventional, prepared by continuously bubbling ozone and therefore O_3 saturated) and continuous experiments with ceramic tubular membranes having different inner surface per volume were performed. The results for the CBZ (i.e. the ozone reactive compound) were similar whatever the process. However, the hydroxyl radical exposure was slightly higher in the conventional experiments for ozone and peroxone processes, which leads to a better abatement of ozone-resistant compounds in the conventional process. Thus, the authors suggest that using a membrane with a high inner surface per volume, like for instance the hollow fibers, leads to a better efficiency of ozonation processes thanks to a more uniform distribution of oxidants (i.e. ozone and peroxone) in the water to be treated.

Concerning the bromate formation, Stylaniou and al. showed that ozone concentration lower than 20 mg/L are required to be under the regulated concentration limit of bromate (i.e. they did not achieve this limit even at a concentration of 0.020 mg/L, which was the lowest concentration used during their experiments). Indeed, European Commission and US EPA defined this limit at 10 µg/L in drinking water (EC directive 98/83; USEPA,1998). The ozone concentration is a very important parameter to minimize the formation of these compounds. In their experiments, Stylaniou et al. found a high bromate concentration of 49 µg/L at 0.8 mgO_3/mgDOC with the ozone process. In these experiments, comparing with conventional process, membrane processes led to a higher bromates' formation. To conclude, the authors suggest that the use of membrane contactor with both a low ozone gas concentration and the highest possible inner surface per volume are required to improve the micropollutants abatement and to reduce the bromates' formation.

Merle et al. worked on a combination of a membrane contactor with advanced oxidation process for the abatement of micropollutants and the minimization of the bromates' formation (Merle et al., 2017). The authors used PTFE hollow fiber membrane. The water flowed inside the fibers, and the gas inside the shell. They focused especially on bromates' production, and studied the abatement of pCBA because of its high reactivity with hydroxyl radicals and low reactivity with molecular ozone (i.e. ozone-resistant compound). Compared to the conventional peroxone process (i.e. with bubbles), this process showed a better abatement of micropollutants and less bromates formation, for groundwater and surface water treatment. For instance, for a groundwater containing 180 µg.L^{-1} of bromides and 0.48 mgDCO.L^{-1}, with a hydrogen peroxide concentration of 5.67 mgH_2O_2.L^{-1}, and an ozone concentration in the gas phase of 0.5 g.Nm^{-3}, an abatement of p-CBA of 95% was achieved after 300 s of residence

time, and less than 0.5 µg/L of bromates were produced. In the conventional process, 8 $\mu g.L^{-1}$ was formed under the same conditions. It can be noted that with a higher ozone concentration in the gas phase (i.e. 1 g/Nm^3, 2.5 g/Nm^3 and 10 g/Nm^3 in these experiments), the p-CBA abatement was better and faster, but more bromates were produced.

6. Modeling of ozone and oxygen mass transfer through membrane contactors for the elimination of micropollutants

Several studies have investigated the modeling of ozone and oxygen transport through membrane contactors during ozonation processes, from the gas phase to the liquid phase. Most of these works focused on applications such as CO_2 absorption, acid gas capture (i.e. gas-liquid absorption), or liquid-liquid extraction (Faiz et al., 2013; Zhang et al., 2014).

The modeling of such processes is useful for a better understanding of the physical and chemical phenomena occurring. It enables the evaluation of parameters' influence, and therefore can lead to an optimization of the modeled process. Before modeling, membrane ozonation was described through global mass transfer coefficients, and therefore could not be scaled-up to different devices or experimental conditions. (Kukuzaki et al., 2010; Stylianou et al., 2016). In addition, modelling can be used in design and optimization of cross-flow membrane modules for multi-components membrane gas absorption processes.

Several types of computational approaches can be seen for ozone transport simulation in membrane contactor processes. Three methods will be presented here. In the first one, dimensionless numbers are used (in particular the Sherwood number) and hypotheses are assumed in order to simplify the equations and to avoid a numerical resolution. In the second approach presented here, ozone concentrations are obtained from the partial pressures. In the last method, software like Comsol Multiphysics for example is used in order to solve the transfer equations and directly determine concentration profiles, by simulating the ozone mass transfer through a membrane into a liquid. A synthesis of several studies on this subject is available in Table 5.

Table 5. Synthesis of the studies about modelling of ozone diffusion with membrane contactors.

Publication	Modeling and determination of	Type of membrane	Investigated parameters
Ozone Mass Transfer Studies in a Hydrophobized Ceramic Membrane Contactor: Experiments and Analysis. (Stylianou et al., 2016)	Concentration of dissolved ozone at the module output	Tubular membrane Porous (Ceramic - Al_2O_3)	Liquid velocity Liquid pH Gas concentration Membrane length Temperature Order of the ozone decomposition reaction
Mass transfer studies in flat-sheet membrane contactor with ozonation (Phattaranawik et al., 2005)	Ozone transfer coefficient (developed indirectly from the oxygen transport) Ozone flux Ozone concentration at membrane/liquid interface	Plane membrane Porous (PVDF)	Flow rates Temperature Matrix for ozone flux determination (pure water/solution of sodium nitrite)
A single tube contactor for testing membrane ozonation (Zoumpouli et al., 2018)	Concentration profiles Transfer resistance Transfer coefficients Ozone flux Residual ozone concentration	Tubular membrane Non porous (PDMS)	Liquid velocity Matrix (pure water/surface water/waste water/solution with humic acid) Membrane diameter Gas concentration
Modeling of ozone mass transfer through non-porous membranes for water treatment (Berry et al., 2017)	Concentration profiles Transfer resistance Overall transfer coefficient	Non porous capillary membrane (PDMS)	Membrane length, Thickness membrane Liquid velocity Gas diffusivity in the membrane Gas solubility in the membrane

6.1. Development of a mass transfer model based on dimensionless numbers

Stylianou, Kostoglou, and Zouboulis studied the ozone mass transfer in a hydrophobized ceramic membrane contactor (Stylianou et al., 2016). The gas was a mixture of ozone and oxygen, and flowed in the shell of the contactor. The liquid was in the tube. Based on experiments, the authors developed a mathematical model, representing the occurring phenomena and extracting the most important parameters. A first step was to model only the mass transfer, without taking into account the enhancement factor due to ozone decomposition. The transfer was considered as a multiphase system with three steps: diffusion in gas phase, transfer through the membrane pores, and diffusion to water. This is therefore a convection-diffusion mechanism. Generally, the steady state partial differential conservation equation is solved in order to obtain the ozone mass transfer. However, the authors used the Leveque solution and the corresponding Sherwood number, since all the experimental conditions matched (e.g. laminar flow). The dissolved ozone concentration at the outlet of the contactor was then obtained thanks to a mass balance and the Sherwood number.

$$\boldsymbol{C_f = C_{eq} + (C_0 - C_{eq}) e^{-4LD_{O3,L}Sh / u_{L,mean} d_i^2}}, \quad [14]$$

With:

- C_f : Solute concentration at the tube outlet (mol.m^{-3})
- C_{eq}: Solubility of ozone in the liquid (C_{eq}= HP_f, where H is a variant of the Henry's law constant in mol.m^{-3}.hPa^{-1} and P_f the partial ozone pressure in hPa) (mol.m^{-3})
- C_0 : Feed ozone concentration (mol.m^{-3})
- L : Total tube length (m)
- $D_{O3,L}$: Diffusivity of ozone in the liquid phase (i.e. water) (m².s^{-1})
- Sh : Sherwood number of the liquid phase (Sh can be described by a global form such as $Sh = \frac{K_L L_c}{D} = A \times Re^B \times Sc^C$, where A, B, C are empirical constants, Sc is the Schmidt number, Re is the Reynolds number, Lc is the hydraulic diameter of the liquid phase, D is the diffusivity, and K_L is the overall mass transfer)
- $u_{L,mean}$: Mean liquid velocity (m.s^{-1})
- d_i : Internal diameter of the tube (m)

Then, the mass transfer model was completed with the ozone decomposition (i.e. a mass transfer and reaction model were defined). Generally, conservation equations (i.e. diffusion and convection terms), and reaction terms, are solved numerically. Transfer and reaction are assumed to occur

simultaneously. Transfer, as mentioned before, is assumed to follow Leveque relation, and reaction rate is assumed to depend on the cross-sectional averaged solute concentration. The governing equation for the perimeter averaged ozone concentration is described by the following equation:

$$\mathbf{u}_{L,mean}\frac{dC}{dz} = \frac{4DSh}{d^2}\left(C_{eq} - C\right) - r_M\ , \qquad [15]$$

By using the Euler explicit numerical discretization scheme with a fine mesh, for example with a discretization at N points with step such as δ=L/N, a set of differential equations results can be found easily.

For Reynolds numbers of the liquid side up to 100 (i.e. laminar regime), dissolved ozone concentration at the outlet of the membrane contactor calculated with the developed model fit well with the experimental results (deviation around 5%). Moreover, ozone properties (e.g. diffusivity, ozone equilibrium concentration, ozone self-decomposition order and rate) calculated from the model fit the experimental and theoretical data. The extrapolation of data for the study of different devices and experimental conditions is possible, by changing the value of major physical parameters (e.g. diffusivity, solubility). The authors also studied the influence of several parameters such as the liquid velocity, the pH, the gas concentration, the membrane length, and the temperature. They came to the conclusion that the pH and the ozone concentration have the greatest impact on the dissolved ozone concentration at the outlet of the contactor. Moreover, they noted that the ozone flux increased with the liquid velocity (i.e. with the Reynolds number).

6.2. Development of a mass transfer model by using transfer coefficient and partial pressures

The mass transport in a membrane contactor (i.e. across concentration boundary layer of gas phase, through porous membrane, and liquid boundary layer) can be described with global and individual mass transfer coefficients. In order to determine these coefficients, the resistance-in-series model can be used. Phattaranawik, Leiknes, and Pronks studied ozone mass transfer in porous flat-sheet membrane contactor, made with PVDF (Phattaranawik et al., 2005). The liquid side Reynolds numbers ranged from 454 to 1469 for the experiments with O_2, and to 1136 for the experiments with O_3, both corresponding to a laminar flow. To model mass transfer without reaction, the authors determined ozone mass transfer coefficients indirectly from oxygen transfer measurements to remove ozone decomposition and potential reactions in the liquid. The oxygen mass transfer coefficient in the liquid phase is correlated to Sherwood number and can be deducted from this correlation. It can also be calculated from the Wilson plot method, a method which is also valid for the determination of the membrane mass transfer coefficient. With this method, the liquid mass transfer and the membrane

mass transfer coefficients can be separated from the overall mass transfer coefficient. The authors focused on liquid mass transfer coefficient. They deduced this coefficient for the ozone from the oxygen coefficient, using in particular the surface renewal theory (see Equation 15).

$$k_{L,O3} = \left(\frac{D_{O3,L}}{D_{O2,L}}\right)^{0.5} \times k_{L,O2} = 0.789 \times k_{L,O2}\ ,$$ (Cussler, 2009) [15]

To model ozone mass transfer with a chemical reaction, an enhancement factor was added to the individual transfer coefficient of the liquid film. The global transfer coefficient is described by the equation [12].

The authors described the procedure followed for calculating ozone fluxes without chemical reaction (i.e. with pure water), and with chemical reaction (i.e. with sodium nitrite solutions). The procedure with pure water can be summarized in several main steps. First, the ozone flux is assumed and the effluent ozone concentrations in both gas and liquid streams are calculated by mass balance. The average ozone concentrations are then determined. The concentrations at both membrane surfaces, and the ozone partial pressures at the membrane surfaces are calculated, and the flux are deducted from these pressures. Finally, the new calculated flux is compared with the flux previously assumed. When the difference between the assumed and the calculated flux is smaller than 0.01%, the procedure is finished. If not, the calculated flux is the new assumed flux, and the procedure begins again (i.e. the loop begins again). With a chemical reaction, the procedure is more complex than without, due to the presence of oxidation. Phattaranawik at al. concluded that both procedures can be used to design the ozonation membrane contactor in pilot scale. However, the mathematical model should be refined with residual ozone concentration because of the authors' assumption of zero effluent ozone concentrations in the liquid stream.

6.3. Determination of concentration profiles with software for the resolution of transfer equations

Another approach is the numerical modeling thanks to Computational Fluid Dynamics (CFD) software (Berry et al., 2017; Zoumpouli et al., 2018). The steps of the CFD simulation set-up are described by Tu et al. (Tu et al., 2018). The first step is to define a domain (2-D or 3-D) and a geometry based on the studied membrane dimensions. For a gas/liquid membrane contactor, 3 domains can be defined: the gas phase, the membrane, the liquid phase. Then, the optimal mesh has to be chosen in order to obtain the best compromise between accuracy and computing time. The model can be scaled if necessary, and the convergence criteria have to be set, representing the acceptable residual after all the iterations. The next step is the specification of the governing equations (i.e. species and momentum

equations), and of the boundary conditions. The CFD software takes care to couple and solve these equations, and therefore concentration profiles are obtained (Berry et al., 2017) .

During their works, Berry et al. used Comsol Multiphysics ® in order to obtain concentration profiles. The simulation was made with the gas flowing inside the tube and the liquid outside, in a non-porous capillary membrane made with PDMS. The gas was pure oxygen or a mixture of ozone and oxygen. Variations from 3.5 to 2210 of the liquid side Reynolds number were performed, corresponding to a laminar flow. The regime was also laminar on the gas side. The equations solved by the software, and their application conditions, are synthetized in Table 6.

The model established by the authors resulted in the determination of the concentration profiles. It can be used as a base for the prediction of the ozone and oxygen transfer for various designs, materials, and hydraulic conditions. Sherwood numbers obtained with this model fit with those found in the literature (Berry et al., 2017) . The main conclusions are as follow. First, the gas solubility is a parameter which cannot be neglected, in particular for the oxygen. The main resistance of the ozone transfer is on the liquid side, and the main resistance of the oxygen transfer is in the membrane.

Zoumpouli et al. had a similar approach than Berry et al. (Zoumpouli et al., 2018). However, the configuration of the membrane contactor was different. The simulation was made with the liquid flowing inside the tube and the gas in the shell, in a non-porous tubular membrane made with PDMS. The gas studied was a mixture of ozone and oxygen. The effect of added peroxone (i.e. H_2O_2) in the liquid phase was also investigated. The liquid side Reynolds number was varied up to 290. For Reynolds numbers less than 100, the simulation results were moderately overpredicted, in comparison to experimental measures. This may be a result of a non-uniform dispersion of O_3 for low flowrates. For Reynolds numbers over 100, results obtained during the experiments fitted well with the simulation results, with an absolute difference lower than 0,5 mg/L. Their main conclusion is the importance of the liquid velocity as a major parameter for the determination of the ozone global transfer, followed, in that order, by the membrane length and the gas concentration.

Table 6. Governing equations of the mass transport used by Berry et al.

		Gas section (0 ≤ r ≤Ri)	*Membrane section (0 ≤ r ≤ Ri+Lm)*	*Liquid section (Ri+Lm≤ r ≤ Ri+Lm+Lw)*
Momentum transport	***Assumptions***	Ideal and incompressible gas Laminar, steady state, and Newtonian flow	Gas velocity negligible because of the low gas permeability in the membranes	Laminar, steady, and fully developed flow Co-current configuration. Constant liquid density and constant liquid viscosity.
	Boundary conditions	Axial symmetry: no flow crossing the boundary ($u_{r,g}$= 0 when r=0) Membrane wall: no-slip ($u_{z,g}$=0 when r=Ri) The velocity in the r-directions at all the boundaries are almost zero ($u_{r,g}$=0) Tube inlet: flow is fully developed and velocity profile is parabolic ($u_{z,g}=2u_{g,mean}[1-(r/Ri)^2]$ Tube outlet: flow is fully developed ($\partial u_{z,g}/\partial z$=0 when z=0)	X	Velocity in the r-directions at all the boundaries almost null ($u_{r,L}$= 0) Membrane wall: no-slip ($u_{z,L}$= 0 when r=Ri+Lm) Inlet: Averaged velocity specified at the inlet ($u_{z,L}=u_{L,mean}$ when z=0) Outlet: Fully developed flow ($\partial u_{z,L}/\partial z$=0 when z=L)
	Equations	Continuity: $\nabla . u_g$ Navier-Stokes: $\rho_g(u_g . \nabla u_g) = -\nabla \rho_g + \mu_g \nabla^2 u_g$	ug=0	Continuity: $\nabla . u_L$ Navier-Stokes: $\rho_L(u_L . \nabla u_L) = -\nabla \rho_L + \mu_L \nabla^2 u_L$
Species transport	***Assumptions***	Transport only by diffusion and convection, no reaction taking place in the system	Transport only by diffusion and convection, no reaction taking place in the system. No mutual interaction between the gases of the mixture (O_2/O_3) (Dhingra and Marand, 1998)	Isotropic mass diffusivity of i
	Boundary conditions	Axial symmetry: no material flow across the boundary ($\partial u_{g,j}/\partial r$=0 when r=0) Tube inlet: $C_{g,j}=C_{g,j,0}$ Tube outlet: the gas flux is predominantly by convection ($\partial u_{g,j}/\partial z$=0 when z=L)	Gas-membrane interface: interfacial transport defined by the solubility laws ($C_{m1,j}=C_{g,j,i}/S_j$ when r=Ri) Membrane inlet: insulated boundary ($\partial C_{m,j}/\partial z$=0 when z=0) Membrane outlet: insulated boundary ($\partial C_{m,j}/\partial z$=0 when z=L)	Concentrations of O_2 and O_3 null: $C_{L,j,0}$=0 Membrane-liquid interface: interfacial transport defined by the solubility laws ($C_{m1,j}=H_j C_{L,j,i}$ when r=Ri+Lm)
	Equations	$u_g . \nabla C_{g,j} = D_{g,j} \nabla^2 C_{g,j}$	$D_{m,j}\left[\frac{1}{r}\frac{\partial\left(r\frac{\partial C_{m,j}}{\partial x}\right)}{\partial r} + \frac{\partial^2 C_{m,j}}{\partial z^2}\right] = 0$	$u_L . \nabla C_{L,j} = D_{L,j} \nabla^2 C_{L,j}$

7. Conclusion

Membrane contactors for ozone diffusion is a recent unit operation for water treatment by ozonation. Using a hollow fiber membrane contactor, ozone is added uniformly to the water to be treated, through many dosing points and with a great mass transfer surface area. It leads to a better transformation rate of micropollutants than with conventional ozonation processes, and potentially to a lower bromates' formation thanks to a lower residual ozone concentration.

In addition, membrane contactors offer other advantages, like its modularity, its small foot print, and the independent flow adjustment for gas and liquid phases. Gas can also be recycled, leading to energy and reagents savings.

Many parameters influence the mass transfer during ozonation using membrane contactors. When carefully chosen, the efficiency of the process can then be greatly enhanced. For instance, the choice of the fiber material used is a crucial parameter. It has to provide a good ozone transfer through the membrane, but resist to ozone even for a long use. PTFE and PVDF membranes seem to be good choices for an ozonation application. The pressures to apply to the different phases also depend on the material chosen. The transmembrane pressure seems to be the major difficulty of membrane contactor technology. It has to be set carefully, in order to avoid bubbling and wetting problems.

The modeling of membrane processes for ozonation is useful to optimize reactor design and operating conditions and to study the influence of membrane properties. This optimization enables to achieve the best pollutant removal, for the minimum by-products' production and the minimum ozone consumption.

An important challenge to overcome will be the development of more efficient membrane material. Hydrophobic membranes have to be manufactured with coating or grafting techniques, which could lead to complicated modification routes and excessive use of chemicals. Moreover, studies about long term stability of the membranes used will be essential to apply the process on an industrial scale. Finally, a key point concerns the manufacture of affordable module with an optimized hydrodynamic and a high mass transfer coefficient.

Conclusions et perspectives du Chapitre I

La nécessité d'améliorer les stations d'épuration actuelles pour permettre l'élimination des micropolluants et une potentielle REUSE amène à rechercher les traitements avancés idoines à la fois d'un point de vue technique et économique.

Dans ce contexte, les contacteurs membranaires apparaissent comme une technologie particulièrement intéressante du fait d'une diffusion de l'ozone transféré à travers la membrane mieux maîtrisée que dans un procédé d'absorption gaz/liquide conventionnel, comme par exemple dans un réacteur à bulles. Leur utilisation dans le cadre de procédés d'oxydation avancée telle que l'ozonation serait à la fois pertinent pour abattre les micropolluants organiques tout en limitant la formation de sous-produits issus des réactions d'oxydation secondaires et potentiellement toxiques, tels que les bromates.

Néanmoins, l'ajout d'une résistance au transfert par rapport à un procédé traditionnel, due à la présence de la membrane, pourrait avoir un impact significatif sur le transfert. Cette résistance sera donc évaluée au cours du Chapitre III et, associée à d'autres résultats, aidera à déterminer les conditions dans lesquelles ce procédé est le plus efficace, ceci avec pour objectif de mieux comprendre quels paramètres sont à prendre en compte lors de la conduite de ce procédé, et à terme d'optimiser la géométrie de cette technologie.

Dans ce sens, la modélisation s'avère être un outil précieux pouvant aider à comprendre les phénomènes physiques et chimiques ayant lieu au sein du contacteur. L'état de l'art sur le sujet a cependant révélé un manque d'information et d'études sur cette thématique. Ainsi, dans le Chapitre V, un modèle visant à combler en partie cette lacune et à mieux comprendre les phénomènes locaux sera proposé.

En outre, les verrous expérimentaux évoqués dans ce chapitre seront pris en compte lors des études réalisées pour la suite de cette thèse, notamment les pressions transmembranaires limitantes (pression de bulle et pression de percée). De plus, le Chapitre I ayant souligné le rôle crucial que joue le matériau du contacteur membranaire dans le transfert de l'ozone et la continuité du procédé au cours du temps, les essais seront réalisés avec un contacteur composé de fibres en PTFE, ce matériau étant particulièrement résistant à l'ozone. Après une certaine durée d'utilisation, son vieillissement sera évalué sur la base d'images réalisées au Microscope Electronique à Balayage.

Bibliographie du Chapitre I

Ahmed, T., Semmens, M.J., 1992a. The use of independently sealed microporous hollow fiber membranes for oxygenation of water: model development. J. Memb. Sci. 69, 11–20.

Ahmed, T., Semmens, M.J., 1992b. Use of sealed end hollow fibers for bubbleless membrane aeration: experimental studies. J. Memb. Sci. 69, 1–10.

Ahmed, T., Semmens, M.J., Voss, M.A., 2004. Oxygen transfer characteristics of hollow-fiber, composite membranes. Adv. Environ. Res. 8, 637–646.

AIDA, 1998. Directive n° 98/83/CE du 03/11/98 relative à la qualité des eaux destinées à la consommation humaine.

Al-Saffar, H.B., Oklany, J.S., Ozturk, B., Hughes, R., 1995. Removal of carbon dioxide from gas streams using a gas/liquid hollow fibre module. Process Saf. Environ. Prot. 73, 144–150.

Alves dos Santos, F.R., Borges, C.P., da Fonseca, F.V., 2015. Polymeric Materials for Membrane Contactor Devices Applied to Water Treatment by Ozonation. Mater. Res. 18, 1015–1022. https://doi.org/10.1590/1516-1439.016715

Amin, S.K., Abdallah, H.A.M., Roushdy, M.H., El-Sherbiny, S.A., 2016. An overview of production and development of ceramic membranes. Int. J. Appl. Eng. Res. 11, 7708–7721.

Antoniou, M.G., Hey, G., Rodríguez Vega, S., Spiliotopoulou, A., Fick, J., Tysklind, M., la Cour Jansen, J., Andersen, H.R., 2013. Required ozone doses for removing pharmaceuticals from wastewater effluents. Sci. Total Environ. 456–457, 42–49. https://doi.org/10.1016/j.scitotenv.2013.03.072

Atchariyawut, S., Jiraratananon, R., Wang, R., 2007. Separation of CO2 from CH4 by using gas–liquid membrane contacting process. J. Memb. Sci. 304, 163–172. https://doi.org/10.1016/j.memsci.2007.07.030

Atchariyawut, S., Phattaranawik, J., Leiknes, T., Jiraratananon, R., 2009. Application of ozonation membrane contacting system for dye wastewater treatment. Sep. Purif. Technol. 66, 153–158. https://doi.org/10.1016/j.seppur.2008.11.011

Bakeri, G., Matsuura, T., Ismail, A.F., Rana, D., 2012. A novel surface modified polyetherimide hollow fiber membrane for gas–liquid contacting processes. Sep. Purif. Technol. 89, 160–170. https://doi.org/10.1016/J.SEPPUR.2012.01.022

Bamperng, S., Suwannachart, T., Atchariyawut, S., Jiraratananon, R., 2010. Ozonation of dye wastewater by membrane contactor using PVDF and PTFE membranes. Sep. Purif. Technol. 72, 186–193. https://doi.org/10.1016/j.seppur.2010.02.006

Bauer, W.G., Fredrickson, A.G., Tsuchiya, H.M., 1963. Mass transfer characteristics of a venturi liquid-gas contactor. Ind. Eng. Chem. Process Des. Dev. 2, 178–187. https://doi.org/10.1021/i260007a002

Behera, S.K., Kim, H.W., Oh, J.-E., Park, H.-S., 2011. Occurrence and removal of antibiotics, hormones and several other pharmaceuticals in wastewater treatment plants of the largest industrial city of Korea. Sci. Total Environ. 409, 4351–4360. https://doi.org/10.1016/J.SCITOTENV.2011.07.015

Berry, M.J., Taylor, C.M., King, W., Chew, Y.M.J., Wenk, J., 2017. Modelling of Ozone Mass-Transfer through Non-Porous Membranes for Water Treatment. Water 9, 452. https://doi.org/10.3390/w9070452

Boon, A.G., 1980. Measurement of aerator performance, in: Papers Presented at the Symposium on the Profitable Aeration of Waste Water, Held at the Sudbury Conference Hall, London, April 1980/Organized and Sponsored by BHRA Fluid Engineering. Cranfield, Eng.: BHRA Fluid Engineering, c1980.

Boucif, N., 2012. Modélisation et simulation de contacteurs membranaires pour les procédés d'absorption de gaz acides par solvant chimique. Lorraine, Nancy.

Bourgin, M., Borowska, E., Helbing, J., Hollender, J., Kaiser, H.-P., Kienle, C., McArdell, C.S., Simon, E., von Gunten, U., 2017. Effect of operational and water quality parameters on conventional ozonation and the advanced oxidation process O3/H2O2: Kinetics of micropollutant abatement, transformation product and bromate formation in a surface water. Water Res. 122, 234–245. https://doi.org/10.1016/j.watres.2017.05.018

Briens, C.L., Huynh, L.X., Large, J.F., Catros, A., Bernard, J.R., Bergougnou, M.A., 1992. Hydrodynamics and gas-liquid mass transfer in a downward venturi-bubble column combination. Chem. Eng. Sci. 47, 3549–3556. https://doi.org/10.1016/0009-2509(92)85069-N

Buffle, M.O., Schumacher, J., Meylan, S., Jekel, M., Von Gunten, U., 2006. Ozonation and advanced oxidation of wastewater: Effect of O3 dose, pH, DOM and HO.-scavengers on ozone decomposition and HO . generation. Ozone Sci. Eng. 28, 247–259. https://doi.org/10.1080/01919510600718825

Cachon, R., Girardon, P., Voilley, A., 2019. Gases in Agro-food Processes.

Chabanon, E., Favre, E., 2017. 3.9 Membranes Contactors for Intensified Gas–Liquid Absorption Processes. Compr. Membr. Sci. Eng. https://doi.org/10.1016/B978-0-12-409547-2.12250-4

Choi, Y.J., Kim, M., 2011. Preparation and characterization of polyvinylidene fluoride by irradiating electron beam. Appl. Chem. Eng. 22, 353–357. https://doi.org/10.1021/ie010553y

Ciora, R.J., Liu, P.K.T., 2003. Ceramic membranes for environmental related applications. Fluid - Part. Sep. J. 15, 51–60.

Côté, P., Bersillon, J.-L., Huyard, A., 1989. Bubble-free aeration using membranes: mass transfer analysis. J. Memb. Sci. 47, 91–106. https://doi.org/https://doi.org/10.1016/S0376-7388(00)80862-5

Cruz-Alcalde, A., Esplugas, S., Sans, C., 2019. Abatement of ozone-recalcitrant micropollutants during municipal wastewater ozonation: Kinetic modelling and surrogate-based control strategies. Chem. Eng. J. 360, 1092–1100. https://doi.org/10.1016/j.cej.2018.10.206

Cussler, E.L., 2009. Diffusion : mass transfer in fluid systems. Cambridge University Press.

deMontigny, D., Tontiwachwuthikul, P., Chakma, A., 2006. Using polypropylene and polytetrafluoroethylene membranes in a membrane contactor for CO2 absorption. J. Memb. Sci. 277, 99–107. https://doi.org/https://doi.org/10.1016/j.memsci.2005.10.024

Dhingra, S.S., Marand, E., 1998. Mixed gas transport study through polymeric membranes. J. Memb. Sci. 141, 45–63. https://doi.org/10.1016/S0376-7388(97)00285-8

Dindore, V.Y., Brilman, D.W.F., Versteeg, G.F., 2005. Modelling of cross-flow membrane contactors: Physical mass transfer processes. J. Memb. Sci. 251, 209–222. https://doi.org/10.1016/j.memsci.2004.11.017

Drioli, E., Criscuoli, A., Curcio, E., 2006. Membrane contactors : fundamentals, applications and potentialities. Elsevier.

Elovitz, M.S., Von Gunten, U., 1999. Hydroxyl Radical/Ozone Ratios During Ozonation Processes. I. The Rct Concept. Ozone Sci. Eng. J. Int. Ozone Assoc. 21, 239–260. https://doi.org/10.1080/01919519908547239

Elovitz, M.S., Von Gunten, U., Kaiser, H.-P., 2000. Hydroxyl Radical/Ozone Ratios During Ozonation Processes. II. The Effect of Temperature, pH, Alkalinity, and DOM Properties. Ozone Sci. Eng. J. Int. Ozone Assoc. 22, 123–150. https://doi.org/10.1080/01919510008547216

Faiz, R., Fallanza, M., Ortiz, I., Li, K., 2013. Separation of olefin/paraffin gas mixtures using ceramic hollow fiber membrane contactors. Ind. Eng. Chem. Res. 52, 7918–7929. https://doi.org/10.1021/ie400870n

Fang, Y., Novak, P.J., Hozalski, R.M., Cussler, E.L., Semmens, M.J., 2004. Condensation studies in gas permeable membranes. J. Memb. Sci. 231, 47–55. https://doi.org/https://doi.org/10.1016/j.memsci.2003.10.039

Gabelman, A., Hwang, S.T., 1999. Hollow fiber membrane contactors. J. Memb. Sci. 159, 61–106. https://doi.org/10.1016/S0376-7388(99)00040-X

Gao, Y., Ji, Y., Li, G., An, T., 2016. Theoretical investigation on the kinetics and mechanisms of hydroxyl radical-induced transformation of parabens and its consequences for toxicity: Influence of alkyl-chain length. Water Res. 91, 77–85. https://doi.org/10.1016/j.watres.2015.12.056

Gogoi, A., Mazumder, P., Tyagi, V.K., Tushara Chaminda, G.G., An, A.K., Kumar, M., 2018. Occurrence and fate of emerging contaminants in water environment: A review. Groundw. Sustain. Dev. 6, 169–180. https://doi.org/10.1016/j.gsd.2017.12.009

Goh, P.S., Naim, R., Rahbari-Sisakht, M., Ismail, A.F., 2019. Modification of membrane hydrophobicity in membrane contactors for environmental remediation. Sep. Purif. Technol. 227, 115721. https://doi.org/10.1016/J.SEPPUR.2019.115721

Gomes, J., Costa, R., Quinta-Ferreira, R.M., Martins, R.C., 2017. Application of ozonation for pharmaceuticals and personal care products removal from water. Sci. Total Environ. 586, 265–283. https://doi.org/10.1016/j.scitotenv.2017.01.216

Gordon, G., 1995. The chemistry and reactions of ozone in our environment. Prog. Nucl. Energy 29, 89–96. https://doi.org/10.1016/0149-1970(95)00031-E

Guerra, K., Pellegrino, J., 2013. Development of a Techno-Economic Model to Compare Ceramic and Polymeric Membranes. Sep. Sci. Technol. 48, 51–65. https://doi.org/10.1080/01496395.2012.690808

Guo, Y., Wang, H., Wang, B., Deng, S., Huang, J., Yu, G., Wang, Y., 2018. Prediction of micropollutant abatement during homogeneous catalytic ozonation by a chemical kinetic model. Water Res. 142, 383–395. https://doi.org/10.1016/j.watres.2018.06.019

Hansen, K.M.S., Spiliotopoulou, A., Chhetri, R.K., Escolà Casas, M., Bester, K., Andersen, H.R., 2016. Ozonation for source treatment of pharmaceuticals in hospital wastewater – Ozone lifetime and required ozone dose. Chem. Eng. J. 290, 507–514. https://doi.org/10.1016/j.cej.2016.01.027

Heeb, M.B., Criquet, J., Zimmermann-Steffens, S.G., Von Gunten, U., 2014. Oxidative treatment of bromide-containing waters: Formation of bromine and its reactions with inorganic and organic compounds - A critical review. Water Res. 48, 15–42. https://doi.org/10.1016/j.watres.2013.08.030

Hollender, J., Zimmermann, S.G., Koepke, S., Krauss, M., McArdell, C.S., Ort, C., Singer, H., von Gunten, U., Siegrist, H., 2009. Elimination of organic micropollutants in a municipal wastewater treatment plant upgraded with a full-scale post-ozonation followed by sand filtration. Environ. Sci. Technol. 43, 7862–7869. https://doi.org/10.1021/es9014629

Huber, M.M., Canonica, S., Park, G.-Y., von Gunten, U., 2003. Oxidation of Pharmaceuticals during Ozonation and Advanced Oxidation Processes. Environ. Sci. Technol. 37, 1016–1024. https://doi.org/10.1021/es025896h

Janknecht, P., Wilderer, P.A., Picard, C., Larbot, A., 2001. Ozone–water contacting by ceramic membranes. Sep. Purif. Technol. 25, 341–346. https://doi.org/https://doi.org/10.1016/S1383-5866(01)00061-2

Jansen, R.H.S., de Rijk, J.W., Zwijnenburg, A., Mulder, M.H.V., Wessling, M., 2005. Hollow fiber membrane contactors—A means to study the reaction kinetics of humic substance ozonation. J. Memb. Sci. 257, 48–59. https://doi.org/10.1016/J.MEMSCI.2004.07.038

Kanakaraju, D., Glass, B.D., Oelgemoller, M., 2018. Advanced oxidation process-mediated removal of pharmaceuticals from water: A review. J. Environ. Manage. 219, 189–207. https://doi.org/10.1016/j.jenvman.2018.04.103

Khaisri, S., deMontigny, D., Tontiwachwuthikul, P., Jiraratananon, R., 2009. Comparing membrane resistance and absorption performance of three different membranes in a gas absorption membrane contactor. Sep. Purif. Technol. 65, 290–297. https://doi.org/10.1016/j.seppur.2008.10.035

Kim, J., Davies, S.H.R., Baumann, M.J., Tarabara, V. V., Masten, S.J., 2008. Effect of ozone dosage and hydrodynamic conditions on the permeate flux in a hybrid ozonation-ceramic ultrafiltration system treating natural waters. J. Memb. Sci. 311, 165–172. https://doi.org/10.1016/j.memsci.2007.12.010

Kukuzaki, M., Fujimoto, K., Kai, S., Ohe, K., Oshima, T., Baba, Y., 2010. Ozone mass transfer in an ozone-water contacting process with Shirasu porous glass (SPG) membranes-A comparative study of hydrophilic and hydrophobic membranes. Sep. Purif. Technol. 72, 347–356. https://doi.org/10.1016/j.seppur.2010.03.004

Kwon, Y.-N., Hong, S., Choi, H., Tak, T., 2012. Surface modification of a polyamide reverse osmosis membrane for chlorine resistance improvement. J. Memb. Sci. 415–416, 192–198. https://doi.org/10.1016/J.MEMSCI.2012.04.056

Kwon, Y.-N., Joksimovic, R., Kim, I.-C., Leckie, J.O., 2011. Effect of bromide on the chlorination of a polyamide membrane. Desalination 280, 80–86. https://doi.org/10.1016/J.DESAL.2011.06.046

Laera, G., Cassano, D., Lopez, A., Pinto, A., Pollice, A., Ricco, G., Mascolo, G., 2012. Removal of organics and degradation products from industrial wastewater by a membrane bioreactor integrated with ozone or UV/H 2O 2 treatment. Environ. Sci. Technol. 46, 1010–1018. https://doi.org/10.1021/es202707w

Lee, Y., Gerrity, D., Lee, M., Bogeat, A.E., Salhi, E., Gamage, S., Trenholm, R.A., Wert, E.C., Snyder, S.A., von Gunten, U., 2013. Prediction of micropollutant elimination during ozonation of municipal wastewater effluents: use of kinetic and water specific information. Environ. Sci. Technol. 47, 5872–5881. https://doi.org/10.1021/es400781r

Lee, Y., Kovalova, L., McArdell, C.S., von Gunten, U., 2014. Prediction of micropollutant elimination during ozonation of a hospital wastewater effluent. Water Res. 64, 134–148. https://doi.org/10.1016/J.WATRES.2014.06.027

Lee, Y., von Gunten, U., 2016. Advances in predicting organic contaminant abatement during ozonation of municipal wastewater effluent: reaction kinetics, transformation products, and changes of biological effects. Environ. Sci. Water Res. Technol. 2, 421–442. https://doi.org/10.1039/C6EW00025H

Leiknes, T., Phattaranawik, J., Boller, M., Von Gunten, U., Pronk, W., 2005. Ozone transfer and design concepts for NOM decolourization in tubular membrane contactor. Chem. Eng. J. 111, 53–61. https://doi.org/10.1016/j.cej.2005.05.007

Li, J., Zhu, L.-P., Xu, Y.-Y., Zhu, B.-K., 2010. Oxygen transfer characteristics of hydrophilic treated polypropylene hollow fiber membranes for bubbleless aeration. J. Memb. Sci. 362, 47–57. https://doi.org/https://doi.org/10.1016/j.memsci.2010.06.013

Lishman, L., Smyth, S.A., Sarafin, K., Kleywegt, S., Toito, J., Peart, T., Lee, B., Servos, M., Beland, M., Seto, P., 2006. Occurrence and reductions of pharmaceuticals and personal care products and estrogens by municipal wastewater treatment plants in Ontario, Canada. Sci. Total Environ. 367, 544–558.

Luo, Y., Guo, W., Ngo, H.H., Nghiem, L.D., Hai, F.I., Zhang, J., Liang, S., Wang, X.C., 2014. A review on the occurrence of micropollutants in the aquatic environment and their fate and removal during wastewater treatment. Sci. Total Environ. 473–474, 619–641. https://doi.org/10.1016/j.scitotenv.2013.12.065

Margot, J., Kienle, C., Magnet, A., Weil, M., Rossi, L., de Alencastro, L.F., Abegglen, C., Thonney, D., Chèvre, N., Schärer, M., Barry, D.A., 2013. Treatment of micropollutants in municipal wastewater: Ozone or powdered activated carbon? Sci. Total Environ. 461–462, 480–498. https://doi.org/10.1016/j.scitotenv.2013.05.034

Mark, J.E., 1999. Polymer Data Handbook. OXFORD UNIVERSITY PRESS.

Mavroudi, M., Kaldis, S.P., Sakellaropoulos, G.P., 2006. A study of mass transfer resistance in membrane gas–liquid contacting processes. J. Memb. Sci. 272, 103–115. https://doi.org/10.1016/J.MEMSCI.2005.07.025

Mecha, A.C., Onyango, M.S., Ochieng, A., Momba, M.N.B., 2016. Impact of ozonation in removing organic micro-pollutants in primary and secondary municipal wastewater: Effect of process parameters. Water Sci. Technol. 74, 756–765. https://doi.org/10.2166/wst.2016.276

Merle, T., Pronk, W., Von Gunten, U., Eawag, †, 2017. MEMBRO 3 X, a Novel Combination of a Membrane Contactor with Advanced Oxidation (O 3 /H 2 O 2) for Simultaneous Micropollutant Abatement and Bromate Minimization. Environ. Sci. Technol. Lett 4, 13. https://doi.org/10.1021/acs.estlett.7b00061

Mori, Y., Oota, T., Hashino, M., Takamura, M., Fujii, Y., 1998. Ozone-microfiltration system. Desalination 117, 211–218. https://doi.org/10.1016/S0011-9164(98)00098-8

Mulder, M., 1996. Basic principles of membrane technology, 2nd ed. ed. Kluwer Academic, Dordrecht ; Boston.

Nakada, N., Shinohara, H., Murata, A., Kiri, K., Managaki, S., Sato, N., Takada, H., 2007. Removal of selected pharmaceuticals and personal care products (PPCPs) and endocrine-disrupting chemicals (EDCs) during sand filtration and ozonation at a municipal sewage treatment plant. Water Res. 41, 4373–4382. https://doi.org/10.1016/J.WATRES.2007.06.038

Nawrocki, J., Kasprzyk-Hordern, B., 2010. The efficiency and mechanisms of catalytic ozonation. Appl. Catal. B Environ. 99, 27–42. https://doi.org/10.1016/j.apcatb.2010.06.033

Nguyen, P.T., 2018. Contacteurs à membranes denses pour les procédés d ' absorption gaz-liquide intensifiés : application à la capture du CO 2 en post combustion Phuc Tien Nguyen To cite this version : HAL Id : tel-01748894 soutenance et mis à disposition de l ' ensemble de .

Nguyen, P.T., Lasseuguette, E., Medina-Gonzalez, Y., Remigy, J.C., Roizard, D., Favre, E., 2011. A dense membrane contactor for intensified CO2 gas/liquid absorption in post-combustion capture. J. Memb. Sci. 377, 261–272. https://doi.org/10.1016/J.MEMSCI.2011.05.003

Nobukawa, T., Sanukida, S., 2000. The genotoxity of by-products by chlorination and ozonation of the river water in the presence of bromide ions. Water Sci. Technol. 42, 259–264. https://doi.org/10.2166/wst.2000.0389

Office fédéral de l'environnement, D.E., 2014. Rapport explicatif concernant la modification de l'ordonnance sur la protection des eaux.

Ozkan, F., Ozturk, M., Baylar, A., 2006. Experimental investigations of air and liquid injection by venturi tubes. Water Environ. J. 20, 114–122. https://doi.org/10.1111/j.1747-6593.2005.00003.x

Pabby, A.K., Sastre, A.M., 2013. State-of-the-art review on hollow fibre contactor technology and membrane-based extraction processes. J. Memb. Sci. 430, 263–303. https://doi.org/10.1016/j.memsci.2012.11.060

Paxéus, N., 2004. Removal of selected non-steroidal anti-inflammatory drugs (NSAIDs), gemfibrozil, carbamazepine, b-blockers, trimethoprim and triclosan in conventional wastewater treatment plants in five EU countries and their discharge to the aquatic environment. Water Sci. Technol. 50, 253–260. https://doi.org/10.2166/wst.2004.0335

Petala, M., Samaras, P., Zouboulis, A., Kungolos, A., Sakellaropoulos, G.P.P., 2008. Influence of ozonation on the in vitro mutagenic and toxic potential of secondary effluents. Water Res. 42, 4929–4940. https://doi.org/10.1016/J.WATRES.2008.09.018

Petala, M., Tsiridis, V., Samaras, P., Zouboulis, A., Sakellaropoulos, G.P.P., 2006. Wastewater reclamation by advanced treatment of secondary effluents. Desalination 195, 109–118. https://doi.org/10.1016/J.DESAL.2005.10.037

Phattaranawik, J., Leiknes, T., Pronk, W., 2005. Mass transfer studies in flat-sheet membrane contactor with ozonation. J. Memb. Sci. 247, 153–167. https://doi.org/10.1016/j.memsci.2004.08.020

Picard, C., Larbot, A., Sarrazin, J., Janknecht, P., Wilderer, P., 2001. Ceramic membranes for ozonation in wastewater treatment. Ann. Chim. - Sci. des Matériaux 26, 13–22. https://doi.org/10.1016/S0151-9107(01)80042-8

Pines, D., Min, K.-N., J. Ergas, S., Reckhow, D., 2005. Investigation of an Ozone Membrane Contactor System. https://doi.org/10.1080/01919510590945750

Prieto-Rodríguez, L., Oller, I., Klamerth, N., Agüera, A., Rodríguez, E.M., Malato, S., 2013. Application of solar AOPs and ozonation for elimination of micropollutants in municipal wastewater treatment plant effluents. Water Res. 47, 1521–1528. https://doi.org/10.1016/j.watres.2012.11.002

Reed, B.W., Semmens, M.J., Cussler, E.L., 1995. Chapter 10 Membrane contactors. Membr. Sci. Technol. 2, 467–498. https://doi.org/10.1016/S0927-5193(06)80012-4

Reungoat, J., Escher, B.I.I., Macova, M., Argaud, F.X.X., Gernjak, W., Keller, J., 2012. Ozonation and

biological activated carbon filtration of wastewater treatment plant effluents. Water Res. 46, 863–872. https://doi.org/10.1016/J.WATRES.2011.11.064

Reungoat, J., Macova, M., Escher, B.I.I., Carswell, S., Mueller, J.F.F., Keller, J., 2010. Removal of micropollutants and reduction of biological activity in a full scale reclamation plant using ozonation and activated carbon filtration. Water Res. 44, 625–637. https://doi.org/10.1016/J.WATRES.2009.09.048

Richardson, S.D., 2003. Disinfection by-products and other emerging contaminants in drinking water. TrAC Trends Anal. Chem. 22, 666–684. https://doi.org/10.1016/S0165-9936(03)01003-3

Rosal, R., Rodríguez, A., Perdigón-Melón, J.A., Petre, A., García-Calvo, E., Gómez, M.J., Agüera, A., Fernández-Alba, A.R., 2010. Occurrence of emerging pollutants in urban wastewater and their removal through biological treatment followed by ozonation. Water Res. 44, 578–588. https://doi.org/10.1016/J.WATRES.2009.07.004

Roustan, M., 2003. Transferts gaz-liquide dans les procédés de traitement des eaux et des effluents gazeux. Éd. Tec & doc, Paris; Londres; New York.

Roustan, M., Debellefontaine, H., Do-Quang, Z., Duguet, J.-P., 1998. Development of a Method for the Determination of Ozone Demand of a Water. Ozone Sci. Eng. 20, 513–520. https://doi.org/10.1080/01919519809480338

Samadi, M.T., Azarian, G., Seifipour, F., Huang, C.P., Yang, X., Poormohammadi, A., 2015. The formation of aldehydes and ketones ozonation by-products and their variation through general water treatment plant in hamadan, Iran. Glob. Nest J. 17, 682–691.

Santos, J.L., Aparicio, I., Alonso, E., 2007. Occurrence and risk assessment of pharmaceutically active compounds in wastewater treatment plants. A case study: Seville city (Spain). Environ. Int. 33, 596–601. https://doi.org/https://doi.org/10.1016/j.envint.2006.09.014

Schlüter-Vorberg, L., Prasse, C., Ternes, T.A., Mückter, H., Coors, A., 2015. Toxification by transformation in conventional and advanced wastewater treatment: the antiviral drug acyclovir. Environ. Sci. Technol. Lett. 2, 342–346. https://doi.org/10.1021/acs.estlett.5b00291

Schwarzenbach, R.P., Escher, B.I., Fenner, K., Hofstetter, T.B., Johnson, C.A., von Gunten, U., Wehrli, B., 2006. The Challenge of Micropollutants in Aquatic Systems. Science (80-.). 313, 1072–1077. https://doi.org/10.1126/science.1127291

Shanbhag, P.V., Guha, A.K., Sirkar, K.K., 1995. Single-phase membrane ozonation of hazardous organic compounds in aqueous streams. J. Hazard. Mater. 41, 95–104. https://doi.org/10.1016/0304-3894(94)00097-Z

Shanbhag, P. V, Guha, A.K., Sirkar, K.K., 1998. Membrane-Based Ozonation of Organic Compounds. Ind. Eng. Chem. Res. 37, 4388–4398. https://doi.org/10.1021/ie980182u

Shen, Z., Semmens, M.J., Collins, A.G., 1990. A novel approach to ozone - water mass transfer using hollow - fiber reactors. Environ. Technol. 11, 597–608. https://doi.org/10.1080/09593339009384902

Smolders, K., Franken, A.C.M.C.M., 1989. Terminology for Membrane Distillation. Desalination 72, 249–262. https://doi.org/10.1016/0011-9164(89)80010-4

Snyder, S.A., Wert, E.C., Rexing, D.J., Zegers, R.E., Drury, D.D., 2006. Ozone oxidation of endocrine disruptors and pharmaceuticals in surface water and wastewater. Ozone Sci. Eng. 28, 445–460. https://doi.org/10.1080/01919510601039726

Sotelo, J.L., Beltrán, F.J., Benitez, F.J., Beltrán-Heredia, J., 1989. Henry's law constant for the ozone-water system. Water Res. 23, 1239–1246. https://doi.org/https://doi.org/10.1016/0043-1354(89)90186-3

Stalter, D., Magdeburg, A., Oehlmann, J., 2010a. Comparative toxicity assessment of ozone and activated carbon treated sewage effluents using an in vivo test battery. Water Res. 44, 2610–2620. https://doi.org/10.1016/J.WATRES.2010.01.023

Stalter, D., Magdeburg, A., Weil, M., Knacker, T., Oehlmann, J., 2010b. Toxication or detoxication? In vivo toxicity assessment of ozonation as advanced wastewater treatment with the rainbow trout. Water Res. 44, 439–448. https://doi.org/10.1016/J.WATRES.2009.07.025

Stylianou, S.K., Katsoyiannis, I.A., Mitrakas, M., Zouboulis, A.I., 2018. Application of a ceramic membrane contacting process for ozone and peroxone treatment of micropollutant contaminated surface water. J. Hazard. Mater. 358, 129–135. https://doi.org/10.1016/j.jhazmat.2018.06.060

Stylianou, S.K., Kostoglou, M., Zouboulis, A.I., 2016. Ozone Mass Transfer Studies in a Hydrophobized Ceramic Membrane Contactor: Experiments and Analysis. Ind. Eng. Chem. Res. 55, 7587–7597. https://doi.org/10.1021/acs.iecr.6b01446

Suez, 2007. SUEZ degremont® water handbook - Selecting ozonation reactors [WWW Document]. URL https://www.suezwaterhandbook.com/processes-and-technologies/oxidation-disinfection/oxidation-and-disinfection-using-ozone/selecting-ozonation-reactors (accessed 3.16.20).

Tootchi, L., Seth, R., Tabe, S., Yang, P., 2013. Transformation products of pharmaceutically active compounds during drinking water ozonation. Water Sci. Technol. Water Supply 13, 1576–1582. https://doi.org/10.2166/ws.2013.172

Tu, J., Yeoh, G.H., Liu, C., 2018. Computational fluid dynamics: A practical approach, Computational Fluid Dynamics: A Practical Approach.

Van Geluwe, S., Braeken, L., Van der Bruggen, B., 2011. Ozone oxidation for the alleviation of membrane fouling by natural organic matter: A review. Water Res. 45, 3551–3570. https://doi.org/10.1016/j.watres.2011.04.016

von Gunten, U., 2003a. Ozonation of drinking water: Part I. Oxidation kinetics and product formation. Water Res. 37, 1443–1467. https://doi.org/10.1016/s0043-1354(02)00457-8

von Gunten, U., 2003b. Ozonation of drinking water: Part II. Disinfection and by-product formation in presence of bromide, iodide or chlorine. Water Res. 37, 1469–1487. https://doi.org/10.1016/S0043-1354(02)00458-X

Von Gunten, U., 2018. Oxidation Processes in Water Treatment: Are We on Track? Environ. Sci. Technol. 52, 5062–5075. https://doi.org/10.1021/acs.est.8b00586

Wang, H., Zhan, J., Yao, W., Wang, B., Deng, S., Huang, J., Yu, G., Wang, Y., 2018. Comparison of pharmaceutical abatement in various water matrices by conventional ozonation, peroxone (O3/H2O2), and an electro-peroxone process. Water Res. 130, 127–138. https://doi.org/10.1016/j.watres.2017.11.054

Wenten, I.G., Julian, H., Panjaitan, N.T., 2012. Ozonation through ceramic membrane contactor for iodide oxidation during iodine recovery from brine water. Desalination 306, 29–34. https://doi.org/10.1016/j.desal.2012.08.032

Wert, E.C., Rosario-Ortiz, F.L., Drury, D.D., Snyder, S.A., 2007. Formation of oxidation byproducts from ozonation of wastewater. Water Res. 41, 1481–1490. https://doi.org/10.1016/J.WATRES.2007.01.020

Westerhoff, P., Song, R., Amy, G., Minear, R., 1997. Applications of ozone decomposition models. Ozone Sci. Eng. 19, 55–73. https://doi.org/10.1080/01919519708547318

Xu, Y., Goh, K., Wang, R., Bae, T.-H., 2019. A review on polymer-based membranes for gas-liquid membrane contacting processes: Current challenges and future direction. Sep. Purif. Technol. 229, 115791. https://doi.org/10.1016/J.SEPPUR.2019.115791

Yao, W., Rehman, S.W.U., Wang, H., Yang, H., Yu, G., Wang, Y., 2018. Pilot-scale evaluation of micropollutant abatements by conventional ozonation, UV/O3, and an electro-peroxone process. Water Res. 138, 106–117. https://doi.org/10.1016/J.WATRES.2018.03.044

Yu, X., An, L., Yang, J., Tu, S.T., Yan, J., 2015. CO2 capture using a superhydrophobic ceramic membrane contactor. J. Memb. Sci. 496, 1–12. https://doi.org/10.1016/j.memsci.2015.08.062

Yue, C., Seth, R., Tabe, S., Zhao, X., Hao, C., Yang, P., Schweitzer, L., Jamal, T., 2009. Evaluation of pilot-scale oxidation of several PPCPs/EDCs (pharmaceuticals and personal care products/endocrine disrupting compounds) during drinking water ozonation treatment. Water Sci. Technol. Water Supply 9, 577–582. https://doi.org/10.2166/ws.2009.573

Zhang, W., Wahlgren, M., Sivik, B., 1989. Membrane Characterization by the Contact Angle Technique II. Characterization of UF-Membranes and Comparison between the Captive Bubble and Sessile Drop as Methods to obtain Water Contact Angles. Desalination 72, 263–273. https://doi.org/10.1016/0011-9164(89)80011-6

Zhang, Z.E., Yan, Y.F., Zhang, L., Ju, S.X., 2014. Hollow fiber membrane contactor absorption of CO2 from the flue gas: review and perspective. Glob. Nest J. 16, 354–373. https://doi.org/10.1109/HICSS.2009.259

Zimmermann, S.G., Wittenwiler, M., Hollender, J., Krauss, M., Ort, C., Siegrist, H., von Gunten, U., 2011. Kinetic assessment and modeling of an ozonation step for full-scale municipal wastewater treatment: Micropollutant oxidation, by-product formation and disinfection. Water Res. 45, 605–617. https://doi.org/10.1016/j.watres.2010.07.080

Zoumpouli, G., Baker, R., Taylor, C., Chippendale, M., Smithers, C., Xian, S., Mattia, D., Chew, J., Wenk, J., 2018. A Single Tube Contactor for Testing Membrane Ozonation. https://doi.org/10.3390/w10101416

Chapitre II

Matériels et méthodes

Liste des symboles et abréviations du Chapitre II

ΔA	Différence d'absorbance entre l'échantillon et le blanc	cm^{-1}
ε	Porosité de la membrane	-
τ	Tortuosité de la membrane	-
γ	Tension de surface	$N.m^{-1}$
ϑ	Angle de contact	radian
$\int [O_3]_L dt$	Exposition à l'ozone moléculaire	M.min
$\int [HO^\circ]_L dt$	Exposition aux radicaux hydroxyles	M.min
AO7	Acide Orange 7	-
b	Chemin optique de la cellule	cm
C_{pCBA}, $C_{pCBA,0}$	Respectivement la concentration en p-CBA dans l'eau à l'instant du prélèvement et à l'instant initial	mol.L-1 ou g.L-1
$C_{O_3\ dissous}$	Concentration en ozone dissous dans le liquide	$mg.L^{-1}$
CBZ	Carbamazépine	-
DCO	Demande Chimique en Oxygène	$mgO_2.L^{-1}$
COD	Carbone Organique Dissous	$mgC.L^{-1}$
COT	Carbone Organique Total	$mgC.L^{-1}$
COV	Composés Organiques Volatils	
f	Constante de proportionnalité	$cm^{-1}.(mg_{O3}.L^{-1})^{-1}$
D_{iso}	Densité de l'isopropanol	$kg.m^{-3}$
D_{PTFE}	Densité du PTFE	$kg.m^{-3}$
$d_{pore,max}$	Diamètre maximal des pores de la membrane	m
HO°	Radicaux hydroxyles	-
HPLC-UV	Chromatographie liquide de haute performance avec un détecteur ultraviolet (ou CLHP-UV)	-
k_{O3}, k_{OH}	Constante de réaction respectivement avec l'ozone moléculaire et les radicaux hydroxyles	$M^{-1}.s^{-1}$
K_{ow}	Coefficient de partage octanol/eau	-
LC-MS/MS	Chromatographie liquide haute performance couplée à la spectrométrie de masse en tandem	-
MES	Matière en suspension	-
MEB	Microscope électronique à balayage	-
p-CBA	Acide para-chlorobenzoïque	-
$P_{percée}$	Pression de Percée	Pa
PTFE	Polytétrafluoroéthylène	-
Rct	Coefficient d'Elovitz	-
SUL	Sulfaméthoxazole	-
SUVA	Absorbance UV spécifique	$L.cm^{-1}.mgCOD^{-1}$
$Vprélevement$	Volume de l'échantillon prélevé	mL
$Vtotal$	Volume total de l'échantillon	mL
w_{we}, w_{dry}	Respectivement le poids de la membrane mouillée et sèche	kg

Chapitre II. Matériels et méthodes

Ce chapitre présente les méthodes, matériels et outils utilisés au cours de ces travaux de thèse. Dans un premier temps, les produits chimiques utilisés sont exposés, plus particulièrement les micropolluants ciblés lors de cette étude. Puis, les matrices et solutions employées sont présentées ainsi que les techniques analytiques associées. Ensuite, les contacteurs membranaires sélectionnés et conçus pour cette thèse sont décrits, ainsi que les techniques de caractérisation adaptées. Enfin, le pilote d'ozonation développé pour cette thèse est présenté ainsi que les méthodes employées pour le suivi de l'ozone et des radicaux hydroxyles.

A noter que les matériels et méthodes sont également spécifiés au sein de chaque chapitre de cette thèse, de par sa construction par article.

1. Produits chimiques utilisés

1.1. Micropolluants ciblés

Deux micropolluants sont ciblés durant ces travaux : la carbamazépine (CBZ) et le sulfaméthoxazole (SUL). Les produits utilisés ont tous une pureté supérieure à 98% et proviennent de Sigma-Aldrich. Le SUL est stocké à température ambiante tandis que la CBZ est stockée à 4°C. Le Tableau 1 présente les principales caractéristiques des composés étudiés. Parmi eux, la CBZ est le composé le plus hydrophobe (Log K_{ow} le plus élevé) et est peu soluble dans l'eau. Il s'agit du composé réagissant le plus rapidement avec les radicaux hydroxyles (k_{OH} le plus élevé) et le moins bien avec l'ozone moléculaire (k_{O3} le plus faible), malgré une constante de réaction restant très élevée par rapport à beaucoup d'autres micropolluants organiques. Le SUL est le composé réagissant le plus rapidement avec l'ozone moléculaire (k_{O3} le plus élevé) et présentant la solubilité la plus élevée.

Ces micropolluants ont été choisis d'une part car il s'agit de produits pharmaceutiques. Ces derniers constituent en effet la majorité des micropolluants rejetés par les stations d'épuration (Bolong et al., 2009). Plusieurs études réalisées à travers le monde ont ainsi montré la présence de ces composés en sortie de station d'épuration, mais également dans les eaux de surface (Ashton et al., 2004; Björlenius et al., 2018; Kolpin et al., 2002; Ternes, 1998; Valdés et al., 2016). D'autre part, les deux molécules ciblées ont été sélectionnées de par leur très bonne réactivité à l'ozonation, comme l'indiquent les constantes de réaction indiquées dans le Tableau 1. Enfin, l'expertise analytique présente au laboratoire a permis de valider ce choix, ces micropolluants ayant déjà été étudiés au cours d'autres travaux.

Tableau 1. Principales caractéristiques des micropolluants ciblés (a (Huber et al., 2003), b (Mathon et al., 2021), c (Beltrán and Rey, 2018)).

Composé	Formule	Masse molaire ($g.mol^{-1}$)	k_{O3} ($M.s^{-1}$)	k_{OH} ($M.s^{-1}$)	Log K_{ow}	Solubilité dans l'eau (25°C, $mg.L^{-1}$)	Formule semi-développée
Carbamazépine (CBZ)	$C_{15}H_{12}N_2O$	236	$3,0 \times 10^5$ [a]	$8,8 \times 10^9$ [b]	2,45 [b]	18 [b]	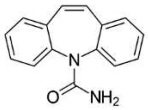
Sulfaméthoxazole (SUL)	$C_{10}H_{11}N_3O_3S$	253	$4,2 \times 10^5$ [c]	$3,2 \times 10^9$ [b]	0,89 [b]	610 [b]	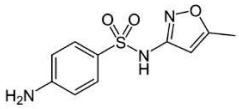

1.2. Autres produits chimiques utilisés

Tableau 2. Origine des produits chimiques utilisés.

Nom (abréviation ou formule)	Pureté ou concentration	Fournisseur	Constantes de réaction
Acide Orange 7 (AO7)	> 85%	Sigma-Aldrich	$k_{O3\text{-}AO7} = 1,20 \times 10^4\ M^{-1}.s^{-1}$ (Gomes et al., 2010)
Acide para-chlorobenzoïque (p-CBA)	99%	Aldrich	$k_{OH\text{-}pCBA} = 5 \times 10^9\ M^{-1}.s^{-1}$ (Neta and Dorfman, 1968) $k_{O3\text{-}pCBA} < 0,15\ M^{-1}.s^{-1}$ (David Yao and Haag, 1991)
Acide phosphorique (H_3PO_4)	84%	Sigma-Aldrich	
Bromure de sodium (NaBr)	> 99%	Sigma-Aldrich	
Fluoroetch®	X	Polyfluor	
Indigo trisulfonate ($C_{16}H_7K_3N_2O_{11}S_3$)	100%	Sigma-Aldrich	$k_{O3\text{-}indigo} > 10^7\ M^{-1}.s^{-1}$ (Bader and Hoigné, 1981)
Iodure de potassium (KI)	> 99,5%	Honeywell Fluka	
Phosphate monosodique (NaH_2PO_4)	> 98%	Sigma-Aldrich	
Sulfite de sodium (Na_2SO_3)	> 98%	Sigma-Aldrich	

2. Matrices étudiées

2.1. Eau pure tamponnée

La matrice constituée d'eau pure tamponnée à pH 3 est réalisée en mélangeant de l'eau déminéralisée (système de purification d'eau Elix® Essential 5 : Carbone Organique Total < 30 ppb, résistivité entre 5 et 15 MΩ·cm) et une solution tampon produite en dissolvant 1,2 $g.L^{-1}$ de phosphate monosodique

(NaH_2PO_4) dans de l'eau déminéralisée et en ajustant le pH avec l'ajout de quelques millilitres d'acide phosphorique (H_3PO_4) concentré à 84%.

2.2. Solution colorée

L'Acide Orange 7 (AO7) présente une constante de réaction avec l'ozone élevée ($k_{O3\text{-}AO7}$ = 1,20 x 10^4 $M^{-1}.s^{-1}$) et est rapide à analyser, d'où son choix dans cette étude en tant que polluant organique modèle. Sa structure moléculaire est présentée dans la figure ci-dessous.

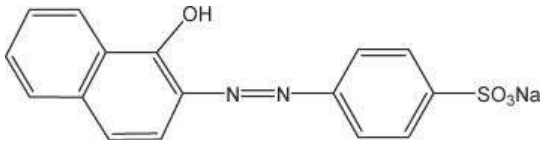

Figure 5. Structure moléculaire de l'Acide Orange 7.

La solution colorée est préparée à partir de la matrice constituée d'eau pure tamponnée (voir section précédente), en ajoutant 5,88 mg.L^{-1} d'AO7 pur à 85%. La solution est mise sous agitation durant minimum 24h afin d'assurer la dissolution complète du colorant. L'absorbance de chaque échantillon est mesurée à l'aide d'un spectrophotomètre UV-visible (UV-2401PC, Shimadzu, Japon) à 484 nm (longueur d'onde d'absorption maximum de ce composé), dans des cuvettes en plastique de 1 cm de chemin optique. Une courbe d'étalonnage permet finalement de relier l'absorbance mesurée à la concentration correspondante en AO7 de l'échantillon.

2.3. Effluent réel de sortie de station d'épuration

2.3.1. Description de la station d'épuration

2.3.1.1. Caractéristiques

La station de la Grande-Motte a été mise en service en 1984 et possède une capacité de 65 000 EH. Elle appartient à la Communauté d'agglomération du Pays de l'Or (composée à ce jour de Mauguio, Candillargues, la Grande-Motte, Lansargues, Mudaison, Palavas-les-Flots, Saint-Aunès et Valergues) et son exploitation est déléguée à la SAUR. Elle rejette les eaux traitées dans le canal du Rhône puis dans l'Etang de l'Or (Sandre, 2019).

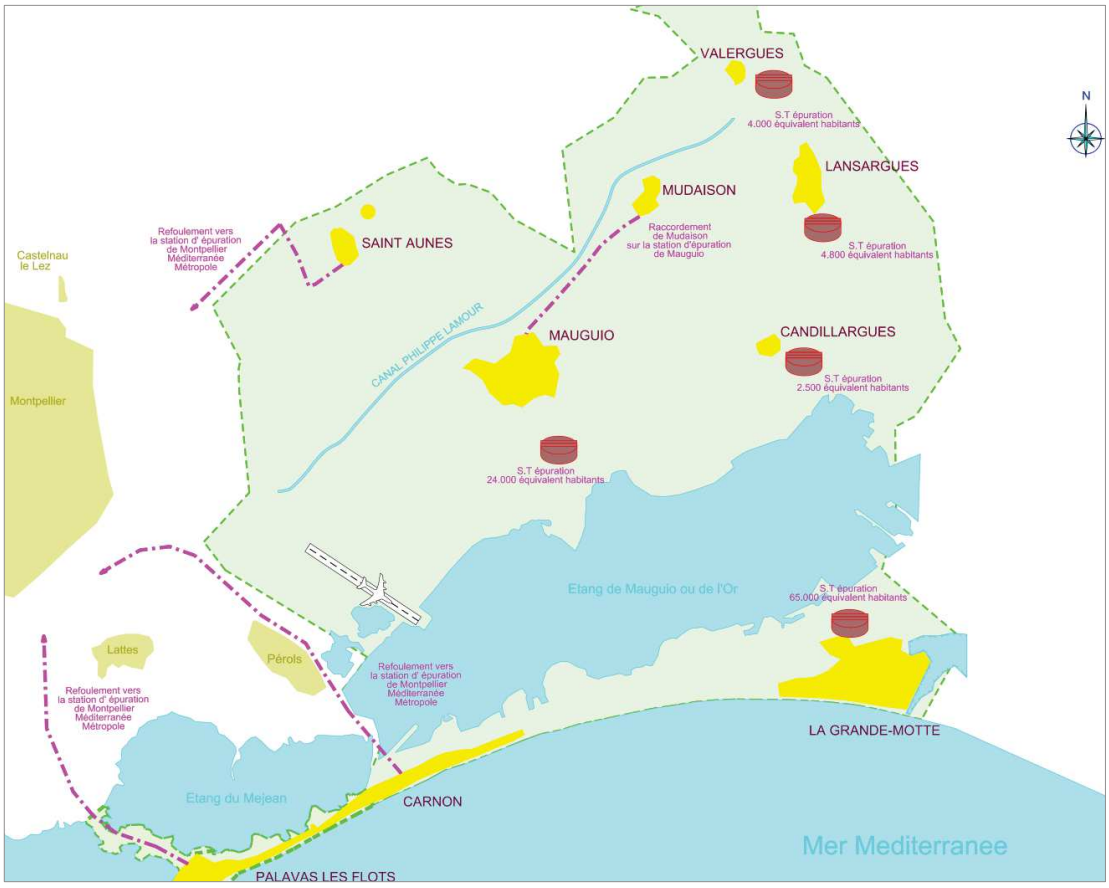

Figure 6. Principales infrastructures rejetant dans l'Etang de l'Or (Agglomération du Pays de l'Or, 2019).

Afin de répondre aux enjeux de la qualité de l'eau de l'étang de l'Or (Figure 6), zone sensible à l'eutrophisation, les procédés utilisés ont été renouvelés en 2012 afin d'avoir un rendement épuratoire particulièrement élevé en azote et phosphore y compris par temps de pluie (Agglomération du Pays de l'Or, 2019). En effet, lors de fortes pluies, le débit en entrée de station augmente. L'excès va ensuite dans le canal et peut potentiellement déborder dans les eaux de baignade.

De plus, du fait de la situation géographique de la station, le débit d'eaux usées à traiter varie fortement en fonction des saisons et des activités associées, plus particulièrement du tourisme saisonnier. Ainsi, bien que la valeur moyenne annuelle en entrée soit de 2936 $m^3.j^{-1}$, le débit de référence retenu est de 5702 $m^3.j^{-1}$ (valeur correspondant au percentile 95) (Ministère de la Transition Ecologique, 2020). Cette variation est due à l'augmentation de la population, multipliée par cinq en été.

Le traitement secondaire utilisé est un procédé à boue activée moyenne charge (bassin aéré). Il est précédé d'un traitement de l'azote par nitrification/dénitrification grâce à des passages successifs dans une zone anaérobie et une zone anoxie. Un traitement supplémentaire par bioréacteur à membrane a été ajouté en juin 2013 afin de sécuriser le traitement et de permettre un abattement bactérien supplémentaire (traitement physique). Des membranes planes immergées de type Kubota Submerged

Membrane Unit® (SMU) (KUBOTA, Japan) sont utilisées. Elles possèdent une surface totale de 16 240 m^2 et une taille de pore moyenne de 0,2 µm. Elles sont réparties dans 4 bassins fonctionnant toute l'année.

Afin d'optimiser le traitement en fonction de la saison (augmentation du débit l'été, faible charge en hiver), deux files identiques ont été mises en place en parallèle en amont des membranes. Ainsi, le volume d'une ligne est de 5770 m^3 alors que le volume total (lorsque les deux files sont utilisées) est de 10222 m^3 (Jacquin, 2017).

Concernant les boues, celles-ci sont traitées par épaississement statique gravitaire et la station produit 345,48 tMS par an. 53% de la Matière Sèche produite sert ensuite au compostage et 48% est épandue (chiffres 2019) (Ministère de la Transition Ecologique, 2020).

2.3.1.2. Prélèvements

Le procédé d'ozonation par contacteur membranaire étudié dans cette thèse a pour but d'être installé en traitement tertiaire des stations d'épuration afin de protéger l'écosystème aquatique et d'envisager la réutilisation des eaux usées traitées. Ainsi, l'objectif est d'étudier l'effet d'une matrice réelle sur le procédé étudié, c'est-à-dire d'une eau en sortie de station d'épuration (eau traitée). Le prélèvement était donc réalisé au niveau du rejet des eaux traitées comme indiqué sur la Figure 7. L'eau était ensuite stockée dans une chambre froide à 4°C en attendant d'être utilisée et conservée pendant maximum un mois.

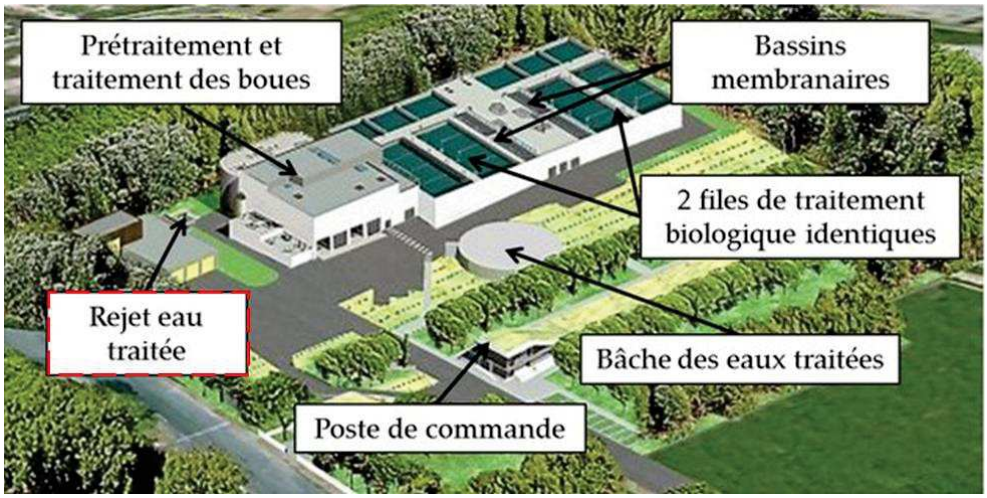

Figure 7. Station d'épuration de la Grande-Motte et lieu des prélèvements (Jacquin, 2017).

Comme énoncé précédemment, le moment du prélèvement (saison) a un impact sur l'eau à traiter ainsi que sur le traitement effectué. Ainsi, l'eau était caractérisée à chaque nouveau prélèvement. La moyenne et l'écart-type obtenus pour ces caractéristiques ainsi que la composition ionique des prélèvements réalisés sont présentés dans les tableaux 3 et 4.

Tableau 3. Paramètres globaux de l'eau prélevée en sortie de la station d'épuration de la Grande-Motte.

Paramètres	Valeur moyenne	Ecart-type
COT (mgC/L)	6.8	0.7
DCO (mgO_2/L)	18.0	1.0
pH	7.7	0.2
SUVA ($L.cm^{-1}.mgC^{-1}$)	0.02	0.01

Tableau 4. Composition ionique moyenne ($mg.L^{-1}$).

Composition ionique moyenne ($mg.L^{-1}$)			
Sodium (Na^+)	88.1 ± 0.8	Bromate (BrO_3^-)	< LOD
Ammonium (NH_4^+)	< LOD	Chlorure (Cl^-)	155 ± 6
Potassium (K^+)	22.6 ± 0.3	Nitrite (NO_2^-)	0.2 ± 0.2
Magnésium (Mg^+)	10.1 ± 0.3	Chlorate (ClO_3^-)	0.5 ± 0.3
Calcium (Ca^{2+})	92.0 ± 0.7	Bromure (Br^-)	0.29 ± 0.03
Sulphate (SO_4^{2-})	84 ± 10	Phosphate (PO_4^{3-})	0.3 ± 0.3

2.3.2. Effluent dopé en micropolluants

Pour chaque essai, un volume de 30L d'effluent prélevé en sortie de la station d'épuration de la Grande-Motte est dopé avec 2 $mg.L^{-1}$ de chaque micropolluant ciblé. La solution est ensuite mise sous agitation durant minimum 24h afin d'assurer la dissolution complète des micropolluants puis injectée dans la cuve d'alimentation du pilote d'ozonation. Une mise à l'équilibre entre la solution et le pilote d'ozonation est ensuite effectuée durant environ 12h grâce à une recirculation du liquide. Simultanément, de l'air comprimé circule dans les fibres afin d'éviter toute pénétration du liquide à travers la membrane. Cette mise à l'équilibre permet aux micropolluants de potentiellement d'adsorber sur le système, en fonction de la constante K_{OW} de chacun d'entre eux. Sans cela, l'abattement mesuré en sortie du procédé après ozonation ne serait pas dû uniquement à l'ozonation mais également à l'adsorption possible sur la cuve, le circuit, ou encore sur la membrane. La concentration initiale de chaque micropolluant avant ozonation est ensuite déterminée en faisant la moyenne de la concentration mesurée sur trois échantillons prélevés dans la cuve et trois échantillons prélevés via le robinet en amont du contacteur membranaire, au début de chaque expérience.

2.3.3. Effluent réel dopée en bromures et p-CBA

La matrice réelle (effluent prélevé en sortie de la station d'épuration de la Grande-Motte) est dopée avec 2 µM de p-CBA et 3 mg.L^{-1} de bromures (à partir de bromure de sodium). La solution est ensuite mise sous agitation durant minimum 24h pour assurer la dissolution complète des produits.

3. Techniques analytiques utilisées

3.1. Mesure de l'ozone dissous

Les robinets présents en amont et en aval du contacteur membranaire permettent de réaliser les prélèvements nécessaires afin d'analyser l'ozone dissous. La concentration en ozone dissous est déterminée à partir de la méthode dite « indigo », développée par Bader et Hoigné en 1981 et compléter en 1982 (Bader and Hoigné, 1982, 1981). Cette méthode se base sur la mesure de l'absorbance d'un colorant bleu indigo à 600 nm. En milieu acide, l'ozone réagit très rapidement avec l'indigo trisulfonate de potassium (constante de réaction supérieure à 10^7 $M^{-1}.s^{-1}$) et forme de l'acide isatin sulfonique, incolore à 600 nm, ce qui va provoquer une diminution de l'absorbance de la solution contenant l'indigo. Ce décroissement est proportionnel avec la quantité d'ozone, la stœchiométrie de cette réaction étant d'une mole d'ozone par mole d'indigo trisulfonate.

La solution mère en indigo trisulfonate de potassium est réalisée par ajout de 0,38 g d'indigo trisulfonate et de 1 mL d'acide phosphorique dans une fiole de 500mL complétée avec de l'eau milli-Q. Elle peut être conservée à l'abri de la lumière et à 4°C. Son absorbance initiale est de 0,20 ± 0,01 cm^{-1}. On renouvelle cette solution lorsqu'une dilution au 1/100 donne une absorbance inférieure ou égale à 0,16 cm^{-1} à 600 nm, soit au bout d'environ 4 mois.

La solution de dosage, ou réactif d'indigo, est produite en fonction de la concentration en ozone dissous que l'on anticipe. Deux solutions filles sont possibles en fonction de la gamme visée. Lors de la mesure, il est recommandé d'ajouter 9 mL de prélèvement à 1 mL de solution fille. Si nécessaire, des dilutions sont possibles avec la deuxième solution de dosage présentée, afin d'atteindre des concentrations plus élevées. Dans ce cas, on ajoute moins de 9 mL de prélèvement, et on complète avec de l'eau Milli-Q.

- **Concentration en ozone dissous entre 0.01 et 0.1 mg.L^{-1} :**

Dans une fiole jaugée de 250 mL, sont ajoutés 5 ml de la solution indigo mère, 2,5 g de dihydrogène phosphate de sodium et 1,7 mL de l'acide phosphorique dans de l'eau Milli-Q, jusqu'au trait de jauge. La solution de dosage est stockée à l'abri de la lumière et à 4°C et est renouvelée lorsque l'absorbance mesurée est inférieure à 80% de l'absorbance initiale soit au bout de 5 jours environ.

- **Concentration en ozone dissous entre 0,05 et 0,3 mg.L-1 :**

Le protocole est le même que dans le cas précédent mais 25 mL de la solution mère sont insérés dans le fiole jaugée, au lieu de 5 mL précédemment.

- **Concentration en ozone dissous supérieure à 0,3 mg.L-1 :**

Pour une concentration supérieure, on dilue le prélèvement de telle sorte que la solution indigo ne devienne pas totalement incolore lorsque l'on injecte notre prélèvement. Dans ce cas, on prépare également le blanc correspondant avec la même dilution.

L'absorbance de chaque échantillon est ensuite mesurée à l'aide d'un spectrophotomètre UV-visible (UV-2401PC, Shimadzu, Japon) à 600 nm dans des cuvettes de 1 cm de chemin optique. La concentration en ozone dissous est finalement calculée à partir de l'équation suivante :

$$C_{O_3\ dissous} = \frac{\Delta A}{\mathrm{f}\times\mathrm{b}} \times \frac{Vtotal}{Vprélevement}\ ,\ [16]$$

Avec : $Vtotal$ le volume total de l'échantillon (soit 10 mL) ; ΔA la différence d'absorbance entre l'échantillon et le blanc (cm^{-1}) ; b le chemin optique de la cellule (cm) ; $Vprélevement$ le volume de l'échantillon (mL, ici 9 mL sauf dilution) ; f la constante de proportionnalité (= 0,42 $cm^{-1}.(mg_{O3}.L^{-1})^{-1}$ ici).

La détermination du facteur f est basée sur le ratio stœchiométrique de 1 mole d'ozone consommé par mole d'indigo, ce qui correspond à une baisse de l'absorbance de 2,104 cm^{-1} par $mol.L^{-1}$ d'ozone, c'est-à-dire une diminution d'absorbance de 0,42 cm^{-1} par $mg.L^{-1}$ d'ozone.

3.2. Techniques analytiques de caractérisation globale

Pour les échantillons collectés après ozonation, 200 µL de Na_2SO_3 (10 $mg.L^{-1}$) sont ajoutés à 2 mL d'échantillon en tant que piégeur (scavenger) de l'ozone dissous résiduel, permettant ainsi de stopper la réaction d'ozonation à l'instant t du prélèvement. Cet ajout n'est pas nécessaire lors de la détermination de l'ozone dissous avec la solution indigo car celle-ci agissait également comme scavenger.

3.2.1. Mesure du pH

Le pH est mesuré grâce à un pH-mètre titrateur Titroline Easy de Schott Instruments, préalablement calibré minimum une fois par semaine avec deux solutions tampons de pH 4,0 et 6,87.

3.2.2. Composition ionique

La concentration des différents ions est déterminée par chromatographie ionique par Mme Valérie Bonniol, à l'Institut Européen des Membranes. Deux colonnes de séparation distinctes, composées

d'une résine échangeuse d'ions et installées en parallèle, sont utilisées (Anions : IonPac AS19 ; Cations : ICS 900, fournies par Thermo Scientific).

Les échantillons sont positionnés dans des vials appropriés et contiennent 50 à 100 µL de la solution à analyser, filtrée à 0,2 µm. Ils sont ensuite injectés grâce à un passeur automatique AS40. Un éluant circule en permanence sur chacune des colonnes, permettant pour l'une l'analyse des anions et pour l'autre l'analyse des cations. Les anions sont analysés à partir d'un chromatographe ICS 1000 équipé d'un suppresseur AERS (4 mm) et d'une colonne IonPac AS19. L'éluant, c'est-à-dire la phase mobile, est du KOH. Les cations sont analysés à partir d'un chromatographe ICS 900 équipé d'un suppresseur CSRS (4mm) et d'une colonne IonPac CS12A. L'éluant est de l'acide méthylsulfonique. La présence d'un suppresseur (membrane semi-perméable) permet d'améliorer la sensibilité de l'analyse en éliminant la conductivité de la phase mobile.

Les ions se fixent sélectivement sur la colonne chromatographique. Ils sont ensuite libérés progressivement en fonction de leur taille, leur charge et leur degré d'hydratation. Chaque espèce ionique est ainsi séparée et détectée par conductimétrie à la sortie de la colonne (cellule conductimétrique DS6 pour les anions et DS5 pour les cations). La concentration de l'espèce ionique dans la solution est directement proportionnelle au signal de conductivité. Un étalonnage est nécessaire au préalable, en fonction des concentrations présumées, afin de déterminer les temps de rétention des ions ciblés et leur concentration.

Ces analyses seront particulièrement utilisées pour le suivi de l'oxydation des bromures en bromate au cours du processus d'ozonation.

3.2.3. Demande Chimique en Oxygène (DCO)

La DCO, ou Demande Chimique en Oxygène, représente la consommation en O_2 par des oxydants chimiques pour oxyder les molécules organiques et minérales présentes dans l'eau. C'est un indicateur global de la pollution d'une eau usée, utilisé dans les stations d'épuration pour contrôler la qualité de l'eau en entrée et en sortie suivant la norme NF T90-101. Les mesures ont été réalisées avec des kits HachLange, le kit étant choisi en fonction de la gamme de concentrations à analyser. Dans notre cas, les kits étaient des DCO LCK 1414, correspondants à une concentration entre 5 et 60 $mgO_2.L^{-1}$.

3.2.4. Carbone Organique Total (COT) et Carbone Organique Dissous (COD)

Le carbone organique total (COT, ou TOC en anglais) est composé de constituants organiques sous formes dissoute et particulaire. L'effluent étudié ici étant en sortie de BRM, l'eau présente une teneur en MES (Matière en Suspension) particulièrement faible (<2 $mg.L^{-1}$). La part particulaire du COT est donc considérée nulle et le COT égal au COD (Carbone Organique Dissous, ou DOC en anglais). De plus,

afin de protéger l'appareil d'analyse utilisé, une filtration sur membrane hydrophile à 0,45 µm est préalablement effectuée. La mesure donnée par l'appareil correspond donc au COD. Le COT est analysé avec un COT-mètre Shimadzu TOC-V CPN. La méthode de mesure NPOC (Non Purgeable Organic Carbon) est sélectionnée et permet le dosage du carbone provenant de l'ensemble des composés organiques de l'échantillon, à l'exception des COV (Composés Organiques Volatils). Chaque échantillon est aspiré et acidifié par de l'acide chlorhydrique à 2 $mol.L^{-1}$ afin de transformer le carbone inorganique en CO_2. Celui-ci est ensuite évacué par stripping grâce à une injection d'O_2. L'échantillon est ensuite chauffé dans un four à 680°C, ce qui oxyde le carbone organique et le libère sous forme de CO_2. Ensuite, un gaz vecteur entraine le CO_2 et permet d'éliminer les halogènes et l'eau par refroidissement. Un détecteur infrarouge permet finalement de mesurer la concentration en CO_2, qui est ensuite convertie en concentration massique de COT grâce à une courbe d'étalonnage.

3.2.5. Absorbance UV-visible

Les spectres UV-Visibles ont été obtenus avec un spectrophotomètre double-faisceaux UV-2401 PC de Shimadzu, en balayant les longueurs d'onde de 200 à 800 nm. Des cuves en quartz avec 1 cm de trajet optique ont été utilisées afin d'avoir un résultat stable dans l'UV. Les spectres obtenus ne permettent pas une quantification de la matière organique présente car ne ceux-ci ne présentent pas de bande d'absorption distincte. Cependant, l'absorbance UV à 254 nm a été mise en évidence par plusieurs travaux de recherche comme étant caractéristique des doubles liaisons (noyaux aromatiques plus particulièrement) et permet ainsi d'étudier l'effet de l'ozone sur ce type de liaisons.

3.2.6. Capacité d'absorbance UV spécifique à 254 nm (SUVA254)

Par définition, la SUVA (ou « Specific UV Absorbance ») est calculée comme le ratio entre l'absorbance d'un échantillon à 254nm (cm^{-1}) sur son COD (en $mg.L^{-1}$). Cet indice permet de comparer l'absorbance à 254 nm de différents échantillons et varie peu pour un effluent secondaire, sa valeur étant située entre 1 et 3 $L.cm^{-1}.mgCOD^{-1}$. Il augmente avec le degré d'aromaticité de la matière organique, et donne ainsi une indication sur « l'insaturation » des liaisons chimiques présentes dans le carbone organique dissous.

3.3. Analyse des micropolluants

Les micropolluants sont analysés sur une installation Waters par chromatographie liquide haute performance (CLHP) couplée à la spectrométrie de masse en tandem (LC-MS/MS). Les analyses sont réalisées par M. Eddy Petit au sein de l'Institut Européen des Membranes. Une colonne XSelect HSS-T3-C18 (100 mm * 21 mm ; 2,5 µm) est utilisée comme phase stationnaire à température ambiante. Le gradient d'élution décrit dans le Tableau 5 est appliqué, comprenant un éluant A, composé de 89,9

% d'eau de qualité CLHP, 10 % d'acétonitrile de qualité CLHP et de 0,1% d'acide formique, et d'un éluant B, composé de 99,9 % d'acétonitrile de qualité CLHP et de 0,1% d'acide formique. Le débit appliqué est de 0,25 $mL.min^{-1}$. La spectrométrie de masse a été préalablement optimisée afin de faciliter le processus d'ionisation et d'atteindre une meilleure sensibilité. En conséquence, les conditions de détection utilisées après optimisation sont les suivantes : potentiel du capillaire de 3,5 kV, tension du cône de 30 V, température de la source de 120°C, température de désolvatation de 450°C, débit de gaz du cône de 50 $NL.h^{-1}$, débit de gaz de désolvatation de 500 $NL.h^{-1}$, et une énergie de collision de 10 V. De l'azote est utilisé en tant que gaz de nébulisation et de l'argon comme gaz de collision. Les courbes de calibration sont réalisées à partir d'une solution étalon constituée de la même matrice que celle des échantillons afin d'éviter les effets de matrice sur la détection, c'est-à-dire d'eau de sortie de la station d'épuration de la Grande-Motte et des deux micropolluants dans des concentrations connues. Une courbe de calibration est réalisée en amont et une autre en aval de chaque série d'analyses afin de corriger la dérive potentielle de l'instrument. Les limites de détection et de quantification sont estimées respectivement à 3 $\mu g.L^{-1}$ et 10 $\mu g.L^{-1}$ pour la CBZ et 0,13 $\mu g.L^{-1}$ et 0,74 $\mu g.L^{-1}$ pour le SUL.

Tableau 5. Gradient d'élution appliqué lors de l'analyse du mixte de micropolluants.

Temps (min)	A (%)	B (%)
0,00	100,0	0,0
0,50	100,0	0,0
4,50	0,0	100,0
5,50	0,0	100,0
6,00	100,0	0,0
10,00	100,0	0,0

3.4. Analyse des p-CBA

L'analyse des p-CBA se fait par HPLC-UV (ou CLHP-UV, Chromatographie liquide de haute performance avec un détecteur ultraviolet) à l'aide d'un système ACQUITY UPLC couplé à un logiciel d'analyse Empower. De la même manière que pour les micropolluants, l'analyse des p-CBA est réalisée par M. Eddy Petit, à l'Institut Européen des Membranes. Le système est muni d'une colonne analytique Nucleodur (Macherey-Nagel) (longueur 50 mm, diamètre intérieur 2 mm, taille des particules 2,7 µm) à température ambiante (T=22°C). La phase mobile est constituée d'une solution A (eau de qualité CLHP + 0,1% (volume/volume) d'acide trifluoroacétique), et d'une solution B (acétonitrile de qualité CLHP + 0,1% (volume/volume) d'acide trifluoroacétique). Le débit utilisé est de 0,25 $mL.min^{-1}$. Une élution isocratique de 3 minutes est appliquée, comprenant 80% de A et 20 % de B, dans laquelle le temps de rétention du p-CBA est de 1,88 min. La détection UV est ensuite réalisée à une longueur d'onde de 240 nm.

4. Détermination du coefficient Rct

L'exposition aux radicaux hydroxyles est déterminée à partir de la mesure de la concentration en p-CBA à partir de l'équation suivante :

$$\int_0^t [HO^\circ]_L dt = \frac{1}{k_{OH-pCBA}} \times \ln\left(\frac{C_{pCBA,0}}{C_{pCBA}}\right), [17]$$

Avec : C_{pCBA} la concentration en p-CBA dans l'eau à l'instant t du prélèvement (mol.L^{-1} or g.L^{-1}) ; $C_{pCBA,0}$ la concentration initiale en p-CBA dans l'eau (mol.L^{-1} or g.L^{-1}) ; et $k_{OH-pCBA}$ la constante de réaction du p-CBA avec HO° (= 5 x 10^9 M^{-1}.s^{-1} (Neta and Dorfman, 1968)). Afin de ne pas perturber le système aqueux et fausser les résultats obtenus, la concentration initiale en p-CBA $[pCBA]_0$ ne doit pas être trop élevée (Pi et al., 2005).

Le coefficient d'Elovitz (Rct), défini tel que rapport entre l'exposition aux radicaux hydroxyles sur l'exposition à l'ozone moléculaire, est ensuite déduit grâce à l'équation suivante (Elovitz and Von Gunten, 1999):

$$Rct = \frac{\int [OH]_L dt}{\int [O_3]_L dt}, [18]$$

Habituellement, Rct varie entre 10^{-9} et 10^{-7} lors de l'ozonation d'eaux naturelles (Elovitz et al., 2000; Elovitz and Von Gunten, 1999).

5. Description des contacteurs membranaires utilisés

5.1. Présentation du contacteur membranaire 65 fibres

Les contacteurs membranaires à 65 fibres utilisés durant ces travaux de thèse sont fournis par l'entreprise française Polymem (Castanet Tolosan / Haute-Garonne) (Figure 8). Leurs caractéristiques sont présentées dans le Tableau 6. Les fibres creuses sont constituées de polytétrafluoroéthylène (PTFE), matériau connu pour être résistant à l'ozone au cours du temps (Bamperng et al., 2010). Les fibres creuses présentent une très grande surface d'échange et rendent ainsi le procédé particulièrement compact.

Figure 8. Contacteur membranaire utilisé.

Tableau 6. Caractéristiques du contacteur membranaire à 65 fibres.

Caractéristiques des fibres en PTFE			
Nombre de fibres *	65	Longueur utile (cm) *	60
Diamètre intérieur (mm) *	0,45	Surface externe utile (m^2)	0,107
Diamètre extérieur (mm) *	0,87	Perméance au N_2 (GPU) *	33 904
Porosité [a]	0,58	Tortuosité [b]	3,47
Volume de liquide dans le contacteur (liquide circulant à l'extérieur des fibres) (m^3) [c]	$3,63 \times 10^{-5}$	Surface d'échange spécifique a (m^2/m^3) [d]	2 948
Caractéristiques du carter en acier inoxydable			
Diamètre intérieur (mm) *	9,5	Taux de remplissage *	54,5%

** Valeurs données par le fournisseur (Polymem, France)*

La porosité de la membrane ε ([a]) a été déterminée par méthode gravimétrique, en pesant sur une balance de précision (Sartorius CPA 225D) un échantillon de membrane sec, puis mouillé dans de l'isopropanol (IPA) (Wang et al., 2010). La masse d'isopropanol (IPA) présente dans les pores d'un échantillon de membrane en était déduite, et la porosité était calculée telle que :

$$\boldsymbol{\varepsilon} = \frac{(\boldsymbol{w_{wet} - w_{dry}})/\boldsymbol{D_{iso}}}{\frac{\boldsymbol{w_{wet} - w_{dry}}}{\boldsymbol{D_{iso}}} + \boldsymbol{w_{dry}}/\boldsymbol{D_{PTFE}}}, \quad [19]$$

Où w_{wet} est le poids de la membrane mouillée, w_{dry} est le poids de la membrane sèche, D_{iso} est la densité de l'isopropanol, et D_{PTFE} la densité du polymère (ici le PTFE).

La mesure était réalisée trois fois pour trois échantillons de membrane différents. La valeur moyenne était ensuite retenue.

La tortuosité τ ([b]) a été calculée à partir de la relation suivante, définie par (Iversen et al., 1997) telle que :

$$\boldsymbol{\tau} = \frac{(\boldsymbol{2-\varepsilon})^{\boldsymbol{2}}}{\boldsymbol{\varepsilon}}, \quad [20]$$

Le volume de liquide ([c]) et l'aire d'échange spécifique ([d]) ont été calculés à partir des données fournies par le constructeur sur les dimensions de l'enveloppe et des fibres du contacteur.

Lors de l'utilisation d'un contacteur membranaire, un paramètre important à contrôler est la pression transmembranaire. En effet, si la différence entre la pression côté liquide et la pression côté gaz est supérieure à la pression dite « de percée », l'eau pénètre à travers les pores de la membrane, ralentissant fortement le transfert de matière. La pression de percée (relative, en Pa) est estimée à partir de l'équation de Young-Laplace telle que :

$$\boldsymbol{P_{percée}} = \frac{\boldsymbol{4 \times \gamma \times \cos\theta}}{\boldsymbol{d_{pore,max}}}, \quad [21]$$

Avec : γ la tension de surface de l'eau avec l'air (= 73 x 10^{-3} N.m^{-1} à 20 °C) ; θ l'angle de contact entre l'eau et la membrane (radians), et $d_{\mathrm{pore,max}}$ le diamètre maximum des pores de la membrane (m) (déterminé à partir des images réalisées au Microscope Electronique à Balayage et analysées avec le logiciel ImageJ®).

Pour les membranes utilisées lors de ces travaux, la pression de percée est estimée **à 0,4 bar**, en considérant un angle de contact supérieur à 102°.

A l'inverse, si la différence entre la pression côté gaz et la pression côté liquide est supérieure à la pression dite "de bulle", l'ozone est diffusé dans l'eau sous forme de bulles et les avantages du contacteur membranaire liés au procédé sans bulle sont perdus. La pression de bulle est déterminée expérimentalement à partir de la démarche suivante, adaptée de la méthode présentée par Khayet et Matsuura (Khayet and Matsuura, 2001). Un contacteur membranaire spécifique sans enveloppe est fabriqué pour ce test à partir du même matériau que celui présent dans le contacteur utilisé lors des essais expérimentaux, c'est-à-dire à partir de fibres en PTFE fournie par l'entreprise Polymem. Ce contacteur spécifique est immergé dans l'eau, avec un circuit de gaz permettant la circulation d'oxygène dans les fibres. La pression de l'oxygène est ensuite augmentée progressivement. La pression de bulle est considérée atteinte lorsque la première bulle apparaît.

Pour les membranes utilisées lors de ces travaux, la pression de bulle est estimée à environ **0,1 bar**. Ainsi, la pression transmembranaire, c'est-à-dire la différence entre la pression entre le côté liquide et celle côté gaz, doit rester entre -0,1 et 0,4 bar.

Au cours de ces travaux, le gaz circule à l'intérieur des fibres et le liquide dans l'enveloppe, à contre-courant (Figure 9).

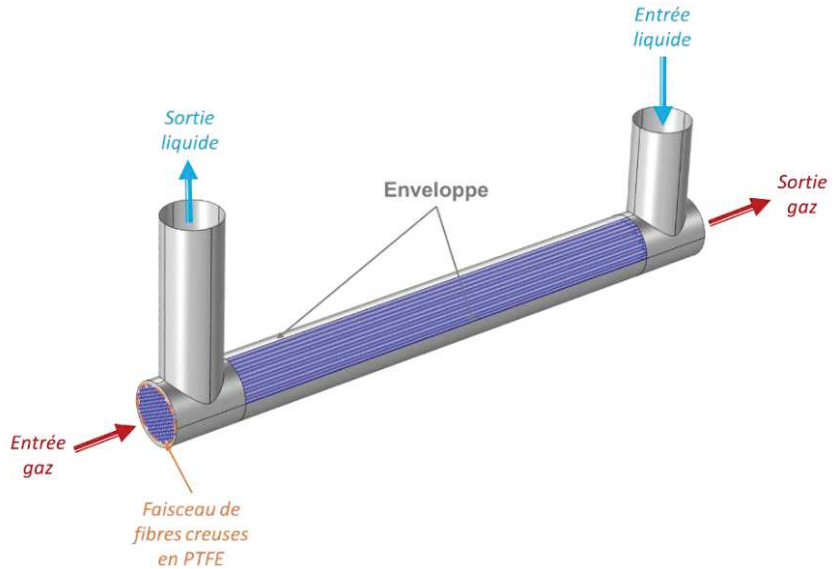

Figure 9. Configuration du contacteur membranaire.

5.2. Présentation du contacteur membranaire 1 fibre

Un contacteur membranaire avec une unique fibre creuse a été fabriqué spécifiquement au sein du laboratoire afin de valider le modèle présenté dans le Chapitre V. La membrane utilisée, une fibre creuse en PTFE, provenait de l'entreprise Polymem, de la même manière que les contacteurs à 65 fibres présentés dans le paragraphe précédent. L'empotage de la fibre dans le carter a été réalisé avec de la résine polyuréthane (voir Figure 10). Afin d'améliorer l'adhérence entre la fibre et la résine, le produit Fluoroetch® (Polyfluor) a été appliqué à l'extrémité de chaque fibre. Les caractéristiques de ce contacteur sont présentées dans le Tableau 7.

Figure 10. Empotage du contacteur membranaire à 1 fibre.

Tableau 7. Caractéristiques du contacteur membranaire à 1 fibre.

Caractéristiques des fibres			
Nombre	1	Longueur utile (cm)	60
Diamètre intérieur (mm) *	0,45	Surface externe utile (m^2)	$1,64 \times 10^{-3}$
Diamètre extérieur (mm) *	0,87	Tortuosité	3,47
Porosité	0,58	Matériau	PTFE
Caractéristiques du carter			
Diamètre intérieur (mm) *	10	Matériau	Téflon (tube) Acier inoxydable (tee)

** Valeurs données par le fournisseur (Polymem, France)*

5.3. Techniques de caractérisation des membranes utilisées

Pour déterminer l'hydrophobicité des fibres avant et après utilisation, les angles de contact sont mesurés avec l'aide de M. Thierry Thami à l'Institut Européen des Membranes. Pour cela, la méthode de la goutte posée est utilisée avec un Digidrop (GBX, France), équipé du logiciel Visiodrop pour l'analyse d'images. Tout d'abord, l'échantillon de fibre est fixé sur une plaque en verre. Une goutte d'eau de 1 µL est ensuite déposée sur la surface à l'aide d'une seringue de précision (aiguille très fine). Une image est alors capturée (Figure 11) et traitée en traçant la ligne de base de la goutte et en ajustant deux tangentes à chaque bordure de la goutte, formant ainsi deux angles de contact (i.e., un angle est mesuré à droite de la goutte et un à gauche, la valeur retenue de l'angle de contact est la moyenne des deux). Chaque mesure est répétée trois fois. Il est important de noter que cette méthode ne

permet pas de quantifier les angles de contact avec précision dans ces travaux. En effet, celle-ci n'est pas idéale dans le cas de surfaces poreuses et non planes, comme c'est le cas ici. Cependant, le volume de la goutte a été adapté au mieux à la taille et à la forme de la fibre afin de pouvoir faire abstraction de la courbure de la surface et que la goutte soit maintenue sur la membrane.

Afin de déterminer le diamètre maximal des pores et d'évaluer l'état de la membrane après utilisation, des images sont réalisées à l'aide d'un Microscope Electronique à Balayage (MEB) Hitachi S-4800 par M. Didier Cot au sein de l'Institut Européen des Membranes (Figure 12). Les échantillons sont préalablement métallisés par une fine couche de platine afin d'améliorer leur conductivité électronique. Le logiciel Image-J est ensuite utilisé pour traiter ces images et en déduire par exemple l'aire moyenne de la surface extérieure des pores, ou encore le diamètre maximum des pores.

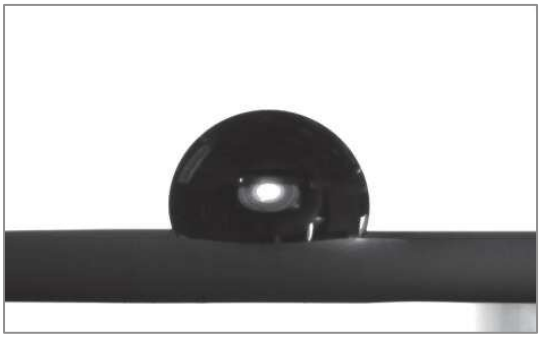

Figure 11. Exemple d'image prise lors de la mesure d'angle de contact sur un échantillon de fibre creuse en PTFE avant ozonation.

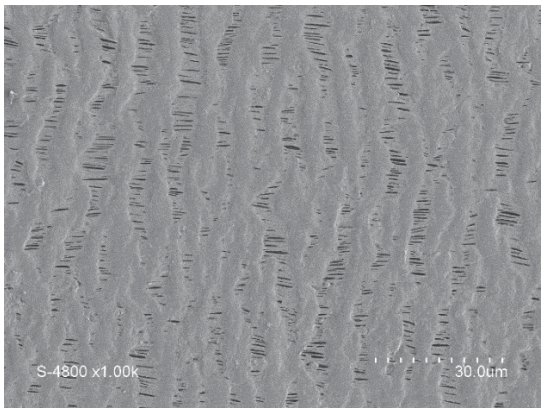

Figure 12. Exemple d'image prise au Microscope Electronique à Balayage sur un échantillon de fibre creuse en PTFE avant ozonation.

6. Description des pilotes d'ozonation

Deux configurations sont possibles pour le dispositif d'ozonation par contacteur membranaire. La mise en place d'un circuit fermé pour le liquide est utilisée lors de l'étude de la formation des bromates afin d'augmenter le temps de résidence dans le contacteur. Elle est également utilisée durant l'étape de mise à l'équilibre réalisée en amont de chaque essai concernant les micropolluants, afin de permettre l'adsorption éventuelle des composés sur le système avant le début du processus d'ozonation. La mise en place d'un circuit ouvert pour le liquide est utilisée pour tous les essais non évoqués précédemment et permet de simplifier les bilans matières par rapport au circuit fermé.

6.1. Dispositif d'ozonation par contacteur membranaire – liquide en circuit fermé

La Figure 13 décrit le dispositif expérimental utilisé pour le procédé d'ozonation lorsque le liquide est recirculé dans le pilote. Le pilote est alimenté en gaz en continu à l'aide d'une bouteille d'oxygène pur et d'un générateur d'ozone (BMT 803 N). Avant de circuler dans le contacteur membranaire, l'ozone est mélangé avec l'oxygène de manière à atteindre le débit de gaz et la concentration en ozone souhaitée. Pour cela, un débitmètre spécifique à l'oxygène et un débitmètre spécifique à l'ozone sont asservis à un logiciel grâce à deux électrovalves. Un analyseur de gaz (BMT 964) est présent pour contrôler la concentration en ozone en amont ou en aval du contacteur membranaire après déshumidification ($C_{O3,gas,in}$ ou $C_{O3,gas,out}$).

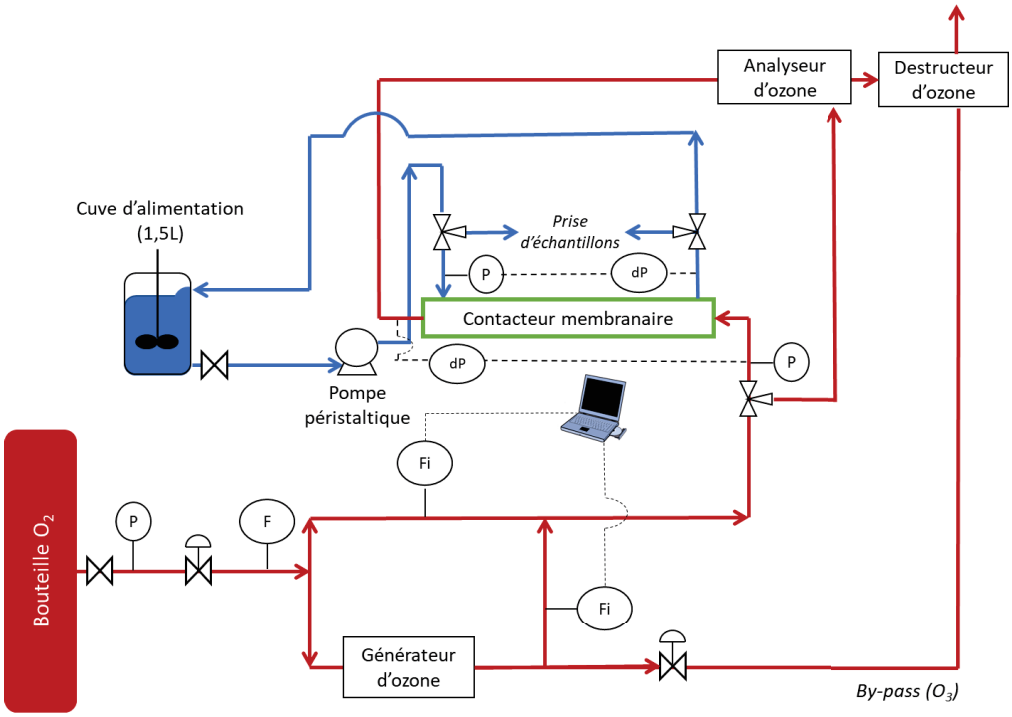

Figure 13. Flowsheet du pilote d'ozonation – liquide en circuit fermé – gaz en circuit ouvert (rouge : circuit gaz, bleu : circuit liquide).

Une cuve en verre de 1,5 L, agitée et thermostatée à 20°C, permet d'alimenter le circuit en liquide. Durant les essais, l'agitateur permet d'homogénéiser l'ozone dissous et le colorant dans la cuve. La circulation du liquide est effectuée grâce à une pompe péristaltique (Watson Marlow 323). Deux robinets (en amont et en aval du contacteur membranaire) sont présents pour prélever les échantillons. Au cours du procédé, l'ozone est transféré de la phase gaz à la phase liquide grâce au gradient de concentration. La membrane agit uniquement comme une barrière entre les deux phases.

6.2. Dispositif d'ozonation par contacteur membranaire – liquide en circuit ouvert

Le pilote d'ozonation par contacteur membranaire utilisé en circuit ouvert est approximativement le même que celui précédemment présenté (Figure 14). Dans cette disposition, le liquide ne s'écoule qu'une seule fois dans le contacteur. Il est ensuite récupéré dans un bidon contenant une solution de KI (iodure de potassium) afin de prévenir tout dégazage de l'ozone résiduel. Afin d'atteindre le régime permanent, une cuve d'alimentation plus grande que celle utilisée en circuit fermé est utilisée (30 L), celle-ci est en acier inoxydable, agitée, et thermostatée à 20°C.

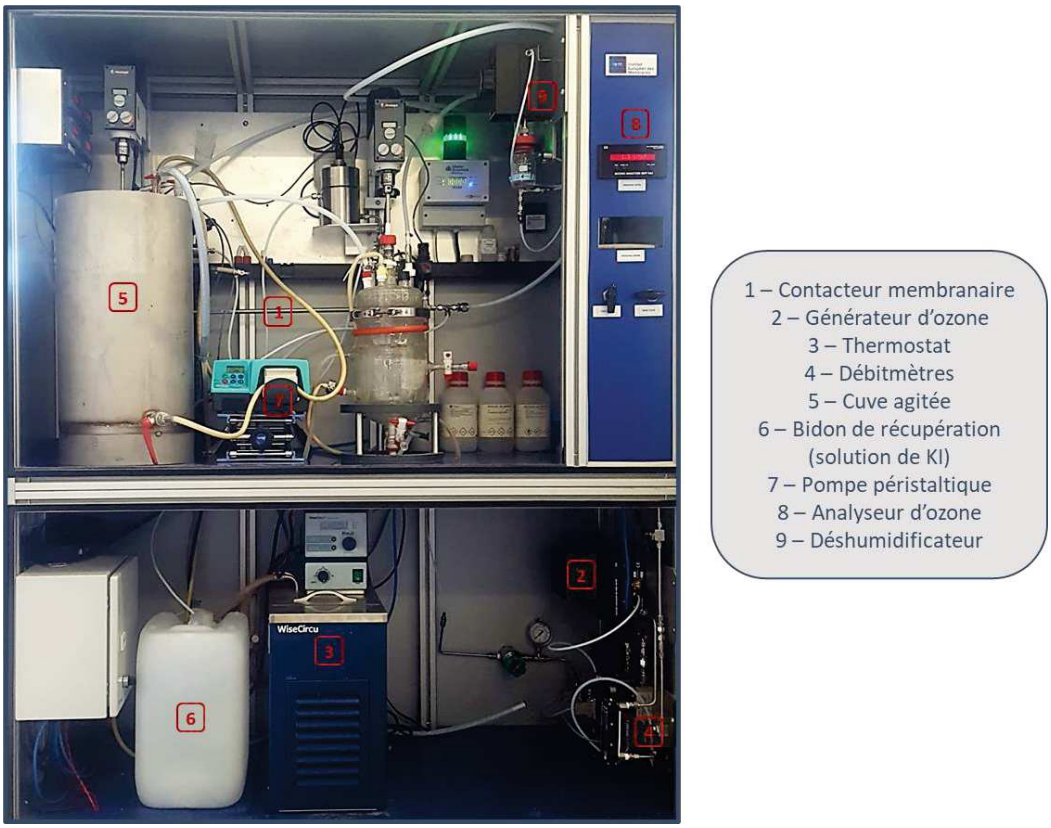

Figure 14. Pilote d'ozonation utilisé en circuit ouvert.

6.3. Dispositif d'ozonation par réacteur semi-batch à bulles

Afin de comparer les résultats obtenus avec le contacteur membranaire à ceux obtenus via un procédé conventionnel, un réacteur semi-batch à bulles est utilisé (Figure 15). Ce réacteur en verre, agité et thermostaté à 20 °C, possède un volume de 4 L. Une pompe de recirculation permet la prise d'échantillons. De la même manière que dans le dispositif d'ozonation par contacteur membranaire, le circuit de gaz est alimenté en continu par une bouteille d'oxygène pur. Un générateur d'ozone (BMT 803 N) convertit une partie de l'oxygène en ozone. Un bouton de réglage situé sur le générateur permet de contrôler la proportion d'ozone généré. Un débitmètre asservi à un logiciel via une électrovalve régule le débit total du mélange de gaz ozone/oxygène. Un analyseur d'ozone (BMT 964),

précédé d'un déshumidificateur protégeant le dispositif, mesure la concentration en ozone dans le gaz en entrée du réacteur ou en sortie, en fonction du mode de circulation sélectionnée. Concrètement, la concentration initiale d'ozone en entrée du réacteur à bulles est réglée avant le début de chaque essai à l'aide de l'analyseur, le circuit gaz étant alors en mode by-pass (i.e. le gaz ne circule pas dans le réacteur). Une fois la manipulation lancée, le gaz circule dans le réacteur via un diffuseur poreux, la valeur indiquée par l'analyseur est alors la concentration en ozone en sortie du réacteur. L'ozone est ensuite détruit dans un dispositif utilisant du charbon actif.

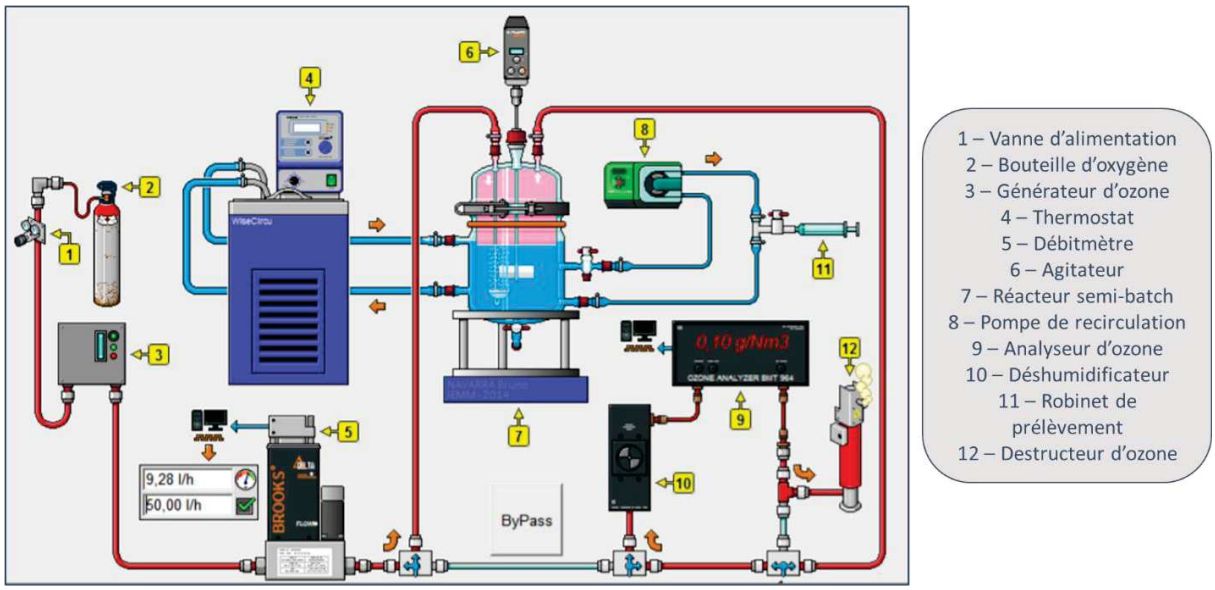

Figure 15. Schéma du pilote d'ozonation avec réacteur semi-batch à bulles, adapté de (Azaïs, 2015).

Bibliographie du Chapitre II

Agglomération du Pays de l'Or, 2019. L'assainissement collectif au Pays de l'Or [WWW Document]. https://www.paysdelor.fr/notre-agglo/eau-et-assainissement/assainissement-collectif/ (accessed 1.15.21).

Ashton, D., Hilton, M., Thomas, K.V. V, 2004. Investigating the environmental transport of human pharmaceuticals to streams in the United Kingdom. Sci. Total Environ. 333, 167–184. https://doi.org/10.1016/J.SCITOTENV.2004.04.062

Azaïs, A., 2015. Ozonation des concentrâts de nanofiltration dans le cadre de la réutilisation des eaux usees urbaines. Thèse de doctorat. Université de Montpellier, Montpellier.

Bader, H., Hoigné, J., 1982. Determination of Ozone In Water By The Indigo Method: A Submitted Standard Method. Ozone Sci. Eng. J. Int. Ozone Assoc. 4, 169–176. https://doi.org/10.1080/01919510390481531

Bader, H., Hoigné, J., 1981. Determination of ozone in water by the indigo method. Water Res. 15, 449–456. https://doi.org/10.1016/0043-1354(81)90054-3

Bamperng, S., Suwannachart, T., Atchariyawut, S., Jiraratananon, R., 2010. Ozonation of dye wastewater by membrane contactor using PVDF and PTFE membranes. Sep. Purif. Technol. 72, 186–193. https://doi.org/10.1016/j.seppur.2010.02.006

Beltrán, F. J., Rey, A., 2018. Free Radical and Direct Ozone Reaction Competition to Remove Priority and Pharmaceutical Water Contaminants with Single and Hydrogen Peroxide Ozonation Systems. Ozone Sci. Eng. 40, 251–265. https://doi.org/10.1080/01919512.2018.1431521

Berry, M.J., Taylor, C.M., King, W., Chew, Y.M.J., Wenk, J., 2017. Modelling of Ozone Mass-Transfer through Non-Porous Membranes for Water Treatment. Water 9, 452. https://doi.org/10.3390/w9070452

Björlenius, B., Ripszám, M., Haglund, P., Lindberg, R.H., Tysklind, M., Fick, J., 2018. Pharmaceutical residues are widespread in Baltic Sea coastal and offshore waters – Screening for pharmaceuticals and modelling of environmental concentrations of carbamazepine. Sci. Total Environ. 633, 1496–1509. https://doi.org/10.1016/j.scitotenv.2018.03.276

Bolong, N., Ismail, A.F., Salim, M.R., Matsuura, T., 2009. A review of the effects of emerging contaminants in wastewater and options for their removal. Desalination 239, 229–246. https://doi.org/10.1016/j.desal.2008.03.020

David Yao, C.C., Haag, W.R., 1991. Rate constants for direct reactions of ozone with several drinking water contaminants. Water Res. 25, 761–773. https://doi.org/10.1016/0043-1354(91)90155-J

Elovitz, M.S., Von Gunten, U., 1999. Hydroxyl Radical/Ozone Ratios During Ozonation Processes. I. The Rct Concept. Ozone Sci. Eng. J. Int. Ozone Assoc. 21, 239–260. https://doi.org/10.1080/01919519908547239

Elovitz, M.S., Von Gunten, U., Kaiser, H.P., 2000. The influence of dissolved organic matter character on ozone decomposition rates and Rct. ACS Symp. Ser. 761, 248–269. https://doi.org/10.1021/bk-2000-0761.ch016

Gomes, A.C., Nunes, J.C., Simões, R.M.S., 2010. Determination of fast ozone oxidation rate for textile dyes by using a continuous quench-flow system. J. Hazard. Mater. 178, 57–65. https://doi.org/10.1016/j.jhazmat.2010.01.043

Huber, M.M., Canonica, S., Park, G.-Y., von Gunten, U., 2003. Oxidation of Pharmaceuticals during

Ozonation and Advanced Oxidation Processes. Environ. Sci. Technol. 37, 1016–1024. https://doi.org/10.1021/es025896h

Iversen, S.B., Bhatia, V.K., Dam-Johansen, K., Jonsson, G., 1997. Characterization of microporous membranes for use in membrane contactors. J. Memb. Sci. 130, 205–217. https://doi.org/10.1016/S0376-7388(97)00026-4

Jacquin, C., 2017. Caractérisation de la Matière Organique Dissoute (DOM) et de ses interactions avec une séparation par membrane pour l'amélioration du contrôle des BioRéacteurs à Membranes (BàM). Thèse de doctorat. Université de Montpellier, Montpellier.

Khayet, M., Matsuura, T., 2001. Preparation and Characterization of Polyvinylidene Fluoride Membranes for Membrane Distillation. Ind. Eng. Chem. Res. 40, 5710–5718. https://doi.org/10.1021/ie010553y

Kolpin, D.W., Furlong, E.T., Meyer, M.T., Thurman, E.M., Zaugg, S.D., Barber, L.B., Buxton, H.T., 2002. Pharmaceuticals, hormones, and other organic wastewater contaminants in U.S. streams, 1999-2000: a national reconnaissance. Environ. Sci. Technol. 36, 1202–1211. https://doi.org/10.1021/es0200903

Mathon, B., Coquery, M., Liu, Z., Penru, Y., Guillon, A., Esperanza, M., Miège, C., Choubert, J.M., 2021. Ozonation of 47 organic micropollutants in secondary treated municipal effluents: Direct and indirect kinetic reaction rates and modelling. Chemosphere 262. https://doi.org/10.1016/j.chemosphere.2020.127969

Ministère de la Transition Ecologique, 2020. Portail d'information sur l'assainissement communal, Situation au 31/12/2019 des stations de traitement des eaux usées, Mise à jour le 14/12/2020, La Grande-Motte : [WWW Document]. http://assainissement.developpement-durable.gouv.fr/station.php?code=060934344001

Neta, P., Dorfman, L.M., 1968. Pulse radiolysis studies. XIII. Rate constants for the reaction of hydroxyl radicals with aromatic compounds in aqueous solutions. ACS Publications.

Pi, Y., Schumacher, J., Jekel, M., 2005. The use of para-chlorobenzoic acid (pCBA) as an ozone/hydroxyl radical probe compound. Ozone Sci. Eng. 27, 431–436. https://doi.org/10.1080/01919510500349309

Sandre, 2019. Jeux de données de référence - Stations de traitement des eaux usées - La Grande Motte. https://www.sandre.eaufrance.fr/urn.php?urn=urn:sandre:donnees:SysTraitementEauxUsees:FRA:code:060934344001:::::html

Ternes, T.A., 1998. Occurrence of drugs in German sewage treatment plants and rivers. Water Res. 32, 3245–3260. https://doi.org/10.1016/S0043-1354(98)00099-2

Valdés, M.E., Huerta, B., Wunderlin, D.A., Bistoni, M.A., Barceló, D., Rodriguez-Mozaz, S., 2016. Bioaccumulation and bioconcentration of carbamazepine and other pharmaceuticals in fish under field and controlled laboratory experiments. Evidences of carbamazepine metabolization by fish. Sci. Total Environ. 557–558, 58–67. https://doi.org/10.1016/j.scitotenv.2016.03.045

Wang, R., Shi, L., Tang, C.Y., Chou, S., Qiu, C., Fane, A.G., 2010. Characterization of novel forward osmosis hollow fiber membranes. J. Memb. Sci. 355, 158–167.

Chapitre III

Evaluation of an ozone diffusion process using a hollow fiber membrane contactor

Liste des symboles et abréviations du Chapitre III

ε	Porosity	-
τ	Tortuosity	-
γ	Surface tension	$N.m^{-1}$
ϑ	Contact angle	radian
A_{outer}, A_{lm}, A_{inner}	Respectively the outer, logarithmic mean, and inner surface area of the membrane	m^2
AO7	Acid Orange 7	-
a	Specific exchange surface of the membrane contactor	$m^2.m^{-3}$
b	stoichiometric coefficient	-
$C_{O3,gas,in}$	Ozone concentration at the gas inlet	$g.Nm^{-3}$ or $mol.m^{-3}$
$C_{O3,gas,out}$	Ozone concentration at the gas outlet	$g.Nm^{-3}$ or $mol.m^{-3}$
C_{O3}	Ozone concentration at the gas inlet in the DOE	$g.Nm^{-3}$
C_1	Dissolved ozone concentration at liquid inlet	$mol.m^{-3}$
C_2	Dissolved ozone concentration at liquid outlet	$mol.m^{-3}$
$C_{Dissolved\ O3\_l}$	Concentration of dissolved ozone at the gas/liquid interface	$mol.m^{-3}$
C_{AO7_lm}	Logarithmic mean of the AO7 concentration at the inlet and at the outlet of the reactor	$mol.L^{-1}$
d_{pore}, $d_{pore,max}$, $d_{m,pore}$,	Respectively the pore diameter, maximum pore diameter, mean pore diameter	m
d_i, d_{lm}, d_o	Respectively the inside, logarithmic mean, and outside diameters of the fibers	m
D_{iso}	IPA density	-
D_{PTFE}	PTFE density	-
$D_{O3,m}$	Effective diffusion coefficient of ozone in the membrane	$m^2.s^{-1}$
$D_{O3,g}$	Diffusion coefficient of ozone in the gas phase	$m^2.s^{-1}$
$D_{Dissolved\ O3,w}$	Diffusion coefficient of ozone in the water	$m^2.s^{-1}$
$D_{AO7,w}$	Diffusivity of AO7 in the water	$m^2.s^{-1}$

D_K	Knudsen diffusion coefficient	$m^2.s^{-1}$
DOE	Design Of Experiments	-
E	Enhancement factor	-
E_{AL}	Limit acceleration factor	-
Ha	Hatta number	-
$H_{O_3,w}$	Partition coefficient of O_3 in water	-
K_L	Overall mass transfer coefficient	$m.s^{-1}$
$K_L a$	Overall mass transfer coefficient	s^{-1}
kc	Decomposition coefficient	s^{-1}
k_m, k_g, k_l	Mass transfer coefficient, respectively in the membrane, in the gas, and in the liquid	$m.s^{-1}$
k_l^r	Mass transfer coefficient in the liquid with a chemical reaction	$m.s^{-1}$
k_2	2nd order reaction constant of AO7 with dissolved ozone	$M^{-1}.s^{-1}$
l_m	Membrane thickness	m
M	Molar mass of ozone	$g.mol^{-1}$
MEB	Microscope Electronique à Balayage	-
$P_{breakthrough}$	Breakthrough pressure	Pa
PP	Polypropylene	-
PTFE	Polytetrafluoroethylene	-
PVDF	Polyvinylidene fluoride	-
Qgas, Qliq	Respectively the gas flow rate and the liquid flow rate	$L.h^{-1}$ or $m^3.s^{-1}$
R	Ideal gas constant	$J.K^{-1}.mol^{-1}$
R_{ov}	Overall resistance to the mass transfer	$s.m^{-1}$
R_g ,R_m, R_l	Respectively the gas, membrane, and liquid resistance to the mass transfer	$s.m^{-1}$
SEM	Scanning Electron Microscopy	-
T	Temperature	Kelvin
V_{tank}	Volume of the feed tank	m^3

w_{dry} , w_{wet}	Respectively the weight of the dry membrane and of the wet membrane	g
WWTP	Wastewater treatment plant	-

Objectifs et approche du Chapitre III

Le Chapitre I a mis en avant l'intérêt d'utiliser un contacteur membranaire lors des procédés d'ozonation pour le traitement tertiaire des eaux afin de lever les verrous identifiés lors de l'utilisation de procédés conventionnels, notamment un contrôle difficile de l'ozone diffusé et la formation non contrôlée de sous-produits issus des différentes réactions d'oxydation. Plus particulièrement, le contacteur membranaire semble être une technologie prometteuse, efficace, abordable pour une application d'élimination des micropolluants organiques tout en minimisant la quantité de bromates formés, et idéale dans le cadre de la réutilisation d'eau usée traitée.

La première étape de ce travail de thèse fût de caractériser complétement le transfert de l'ozone de la phase gaz vers la phase liquide dans un contacteur membranaire avec des fibres creuses en PTFE (polytétrafluoroéthylène). Le Chapitre I avait en effet mis en évidence la bonne résistance à l'ozonation au cours du temps de ce matériau polymère. Lors des essais expérimentaux, la configuration in/out a été utilisée, ce qui signifie que l'ozone était transféré depuis l'intérieur des fibres (in), où le gaz circulait, vers l'extérieur des fibres (out), où le liquide circulait. L'objectif était ainsi d'éviter tout colmatage des membranes (les fibres creuses ayant un diamètre inférieur à 1 mm) lors d'une application avec une eau réelle en sortie de traitement secondaire pouvant présenter une fraction particulaire ou colloïdale.

Dans un premier temps, le coefficient global de transfert K_La a été déterminé dans des conditions précises (débit de liquide, débit de gaz et concentration en ozone dans la phase gaz fixés) et comparé à ceux présentés dans la littérature pour des réacteurs conventionnels. La part de la résistance au transfert due à la membrane en a été déduite. Dans un second temps, l'impact de différents paramètres mis en évidence dans le Chapitre I (débit de liquide, débit de gaz et concentration initiale dans la phase gazeuse) a été examiné dans une matrice d'eau pure tamponnée à pH acide afin d'estimer uniquement le transfert physique de l'ozone, c'est-à-dire sans présence de réaction chimique dans la phase liquide ni de décomposition de l'ozone moléculaire. Enfin, l'ozonation d'une solution acide colorée avec de l'Acide Orange 7, choisi comme modèle de polluant organique, a été étudiée afin d'évaluer l'impact de l'ajout d'une réaction chimique dans la phase liquide sur le transfert d'ozone et ainsi de déterminer le facteur d'accélération engendré par cette réaction.

En parallèle, le vieillissement d'un des contacteurs utilisés a été examiné à l'aide de différentes méthodes de caractérisation, notamment grâce à l'analyse d'images réalisées par microscope électronique à balayage (MEB) par M. Didier Cot, à l'Institut Européen des Membranes.

De cette manière, ce travail contribue à une meilleure compréhension des procédés d'ozonation par contacteur membranaire pour la réutilisation d'eau usée traitée.

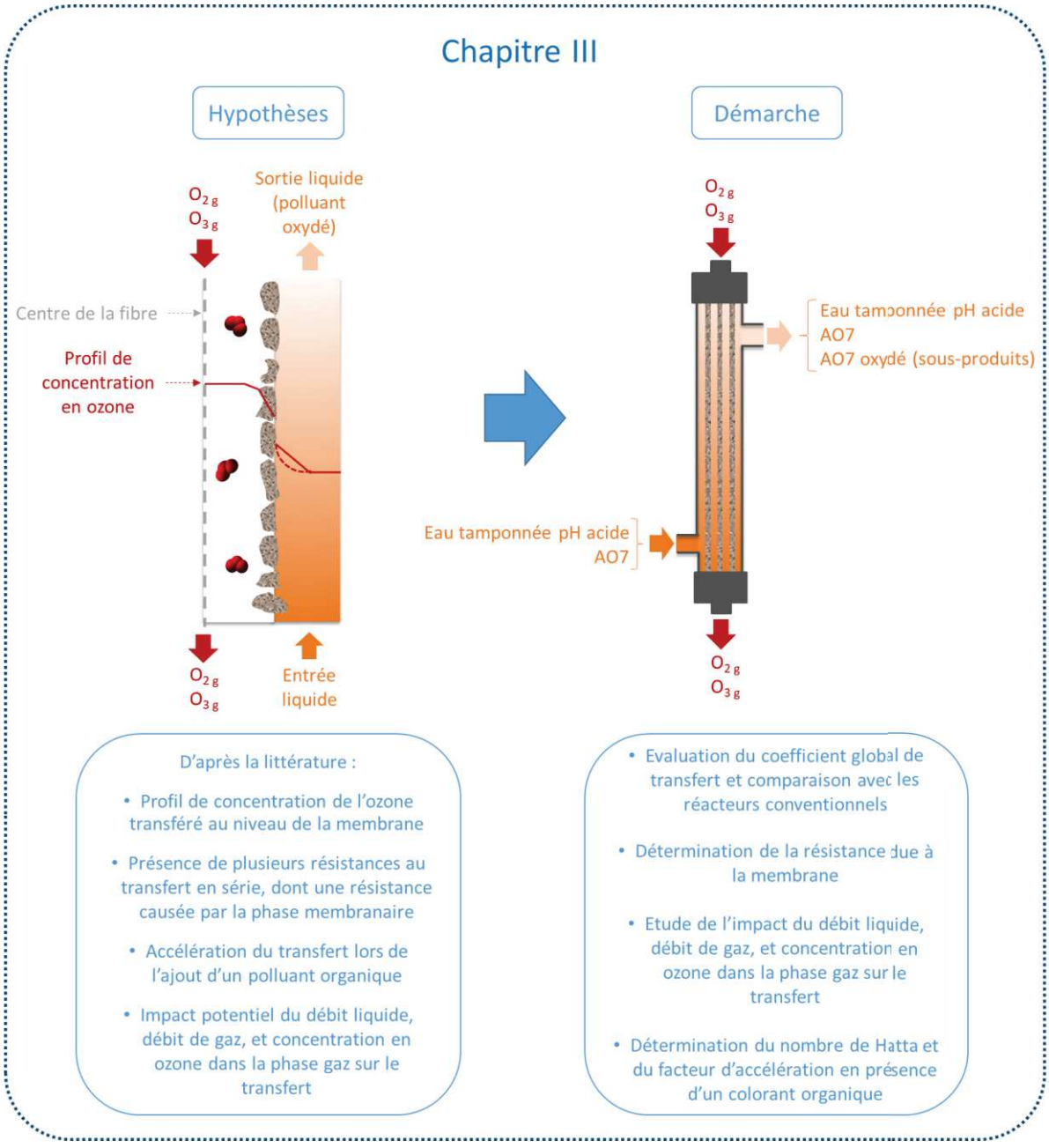
Chapitre III
Hypothèses
Démarche
$O_{2\,g}$
$O_{3\,g}$
Sortie liquide (polluant oxydé)
Centre de la fibre
Profil de concentration en ozone
Entrée liquide
Eau tamponnée pH acide
AO7
AO7 oxydé (sous-produits)
D'après la littérature :
• Profil de concentration de l'ozone transféré au niveau de la membrane
• Présence de plusieurs résistances au transfert en série, dont une résistance causée par la phase membranaire
• Accélération du transfert lors de l'ajout d'un polluant organique
• Impact potentiel du débit liquide, débit de gaz, et concentration en ozone dans la phase gaz sur le transfert
• Evaluation du coefficient global de transfert et comparaison avec les réacteurs conventionnels
• Détermination de la résistance due à la membrane
• Etude de l'impact du débit liquide, débit de gaz, et concentration en ozone dans la phase gaz sur le transfert
• Détermination du nombre de Hatta et du facteur d'accélération en présence d'un colorant organique

[1]

Evaluation of an ozone diffusion process using a hollow fiber membrane contactor

Alice Schmitt[a], Julie Mendret[a], Stephan Brosillon[a]

[a] IEM, University of Montpellier, CNRS, ENSCM, Montpellier, France

Published in Chemical Engineering Research and Design

Abstract

Conventional ozonation processes efficiently remove micropollutants in water treatment, but uncontrolled ozone dosing can produce problematic by-products. Bubbleless operation could help overcome this hurdle. To evaluate this alternative, ozonation was carried out using a polytetrafluoroethylene (PTFE) hollow fiber membrane contactor. The objective was to conduct an extensive characterization of the ozone transfer in an in/out configuration. The overall mass transfer coefficient K_La was determined and was higher than in bubble columns. The transfer resistance due to the membrane was estimated to be lower than 1%. The impact of several variables (liquid flowrate, gas flowrate, and ozone concentration) on the ozone transfer was studied. Ozone concentration was the variable that most increased ozone transfer, followed by the liquid flowrate and then to a lesser extent the gas flowrate. The impact of the presence of a reaction in the water was also evaluated using an organic dye (Acid Orange 7). The Hatta number and the acceleration factor were calculated, corresponding to a reaction that took place partially in the liquid film and in the liquid bulk. Finally, the impact of ozone on membrane material over time was evaluated.

Graphical abstract

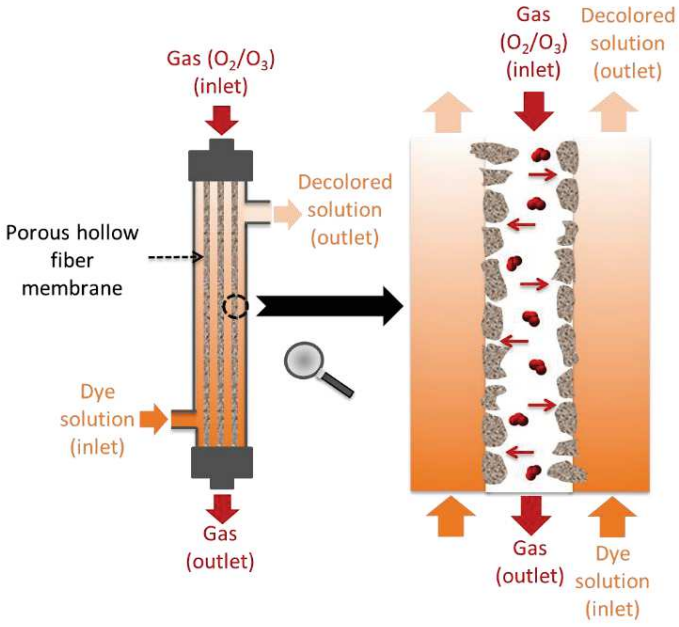

1. Introduction

Drinking water resources are precious and scarce. Their quality and quantities are decreasing significantly as the population rises. To preserve these resources and the water ecosystem, wastewater treatment plants (WWTPs) need to be upgraded by an advanced treatment to ensure the elimination of micropollutants, defined as harmful substances detectable in the environment at very low concentrations (ng.L^{-1} to µg.L^{-1}). Wastewater treatment plants are one of the main sources of organic micropollutants released into the aquatic receiving environment. The micropollutants released by WWTPs are mostly active ingredients of pharmaceuticals (Bolong et al., 2009). Activated carbon adsorption and ozonation are two processes that can used to treat organic micropollutants in wastewater (Margot et al., 2013). The efficiency of activated carbon depends on dose of powdered activated carbon, regeneration of activated carbon granules, contact time, and the presence of natural organic matter, which can diminish micropollutant removal (Guillossou et al., 2020; Luo et al., 2014). Ozonation is effective and economic, easy to automate, and clean to handle. It offers a chemical way to remove 90% of emerging contaminants and can be simply incorporated into both existing and new applications (Prieto-Rodríguez et al., 2013; Snyder et al., 2006). During ozonation, a targeted substance is degraded by direct and indirect oxidation (unlike activated carbon, which only adsorbs). In addition, ozone is a disinfectant that can be used to inactivate some of the pathogens present in wastewater. Ozonation is thus a very appealing technology for water reuse, and it can be used coupled to other technologies in a multiple-barrier concept. However, ozone in water treatment is generally bubbled through diffusers. Bubbling has drawbacks, such as stripping of volatile organic compounds, high reactor footprints, mass transfer limitations (whence high energy costs) and foaming. Another disadvantage is the release, in some cases, of by-products of the oxidation reaction that may be more hazardous than the original pollutants (Gogoi et al., 2018; Schlüter-Vorberg et al., 2015). This concern often stems from uncontrolled ozone dosage. To overcome all these problems, the recent use of membrane contactors for ozone diffusion in water treatment offers an attractive solution, by virtue of its bubbleless operation (Schmitt et al., 2020). Membrane contactors have recently emerged as a good alternative to classic reactors for the transfer of gas to a liquid phase (Pabby and Sastre, 2013), and to control the dosing of ozone during ozonation processes by injecting it across the membrane through multiple dosing points (Merle et al., 2017). At neutral pH, ozone decomposition into hydroxyl radicals will allow the removal of a wider range of micropollutants. Simultaneously, the use of a membrane contactor for ozonation of water containing bromides may minimize the formation of bromates (regulated in drinking water because of their carcinogenic potential), through many ozone dosing points, leaving less residual ozone. Hence the use of this method for applications such as micropollutant treatment and bromate minimization appears very promising.

Membrane contactor technology for ozonation of water is not yet well described, and more work is needed to fully characterize the process. When ozone contactors are used, two configurations are possible. In one, the liquid flows inside the membrane, and the gas in the shell (i.e., outside the membrane). In the other, phases (liquid and gas) are reversed. Membranes can have various geometries: plane, tubular, capillary or hollow fiber. These last three forms are often used to transfer gas (e.g., ozone) to water, and differ in their pore diameter. Hollow fiber membranes have very small diameters (internal diameter < 0.5 mm), giving very large exchange surface areas per unit volume (Schmitt et al., 2020). To the best of the authors' knowledge, only one article to date reports on an experimental investigation of ozone transfer through a membrane contactor (tubular membrane) with the gas circulating inside the fibers and the liquid in the shell (i.e., in/out configuration) (Wenten et al., 2012). This configuration offers the main advantage of a lower risk of membrane fouling thanks to the circulation of the gas in the fibers whose the diameter is smaller than 1 mm instead of the treated wastewater which could have suspended matter. Wenten et al. had already shown that this configuration could produce a better oxidation of iodide into iodine, for instance. The authors suggested that the poorer result obtained with the out/in configuration could be due to a reaction between ozone and membrane ceramic material. It would thus be useful to confirm this observation and extend it, both for components other than iodide, and for other membranes such as polymer membranes, which are less costly and easier to use owing to their robustness. This was the objective of the present work.

Polymer hollow fiber membranes were used instead of the ceramic tubular membranes in Wenten et al. The overall goal of this work was to fully characterize the transfer of ozone from the gas phase to the liquid phase in an in/out hollow fiber membrane contactor. The aim was to determine (i) the impact of several operating variables (liquid flow rate, gas flow rate, ozone concentration in the gas mix), (ii) the process efficiency for the abatement of an organic dye (Acid Orange 7) as model solution, and (iii) the effect of the presence of ozone on membrane durability. This work thus contributes to a better understanding of the ozonation process for wastewater reuse using membrane contactors.

2. Materials and methods

2.1. Membrane contactor technology

The membrane contactor used in this work was supplied by Polymem (France). Its characteristics are listed in Table 2. Gas circulates inside the fibers and liquid in the shell by counter-current flow (Figure 16.b). The hollow fibers were made of polytetrafluoroethylene (PTFE), known to be highly ozone-resistant over time (Bamperng et al., 2010). The hollow fiber form enables a very compact process through a large exchange surface area.

Table 2. Membrane contactor technical specifications.

PTFE fibers			
Number *	65	Effective length (cm) *	60
Inside diameter (mm) *	0.45	Effective outside surface (m^2)	0.107
Outside diameter (mm) *	0.87	N_2 permeance (GPU) *	33,904
Porosity [a]	0.58	Tortuosity [b]	3.47
Liquid volume (m^3) [c]	3.63×10^{-5}	Specific exchange surface *a* (m^2/m^3) [d]	2,948
Stainless steel shell			
Inside diameter (mm) *	9.5	Packing fraction *	54.5%

** Values specified by the manufacturer (Polymem, France)*

The membrane porosity ε ([a]) was determined gravimetrically (Sartorius CPA 225D balance), by measuring the mass of isopropanol (IPA) inside the membrane pores (Wang et al., 2010). The porosity was calculated as:

$$\boldsymbol{\varepsilon} = \frac{(\boldsymbol{w_{wet} - w_{dry}})/\boldsymbol{D_{iso}}}{\frac{\boldsymbol{w_{wet} - w_{dry}}}{\boldsymbol{D_{iso}}} + \boldsymbol{w_{dry}}/\boldsymbol{D_{PTFE}}} \text{ , [22]}$$

where w_{wet} is the weight of the wet membrane, w_{dry} is the weight of the dry membrane, D_{iso} is the IPA density, and D_{PTFE} is the polymer density.

The tortuosity factor τ ([b]) was estimated by the porosity-tortuosity relationship defined by (Iversen et al., 1997) as:

$$\boldsymbol{\tau} = \frac{(\boldsymbol{2-\varepsilon})^2}{\boldsymbol{\varepsilon}} \text{ , [23]}$$

The liquid volume ([c]) and the specific exchange surface area ([d]) were calculated from the shell and fiber properties given by the manufacturer.

When using a membrane contactor, a very important variable to check is the transmembrane pressure. If the ratio of the pressure on the liquid side to the pressure on the gas side is higher than the "breakthrough pressure", wetting of the membrane pores occurs (i.e., the liquid penetrates the membrane pores), lowering the mass transfer. The breakthrough pressure (relative, in Pa) is defined by the Young-Laplace equation as:

$$\boldsymbol{P_{breakthrough}} = \frac{\boldsymbol{4 \times \gamma \times \cos\theta}}{\boldsymbol{d_{pore,max}}} \text{ , [24]}$$

where γ is the surface tension of water with air (= 73 x 10^{-3} $N.m^{-1}$ at 20 °C), θ is the contact angle between the membrane and the water (radians), and $d_{pore,max}$ is the maximum pore diameter (m) (determined from fiber SEM pictures analyzed with ImageJ® software).

In this work, the breakthrough pressure was estimated to be 0.4 bar (taking the contact angle between the material and the water to be greater than 102°).

Conversely, if the ratio of the pressure on the gas side to the pressure on the liquid side is higher than the "bubble pressure", there is ozone dispersion in water by bubbles. In this case, one of the main advantages of the membrane contactor, which is to transfer ozone uniformly to the water to be treated in a bubbleless operation, is lost. The bubble pressure was experimentally determined with the following method, adapted from the method presented by Khayet and Matsuura (Khayet and Matsuura, 2001). A special membrane contactor was produced for this test, with PTFE fibers provided by the same supplier (Polymem) as for the membrane contactor used in the experiments, but without a shell. Oxygen circulated inside the membrane fibers immersed in water. The oxygen pressure was then gently increased stepwise. The bubble pressure was considered attained when the first bubble was observable. With this method, the bubble pressure was estimated to be about 0.1 bar. Hence the transmembrane pressure (i.e., the difference between the pressure on the liquid side and the pressure on the gas side) had to stay between −0.1 and 0.4 bar.

To evaluate the hydrophobicity of the fibers before and after use, contact angle was measured using the sessile drop method with a GBX meter (Digidrop, France) equipped with image analysis software (Visiodrop). First, fibers were fixed on a glass plate. A droplet of water (1 µL) was then deposited on the film surface with a precision syringe. The method is based on image processing and curve fitting for contact angle measurement from a theoretical meridian drop profile, determining two contact angles between the baseline of the drop and the tangents at the drop boundary (i.e., one angle is measured on the right and one on the left, the final contact angle being the average of the two values). Each measurement was repeated three times.

Scanning electron microscopy (SEM) pictures were obtained using a Hitachi S-4800 instrument to evaluate the state of the fibers and their deterioration after use. Samples were previously metalized with a thin layer of platinum to improve their electronic conductivity.

2.2. Ozonation: pilots and methods

2.2.1. Description of the ozonation pilot with membrane contactor – liquid in closed loop

Figure 16.a depicts the experimental set-up used for the ozonation process. When the liquid was in a closed loop, this ozonation lab-scale pilot consisted of a membrane contactor (see Section 2.1 for description) continuously fed by an ozone generator (BMT 803 N) from a lab-grade pure oxygen tank. Before circulating in the gas side of the membrane contactor, the ozone was diluted with the oxygen to achieve the desired gas flowrate. An ozone gas analyzer (BMT 964) was used to monitor the gas

ozone concentration ($C_{O3,gas,in}$) after dehumidification. Two electrovalves connected to a computer were used to determine the desired concentration of the oxygen/ozone mixture.

The liquid flowed into the pilot from a stirred 1.5 L glass tank under thermostatic control (20 °C). During the experiment, an agitator was used to homogenize dissolved ozone and dye concentrations in the tank. A peristaltic pump (Watson Marlow 323) was used for the liquid circulation. Two taps (upstream and downstream of the membrane contactor) were used for sampling.

Ozone was transferred from the gas phase of the membrane contactor to the liquid phase, along a concentration gradient. The membrane in the contactor acted as a barrier.

The main advantage of this configuration was to increase the residence time in the membrane contactor and has thus been used for the K_La determination (Section 3.1).

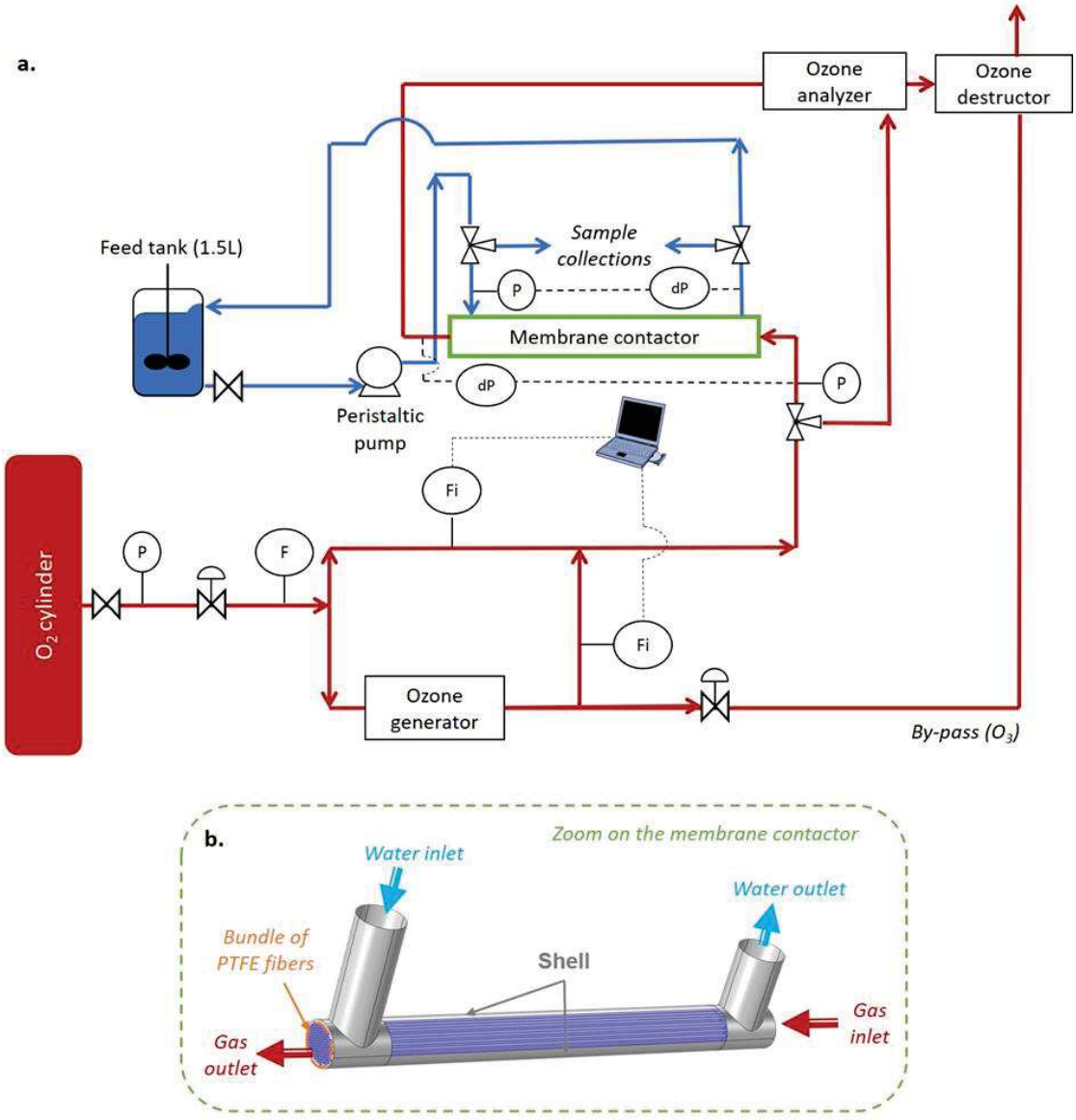

Figure 16. a. Flowsheet of the ozonation pilot - liquid in closed loop - gas in open circuit (red: gas stream, blue: liquid stream); b. Zoom on the configuration of the membrane contactor.

2.2.2. Description of the ozonation pilot with membrane contactor – liquid in open circuit

The ozonation pilot with the liquid flowing in an open circuit was almost the same as in the closed loop. The main difference was that the liquid circulated only once in the membrane contactor. The liquid was then recovered in a container with KI solution to prevent the ozone degassing. To achieve the steady-state values, a larger feed tank was used (30 L). The tank was made of stainless steel, stirred, and under thermostatic control (20 °C). The main advantage of this configuration was the simplification of the mass balances in comparison to that with the liquid in closed loop. Therefore, this configuration has been used for the study of the impact of several variables on the ozone transfer and for the experiments with AO7 (Sections 3.3 and 3.4).

2.2.3. Description of the ozonation pilot with bubble column (batch reactor)

To compare the results obtained with the membrane contactor with those obtained with a conventional process, a semi-batch bubble reactor was also used (see Figure 17Figure 15.). A 4 L glass reactor was stirred using an agitator to homogenize the liquid and kept under thermostatic control (20 °C). A recirculating pump was used for sampling. As in the previously described ozonation pilot with the membrane contactor, an oxygen cylinder fed the gas circuit. A gas flowmeter was then used to regulate gas flowrate upstream of an ozone generator (BMT 803 N). The ozone generator was used to convert part of the pure oxygen into ozone. The amount of ozone produced by the generator could be manually regulated with a setting knob. The gas mixture obtained therefore comprised ozone and oxygen. An electrovalve connected to a computer was used to set the gas flowrate and obtain the desired concentration of the gas mixture. Two options were then possible. The first was for the gas mixture to flow through the by-pass and be analyzed with an ozone analyzer (BMT 964) and then processed in an ozone destructor, in the same way as with the ozonation pilot with the membrane contactor. The ozone concentration given by the analyzer was then the ozone concentration in the gas at the inlet to the process. The other option was for the gas mixture to flow inside the semi-batch reactor with a porous diffuser, and then be analyzed and deozonated. The ozone concentration given by the analyzer was then the ozone concentration in the gas at the outlet from the bubble column. The analyzer was preceded by a dehumidifier to remove any humidity in the gas and protect the device. The residual ozone was destroyed by the ozone destructor using active carbon.

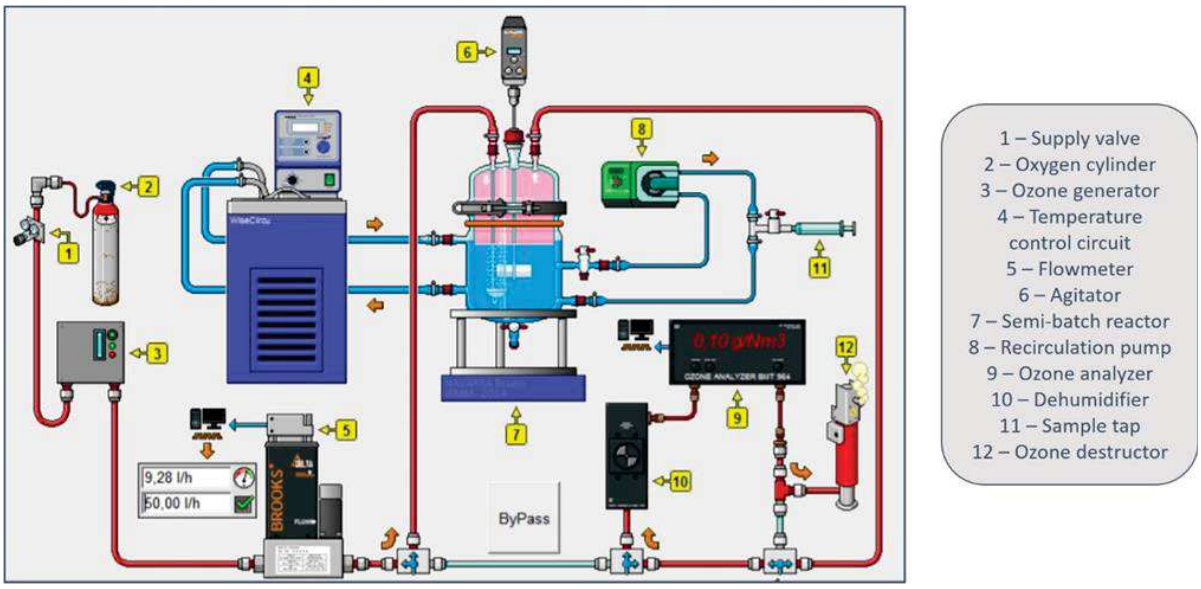

Figure 17. Scheme of the ozonation pilot with bubble column.

2.2.4. Design of experiments: determination and interpretation

The analysis of the experimental data obtained with a 2^3 factorial design of experiments (DOE) was conducted to compare the significance and the impact of three variables on the ozone transfer, namely the liquid flow rate (Q_{liq}), the gas flow rate (Q_{gas}), and the ozone concentration at the gas inlet (C_{O3}). For each variable, three levels were tested (a minimum, a central point, and a maximum). Variables and their minima and maxima were chosen after a preliminary study of the literature, and were adapted to the capacity of the experimental pilot used (Schmitt et al., 2020). Minitab 19® software was used to establish and interpret the DOE.

2.2.5. Ozone analysis

The indigo method (Bader and Hoigné, 1982) was used to determine the dissolved ozone concentration in the liquid phase. Once the experiment had started, the ozone gas analyzer (BMT 964) was used to analyze the gas ozone concentration at the outlet from the membrane contactor ($C_{O3,gas,out}$) (after dehumidification).

2.2.6. Inhibition of hydroxyl radicals

During the ozonation reaction, several mechanisms act in parallel. Dissolved ozone can both react directly with the pollutant, or indirectly due to its decomposition into hydroxyl radicals (Roustan, 2003; Schmitt et al., 2020). The different matrices used in this work were buffered at acid pH (pH ≈ 3) to limit ozone decomposition (i.e., decomposition of molecular ozone into hydroxyl radicals), and therefore facilitate understanding of the ozone transfer. The buffered solution used was made by dissolving 1.2

$g.L^{-1}$ of sodium dihydrogen phosphate (NaH_2PO_4) in deionized water and then adjusting the pH with a few milliliters of 84% phosphoric acid (H_3PO_4). The pH of the final buffered solution was 2.2.

2.3. Matrix characterization

- **Buffered water**

Buffered water was made by mixing demineralized water (total organic carbon < 30 ppb) and the buffered solution described in the section "Inhibition of the hydroxyl radicals" to adjust the pH. The final pH of the matrix was 3.

- **Solution colored with Acid Orange 7 (AO7)**

Acid Orange 7 (AO7) ($C_{16}H_{11}N_2NaO_4S$, purity > 85 %), also called Orange II, was obtained from Sigma and used without further purification. AO7 was chosen as a model for organic pollutants owing to its high reactivity with molecular ozone and ease of analysis. AO7 concentration was measured in a 1 cm plastic cuvette using a UV-VIS spectrophotometer (UV-2401PC, Shimadzu, Japan) at wavelength 484 nm (at which the absorption of AO7 is maximum).

2.4. Theoretical approach to ozone mass transfer in a membrane contactor

Figure 18 depicts the mass transfer in a gas-liquid membrane contactor. The membrane is hydrophobic, and so membrane pores are filled by the gas (i.e., non-wetted). The compound of interest (i.e., the ozone) encounters three flow resistances in series going from the bulk of the gas phase to the bulk of the liquid phase: the gas film (the gas-membrane boundary layer), the membrane, and the liquid film (the membrane-liquid boundary layer). At the interface between gas and liquid, the concentration profile is discontinuous and obeys Henry's law (Gabelman and Hwang, 1999).

Figure 18. Ozone concentration profile in a membrane contactor (adapted from Schmitt et al., 2020).

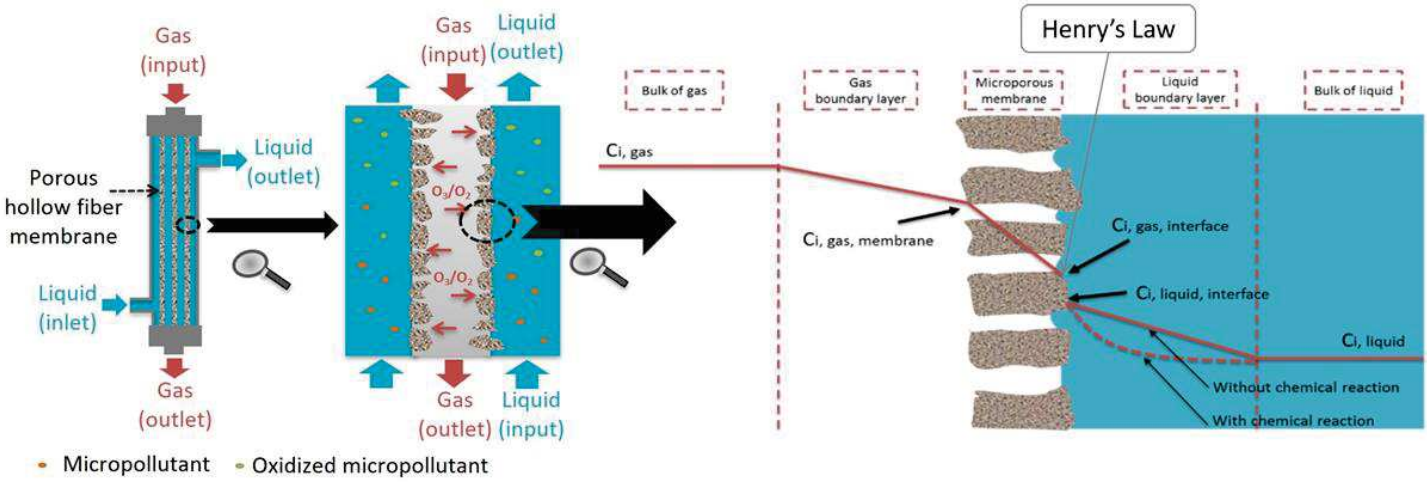

The overall mass transfer resistance, relative to the liquid side, is the sum of the individual mass transfer resistance in each phase and can be defined as $R_{ov} = 1/K_L$. For a membrane contactor where the liquid flows in the shell (i.e., outside the membrane) and the gas flows inside the fibers, it can be described as (Kukuzaki et al., 2010):

$$\frac{\mathbf{1}}{\boldsymbol{K_{\mathrm{L}}}\times\boldsymbol{A_{\mathrm{outer}}}} = \frac{\mathbf{1}}{\boldsymbol{H_{O_3,w}}\times\boldsymbol{k_{\mathrm{g}}}\times\boldsymbol{A_{\mathrm{inner}}}} + \frac{\mathbf{1}}{\boldsymbol{H_{O_3,w}}\times\boldsymbol{k_{\mathrm{m}}}\times\boldsymbol{A_{\mathrm{lm}}}} + \frac{\mathbf{1}}{\boldsymbol{k_l}\times\boldsymbol{A_{\mathrm{outer}}}}, \quad [25]$$

where K_L is the overall mass transfer coefficient (m.s^{-1}), k_m, k_g, k_l are the mass transfer coefficient in the membrane, in the gas, and in the liquid respectively (m.s^{-1}), A_{outer}, A_{lm}, A_{inner} are the outer, logarithmic mean, and inner surface area of the membrane respectively (m^2), $H_{O_3,w}$ is the partition coefficient of O_3 in water (dimensionless), which can be described by Henry's law as $H = (C_{O3,g}/C_{O3,l})$eq: for the dissolution of ozone in water, its value is 3.823 (mg/L)/(mg/L) at 295 K (Atchariyawut et al., 2009) and is reduced to 2.907 at 295 degrees Kelvin (Roustan, 2003).

After simplification of Equation 4, the global mass transfer coefficient can be expressed as:

$$\frac{\mathbf{1}}{\boldsymbol{K_{\mathrm{L}}}} = \frac{\boldsymbol{d_{\mathrm{o}}}}{\boldsymbol{H_{O_3,w}}\times\boldsymbol{k_{\mathrm{g}}}\times\boldsymbol{d_{\mathrm{i}}}} + \frac{\boldsymbol{d_{\mathrm{o}}}}{\boldsymbol{H_{O_3,w}}\times\boldsymbol{k_{\mathrm{m}}}\times\boldsymbol{d_{\mathrm{lm}}}} + \frac{\mathbf{1}}{\boldsymbol{k_l^r}}, \quad [26]$$

where d_i, d_{lm}, d_o are respectively the inside, logarithmic mean, and outside diameters of the fibers (m). In Equation 25, describing the overall mass transfer from the resistance-in-series model, when a chemical reaction occurs, k_l can be replaced by k_l^r, defined as $k_l^r = Ek_L$. E is the enhancement factor, described by $E = \frac{J_{O_3 \text{ with reaction}}}{J_{O_3 \text{ without reaction}}}$. It takes into account the effect of the reaction on the mass transfer, increasing by the rise in the concentration gradient (Nguyen, 2011). The resistance on the liquid side is therefore reduced by the presence of a chemical reaction in the liquid.

The membrane mass coefficient can be calculated from the membrane structure properties (Bamperng et al., 2010; Mavroudi et al., 2006) as:

$$\boldsymbol{k_{\mathrm{m}}} = \frac{\boldsymbol{D_{\mathrm{O3,m}}}\times\boldsymbol{\varepsilon}}{\boldsymbol{\tau}\times\boldsymbol{l_{\mathrm{m}}}}, \quad [27]$$

where $D_{O3,m}$ is the effective diffusion coefficient of ozone in the membrane (m^2.s^{-1}) and l_m the membrane thickness (m). Inside the membrane pores, gas can flow by molecular diffusion and Knudsen diffusion. $D_{O3,m}$ can therefore be expressed as Equation 7 (Jansen et al., 2005).

$$\boldsymbol{D_{\mathrm{O3,m}}} = \frac{\mathbf{1}}{\frac{\mathbf{1}}{\boldsymbol{D_{\mathrm{O_3,g}}}}+\frac{\mathbf{1}}{\boldsymbol{D_{\mathrm{K}}}}} = \frac{\mathbf{1}}{\frac{\mathbf{1}}{\boldsymbol{D_{\mathrm{O_3,g}}}}+\frac{\mathbf{1}}{\frac{\boldsymbol{d_{\mathrm{pore}}}}{\mathbf{3}}\sqrt{\frac{\mathbf{8}\boldsymbol{RT}}{\boldsymbol{\pi M}}}}}, \quad [28]$$

where D_K is the Knudsen diffusion coefficient, defined by $D_K = \frac{d_{m,pore}}{3}\sqrt{\frac{8RT}{\pi M}}$ ($m^2.s^{-1}$), $D_{O3,g}$ is the diffusion coefficient of ozone in the gas phase ($m^2.s^{-1}$) (= 2.00×10^{-5} $m^2.s^{-1}$ at 20 °C (Bamperng et al., 2010)), T is the temperature (293.15 degrees Kelvin), M is the molar mass of ozone (47.998 $g.mol^{-1}$, R is the ideal gas constant (8.3145 $J.K^{-1}.mol^{-1}$, and $d_{m,pore}$ is the mean pore diameter (m) (0.777 µm for the membrane contactor used).

This last value (the average membrane pore size) was determined by liquid-gas displacement porometry, using a PMR-2000-LL-R porometer (IFTS-France). The pores of the sample were filled with IPA during a first wetting step. Nitrogen gas was then fed through the membrane and its flowrate was measured as a function of the applied pressure. Pore dimension was next calculated by applying Laplace's law, which is expressed in Equation 8.

$$\boldsymbol{\Delta P = \frac{4\gamma \cos\theta}{d_{pore}}}, \text{ [29]}$$

where γ is the interfacial tension of IPA, ΔP is the differential of applied pressure, θ is the contact angle between the membrane and the IPA, and d_{pore} is the pore diameter.

3. Results and discussion

3.1. Determination of the global transfer coefficient K_La

The overall material balance was first established. The conditions of liquid flow strongly impact the liquid transfer coefficient, and thereby the value of K_La, which represents a sum of the different coefficients. Determining K_La is thus essential to compare several reactors. Turbulent flow of gas and liquid phases makes the description of the velocity fields very complicated, and so overall coefficients are indispensable for the mass balance equation. In addition, the modeling of the ozone transfer through a membrane contactor with computational fluid dynamics software could provide a better comprehension of the local phenomena occurring, and so enable optimization of the contactor design for a better transfer.

To determine the overall transfer coefficient K_La, experiments were carried out with recirculation of the liquid (see Figure 16.a) to better visualize the increase in dissolved ozone concentration during the transitional regime. Pure water buffered at acid pH was used to avoid decomposition of the molecular ozone into hydroxyl radicals. We note that pH variation from 1 to 9 does not impact the K_La value (Ferre-Aracil et al., 2015; Kuosa and Kallas, 2010). The material balance is described below; the notation is presented in Figure 19.

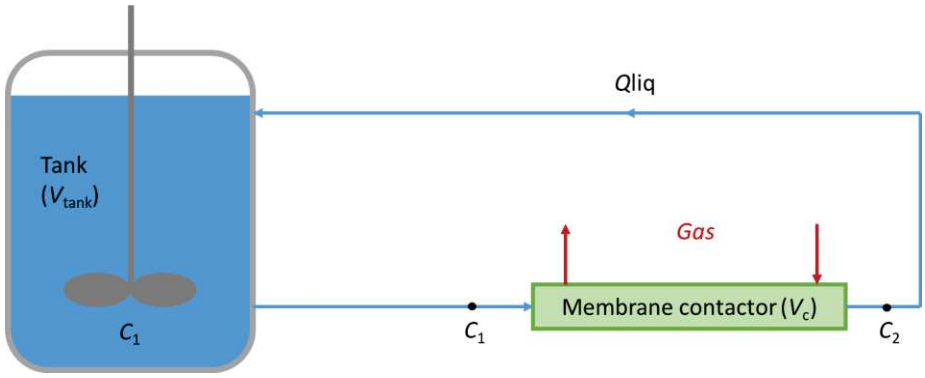

Figure 19. Simplified scheme of the process for K_La determination.

The mass balance in the tank cannot be neglected to determine K_La as in Equations 30 and 31.

$$\boldsymbol{Q_{liq} C_2 dt = Q_{liq} C_1 dt + V_{tank} dC_1}\,, \quad [30]$$

$$\boldsymbol{Q_{liq}(C_2 - C_1)dt = V_{tank} dC_1}\,, \quad [31]$$

where Q_{liq} is the liquid flowrate, C_1 is the dissolved ozone concentration at the membrane contactor inlet, C_2 is the dissolved ozone concentration at the membrane contactor outlet, and V_{tank} is the volume of the feed tank, which is agitated.

The mass balance on the membrane contactor, where the ozone is transferred to the water, is then specified in Equation 32.

$$\boldsymbol{Q(C_2 - C_1) = K_L a\, V_c\, \Delta C}\,, \quad [32]$$

Where

$$\boldsymbol{\Delta C = C^* - \overline{C} = \frac{C_2^* - C_1^*}{\ln\left(\frac{C_2^*}{C_1^*}\right)} - \overline{C} \approx \frac{C_2^* - C_1^*}{\ln\left(\frac{C_2^*}{C_1^*}\right)} - C_1}\,. \quad [33]$$

Equation 34 was established by combining Equations 32 and 33. After integration, the overall transfer coefficient can be deduced (Equation 35). Initially, there is no dissolved ozone in the liquid phase (i.e., boundary condition is $C(t_0) = 0$).

$$\boldsymbol{K_L a\, V_c\, \Delta C\, dt = V_{tank} dC_1}\,, \quad [34]$$

$$\boldsymbol{\ln(C^* - C_1) = \frac{-K_L a\, V_c}{V_{tank}} t + \ln(C^*)}\,. \quad [35]$$

The value of the ozone K_La in pure water with no reaction was found to be 1.412×10^{-1} s^{-1}, neglecting the coefficient for the decomposition of molecular ozone into hydroxyl radicals owing to the acid pH of the water (pH = 3). The decomposition coefficient kc at this pH is 4×10^{-4} s^{-1} (Roth and Sullivan,

1981). In conventional ozonation processes, K_La is estimated at between 5×10^{-3} and 2.7×10^{-2} s^{-1} (for bubble columns) (Beltrán et al., 1997; Roustan et al., 1996). The mass transfer obtained in this study is therefore better than with bubble columns.

The specific exchange surface a, calculated from the volume of liquid in the shell of the contactor and the effective exchange surface, is about 2948 $m^2.m^{-3}$. Therefore, K_L was estimated to be 4.789×10^{-5} $m.s^{-1}$. Taking into account kc, K_L is 4.775×10^{-5} $m.s^{-1}$, only 0.3% of relative deviation compared to the previous value.

This value is higher than those presented by Pines et al. for a similar Reynolds number (about 400), which were about 2×10^{-5} $m.s^{-1}$ depending on the membrane material used (Pines et al., 2005). However, Pines et al. presented higher values of K_L at higher Reynolds numbers (e.g., $K_L = 7.6 \times 10^{-5}$ $m.s^{-1}$ at Re = 2000). This result proves the presence of a significant transfer resistance on the liquid side and highlights the importance of the reduction of liquid film thickness, with, for example, a greater turbulence, to optimize the ozone transfer.

Owing to the membrane resistance and to the low pressure difference between the two phases, K_L obtained with membrane contactors is lower than K_L obtained with bubble reactors (Leiknes et al., 2005). However, the main advantage of this new process is the specific exchange surface (a, in $m^2.m^{-3}$) which is particularly high in a membrane contactor. Consequently, the mass transfer K_La remains competitive with conventional processes. To achieve a larger specific exchange surface, a large quantity of membrane is required, leading to a high membrane construction cost before the ozonation process can be set up. However, a significantly lower operating cost is expected after the installation owing to the gas recycling. Because higher consumption of the produced ozone is achieved, less ozone needs to be generated (ozone production is expensive), and an ozone destructor is no longer needed (Stylianou et al., 2015b). In addition, the gas is supposed to be dry at the outlet of the contactor and then could be injected in the ozone generator. In this study, recycling the residual ozone at the gas outlet could lead to an economy of production of about 10 $g.Nm^{-3}$ of gaseous ozone and should have been complemented with newly generated ozone to achieve the desired concentration.

The overall transfer coefficient K_L depends mostly on the liquid flow conditions. As a consequence, this coefficient will be used later to study the ozone transfer with a reaction (i.e., chemical reaction with organic matter, such as a dye or organic micropollutants or decomposition of molecular ozone), both in open and closed liquid circulation and at the same liquid flowrate.

3.2. Determination of the membrane transfer coefficient and of the resistance induced by the membrane

The membrane transfer coefficient was determined by the method described in Section 2.4. The intermediate calculations and the final value of k_m are presented in Table 3 and compared with the results obtained in the study of Bamperng et al (Bamperng et al., 2010).

Table 3. Comparison of membrane mass transfer coefficients.

Membrane material	ε	τ	d_p (µm)	l_m (m)	$D_{O3,g}$ (m².s⁻¹)	D_K (m².s⁻¹)	$D_{O3,m}$ (m².s⁻¹)	k_m (m.s⁻¹)	Source
PTFE	0.58	3.48	0.78	2.10×10^{-4}	2.00×10^{-5}	2.95×10^{-6}	2.57×10^{-6}	0.20×10^{-2}	*This study*
PTFE	0.40	6.40	0.30	1.86×10^{-4}	2.08×10^{-5}	3.64×10^{-5}	1.32×10^{-5}	0.44×10^{-2}	*Bamperng et al., 2010*
PVDF	0.75	2.08	0.20	1.75×10^{-4}	2.08×10^{-5}	2.43×10^{-5}	1.12×10^{-5}	2.31×10^{-2}	*Bamperng et al., 2010*

The diffusivity of ozone in the membrane obtained in this work was one order of magnitude lower than in the study of Bamperng et al., even for a similar material (PTFE). This emphasizes the importance of the structural material used. More specifically, these results showed the impact of the membrane thickness on the ozone transfer in the membrane. The porosity and the pore diameter were higher in this work, and still led to a lower final transfer coefficient. The notable difference between the k_m values obtained can therefore be explained by the thickness difference.

Considering the overall resistance $R_{ov} = \frac{1}{K_L} = R_g + R_m + R_l$, the membrane resistance (R_m) and the part of the overall resistance due to the membrane (R_m/R_{ov}) were calculated from Equation 4. The membrane resistance was found to be 1.87×10^2 s.m^{-1}, less than 1% of the overall resistance. This percentage is the same as that found by Hasanoğlu et al. in their work on ammonia extraction with a hollow fiber membrane contactor (Hasanoğlu et al., 2013). By contrast, Khaisri et al. estimated this percentage at 40% in their study on CO_2 absorption with a PTFE hollow fiber membrane contactor (Khaisri et al., 2009). However, they assumed that membrane pores were partially wetted, leading to a higher membrane resistance than with non-wetted pores. The authors also compared three different membrane materials – PTFE, PP (polypropylene), and PVDF (polyvinylidene fluoride). The lowest membrane resistance was obtained for the PTFE material. We note that the method used to determine membrane resistance was not the same as in our work (the Wilson plot method was used).

In this study, due to the low proportion of the membrane in the overall resistance, the impact of the membrane thickness on the overall resistance is very restricted because of the dominating liquid side resistance. However, Bein et al. highlighted in a previous study that if it was generally the case for the hydrophobic fluoropolymers, it was not for inorganic or hydrophilic materials like for instance for

PDMS (polydimethylsiloxane), hydrophilic PVDF, or α-Al2O3 (Bein et al., 2021). With these materials, the membrane resistance can be significant, and thus the membrane thickness becomes a key parameter.

In addition, the resistance in the gas phase could be neglected relative to the resistance in the liquid phase, owing to the ozone diffusion coefficient in the gas phase, which is 4 orders of magnitude higher than in the water ($D_{\text{Dissolved O3,w}}$ = 1.708 × 10^{-9} $m^2.s^{-1}$ at 20 °C (Johnson and Davis, 1996), $D_{O3,g}$ = 1.00 × 10^{-5} $m^2.s^{-1}$ at 20 °C (Bamperng et al., 2010)). Therefore, most of the mass transfer resistance is on the liquid side, highlighting the key role of the liquid flow when using a membrane contactor for a gas liquid absorption application. This result agrees with the conclusion of Phattaranawik et al. in their study on mass transfer in a flat-sheet membrane contactor with ozonation: the ozone mass transport is controlled by the mass transfer resistance in the liquid film (Phattaranawik et al., 2005).

3.3. Study of the ozonation of pure water through a membrane contactor: impact of several variables on the ozone transfer

The analysis of the experimental data obtained with a 2^3 factorial design of experiments (DOE) was conducted to compare the significance and the impact of three variables on the ozone transfer, namely the liquid flow rate (Q_{liq}), the gas flow rate (Q_{gas}), and the ozone concentration at the inlet to the gas phase (C_{O3}). The DOE described in Table 4 was first followed. The experiments were carried out with the liquid phase in open circuit.

Table 4. DOE for the study of ozone transfer in buffered pure water.

Test number	Q_{liq} ($L.h^{-1}$)	Q_{gas} ($L.h^{-1}$)	C_{O3} ($g.Nm^{-3}$)
1	75	30	30
2	56.6	30	30
3	75	8	30
4	56.6	8	30
5	75	30	15
6	56.6	30	15
7	75	8	15
8	56.6	8	15
9	65.8	19	22.5
10	65.8	19	22.5
11	65.8	19	22.5

The mean response obtained for each experiment, corresponding to the ozone transferred from the gas phase to the liquid phase, was plotted on the Figure 20. This dose was calculated using two different methods. The first was a mass balance on the gas phase (i.e., the difference between the quantity of ozone at the inlet and at the outlet of the membrane contactor). The second was the

determination of the dissolved ozone concentration in the liquid phase. Each experiment was at least duplicated, and the error bars correspond to the standard deviations.

Systematically, experiments were conducted at acid pH using a buffered solution (see Section 2.3), thus avoiding the decomposition of molecular ozone into hydroxyl radical. Pure water was used (TOC < 200 ppb), thus avoiding the reaction of dissolved ozone with substances in the liquid phase. Consequently, the result (i.e., the transferred ozone) is expected to be the same whichever method is used. Consistent results were obtained with the two methods. The method of the mass balance on the gas phase was chosen for the statistical analysis of the data.

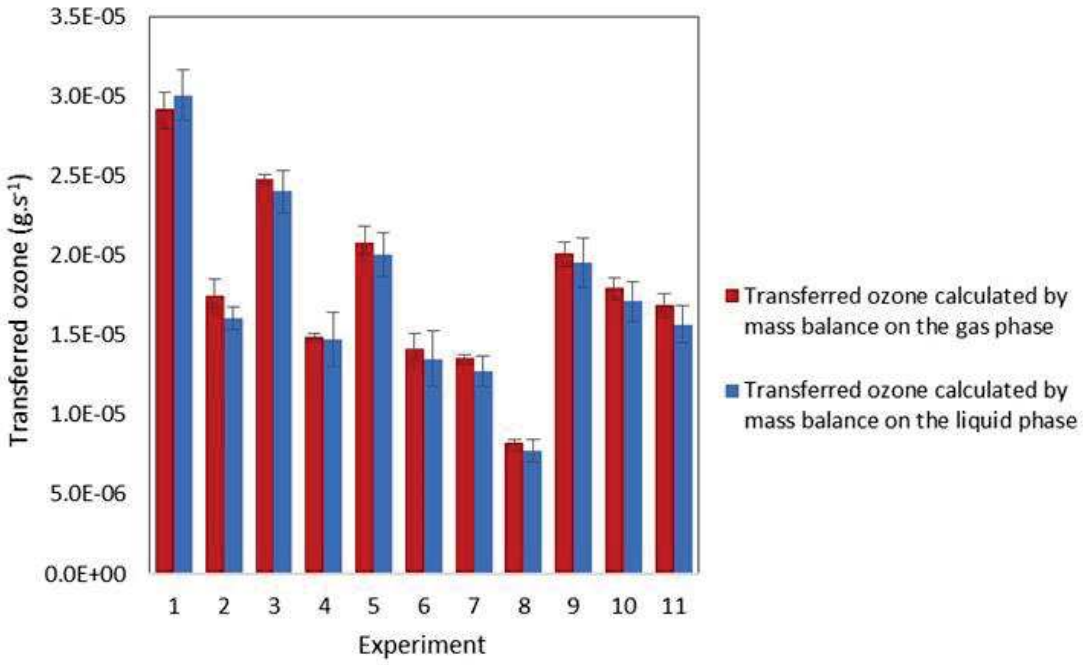

Figure 20. Transferred ozone calculated by mass balance on the gas phase vs by mass balance on the liquid phase.

A linear model was used for the interpretation of these results. The Pareto chart, where dominating and influential factors can be deduced, was plotted using Minitab 19 Statistical software on the Figure 21 (Wenten et al., 2012). Terms with longer bars have more influence on the response. The red line is the effect size at the 0.10 level of significance. Grey bars represent non-significant terms that were removed from the model. The response was the dose of ozone transferred by mass balance on the gas phase. The results showed that the three factors studied (liquid flow rate (A), gas flow rate (B), and ozone concentration at the gas inlet (C)) were influential on the dose of transferred ozone. Only the interaction factor between the liquid flow rate and the ozone concentration at the gas inlet had a significant influence on the response. Liquid flow rate was the variable with the most influence, followed by ozone concentration at the gas inlet rate, then gas flow rate and finally liquid flow coupled with ozone concentration.

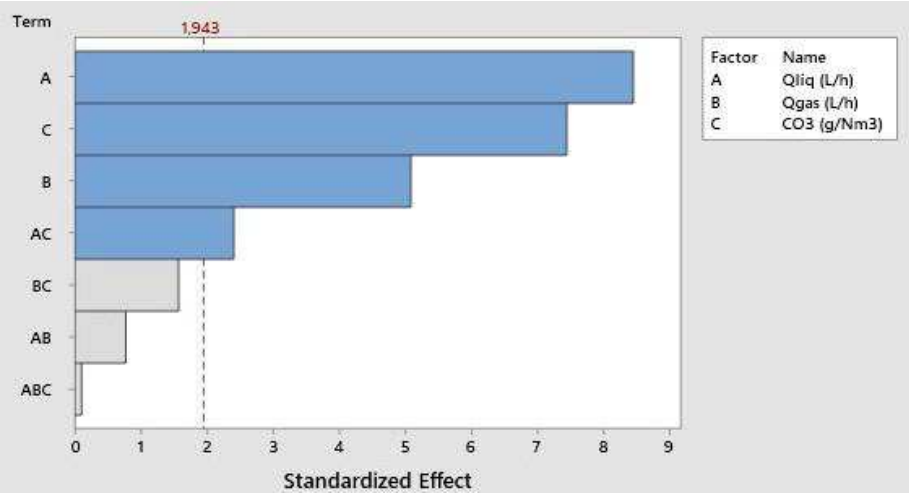

Figure 21. Pareto Chart of Standardized Effects (Response is dose of transferred ozone; α = 0.1).

To maximize the dose of transferred ozone, the optimal factor settings were *Q*liq = 75 L/h, *Q*gas = 30 L/h and CO_3gas = 30 g/Nm^3. Under these conditions, the predicted dose of transferred ozone with the adjusted quadratic model was 2.96 × 10^{-5} g/s. The regression equation of the dose of transferred ozone is defined in Equation 36, and explains 96.36% of the variation of the dose transferred (i.e., R^2 = 96.36%).

$$\textbf{Dose transferred } (\times 10^5) = -0.18 + 0.0066\, Qliq + 0.02295\, Qgas - 0.0649\, CO_3gas + 0.001735\, (Qliq \times CO_3gas), \quad [36]$$

where Dose transferred is the dose of ozone transferred from the gas phase to the liquid phase by mass balance on the gas phase (in g/s, multiply the result by 10^{-5}), *Qliq* is the liquid flow rate (in L/h), *Qgas* is the gas flow rate (in L/h), and CO_3gas is the ozone concentration at the inlet to the gas phase (in g/Nm^3)

The model was also checked by analysis of the residuals, and no unusual data point was found.

3.4. Study of the ozonation of Acid Orange 7 (AO7) through the membrane contactor: acceleration factor

The experiments with pure water recirculating enabled the determination of the ozone K_La in the membrane contactor, which is the same when the liquid phase is not pure water (for identical liquid flow conditions). To study the impact of an irreversible chemical reaction on the ozone transfer, Acid Orange 7 (AO7), a dye highly reactive to molecular ozone (k_{O3} = 1.20 x 10^4 M^{-1}.s^{-1}), was selected. The effects of operating conditions on mass transfer performance were investigated in the previous section and enabled the choice of appropriate conditions for dye removal (i.e., AO7 abatement). Experiments with AO7 solution were carried out, at an initial concentration of about 5 mg.L^{-1}. Material balances

established in Section 3.1. could not be easily resolved with the presence of a reaction, mainly because the reaction took place not only in the membrane contactor but also inside the tank. Several variables therefore depended on time. The study of AO7 removal was thus conducted with water in an open loop (i.e., there was no recirculation of the liquid phase in the membrane contactor). In this process, ozone was transferred from the gas phase to the liquid phase through the membrane. Once dissolved, it reacted with the dye in the solution. Comparison between pure water and dye experiments carried out with liquid in the open loop showed a higher ozone transfer in the presence of AO7 (1.27 $g.h^{-1}.m^{-2}$ instead of 0.84 $g.h^{-1}.m^{-2}$ with buffered water), indicating the existence of an acceleration factor due to the decoloring reaction. This can be explained by the steepened concentration gradient due to the reaction with the dissolved ozone.

The reaction can be described by Equation 16 where *b* is the stoichiometric coefficient of the reaction.

$$\mathbf{O_{3\,(L)} + \mathit{b}\ AO7_{(L)} \rightarrow Products} \quad [37]$$

Molecular ozone could also react with degradation by-products of AO7. However, the low residence time (< 2 s) in the contactor, combined with the high reaction constant of AO7 with O_3, make the theoretical reactions that could ensue negligible.

As seen previously (see Section 0), the mass transfer mechanism in the membrane contactor is divided into several regions (see Figure 18). The objective was here to identify where the reaction took place and whether it had any impact on the mass transfer. To identify the reaction regime during the reaction between AO7 and dissolved ozone, the Hatta number was calculated.

$$\mathbf{Ha} = \frac{\sqrt{k_2\, C_{AO7\_lm} D_{Dissolved\ O3-Water}}}{k_L}, \quad [38]$$

where k_2 is the 2nd order reaction constant of AO7 with dissolved ozone (= 1.20×10^4 $M^{-1}.s^{-1}$ (Gomes et al., 2010)), C_{AO7_lm} is the logarithmic mean of the AO7 concentration at the inlet and at the outlet of the reactor (= 1.216 x 10^{-5} $mol.L^{-1}$), $D_{Dissolved\ O3\text{-}Water}$ is the diffusivity of dissolved ozone in the water (= 1.708×10^{-9} $m^2.s^{-1}$ at 20 °C (Johnson and Davis, 1996)), and k_L is the liquid transfer coefficient ≈ K_L because of the low membrane and gas resistances (= 4.789×10^{-5} $m.s^{-1}$, see Section 3.1)

The Hatta number was found to be 0.33. According to Roustan, this corresponds to a moderately fast reaction, which takes place partially in the liquid film and partially in the liquid bulk (Roustan, 2003). The most suitable reactor to promote this type of reaction has a high interfacial area and a high liquid retention time. In this work, the use of hollow fibers gave a high interfacial area, but the liquid retention time was very short (1.7 s). The use of a lower liquid flowrate would probably have improved

the reaction between dissolved ozone and AO7 in the liquid bulk, thus yielding a better AO7 abatement.

The acceleration factor (*E*) corresponds to the ratio of the material flow transferred at the gas/liquid interface without a chemical reaction to that with a chemical reaction. Ha was found to exceed 0.3, implying E > 1. For a second order reaction (i.e., $r = kC_{O3}C_{AO7}$), *E* could be determined with precision and is defined as:

$$\boldsymbol{E} = \frac{\mathbf{Ha}\sqrt{\frac{E_{\mathbf{AL}}-E}{E_{\mathbf{AL}}-1}}}{\tanh\left[\mathbf{Ha}\sqrt{\frac{E_{\mathbf{AL}}-E}{E_{\mathbf{AL}}-1}}\right]} \text{ , [39]}$$

where E_{AL} is called the "limit acceleration factor", and is described by Equation 40.

$$\boldsymbol{E_{\mathbf{AL}}} = \mathbf{1} + \frac{\boldsymbol{D_{\mathbf{AO7,w}}}\,\boldsymbol{C_{\mathbf{AO7\_lm}}}}{\mathbf{b}\,\boldsymbol{D_{\mathbf{Dissolved\ O3,w}}}\,\boldsymbol{C_{\mathbf{Dissolved\ O3\_I}}}} \text{ , [40]}$$

where $D_{AO7,w}$ is the diffusivity of AO7 in the water (= 8.48 × 10^{-10} $m^2.s^{-1}$ at 20 °C (Hori et al., 1987)), and $C_{Dissolved\ O3\_I}$ is the concentration of dissolved ozone at the gas/liquid interface (= 1.55 × 10^{-4} $mol.L^{-1}$ according to the Henry's law).

Solving Equation 18, the acceleration factor was calculated to be 1.03. This result implies that the ozone mass transfer was slightly accelerated by the reaction between AO7 and dissolved ozone, and that the resistance on the liquid side was slightly lower in the presence of AO7 than without (i.e., lower with chemical absorption than with physical absorption) (see Section 0).

To compare the AO7 abatement obtained using the membrane contactor with a conventional process, an experiment was conducted with a bubble column (see Section 2.2). The initial AO7 concentration was approximately the same as in the membrane contactor experiments (i.e., about 5 $mg.L^{-1}$). The average abatement obtained with the membrane contactor (i.e., 34%) in a very short residence time (i.e., < 2 s) was achieved in over 5 minutes with the bubble column (and 100% decoloring was achieved in 15 min). The membrane contactor therefore holds promise, but it must be noted that although the applied ozone fluxes in $g.h^{-1}$ were close in the membrane contactor and in the bubble column experiments, both applied ozone flow and transferred ozone flow in $g.h^{-1}._{treated}L^{-1}$ were significantly higher in the membrane contactor experiments, largely explaining the marked difference between the residence time of the two reactors to achieve 34% AO7 abatement (see Table 5).

In Table 5, an average of the result obtained with the membrane contactor is given (experiments had been performed in triplicate). The associated standard deviation is also indicated. We see that the applied ozone flow in the membrane contactor experiments was 89 times higher than in the conventional process experiment. The AO7 concentration time course obtained with the bubble

column showed that AO7 abatement was proportional to the time (only one run). We can therefore assume that with an applied ozone flow of 6.596 $g.h^{-1}.{}_{treated}L^{-1}$ (i.e., 89 × 0.074 $g.h^{-1}.{}_{treated}L^{-1}$), a residence time of 3.37 s (i.e., 5.08 / 89 min) would be required to achieve 34% AO7 abatement in the bubble column, twice the time taken by the membrane contactor to do the same. This calculation is a first approach and should be consolidated by a duplication of experiments in a bubble column.

Table 5. Comparison between membrane contactor and bubble column for AO7 removal.

Reactor used	$C_{O_3,gas\ inlet}$ ($g.Nm^{-3}$)	$C_{O_3,gas\ outlet}$ ($g.Nm^{-3}$)	$C_{O_3,liq\ outlet}$ ($mg.L^{-1}$)	$C_{AO7\ inlet}$ ($mg.L^{-1}$)	$C_{AO7\ outlet}$ ($mg.L^{-1}$)	Applied ozone * ($g.h^{-1}$)	Applied ozone * ($g.h^{-1}.{}_{treated}L^{-1}$)	Transferred ozone ** ($g.h^{-1}$)	Transferred ozone ** ($g.h^{-1}.{}_{treated}L^{-1}$)	Residence time of the liquid for 34% AO7 abatement ***
Membrane contactor	30.0 (+/- 0.3)	13.0 (+/- 0.4)	0.1 (+/- 0.1)	5.2 (+/- 0.4)	3.5 (+/- 0.2)	0.240 (+/- 0.002)	6.596 (+/- 0.066)	0.136 (+/- 0.004)	3.733 (+/- 0.125)	1.7 s
Bubble column	37.0 (+/- 0.5)	*n.a.*	*n.a.*	4.2 (+/- 0.1)	*n.a.* (0 at the end of the experiment)	0.296	0.074	0.236	0.059	5.08 min

* Calculated from the gas at the inlet
** Calculated by mass balance on the gas phase
***Initial AO7 concentration (≈ $5mg.L^{-1}$)
n.a.: Not available due to time-dependance

3.5. Impact of ozone on membrane material

After about 40 hours of exposition to ozone environment, despite correct transmembrane pressures (in particular the breakthrough pressure, see Section 2.1), a large volume of liquid was observed on the gas side. This time corresponded to the circulation of about 10 g of ozone gas through the contactor. This value was estimated by cumulating, for all the experiments, the mass flow rate in the gas phase at the inlet to the contactor. The same problem occurred for several membrane contactors that were similar (same material, number of fibers, and supplier). Once watertightness was lost, large volumes of water were found at the gas outlet in each experiment. The membrane contactor was therefore replaced.

Several hypotheses can explain the presence water in the gas outlet. First, a large amount of water may have flowed through the membrane pores and then circulated inside the fibers to the gas outlet. A smaller amount might not be visible but would also affect the ozone transfer. The presence of water in the pores, even partial, is a major problem because it significantly reduces the transfer of ozone from the gas to the liquid phase owing to the lower diffusivity of ozone in the liquid than in the gas phase (see Section 3.2). This could have happened if the breakthrough pressure had been locally exceeded, for example through a change in water flow or in hydrophobicity. Visually, it was not

possible to check partial or complete penetration of water inside the membrane pores during the experiments. However, liquid was in these cases visible at the gas outlet.

Another hypothesis is a loss of seal at the potted part, which is where fibers are bonded in place using resin, joining the shell to the fibers. The potting of a membrane contactor, particularly if it is for an ozonation or oxidation application, is a difficult process because it must fulfill several requirements. First, the resin must adhere to the membrane material used, and PTFE is notably adhesion-resistant. The resin must also be durable. Here, fibers all came unstuck on one side of the contactor. This last hypothesis was therefore taken as most probable.

A test validated that the potting was no longer sealed and watertight. The resin used for the potting of the membrane contactors used in this work was polyurethane resin. It proved not to be resistant to ozone attack over time. Polyurethane resin is considered to have a good ozone resistance (Irfan, 1998). However, Sleeper and Henry showed in their tests on durability of materials exposed to ozone that polyurethane sealant was immediately degraded by ozone. Some research is reported in the literature on the production of specific products for this field. For instance, a patent has been filed for making a polyurethane resin specifically for use with ozone (Yoon et al., 2011).

It was also notable that fibers came unstuck on only one side (the gas outlet), which is the side where there was the lowest dissolved ozone concentration and gaseous ozone concentration. No explanation was found for this particularity. One hypothesis is the transmembrane pressure, which was checked at the inlet and at the outlet of the contactor, but which could locally exceed the breakthrough pressure. The water enters the contactor perpendicularly. This could potentially explain the presence of water (and of dissolved ozone) inside the fibers on this side. As observed by other authors, dissolved ozone is more aggressive toward materials than gaseous ozone, which could explain why this side was attacked first (Sleeper and Henry, 2002). With time, fibers would come off on both sides.

To evaluate the deterioration of the fiber properties over time and to determine whether this deterioration could favor water penetration inside, analysis of hydrophobicity and material structure was carried out by contact angle measurements and SEM images.

The following SEM images (Figure 22) show the tested samples according to their location, both for outer surface and lumen of samples, with several magnifications. Figure 22 shows that the lumen side was less damaged than the outer surface for every location in the contactor. These results suggest there was very little reaction between the ozone and the membrane material inside the fibers. Material balances could therefore be established without taking into account the presence of a reaction between gaseous ozone and the material. Conversely, the outer surfaces of fibers were particularly damaged, especially in the middle of the contactor. A torn crust was visible, which could

induce a modification of the membrane porosity and so could explain the water penetration inside the fibers. There was clearly some reaction between the ozone and the membrane material on the outer surface. According to Fujimoto et al., peroxides are formed on the PDMS surface when ozone is in the presence of water (Fujimoto et al., 1993; Zoumpouli et al., 2018). However, according to the authors (Fujimoto et al.), this does not occur on a Teflon surface, and therefore should not happen on a PTFE surface. The difference between the results obtained (i.e., for the lumen side and for the outer surface of the fiber) could thus be explained by the greater aggressivity of the dissolved ozone relative to gaseous ozone (Sleeper and Henry, 2002).

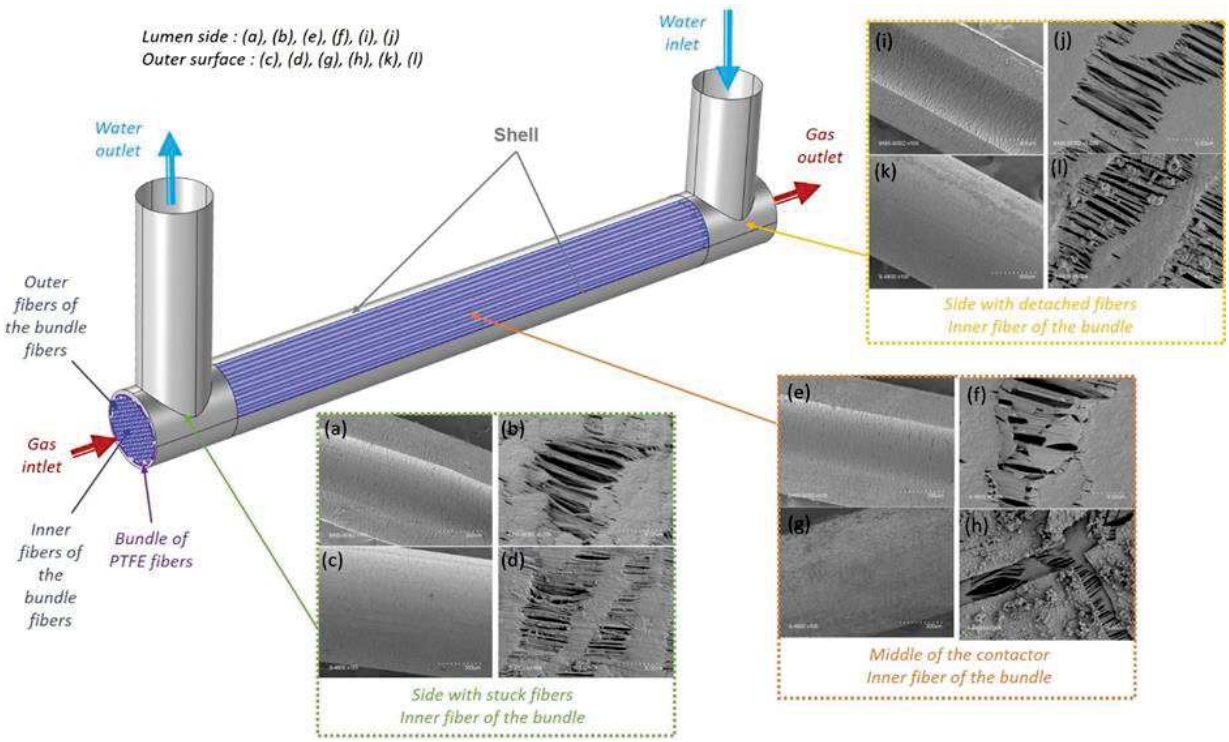

Figure 22. SEM images of an inner fiber sample of the bundle at different locations for lumen side and outer surface.

Contact angles were investigated on the same samples as previously. Importantly, the values obtained were qualitative but not quantitative, so must be considered with caution. The contact angles measured with the analytical method used (see Section 2.1) depended on the porosity, roughness, and hydration state of the membrane. This method is ill-adapted to a non-planar surface such as the hollow fiber in this work (porous hollow fiber membrane). However, by depositing a very small volume of water on the surface to be analyzed, the material being hydrophobic, contact angles were measured without being exactly quantified. Contact angle measurements revealed no alteration of the membrane hydrophobicity whatever the location of the sample. A change in the membrane hydrophobicity did not therefore account for the penetration of a large volume of water inside fibers.

To conclude, the factor limiting the use of the membrane contactor over time seems to be the potting, particularly the resin used to bond the fibers. The loss of adhesion of the fibers inside the resin explains the loss of seal after a period of ozonation. However, the membrane material also presented significant alterations over time, specifically on the outer surface of the fibers, which was in contact with dissolved ozone.

According to the literature, PTFE is one of the best polymeric materials for resisting ozonation over time (Bein et al., 2021). Bamperng et al. observed no modification of the PTFE after more than 16 hours of exposure to an ozone environment concentrated at 40 $g.Nm^{-3}$ (Bamperng et al., 2010). Santos et al. had the same observation for an ozone exposure of 5.25 $g.h^{-1}$ during 4 hours, corresponding to 21 g of ozone, which is twice the amount achieved in this study (Alves dos Santos et al., 2015). However, their study was made with gaseous ozone, which is supposed to be less aggressive than dissolved ozone (Sleeper and Henry, 2002). Furthermore, Bein et al. suggested that even if no changes have already been reported for PTFE, unlimited stability cannot be guaranteed in the case of a long-term exposure due to the scarcity of the existing data and to the problems of chemical stability reported in the case of harsh conditions, like for instance defluorination during chemical cleaning (Bein et al., 2021).

According to the SEM images presented in this work (Figure 22), PTFE material could not be suitable for membrane contactors in practical application of ozonation. The study of another material, such as PVDF, also known for being resistant to ozone oxidation, would be useful to compare results. However, in a previous study, Bamperng et al. compared PTFE and PVDF and observed for this last a significant reduction of the mass transfer of 30% over 16h at the same ozone concentration (40 $g.Nm^{-3}$) (Bamperng et al., 2010). Previous studies have recently pointed out the unsuitability of polymeric membranes for treatment involving oxidizing agents such as ozone (Shanbhag et al., 1998).

Some research on ozonation with ceramic (i.e., chemically inert) membrane contactors has been conducted (Heng et al., 2007; Jansen et al., 2005; Stylianos et al., 2015b). However, the production of ceramic membranes in the form of hollow fibers (very small diameter fiber in order to obtain the largest possible exchange surface area) is still being developed (Dashti and Asghari, 2015). In addition, ceramic membranes are generally more hydrophilic than the polymerics, and thus water could more easily penetrate in the pores and decrease the mass transfer in the case of a porous membrane. The addition of a hydrophobic layer could be a solution (Stylianou et al., 2015a). Nevertheless, no study has been made at this time about the chemical stability of these layers after a long-term exposure to ozone (Bein et al., 2021). Simultaneously, the use of nonporous membranes (ceramic or polymeric) could avoid the transmembrane pressure problem (i.e., the requirement not to exceed the breakthrough pressure and the bubble pressure). One disadvantage would be the higher mass transfer

resistance using dense membranes compared to porous membranes owing to their higher membrane resistance. However, Pines et al. demonstrated in their work that the overall mass transfer was not necessarily lower with nonporous membranes than with polymeric membranes (Pines et al., 2005). Another solution would be to use composite membranes with a porous support and a dense layer. This would eliminate any problem of transmembrane pressure while reducing membrane resistance thanks to the porous part (compared with dense membranes) (Chabanon, 2011; Favre and Roizard, 2012). Finally, one other solution could be to deposit a thin layer of an ozone-resistant material around the hollow fibers, for example by soaking, on the potted part of the contactor to prevent fiber detachment.

4. Conclusions

This study set out to gain more knowledge on the ozonation process using an in/out membrane contactor. A full characterization was performed using water and a model pollutant. The main conclusions are as follows:

- The overall mass transfer coefficient $K_L a$ measured in this study showed that the membrane contactor is an advantageous device for ozonation compared with conventional processes, despite the addition of a resistance to the mass transfer (i.e., the membrane resistance), particularly because of its large specific exchange surface area.
- The mass transfer resistance due to the membrane depends on the material used. It represents less than 1% of the overall resistance. The $K_L a$ value therefore depends mainly on the liquid flow conditions.
- The main variables that have an impact on the ozone transfer are the ozone concentration in the gas phase and the liquid flowrate. Conversely, gas flowrate has very little impact on the ozone transfer.
- The results obtained with AO7 solutions prove that the membrane contactor can be effective for organic pollutant ozonation, even at very short contact times.
- When a chemical reaction takes place in the liquid, an acceleration of the ozone transfer occurs, owing to the steepened concentration gradient. The presence of organic micropollutants could therefore favor ozone transfer through a membrane contactor.
- This work is a preliminary study for the ozonation of organic micropollutants with membrane contactors in the same process configuration.

Conclusions et perspectives du Chapitre III

Ce chapitre a permis une meilleure compréhension de l'ozonation par contacteur membranaire grâce à la caractérisation complète du transfert d'ozone en présence d'eau pure tamponnée puis d'un polluant organique choisi comme modèle, au sein d'un contacteur membranaire composé de fibres creuses en PTFE en configuration in/out.

Cette configuration, dans laquelle le gaz circule à l'intérieur des fibres creuses, présenterait l'avantage d'éviter les problèmes liés au colmatage de la membrane, ce qui est particulièrement important dans le cas d'application avec une eau réelle.

Comme annoncé dans le Chapitre I, les contacteurs membranaires apparaissent comme une technologie particulièrement intéressante pour les procédés d'ozonation en comparaison des procédés d'ozonation conventionnels. Plus particulièrement, ils sont efficaces pour l'ozonation de colorants organiques, tel que l'Acide Orange 7 étudié dans ce chapitre, y compris pour de très faibles temps de séjours (de l'ordre de quelques secondes) (Atchariyawut et al., 2009; Bamperng et al., 2010). Ils sembleraient donc être appropriés dans un objectif d'élimination des micropolluants organiques présents en sortie de station d'épuration.

La valeur du coefficient de transfert global $K_L a$ déterminée dans ce chapitre est supérieure à celle des réacteurs traditionnels, en grande partie grâce à la très grande surface d'échange offerte par la membrane et sa géométrie en forme de fibres creuses. Cette étude a également montré que la résistance au transfert due à la membrane était très faible (moins de 1% de la résistance totale). Néanmoins, d'après le Chapitre I, cette proportion peut rapidement augmenter en cas de dépassement de la pression de percée, celle-ci entraînant la pénétration d'eau dans les pores de la membrane, freinant considérablement le transfert de l'ozone.

En conséquence, le coefficient de transfert global $K_L a$ dépend principalement des conditions d'écoulement de la phase liquide. Ainsi, en favorisant l'écoulement par exemple grâce à un débit liquide plus élevé ou encore à la mise en place de chicanes ou de mélangeurs statiques dans l'enveloppe du contacteur, ce coefficient pourrait encore être augmenté. En outre, en complément du débit liquide, la concentration en ozone appliquée dans la phase gaz a également un impact significatif et positif sur le transfert, ce qui confirme les résultats recueillis dans la littérature et cités dans le Chapitre I.

D'autre part, la présence d'un polluant organique réagissant avec l'ozone dans la phase liquide a un impact positif sur le transfert, en favorisant un gradient de concentration en ozone plus élevé que celui

existant dans le cas d'un transfert purement physique. Un facteur d'accélération a ainsi été déduit, relativement faible et spécifique à la réaction et au procédé étudiés.

Le matériau utilisé, c'est-à-dire le PTFE, est d'après le Chapitre I l'un des matériaux polymères les plus résistants à l'ozonation. Cependant, il s'est révélé dans notre étude que la surface des fibres avait subi des modifications au cours du temps. De plus, la résine utilisée pour faire l'étanchéité du contacteur membranaire n'a pas résisté aux essais réalisés et le contacteur a donc été changé plusieurs fois au cours de ces travaux de thèse. Ces observations ont souligné l'importance du choix des matériaux lors de la fabrication des contacteurs membranaires en fonction de leur application, constituant un facteur essentiel de leur longévité. Pour une application d'ozonation, ils doivent simultanément garantir un bon transfert de matière et résister à l'oxydation par cette même matière, particulièrement puissante dans le cas de l'ozone ou encore de radicaux hydroxyles.

L'utilisation de matériaux céramiques permettrait de surmonter ce verrou. Néanmoins, la fabrication de membranes inorganiques en géométrie fibre creuse est encore difficilement praticable. Comme mis en avant dans le Chapitre I, une autre solution envisageable à laquelle plusieurs études se sont intéressées serait l'utilisation de membranes composites possédant une fine couche dense recouvrant le matériau poreux servant de base à la structure (Chabanon, 2011; Favre and Svendsen, 2012). La présence de cette peau permettrait de s'affranchir des problèmes liés aux pressions transmembranaires (pression de bulle et pression de percée) qui se sont avérées être une des limites rencontrées lors des expériences réalisées. En empêchant l'eau de pénétrer dans la membrane, la couche dense protègerait le cœur de la membrane de l'ozone dissous, celui-ci étant plus agressif que l'ozone sous forme gazeuse (Sleeper and Henry, 2002). L'avantage de la membrane composite d'être composée d'une fine peau dense tout en conservant une base poreuse est de limiter la résistance au transfert due à la membrane. Cependant, cette couche doit elle aussi être conçue dans un matériau résistant à l'oxydation et plus spécifiquement à l'ozonation.

Ainsi, ce chapitre était une étude de caractérisation préliminaire aux travaux concernant l'application de ce même procédé à l'élimination de micropolluants organiques tout en minimisant la formation de bromates lors d'un traitement tertiaire en station d'épuration.

Bibliographie du Chapitre III

Alves dos Santos, F.R., Borges, C.P., da Fonseca, F.V., 2015. Polymeric Materials for Membrane Contactor Devices Applied to Water Treatment by Ozonation. Mater. Res. 18, 1015–1022. https://doi.org/10.1590/1516-1439.016715

Atchariyawut, S., Phattaranawik, J., Leiknes, T., Jiraratananon, R., 2009. Application of ozonation membrane contacting system for dye wastewater treatment. Sep. Purif. Technol. 66, 153–158. https://doi.org/10.1016/j.seppur.2008.11.011

Bader, H., Hoigné, J., 1982. Determination of Ozone In Water By The Indigo Method: A Submitted Standard Method. Ozone Sci. Eng. J. Int. Ozone Assoc. 4, 169–176. https://doi.org/10.1080/01919510390481531

Bamperng, S., Suwannachart, T., Atchariyawut, S., Jiraratananon, R., 2010. Ozonation of dye wastewater by membrane contactor using PVDF and PTFE membranes. Sep. Purif. Technol. 72, 186–193. https://doi.org/10.1016/j.seppur.2010.02.006

Bein, E., Zucker, I., Drewes, J.E., Hübner, U., 2021. Ozone membrane contactors for water and wastewater treatment: A critical review on materials selection, mass transfer and process design. Chem. Eng. J. 413. https://doi.org/10.1016/j.cej.2020.127393

Beltrán, F.J., García-Araya, J.F., Encinar, J.M., 1997. Henry and mass transfer coefficients in the ozonation of wastewaters. Ozone Sci. Eng. 19, 281–296. https://doi.org/10.1080/01919519708547307

Bolong, N., Ismail, A.F., Salim, M.R., Matsuura, T., 2009. A review of the effects of emerging contaminants in wastewater and options for their removal. Desalination 239, 229–246. https://doi.org/10.1016/j.desal.2008.03.020

Chabanon, E., 2011. Contacteurs à membranes composites et contacteurs microporeux pour procédés gaz-liquide intensifiés de captage du CO2 en post-combustion : expérimentation et modélisation. Génie des procédés. École Nationale Supérieure des Mines de Paris : thèse de doctorat. Français. <NNT : 2011ENMP0061>. <pastel-00677145>

Dashti, A., Asghari, M., 2015. Recent Progresses in Ceramic Hollow-Fiber Membranes. ChemBioEng Rev. 2, 54–70. https://doi.org/https://doi.org/10.1002/cben.201400014

Favre, D., Roizard, E., 2012. Conception et étude de contacteurs gaz/liquide à peau dense pour le captage du dioxyde de carbone - Une étape importante pour l'intensification du captage en postcombustion. Tech. Ing. Base documentaire : TIB495DUO. Ref. article : re166.

Favre, E., Svendsen, H.F., 2012. Membrane contactors for intensified post-combustion carbon dioxide capture by gas-liquid absorption processes. J. Memb. Sci. https://doi.org/10.1016/j.memsci.2012.03.019

Ferre-Aracil, J., Cardona, S.C., Navarro-Laboulais, J., 2015. Determination and validation of Henry's constant for ozone in phosphate buffers using different analytical methodologies. Ozone Sci. Eng. 37, 106–118.

Fujimoto, K., Takebayashi, Y., Inoue, H., Ikada, Y., 1993. Ozone-induced graft polymerization onto polymer surface. J. Polym. Sci. Part A Polym. Chem. 31, 1035–1043. https://doi.org/10.1002/pola.1993.080310426

Gabelman, A., Hwang, S.T., 1999. Hollow fiber membrane contactors. J. Memb. Sci. 159, 61–106. https://doi.org/10.1016/S0376-7388(99)00040-X

Gogoi, A., Mazumder, P., Tyagi, V.K., Tushara Chaminda, G.G., An, A.K., Kumar, M., 2018. Occurrence and fate of emerging contaminants in water environment: A review. Groundw. Sustain. Dev. 6, 169–180. https://doi.org/10.1016/j.gsd.2017.12.009

Gomes, A.C., Nunes, J.C., Simões, R.M.S., 2010. Determination of fast ozone oxidation rate for textile dyes by using a continuous quench-flow system. J. Hazard. Mater. 178, 57–65. https://doi.org/10.1016/j.jhazmat.2010.01.043

Guillossou, R., Le Roux, J., Brosillon, S., Mailler, R., Vulliet, E., Morlay, C., Nauleau, F., Rocher, V., Gaspéri, J., 2020. Benefits of ozonation before activated carbon adsorption for the removal of organic micropollutants from wastewater effluents. Chemosphere 245. https://doi.org/10.1016/j.chemosphere.2019.125530

Hasanoğlu, A., Romero, J., Plaza, A., Silva, W., 2013. Gas-filled membrane absorption: A review of three different applications to describe the mass transfer by means of a unified approach. Desalin. Water Treat. 51, 5649–5663. https://doi.org/10.1080/19443994.2013.769603

Heng, S., Yeung, K.L., Djafer, M., Schrotter, J.-C., 2007. A novel membrane reactor for ozone water treatment. J. Memb. Sci. 289, 67–75. https://doi.org/10.1016/j.memsci.2006.11.039

Hori, T., Kamon, N., Kojima, H., Rohner, R.M., Zollinger, H., 1987. Structure correlation between diffusion coefficients of simple organic compounds and of anionic and cationic dyes in water. J. Soc. Dye. Colour. 103, 265–270. https://doi.org/10.1111/j.1478-4408.1987.tb01119.x

Irfan, M.H., 1998. Polyurethanes in the construction industry, in: Chemistry and Technology of Thermosetting Polymers in Construction Applications. Dordrecht, pp. 123–144.

Iversen, S.B., Bhatia, V.K., Dam-Johansen, K., Jonsson, G., 1997. Characterization of microporous membranes for use in membrane contactors. J. Memb. Sci. 130, 205–217. https://doi.org/10.1016/S0376-7388(97)00026-4

Jansen, R.H.S., de Rijk, J.W., Zwijnenburg, A., Mulder, M.H.V., Wessling, M., 2005. Hollow fiber membrane contactors—A means to study the reaction kinetics of humic substance ozonation. J. Memb. Sci. 257, 48–59. https://doi.org/10.1016/J.MEMSCI.2004.07.038

Johnson, P.N., Davis, R.A., 1996. Diffusivity of ozone in water. J. Chem. Eng. Data 41, 1485–1487. https://doi.org/10.1021/je9602125

Khaisri, S., deMontigny, D., Tontiwachwuthikul, P., Jiraratananon, R., 2009. Comparing membrane resistance and absorption performance of three different membranes in a gas absorption membrane contactor. Sep. Purif. Technol. 65, 290–297. https://doi.org/10.1016/j.seppur.2008.10.035

Khayet, M., Matsuura, T., 2001. Preparation and Characterization of Polyvinylidene Fluoride Membranes for Membrane Distillation. Ind. Eng. Chem. Res. 40, 5710–5718. https://doi.org/10.1021/ie010553y

Kukuzaki, M., Fujimoto, K., Kai, S., Ohe, K., Oshima, T., Baba, Y., 2010. Ozone mass transfer in an ozone-water contacting process with Shirasu porous glass (SPG) membranes-A comparative study of hydrophilic and hydrophobic membranes. Sep. Purif. Technol. 72, 347–356. https://doi.org/10.1016/j.seppur.2010.03.004

Kuosa, M., Kallas, J., 2010. Multicomponent reaction models in ozonation and reduction in the number of model parameters. J. Hazard. Mater. 183, 823–832. https://doi.org/10.1016/j.jhazmat.2010.07.101

Leiknes, T., Phattaranawik, J., Boller, M., Von Gunten, U., Pronk, W., 2005. Ozone transfer and design

concepts for NOM decolourization in tubular membrane contactor. Chem. Eng. J. 111, 53–61. https://doi.org/10.1016/j.cej.2005.05.007

Luo, Y., Guo, W., Ngo, H.H., Nghiem, L.D., Hai, F.I., Zhang, J., Liang, S., Wang, X.C., 2014. A review on the occurrence of micropollutants in the aquatic environment and their fate and removal during wastewater treatment. Sci. Total Environ. 473–474, 619–641. https://doi.org/10.1016/j.scitotenv.2013.12.065

Margot, J., Kienle, C., Magnet, A., Weil, M., Rossi, L., de Alencastro, L.F., Abegglen, C., Thonney, D., Chèvre, N., Schärer, M., Barry, D.A., 2013. Treatment of micropollutants in municipal wastewater: Ozone or powdered activated carbon? Sci. Total Environ. 461–462, 480–498. https://doi.org/10.1016/j.scitotenv.2013.05.034

Mavroudi, M., Kaldis, S.P., Sakellaropoulos, G.P., 2006. A study of mass transfer resistance in membrane gas–liquid contacting processes. J. Memb. Sci. 272, 103–115. https://doi.org/10.1016/J.MEMSCI.2005.07.025

Merle, T., Pronk, W., Von Gunten, U., Eawag, †, 2017. MEMBRO 3 X, a Novel Combination of a Membrane Contactor with Advanced Oxidation (O 3 /H 2 O 2) for Simultaneous Micropollutant Abatement and Bromate Minimization. Environ. Sci. Technol. Lett 4, 13. https://doi.org/10.1021/acs.estlett.7b00061

Nguyen, P.T., 2011. Contacteurs à membranes denses pour les procédés d'absorption gaz-liquide intensifiés : application à la capture du CO 2 en post combustion. Thèse de doctorat. Institut National Polytechnique de Lorraine. Français.

Pabby, A.K., Sastre, A.M., 2013. State-of-the-art review on hollow fibre contactor technology and membrane-based extraction processes. J. Memb. Sci. 430, 263–303. https://doi.org/10.1016/j.memsci.2012.11.060

Phattaranawik, J., Leiknes, T., Pronk, W., 2005. Mass transfer studies in flat-sheet membrane contactor with ozonation. J. Memb. Sci. 247, 153–167. https://doi.org/10.1016/j.memsci.2004.08.020

Pines, D., Min, K.-N., J. Ergas, S., Reckhow, D., 2005. Investigation of an Ozone Membrane Contactor System. https://doi.org/10.1080/01919510590945750

Prieto-Rodríguez, L., Oller, I., Klamerth, N., Agüera, A., Rodríguez, E.M., Malato, S., 2013. Application of solar AOPs and ozonation for elimination of micropollutants in municipal wastewater treatment plant effluents. Water Res. 47, 1521–1528. https://doi.org/10.1016/j.watres.2012.11.002

Roth, J.A., Sullivan, D.E., 1981. Solubility of ozone in water 137–140.

Roustan, M., 2003. Transferts gaz-liquide dans les procédés de traitement des eaux et des effluents gazeux. Éd. Tec & doc, Paris.

Roustan, M., Wang, R.Y., Wolbert, D., 1996. Modeling hydrodynamics and mass transfer parameters in a continuous ozone bubble column. Ozone Sci. Eng. 18, 99–115. https://doi.org/10.1080/01919519608547331

Schlüter-Vorberg, L., Prasse, C., Ternes, T.A., Mückter, H., Coors, A., 2015. Toxification by transformation in conventional and advanced wastewater treatment: the antiviral drug acyclovir. Environ. Sci. Technol. Lett. 2, 342–346. https://doi.org/10.1021/acs.estlett.5b00291

Schmitt, A., Mendret, J., Roustan, M., Brosillon, S., 2020. Ozonation using hollow fiber contactor technology and its perspectives for micropollutants removal in water: A review. Sci. Total

Environ. vol. 729, p. 138664. https://doi.org/10.1016/j.scitotenv.2020.138664

Shanbhag, P. V, Guha, A.K., Sirkar, K.K., 1998. Membrane-Based Ozonation of Organic Compounds. Ind. Eng. Chem. Res. 37, 4388–4398. https://doi.org/10.1021/ie980182u

Sleeper, W., Henry, D., 2002. Durability Test Results of Construction and Process Materials Exposed to Liquid and Gas Phase Ozone. Ozone Sci. Eng. 9512, 249–260. https://doi.org/10.1080/01919510208901616

Snyder, S.A., Wert, E.C., Rexing, D.J., Zegers, R.E., Drury, D.D., 2006. Ozone oxidation of endocrine disruptors and pharmaceuticals in surface water and wastewater. Ozone Sci. Eng. 28, 445–460. https://doi.org/10.1080/01919510601039726

Stylianou, S. K., Sklari, S.D., Zamboulis, D., Zaspalis, V.T., Zouboulis, A.I., 2015a. Development of bubble-less ozonation and membrane filtration process for the treatment of contaminated water. J. Memb. Sci. 492, 40–47. https://doi.org/10.1016/j.memsci.2015.05.036

Stylianou, S. K., Szymanska, K., Katsoyiannis, I.A., Zouboulis, A.I., 2015b. Novel Water Treatment Processes Based on Hybrid Membrane-Ozonation Systems: A Novel Ceramic Membrane Contactor for Bubbleless Ozonation of Emerging Micropollutants. J. Chem. 2015, 1–12. https://doi.org/10.1155/2015/214927

Wang, R., Shi, L., Tang, C.Y., Chou, S., Qiu, C., Fane, A.G., 2010. Characterization of novel forward osmosis hollow fiber membranes. J. Memb. Sci. 355, 158–167. https://doi.org/10.1016/j.memsci.2010.03.017

Wenten, I.G., Julian, H., Panjaitan, N.T., 2012. Ozonation through ceramic membrane contactor for iodide oxidation during iodine recovery from brine water. Desalination 306, 29–34. https://doi.org/10.1016/j.desal.2012.08.032

Yoon, I., Jeon, I., Wi, O., Park, C., Hong, Y., 2011. Ozone resistant polyurethane composition and process of preparing same.

Zoumpouli, G., Baker, R., Taylor, C., Chippendale, M., Smithers, C., Xian, S., Mattia, D., Chew, J., Wenk, J., 2018. A Single Tube Contactor for Testing Membrane Ozonation. https://doi.org/10.3390/w10101416

Chapitre IV

Diffusion of ozone through a hollow fiber membrane contactor for pharmaceuticals removal and bromate minimization

Liste des symboles et abréviations du Chapitre IV

$\boldsymbol{\varepsilon}$	Porosity	-
$\boldsymbol{\tau}$	Tortuosity	-
$\boldsymbol{\gamma}$	Surface tension	$N.m^{-1}$
$\boldsymbol{\vartheta}$	Contact angle	radian
$\int C_{O3,liq}\, dt$	Exposure to molecular ozone	M.min
$\int C_{HO^{\circ},liq}\, dt$	Exposure to hydroxyl radicals	M.min
C_{Br^-}	Concentration of bromide	$mg.L^{-1}$
C_{BrO3^-}	Concentration of bromate	$mg.L^{-1}$
$C_{O3,w}$	Concentration of dissolved ozone in the liquid phase	$mg.L^{-1}$
$C_{O3,g,\ inlet}$	Concentration of ozone at the inlet of the gas phase	$g.Nm^{-3}$
C_{pCBA}, $C_{pCBA,0}$	Respectively the concentration of *p*CBA in the water at a given point in time and the initial concentration of *p*CBA in the water	$mol.L^{-1}$ or $g.L^{-1}$
$C_{CBZ\ inlet}$, $C_{SUL\ inlet}$	Respectively the concentration of CBZ and of SUL at the inlet of the liquid phase	$mg.L^{-1}$
$C_{CBZ\ outlet}$, $C_{SUL\ outlet}$	Respectively the concentration of CBZ and of SUL at the outlet of the liquid phase	$mg.L^{-1}$
CBZ	Carbamazepine	-
COD	Chemical Oxygen Demand	$mgO_2.L^{-1}$
$d_{\mathrm{pore,max}}$	Maximum pore diameter	m
HO°	Hydroxyl radical	-
H_2O_2	Peroxone	-
k_{O3}, k_{OH}	Reaction rate constants respectively with molecular ozone and with hydroxyl radicals	$M^{-1}.s^{-1}$
LC-MS/MS	Liquid chromatography-tandem mass spectrometry /	-

LOD, LOQ	Respectively the limit of detection and of Quantification	-
p-CBA	*p*-chlorobenzoic acid	-
MBR	Membrane bioreactor	-
MP	Micropollutant	-
MW	Molecular weight	$g.mol^{-1}$
NOM	Natural Organic Matter	-
***Q*gas, *Q*liq**	Respectively the gas flow rate and the liquid flow rate	$L.h^{-1}$
O_3	Molecular ozone	-
$P_{\mathbf{breakthrough}}$	Breakthrough pressure	Pa
S	Exchange surface	m^2
SEM	Scanning electron microscopy	
SUL	Sulfamethoxazole	-
TOC	Total Organic Carbon	$mgC.L^{-1}$
WWTP	Wastewater treatment plant	-

Objectifs et approche du Chapitre IV

Après avoir caractérisé le transfert d'ozone dans le Chapitre III, les travaux réalisés dans le cadre de cette thèse se sont focalisés sur le domaine d'application pour lequel l'utilisation du contacteur membranaire semblait particulièrement appropriée, notamment à des fins de REUSE.

Le Chapitre I a montré que les premières études concernant l'élimination de micropolluants organiques par contacteur membranaire présentaient des résultats positifs et très encourageants. Plus récemment, de nouvelles études (Merle et al., 2017; Stylianou et al., 2018) ont souligné l'intérêt du contacteur membranaire dans les procédés d'ozonation avancée lors du traitement des micropolluants afin de limiter la quantité d'ozone résiduel produit grâce aux multiples points de dosage que les membranes possèdent, et ainsi la quantité de bromates formés. Néanmoins, l'état de l'art réalisé sur ce sujet a montré qu'un effort devait encore être fait afin de mieux comprendre les phénomènes de transfert et réactionnels ayant lieu à l'interface avec la membrane et au sein des deux phases et de mieux définir les conditions permettant possiblement de minimiser les bromates formés.

L'étude présentée dans ce chapitre porte donc dans un premier temps sur l'élimination de deux micropolluants organiques d'origine pharmaceutique (la carbamazépine et le sulfaméthoxazole), ceux-ci étant retrouvés en grande quantité dans les eaux de sortie de station d'épuration mais également dans les eaux de surface. Ces composés ont été sélectionnés de par leur constante de réaction avec l'ozone élevée, qui en font de bons candidats pour ce type de procédé, leur occurrence dans les eaux de sortie de station d'épuration ainsi que dans la littérature et l'expertise d'analyse qui était présente au laboratoire concernant ces composés (analysés par LCMS/MS par M. Eddy Petit). La matrice utilisée était une eau de sortie de station d'épuration afin de prendre en compte l'impact de la matrice aqueuse, celui-ci étant non négligeable d'après la littérature (Lado Ribeiro et al., 2019). Cette matrice réelle était néanmoins dopée avec les MP ciblés afin d'être au-dessus des limites de quantification de l'appareil d'analyse utilisé, y compris après ozonation.

Dans un second temps, l'étude de la formation des bromates lors de l'ozonation d'un effluent secondaire par contacteur membranaire a été réalisée. Le liquide était alors recirculé afin d'augmenter le temps de séjour dans le contacteur et de pouvoir comparer les résultats obtenus à ceux d'un réacteur semi-batch à bulles. La matrice réelle était cette fois dopée avec des bromures ainsi que de l'acide para-chlorobenzoïque (p-CBA). Les bromures étaient ajoutés afin de s'affranchir des contraintes liées aux limites de quantification des bromures et bromates avec l'appareil d'analyse utilisé, la matrice initiale n'en contenant que très peu. La chromatographie ionique était réalisée par Mme Valérie Bonniol, à l'Institut Européen des Membranes. Le p-CBA servait quant à lui à contrôler la quantité de

radicaux hydroxyles présents au cours du temps, issus de la décomposition de l'ozone moléculaire et à l'origine de l'abattement rapide d'un grand nombre de micropolluants.

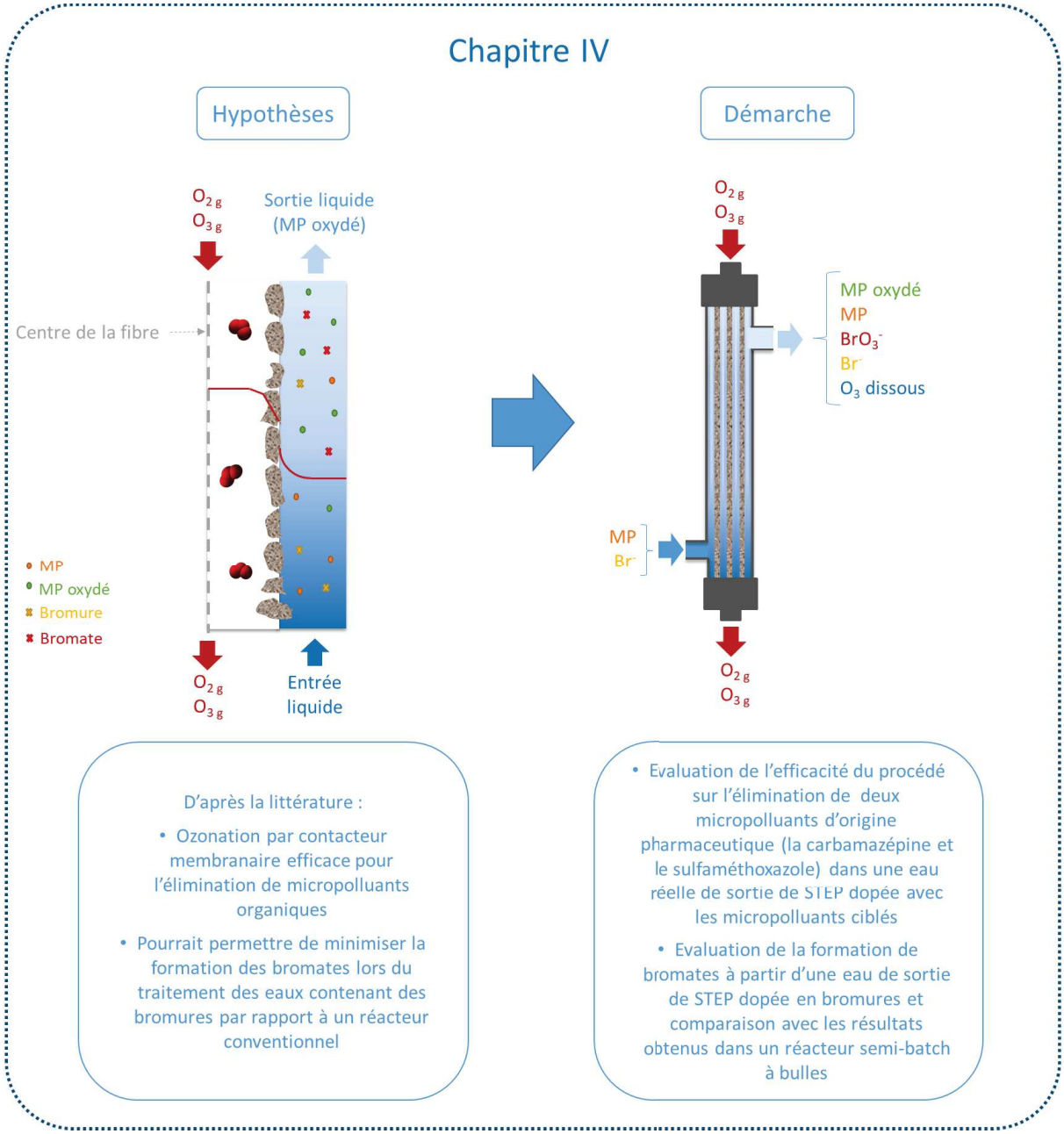

Diffusion of ozone through a hollow fiber membrane contactor for pharmaceuticals removal and bromate minimization

Alice Schmitt[a], Julie Mendret[a], Stephan Brosillon[a]

[a] IEM, University of Montpellier, CNRS, ENSCM, Montpellier, France

Abstract

Ozonation has been used for a long time for disinfection and oxidation in water treatment. Recently, this process has been pointed out as a solution against emerging contaminants. With hollow fibers membrane contactors, ozone is transferred to the water to be treated with a bubbleless operation and a defined exchange surface. Thanks to a lower residual ozone concentration, this device could limit ozonation by-products potentially formed, especially bromates which are regulated in drinking water. The aim of this study is to evaluate ozonation with membrane contactors for pharmaceuticals abatement and bromate minimization, compared to bubble columns in wastewater. To monitor hydroxyl radicals provided from molecular ozone decomposition and more oxidizing, *p*-chlorobenzoic acid (*p*-CBA) tracking, an ozone-resistant compound, is essential. To achieve that goal, a membrane contactor with 65 polytetrafluoroethylene hollow fibers, 0.107 m² exchange surface, 60 cm effective length, 0.45 mm/0.87 mm fiber inner/external diameter respectively, was used for the ozonation of real treated wastewater doped with 2 µM *p*-CBA and 3 $mg.L^{-1}$ bromide. The water was also spiked with two pharmaceuticals (carbamazepine and sulfamethoxazole) to evaluate the process efficiency on their abatements.

For a 100% *p*-CBA abatement, 1,600 $\mu g.L^{-1}$ was formed with the membrane contactor whereas 3,486 $\mu g.L^{-1}$ was formed with a bubble column at the same pH. This result highlights the possibility to produce a significant amount of hydroxyl radical with moderate bromate formation in real wastewater. Using the membrane contactor to treat carbamazepine, and sulfamethoxazole in real wastewater for very short contact times (about 2s), enables to achieve high fluxes of removed micropollutant depending on their reactivity towards ozone and hydroxyl radicals, without bromate formation. Membrane contactors are therefore a good alternative to bubble columns for simultaneous treatment of refractive pollutants in wastewater treatments and bromate minimization.

1. Introduction

Nowadays, the increasing presence and accumulation of micropollutants (MPs) in natural waters is a major environmental concern. MPs are harmful substances, detectable in the environment at very low concentrations (order of magnitude ng/L up to µg/L), and may be responsible for negative effects on

living organisms due to their toxicity, persistency, or bioaccumulation. Their impact, and particularly their additive effect, is yet unknown (Fent et al., 2006; Luo et al., 2014). A chronic exposure by drinking water consumption could therefore cause disastrous consequences on the health. In order to preserve water resources, wastewater treatment plants (WWTPs), which are one of the main sources of release of organic MPs in the aquatic receiving environment, need to be upgraded by an advanced treatment to ensure the elimination of these pollutants (Petrie et al., 2015). MPs can be classified in several categories, including pharmaceuticals whose the presence in aqueous environments is due to therapeutic drugs, personal hygiene products, but also hospital and pharmaceutical industry effluents (Khan et al., 2020; Shojaee Nasirabadi et al., 2016). Pharmaceuticals constitute the major part of the MPs released by WWTP (Bolong et al., 2009). Several studies showed their presence in the WWTP effluents but also in surface waters around the world (Ashton et al., 2004; Björlenius et al., 2018; Kolpin et al., 2002; Ternes, 1998; Valdés et al., 2016).

Among the pharmaceuticals, carbamazepine (CBZ) is an anti-epileptic drug used in many countries and is little or not at all removed in conventional WWTP (Björlenius et al., 2018; UNESCO and HELCOM, 2017). This compound is thus widespread in WWTP secondary effluent and has been widely reported in the literature (Cabeza et al., 2012; Luo et al., 2014; Rosal et al., 2010; Yang et al., 2017). Some studies have also highlighted its presence in surface waters, (Björlenius et al., 2018; Kråkström et al., 2020; Valdés et al., 2016). In the same way, sulfamethoxazole is an antibiotics which is frequently found in surface waters and in WWTP effluents worldwide (Ashton et al., 2004; Hirsch et al., 1999; Kolpin et al., 2002; Loos et al., 2013; Luo et al., 2011).

As a consequence, WWTPs must be upgraded by an advanced treatment for micropollutants abatement with suitable and economic options such as ozonation. In recent decades, ozonation processes have been successfully used to remove organic micropollutants, sometimes combined with another process as a polishing step (Bourgin et al., 2017; Gomes et al., 2017; Lee et al., 2014; Lee and von Gunten, 2016; Reungoat et al., 2010; Vittenet et al., 2015; Yao et al., 2018). The strong oxidizing power of molecular ozone is associated to the even stronger oxidizing power of the hydroxyl radicals, originating from the ozone decomposition, and lead to the removal of most organic compounds (von Gunten, 2003a). In addition, reaction rate constants of the organic MP with hydroxyl radicals are generally significantly higher than those with molecular ozone (i.e. $k_{O3} = 10^5\ M^{-1}.s^{-1}$ for the most reactive compounds while k_{OH} is often superior to $10^9\ M^{-1}.s^{-1}$) (Von Sonntag and Von Gunten, 2012). However, during ozonation processes, the matrix has to be taken into account as a scavenger of hydroxyl radicals due to the Natural Organic Matter (NOM) and the carbonates present in the water. According to the matrix, a higher ozone dose shall be applied (Stylianos K. Stylianou et al., 2018).

Conventional ozonation processes (e.g. ozonation rooms) employ ozone dispersion in the form of bubbles, leading to several disadvantages such as the generation of by-products sometimes more dangerous than the initial products (Richardson et al., 2007). For instance, bromates are produced during the ozonation of waters containing bromides and are regulated in drinking water due to their carcinogenic potential (Soltermann et al., 2017; von Gunten, 2003b). European Commission and US EPA defined this limit at 10 $\mu g.L^{-1}$ in drinking water (AIDA, 1998; USEPA, 1998). Bromates are due to an excess of residual ozone, caused by the difficulty to control the ozone dosage in conventional processes (Pinkernell and Von Gunten, 2001; von Gunten, 2003b). By transferring it in small quantities through the many membrane pores, membrane contactors seem to be promising devices to overcome this issue and simultaneously remove MP while minimizing the formation of bromates (Merle et al., 2017; Stylianos K Stylianou et al., 2018; Stylianos K. Stylianou et al., 2018). The membrane acts as a barrier between the two phases and the mass transfer occurs by diffusion (and not by dispersion) due to a concentration gradient (Schmitt et al., 2020). Ozone is hence transferred uniformly to the water to be treated, with a bubbleless process.

To the best of the authors' knowledge, only two studies have examined the formation of bromate during the ozonation through an out/in membrane contactor. Merle et al. studied the ozonation with ozone and peroxone (i.e. O_3/H_2O_2) of para-chlorobenzoic acid (p-CBA) which is an HO° very reactive compound and an O_3 resistant compound, through a polytetrafluoroethylene (PTFE) hollow fibers membrane contactor. In order to evaluate the bromates formation during the ozonation, the matrix (i.e. a groundwater, a river water and a lake water) were spiked with bromides and p-CBA. The Merle et al's results showed the p-CBA abatement and bromates formation for different ozone gas concentration, liquid residence time, and H_2O_2 doses. Higher residence times led to higher p-CPA removals but also higher bromates concentrations. Both increased with the ozone gas concentration. The highest H_2O_2 dose led to a better MP abatement but a higher bromates formation. They compared the membrane contactor performance to that of the conventional peroxone process (gas bubble injection). Results between the two processes were varying, depending on the tested conditions. When the ozone concentration in the gas phase was above 10 $g.Nm^{-3}$, the conventional process showed better results than the membrane contactor with groundwater, whatever the conditions. For the lake water, the membrane contactor showed better performances up to 5 $g.Nm^{-3}$ of ozone in the gas phase. For the river lake, less bromates were produced with the membrane contactor for a p-CBA removal superior to 80%. Nevertheless, it seems important to highlight that for an ozone gas concentration up to 5 $g.Nm^{-3}$, whatever the conditions and the matrix, the bromates concentration never exceeded 10 $\mu g.L^{-1}$ (i.e. the regulatory limit in EU). Stylianou et al. worked on the ozonation of four micropollutants (i.e. carbamazepine, benzotriazole, p-CBA and atrazine) with O_3 and H_2O_2 via a ceramic tubular

membrane contactor. The matrix (i.e. river water from Aliakmonas River, Greece) was spiked with the four selected micropollutants. They showed that the addition of peroxone had a variable effect (i.e. positive or negative) on the MP abatement, depending on the compound, and that a high concentration of bromates was produced with membrane contactor (higher than the regulatory limit of 10 $\mu g.L^{-1}$). They compared the results obtained with conventional experiments and those obtained with two membrane contactors having differing inner diameters (and exchange surfaces). They concluded that membrane contactors should have the highest possible inner surface per volume and that a low ozone concentration in the gas was required in order to minimize bromate formation.

The state of art thus exhibits that efforts should still be done on the evaluation of ozonation process when using membrane contactors for an application of tertiary water treatment, more specifically for the treatment of emerging pollutants. The objective of the present study lies in the evaluation of the performance of a in/out PTFE hollow fiber membrane contactor on the removal of two pharmaceuticals (i.e. carbamazepine and sulfamethoxazole) in a real wastewater (La Grande-Motte, France). Very few works have been carried out in the configuration in/out (Berry et al., 2017; Wenten et al., 2012). The configuration offers yet the main advantage of a lower risk of membrane fouling thanks to the circulation of the gas in the fibers whose the diameter is smaller than 1 mm instead of the treated wastewater which could have suspended matter. The matrix was spiked with the targeted compounds in order to overcome the constraints associated to the limit of detection (LOD) and of Quantification (LOQ) during the analyses. The second part of the study concerns the bromates formation. Experiments made with the membrane contactor were compared with those of a semi-batch bubble reactor in the same conditions. For this study, the matrix (i.e. WWTP effluent) was spiked with bromides (for LOQ and LOD constraints) and p-CBA in order to monitor hydroxyl radicals provided from molecular ozone decomposition and more oxidizing. The membrane contactor used had previously been fully characterized in the Chapter III.

2. Materials and methods

2.1. Chemicals

High purity (>98%) chemicals were used (analytical grade), all from Sigma-Aldrich (Saint-Quentin Fallavier, France).

Two pharmaceuticals (carbamazepine (CBZ) and sulfamethoxazole (SUL)) were purchased from Sigma-Aldrich. Their main characteristics are presented in Table 6. CBZ was stocked at 4°C whereas SUL was stocked at room temperature.

Table 6. Main characteristics of the targeted micropollutants ([a] (Huber et al., 2003), [b] (Mathon et al., 2021), c (Beltrán and Rey, 2018)).

Compound	Formula	MW ($g.mol^{-1}$)	k_{O3} ($M^{-1}.s^{-1}$)	k_{OH} ($M^{-1}.s^{-1}$)	Log K_{ow}	Solubility in water (25°C, $mg.L^{-1}$)	Semi-developped formula
Carbamazepine (CBZ)	$C_{15}H_{12}N_2O$	236	3.0×10^5 [a]	8.8×10^9 [b]	2.45 [b]	18 [b]	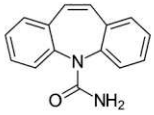
Sulfamethoxazole (SUL)	$C_{10}H_{11}N_3O_3S$	253	4.2×10^5 [c]	3.2×10^9 [b]	0.89 [b]	610 [b]	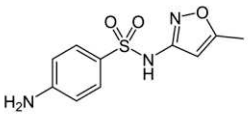

Potassium indigotrisulfonate ($C_{16}H_7K_3N_2O_{11}S_3$, MW = 617 $g.mol^{-1}$) and sodium sulfite (Na_2SO_3, MW = 126 $g.mol^{-}$) were used as ozone-scavenging reagents. Both were stocked at 4°C.

Sodium bromide anhydrous (BrNa, MW = 103 $g.mol^{-1}$) and 4-Chlorobenzoic acid (p-CBA) ($C_7H_5ClO_2$, MW = 157 $g.mol^{-1}$) were used to spike the matrix during the experiments on bromate formation. Both were stocked at room temperature.

2.2. Matrix studied

2.2.1. Real WWTP effluent

Real treated wastewater coming from a WWTP closed to Montpellier (La Grande-Motte, France) was used as a complex matrix. This WWTP has a maximum capacity of 65,000 population equivalent and treats 5,702 $m^3.d^{-1}$ of domestic wastewater on average, depending on the season, due to the increase of the population by 5 during the summer (seaside resort). Nitrogen removal is performed thanks to a nitrification/denitrification biological process with anaerobic zones alternating with anoxia zones. The WWTP is then equipped with an activated sludge process in an aerated basin (medium load). At the outlet, the WWTP has the particularity to owning a membrane bioreactor (MBR) with Submerged Membrane Units (SMU RW400) (KUBOTA, Japan), composed of flat sheet microporous membranes made of chlorinated polyethylene. Membranes have a total surface of 16,240 m^2 and an average pore size of 0.2 µm (ultrafiltration). The characteristics of the MBR permeate, corresponding to the WWTP effluent, are presented in Table 7 and Table 8. In order to optimize the treatment according to the season (high flow rate during summer time and low load during winter), two identical files are present upstream of the MBR (5,770 m^3 per file), the second being applied exclusively during summer. Concerning the sewage sludge, those are treated with static thickening by gravity, and represent 345.48 tons dry matter per year. The effluent was sampled at the outlet of the MBR and stored at 4°C after sampling in order to limit the variation of the composition.

Table 7. Global parameters of the WWTP effluent.

Parameters	Mean value	Standard deviation
TOC (mgC/L)	6.8	0.7
COD (mgO_2/L)	18.0	1.0
pH	7.7	0.2
SUVA ($L.cm^{-1}.mgC^{-1}$)	0.02	0.01

Table 8. Ionic composition of the WWTP effluent.

Average ionic composition (mg/L)			
Sodium (Na^+)	88.1 ± 0.8	Bromate (BrO_3^-)	< LOD
Ammonium (NH_4^+)	< LOD	Chloride (Cl^-)	155 ± 6
Potassium (K^+)	22.6 ± 0.3	Nitrite (NO_2^-)	0.2 ± 0.2
Magnesium (Mg^+)	10.1 ± 0.3	Chlorate (ClO_3^-)	0.5 ± 0.3
Calcium (Ca^{2+})	92.0 ± 0.7	Bromide (Br^-)	0.29 ± 0.03
Sulphate (SO_4^{2-})	84 ± 10	Phosphate (PO_4^{3-})	0.3 ± 0.3

2.2.2. Solution spiked with the targeted MP

A volume of 30 L of the real matrix (i.e. real treated wastewater) was spiked with 2 $mg.L^{-1}$ of each MP studied. The solution was then agitated during at least 24h (to ensure complete dissolution of the MPs), before being incorporated in the feed tank. The solution was then balanced with the system (i.e. the ozonation pilot) thanks to a liquid recirculation during about 12h, with compressed air circulating inside the fibers to prevent the penetration of water in the membrane pores. This balance was established in order to allow the potential adsorption of MP in the system (depending of the K_{OW} of the MP). The initial concentration of each MP was then measured by analyzing three samples from the feed tank (after balancing) and three samples from the tap upstream the membrane contactor. The average value of these samples was kept as initial concentration of each MP for the results interpretation.

2.2.3. Bromide solution

The real matrix was spiked with 2 µM of p-CBA and 3 $mg.L^{-1}$ of bromide (Br^-) by means of BrNa. The solution was then agitated during at least 24h to ensure the complete dissolution of the chemicals.

It is worthy of note that the initial concentration of bromide in the matrix during the summer was significantly higher (up to 1.6 $mg.L^{-1}$) than during the winter (0.3 $mg.L^{-1}$in average), before being spiked. Indeed, the water used in this work came from the WWTP outlet of a touristic city, characterized by its resort area. During all the experiments, the effluent had been spiked with the same quantity of bromides, whatever the initial bromide concentration. Consequently, the initial concentration of bromide was lower for the experiments with the membrane contactor than with the bubble reactor. This difference has been taken into account during the interpretation of the experimental results by normalizing the bromate and bromide concentrations with the initial bromide concentration.

Nevertheless, a higher initial concentration of bromide promotes the production of more bromates due to the kinetics of bromate formation which is depending on the bromide concentration.

2.3. Analytical methods

2.3.1. Ozone analysis

Indigo method (Bader and Hoigné, 1982) was used to determine the dissolved ozone concentration in the liquid phase.

2.3.2. MP analyses

Liquid chromatography-tandem mass spectrometry (LC-MS/MS) was used to quantify the mix of MPs and was performed with a Waters® device. A column with XSelect® HSS-T3-C18 resin (100 mm * 21 mm), 2.5 µm particles size was used as the stationary phase at room temperature, with eluent A (90 % HPLC grade water + 10 % HPLC grade acetonitrile (ACN) + 0.1% formic acid) and eluent B (ACN + 0.1% formic acid). The flow-rate was 0.25 $mL.min^{-1}$ and the gradient elution profile described in the Chapter II (Tableau 5) was applied. To achieve the best sensitivity, the MS was adjusted to facilitate the ionization process and the detection conditions were: capillary potential 3.5 kV, cone voltage 30 V, source temperature 120°C, desolvation temperature 450°C, cone gas flow 50 $NL.h^{-1}$, desolvation gas flow of 500 $NL.h^{-1}$, and collision energy of 10 V. Nitrogen was used as a nebulizer gas and argon as a collision gas. The calibration curves were made in the same matrix as the samples to avoid matrix effects on detection (i.e. calibration curves were made using WWTP effluent with known concentrations of MP). Two calibration curves were made for each MP, by analyzing standard samples before and after analyte samples, to avoid instrumental drift. The LOD and LOQ are respectively estimated about 3 $\mu g.L^{-1}$ and 10 $\mu g.L^{-1}$ for the CBZ, 0.13 $\mu g.L^{-1}$ and 0.74 $\mu g.L^{-1}$ for the SUL.

2.3.3. pCBA analysis

Analyses of pCBA were performed by HPLC-UV on a Waters Acquity UPLC system, coupled to Empower analyst software, fitted with a NucleoShell (Macherey-Nagel) column (50 mm length * 2 mm inside diameter - 2.7 µm particles size) at ambient temperature (T=22°C). The mobile phase was constituted of buffer A (HPLC grade water + 0.1% (v/v) trifluoroacetic acid) and buffer B (HPLC grade acetronitrile + 0.1% (v/v) trifluoroacetic acid). The flow rate was 0.25 $mL.min^{-1}$. Isocratic run of 3 min was applied with 80% of A and 20% of B, in which the retention time of pCBA was 1.88 min. UV detection was performed at λ = 240 nm.

For the samples collected after the ozonation, 200 µL of Na_2SO_3 (10 $mg.L^{-1}$) were added to 2 mL of sample as scavenger of the dissolved ozone.

2.3.4. Real WWTP effluent characterization / Global indicator for pollution monitoring

Analyses of pH were performed with a titrator pHmeter (Titroline Easy, Schott Instruments) calibrated with two buffer solutions (pH = 4.0 and 6.87). COD values were measured using Hach kits LCK 1414 (5-60 mgO_2/L).

TOC analyses were performed using a TOC-VCSN Shimadzu analyzer (Shimadzu Japan) after filtration of the samples through a 0.45 µm filter. UV254 absorbance and SUVA were used to track a relative amount of unsaturated and/or aromatic carbon of Natural Organic Matter (NOM) (Weishaar et al., 2003). The specific UV absorbance ($SUVA_{254}$) was determined from the ratio of UV254 absorbance on TOC value. UV254 absorbance was measured in a 1 cm quartz cuvette using a UV-vis spectrophotometer (UV-2401PC, Shimadzu, Japan).

Concentrations of anions and cations were measured in using an ion chromatograph ICS-1000 equipped with a AERS suppressor (4 mm), an IonPac AS19 column and a DS6 conductivity detector for anions, and an ICS-900 equipped with a CSRS suppressor (4 mm), an IonPac CS12A column and a DS5 conductivity detector for cations (Dionex, Thermo Scientific). Samples were added automatically with a sample changer (AS40).

For the samples collected after ozonation, 200 µL of Na_2SO_3 (10 $mg.L^{-1}$) were added to 2 mL of sample as scavenger of the dissolved ozone.

2.4. Membrane contactor technology

The membrane contactor used in this work was supplied by Polymem (France). Its characteristics are listed in Table 9. Gas circulates inside the fibers and liquid in the shell by counter-current flow (Figure 23).

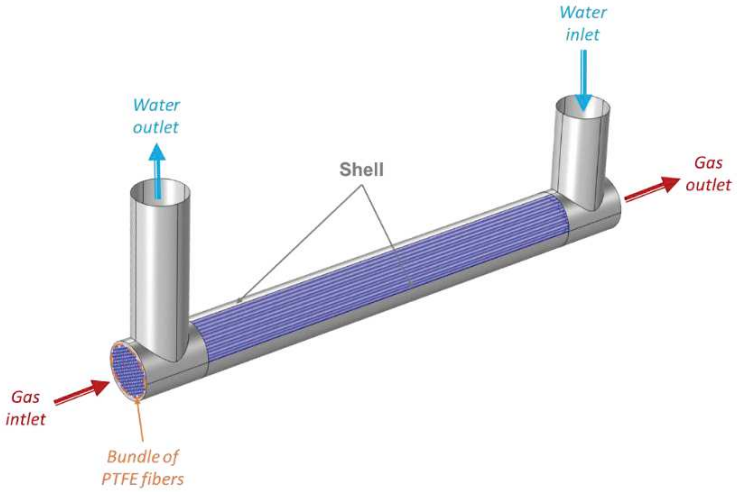

Figure 23. Configuration of the membrane contactor.

The hollow fibers were made of polytetrafluoroethylene (PTFE), known to be highly ozone-resistant over time (Bamperng et al., 2010). The hollow fiber form enables a very compact process through a large exchange surface area.

Table 9. Membrane contactor technical specifications.

PTFE fibers			
Number *	65	Effective length (cm) *	60
Inside diameter (mm) *	0.45	Effective outside surface (m^2)	0.107
Outside diameter (mm) *	0.87	N_2 permeance (GPU) *	33,904
Porosity [a]	0.58	Tortuosity [b]	3.47
Liquid volume (m^3) [c]	3.63×10^{-5}	Specific exchange surface *a* (m^2/m^3) [d]	2,948
Stainless steel shell			
Inside diameter (mm) *	9.5	Filling rate *	54.5%

** Values specified by the manufacturer (Polymem, France)*

The membrane porosity ε ([a]) was determined gravimetrically (Sartorius CPA 225D balance), by measuring the mass of isopropanol (IPA) inside the membrane pores (Wang et al., 2010). The porosity was calculated as:

$$\boldsymbol{\varepsilon} = \frac{(\boldsymbol{w_{wet} - w_{dry}})/\boldsymbol{D_{iso}}}{\frac{\boldsymbol{w_{wet} - w_{dry}}}{\boldsymbol{D_{iso}}} + \boldsymbol{w_{dry}}/\boldsymbol{D_{PTFE}}} \text{ , [41]}$$

where w_{wet} is the weight of the wet membrane, w_{dry} is the weight of the dry membrane, D_{iso} is the IPA density, and D_{PTFE} is the polymer density.

The tortuosity factor τ ([b]) was estimated by the porosity-tortuosity relationship defined by (Iversen et al., 1997) as:

$$\boldsymbol{\tau} = \frac{(\boldsymbol{2-\varepsilon})^2}{\boldsymbol{\varepsilon}} \text{ , [42]}$$

The liquid volume ([c]) and the specific exchange surface area ([d]) were calculated from the shell and fiber properties given by the manufacturer.

When using a membrane contactor, a very important variable to check is the transmembrane pressure. If the ratio of the pressure on the liquid side to the pressure on the gas side is higher than the "breakthrough pressure", wetting of the membrane pores occurs (i.e., the liquid penetrates the membrane pores), lowering the mass transfer. The breakthrough pressure (relative, in Pa) is defined by the Young-Laplace equation as:

$$\boldsymbol{P_{breakthrough}} = \frac{\boldsymbol{4 \times \gamma \times \cos\theta}}{\boldsymbol{d_{pore,max}}} \text{ , [43]}$$

where γ is the surface tension of water with air (= 73 x 10^{-3} N.m^{-1} at 20 °C), θ is the contact angle between the membrane and the water (radians), and $d_{\mathrm{pore,max}}$ is the maximum pore diameter (m) (determined from fiber SEM pictures analyzed with ImageJ® software)

In this work, the breakthrough pressure was estimated to be 0.4 bar (taking the contact angle between the material and the water to be greater than 102°).

Conversely, if the ratio of the pressure on the gas side to the pressure on the liquid side is higher than the "bubble pressure", there is ozone dispersion in water by bubbles. In this case, one of the main advantages of the membrane contactor, which is to transfer ozone uniformly to the water to be treated in a bubbleless operation, is lost. The bubble pressure was experimentally determined with the following method, adapted from the method presented by Khayet and Matsuura (Khayet and Matsuura, 2001). A special membrane contactor was produced for this test, with PTFE fibers provided by the same supplier (Polymem) as for the membrane contactor used in the experiments, but without a shell. Oxygen circulated inside the membrane fibers immersed in water. The oxygen pressure was then gently increased stepwise. The bubble pressure was considered attained when the first bubble was observable. With this method, the bubble pressure was estimated to be about 0.1 bar. Hence the transmembrane pressure (i.e., the difference between the pressure on the liquid side and the pressure on the gas side) had to stay between −0.1 and 0.4 bar.

To evaluate the hydrophobicity of the fibers before and after use, contact angle was measured using the sessile drop method with a GBX meter (Digidrop, France) equipped with image analysis software (Visiodrop). First, fibers were fixed on a glass plate. A droplet of water (1 µL) was then deposited on the film surface with a precision syringe. The method is based on image processing and curve fitting for contact angle measurement from a theoretical meridian drop profile, determining two contact angles between the baseline of the drop and the tangents at the drop boundary (i.e., one angle is measured on the right and one on the left, the final contact angle being the average of the two values). Each measurement was repeated three times.

Scanning electron microscopy (SEM) pictures were obtained using a Hitachi S-4800 instrument to evaluate the state of the fibers and their deterioration after use. Samples were previously metalized with a thin layer of platinum to improve their electronic conductivity.

2.5. Ozonation pilots

2.5.1. Description of the ozonation pilot with membrane contactor – liquid in closed-loop

Figure 24 depicts the experimental set-up used for ozonation process. When the liquid was in a closed loop, this ozonation lab-scale pilot consisted of a membrane contactor continuously feed by an ozone generator (BMT 803 N) from a lab-grade pure oxygen tank. Before circulating in the gas side of the membrane contactor, the ozone was diluted with the oxygen to achieve the desired gas flowrate. An ozone gas analyzer (BMT 964) was used to monitor the gas ozone concentration ($C_{O3,g,inlet}$) after dehumidification. Two electrovalves connected to a computer were used to determine the desired concentration of the oxygen/ozone mixture.

The liquid flowed into the pilot from a stirred 1.5 L glass tank under thermostatic control (20°C). During the experiment, an agitator was used to homogenize dissolved ozone and MP concentrations in the tank. A peristaltic pump (Watson Marlow 323) was used for the liquid circulation. Two taps (upstream and downstream of the membrane contactor) were used for sampling. Ozone was transferred from the gas phase of the membrane contactor to the liquid phase, thanks to a concentration gradient. The ozone gas analyzer (BMT 964) was used once the experiment started to analyze the gas ozone concentration at the outlet of the membrane contactor ($C_{O3,gas,outlet}$) (after dehumidification).

The main advantage of this configuration was to increase the residence time in the membrane contactor and has thus been used for the study of the bromates formation. Indeed, the liquid in open loop did not lead to an evolution of the bromate concentration due to the very short residence time (< 3s) in the contactor in this case and to the lack of sensitivity of the ion chromatography. Therefore, no bromates were detected when the open loop was used.

In addition, this configuration has been used during the preliminary step of the experiments with the targeted MPs. This step led to the equilibrium between the MPs and the system (i.e. pipework, membrane contactor, and feed tank) by leaving the possibility for the MPs to adsorb to the system before beginning the ozonation. During this step, compressed air was circulating inside the fibers in order to avoid the penetration of liquid in the membrane pores. The MPs concentrations were then measured and considered as the initial concentrations for the study of the process of ozonation. Therefore, the removal due to a potential adsorption on the system was deleted for the study of the MPs removal (i.e. MPs removal was only due to the ozonation).

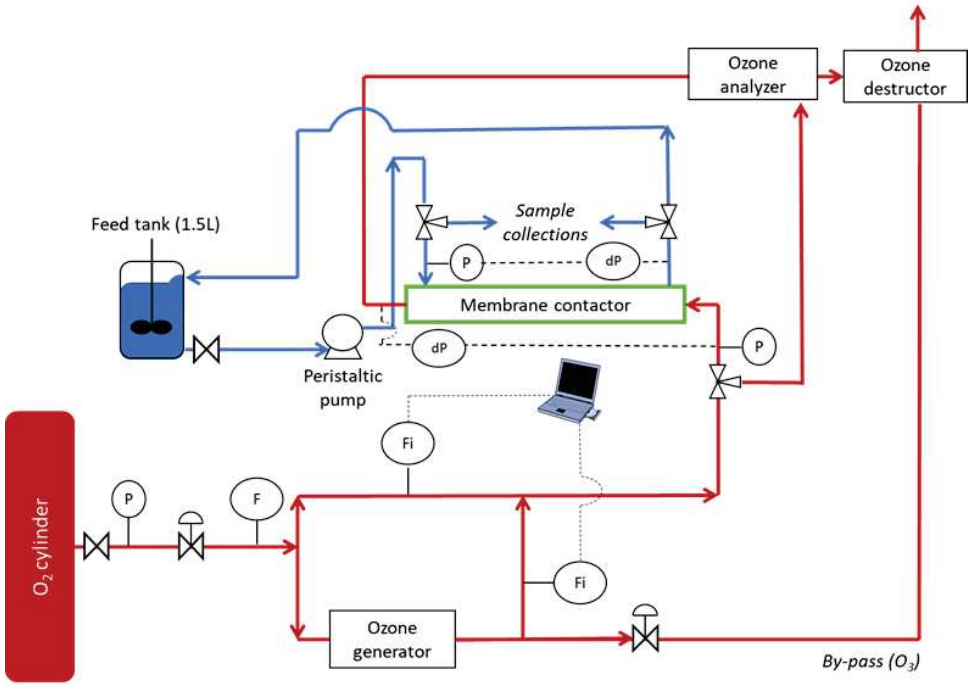

Figure 24. Flowsheet of the ozonation pilot - liquid in closed loop - gas in open circuit (red: gas stream, blue: liquid stream).

2.5.2. Description of the ozonation pilot with membrane contactor – liquid in open circuit

The ozonation pilot with the liquid flowing in an open circuit was almost the same as in the closed loop. The main difference was that the liquid circulated only once in the membrane contactor. The liquid was then recovered in a container with KI solution to prevent the ozone degassing. To achieve the steady-state values, a larger feed tank was used (30L). The tank was made of stainless steel, stirred, and under thermostatic control (20°C). The main advantage of this configuration was the simplification of the mass balances in comparison to that with the liquid in closed loop, and has thus been used for the study of the targeted MPs removal. A duplicate was made for each experiment, and a triplicate for the reference test (identified in the Table 10 by number 1). Before the start of each experiment, the configuration with the liquid in closed-loop was used in order to achieve the balance between the system (i.e. the membrane contactor and the piping) and the MP, due to potential adsorption of the MP on the system. At the beginning of each experiment, three samples were collected in the tank and three samples were collected via the tap located at the inlet of the membrane contactor. Once the steady state achieved, six samples of liquid were collected at the outlet of the membrane contactor.

2.5.3. Description of the ozonation pilot with bubble column (semi-batch reactor)

To compare the results obtained with the membrane contactor with those obtained with a conventional process, a semi-batch bubble reactor was also used (see Figure 15.). A 4 L glass reactor was stirred using an agitator to homogenize the liquid and kept under thermostatic control (20°C). A

recirculating pump was used for sampling. As in the previously described ozonation pilot with membrane contactor, an oxygen cylinder fed the gas circuit. A gas flowmeter was then used to regulate gas flowrate upstream of an ozone generator (BMT 803 N). The ozone generator was used to convert part of the pure oxygen into ozone. The amount of ozone produced by the generator could be manually regulated with a setting knob. The gas mixture obtained therefore comprised ozone and oxygen. An electrovalve connected to a computer was used to set the gas flowrate and obtain the desired concentration of the gas mixture. Two options were then possible. The first was for the gas mixture to flow through the by-pass and be analyzed with an ozone analyzer (BMT 964) and then processed in an ozone destructor, in the same way as with the ozonation pilot with the membrane contactor. The ozone concentration given by the analyzer was then the ozone concentration in the gas at the inlet of the process. The other option was for the gas mixture to flow inside the semi-batch reactor with a porous diffuser and then be analyzed. The ozone concentration given by the analyzer was then the ozone concentration in the gas at the outlet from the bubble column. The analyzer was preceded by a dehumidifier to remove any humidity in the gas and protect the device. The residual ozone was destroyed by the ozone destructor using active carbon.

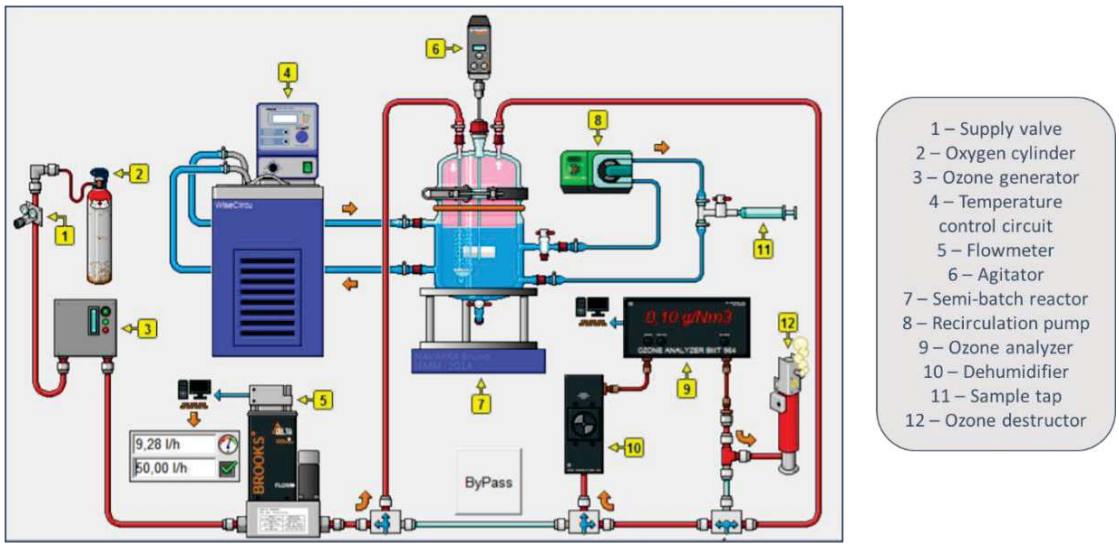

Figure 25. Scheme of the ozonation pilot with bubble column.

2.6. Exposure to hydroxyl radicals and molecular ozone

The exposure to hydroxyl radicals (M.min) was determined from the tracking of the pCBA such as:

$$\int_0^t C_{HO^\circ,liq}\, dt = \frac{1}{k_{OH-pCBA}} \times \ln\left(\frac{C_{pCBA,0}}{C_{pCBA}}\right) \text{, [44]}$$

Where C_{pCBA} was the concentration of *p*CBA in the water at a given point in time (mol.L^{-1} or g.L^{-1}), $C_{pCBA,0}$ was the initial concentration of *p*CBA in the water (mol.L^{-1} or g.L^{-1}), and $k_{OH-pCBA}$ was the

reaction rate constant of *p*CBA with HO° (= 5 x 10^9 $M^{-1}.s^{-1}$ (Neta and Dorfman, 1968)). In order not to disturb the water system and thus not to produce misleading results, $[pCBA]_0$ had not to be too higher (Pi et al., 2005).

The exposure to molecular ozone (M.min) was defined such as $\int C_{O3,liq}\, dt$ where $C_{O3,liq}$ was the dissolved ozone measured with indigo method.

3. Results and discussions

3.1. Study of the ozonation of targeted micropollutants through a PTFE hollow fiber membrane contactor

Results are reported as means with standard deviations (in brackets) with global parameters associated to each experiment (Table 10).

Table 10. Global parameters and objectives of the experiments with the targeted MP.

Experiment	1	2	3	4	5	6	7
Objective	Reference	Variation of the gas concentration	Variation of the gas concentration	Variation of the liquid flowrate	3 successive passages of the liquid in the membrane contactor (variation of the residence time)		
Qliq ($L.h^{-1}$)	46.2	46.2	46.2	92.3	47.8		
Qgas ($L.h^{-1}$)	8						
$C_{O3,g,\ inlet}$ ($g.Nm^{-3}$)	14.7 (0.1)	22.8 (0.4)	30.6 (0.2)	15.2 (0.5)	14.9 (0.1)		
pH	7.9 (0.1)	7.5 (0.1)	8.0 (0.1)	7.5 (0.1)	7.6 (0.1)		
$C_{CBZ\ inlet}$ ($mg.L^{-1}$)	1.92 (0.12)	1.98 (0.02)	2.22 (0.1)	1.92 (0.03)	1.98 (0.03)	1.54 (0.07)	1.31 (0.07)
$C_{SUL\ inlet}$ ($mg.L^{-1}$)	1.95 (0.11)	1.91 (0.02)	2.04 (0.06)	1.85 (0.07)	1.84 (0.03)	1.42 (0.08)	1.16 (0.08)

In the experiments, the pH varied from 7.5 to 8, depending on the pH of the water collected at the outlet of the WWTP.

3.1.1. Effect of the ozonation on the global parameters

During the ozonation, the ozone does not react only with the MP but also with the carbon or ions included in the matrix studied. The Figure 26 and Figure 27 summarize the global parameters of the water before and after each experiment (described in the Table 10), more specifically the Dissolved Organic Carbon (DOC), the Chemical Oxygen Demand (COD), and the SUVA index.

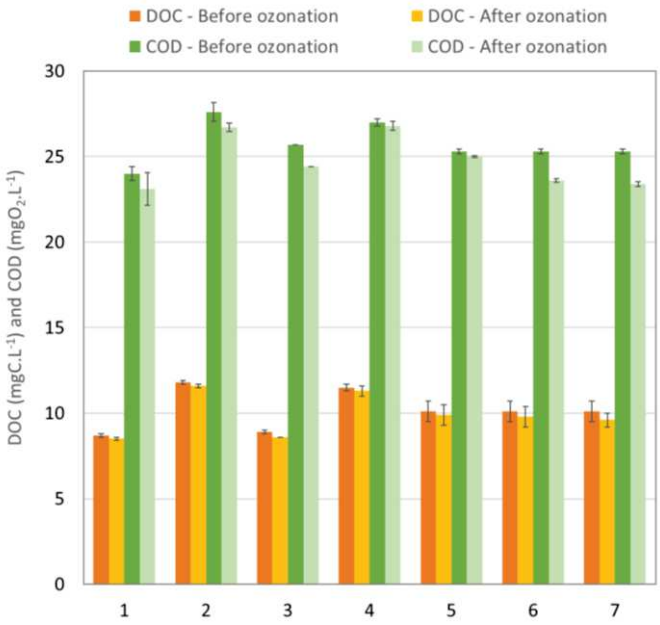

Figure 26. DOC and COD before and after each experiment of ozonation. The number indicated on the x axis corresponds to the number of the experiments in table 10.

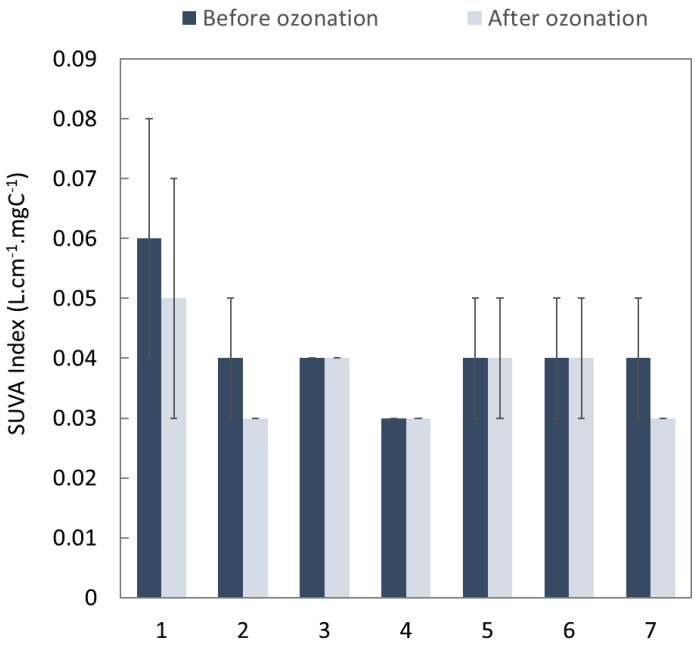

Figure 27. SUVA index before and after each experiment of ozonation. The number indicated on the x axis corresponds to the number of the experiments in table 10.

The differences between the DOC before ozonation for each experiment (Figure 26) are explained by the composition of the water collected at the outlet of the WWTP which depends on the season. The DOC was very little reduced by the ozonation. This can be explained by the short residence time in the contactor, which did not lead to the complete oxidation of the compounds. In particular, the MP were transformed into metabolites which are also organic compounds. For this same reason, the aromaticity of the water, which is characterized by the SUVA index (Figure 27), representative of the double bonds'

quantity, and typically impacted during conventional ozonation processes, did not evolve during the experiments, or was comprised in the standard deviation. Only the COD (Figure 26) showed a decrease more significant (but remaining low), with a reduction up to 7.5% in the case of the recirculation, after the third run (8th experiment). This emphasizes the importance of the residence time to enhance the overall quality of the water, a duration of 3s being not enough to have an impact on the global parameters but sufficient to remove a substantial amount of MP.

3.1.2. Effect of the ozone concentration

In this series of experiments, the concentration of ozone in the gas phase at the inlet of the contactor was varied (i.e. the concentration was fixed at 15 g.Nm^{-3}, 22.5 g.Nm^{-3} and 30 g.Nm^{-3}, columns 1, 2 and 3 in table 5). The liquid flowrate was fixed at 46.2 L.h^{-1} and the gas flowrate at 8L.h^{-1}. The concentrations of CBZ and SUL at the inlet were respectively 1.92 +/- 0.12 and 1.95 +/- 0.11.

The Figure 28.a shows the abatement of each targeted MP for the different concentrations of ozone in the gas phase. A better removal was achieved for all the MP studied when the concentration was increasing. This confirms the results obtained in the Chapter III, where this parameter had been highlighted as having a significant impact on the ozone transfer.

On the Figure 28, it is noticeable that the SUL abatement was similar to the CBZ abatement (in the standard deviations). Indeed, molecular mechanisms are promoted when k_{O3} > 10^4 M^{-1}.s^{-1} and the kinetic constants of the reaction between CBZ with ozone and SUL with ozone are 3.0 x 10^5 M^{-1}.s^{-1} and 4.2 x 10^5 M^{-1}.s^{-1} respectively (Bourgin et al., 2017; Schmitt et al., 2020). Therefore, the molecular mechanism was the main way of action for the targeted MP removal and the reaction of CBZ with ozone was as fast as SUL with ozone.

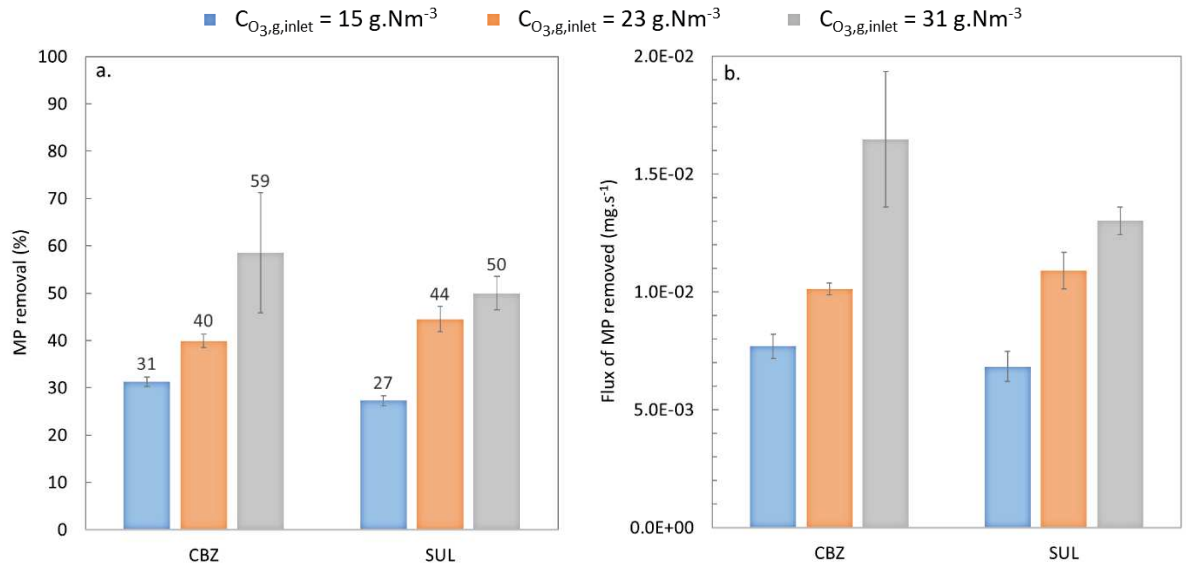

Figure 28. Abatement of CBZ and SUL for an ozone concentration at the inlet of the gas phase of 15, 23, and 31 g.Nm^{-3}, a liquid flowrate of 46.2 L.h^{-1}, a gas flowrate of 8 L.h^{-1}, at neutral pH.

An observation can be made about the abatement percentages, which were lower than those achievable with conventional ozonation processes, where the removal could achieve 100% for CBZ and between 97 and 99% for SUL (Mathon et al., 2021). It seems therefore important to mention that in our study the removal was achieved for a very short residence time of 2.8 s in the membrane contactor instead of between 10 and 30 min in a traditional process (at full-scale WWTP) (Penru et al., 2017). A part of the study of Mathon et al. about the ozonation of MPs involved batch experiments with real treated wastewater (Mathon et al., 2021). A volume of 30L of water was spiked with 0.01 $mg.L^{-1}$ of CBZ. A specific dose of ozone transferred of 1.6 $gO_3.gDOC^{-1}$ was applied during 15 min. The authors showed that 100% of CBZ was removed in about 125s, corresponding to a flux of MP removed of 2.4 x 10^{-3} $mg.s^{-1}$, which is lower than in our study. Furthermore, a CBZ abatement of about 41% was achieved in 60s, which is more than 20 times longer than in our study for a similar abatement. It seems also important to note that the specific dose of ozone transferred in the experiments presented in Figure 28 was comprised between 0.14 and 0.21 $gO_3.gDOC^{-1}$ instead of 1.6 $gO_3.gDOC^{-1}$ in the study of Mathon et al., that could explain a lower MPs abatement.

In addition, the quantity of MP removed was high despite the percentages of abatement relatively low, due to the higher initial concentration in our experiments than in the reality (i.e. at the outlet of WWTP) or in other studies, where the concentration of MP varies from the $ng.L^{-1}$ up to the $\mu g.L^{-1}$.

Moreover, the present results were obtained with a membrane contactor having an exchange surface area of 0.107 m². Membrane contactors have the big advantage to be flexible: the surface of membrane (i.e. the exchange surface) can easily be increased while preserving a low footprint compared to conventional processes.

3.1.3. Effect of the liquid flowrate

In order to study the effect of the liquid flowrate, experiments were realized at two liquid flowrates of 46.2 $L.h^{-1}$ and 92.3 $L.h^{-1}$, a gas flowrate of 8 $L.h^{-1}$, and an ozone concentration at the inlet of the gas phase of about 15 $g.Nm^{-3}$. The results are presented on the Table 11 and the Figure 29.

The Figure 29 shows that more MP were removed when the liquid flowrate was doubled. It is explained by a higher flux of transferred ozone when the liquid flowrate is increased, thanks to the diminution of the transfer resistance in the boundary layer between the liquid and the membrane. Indeed, the thickness of this boundary layer become thinner when the liquid flowrate is increased. The removal of MPs was thus better at a higher liquid flowrate despite a shorter residence time in the membrane contactor.

Table 11. Results obtained on the elimination of MPs and transferred ozone during the experiments with the two liquid flowrates.

Liquid flowrate	46.2 $L.h^{-1}$		92.3 $L.h^{-1}$	
Transferred ozone ($mg.min^{-1}$)	0.92		1.80	
MP	*CBZ*	*SUL*	*CBZ*	*SUL*
Concentration of MP at the inlet ($mg.L^{-1}$)	1.92 (0.12)	1.95 (0.11)	1.92 (0.04)	1.85 (0.07)
Concentration of MP at the outlet ($mg.L^{-1}$)	1.32 (0.09)	1.42 (0.06)	1.39 (0.03)	1.34 (0.08)
Flux of MP removed ($mg.s^{-1}$)	7.69×10^{-3} (5.13×10^{-4})	6.79×10^{-3} (5.98×10^{-4})	1.35×10^{-2} (1.41×10^{-3})	1.315×10^{-2} (2.56×10^{-4})

On the Figure 29, we can observe that the SUL abatement was similar to the CBZ abatement (in the standard deviations). In the same way as on the Figure 28, these results are consistent with the assumption that the molecular mechanism was the main way of action for the MP removal.

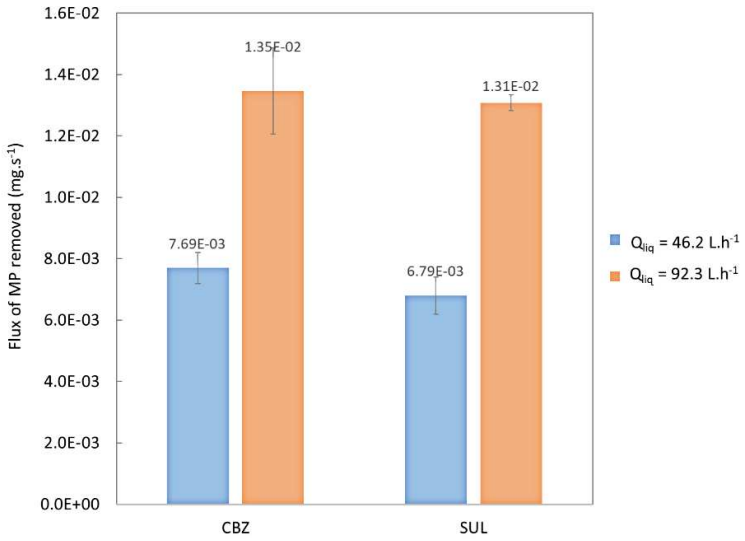

Figure 29. Flux of CBZ and SUL removed for a liquid flowrate of 46.2 $L.h^{-1}$ and 92.3 $L.h^{-1}$, an ozone concentration at the inlet of the gas phase of 15 $g.Nm^{-3}$, a gas flowrate of 8 $L.h^{-1}$, at neutral pH.

3.1.4. Effect of the residence time – recirculation system

The effect of the recirculation of the water was also studied, increasing the residence time in the membrane contactor from 2.7 s at the first run, to 5.4 s at the second run then 8.1 s at the third run. These experiments were different of the protocol of the part 3.1.2. During these experiments, the liquid flowrate was fixed at 47.8 $L.h^{-1}$, the gas flowrate at 8$L.h^{-1}$, and the concentration of ozone at the

inlet of the gas phase at about 15 $g.Nm^{-3}$. These experiments were equivalent to a scheme with three membrane contactors in series. One can note that the rise of the liquid flowrate had also an impact on the residence time, but mostly on the flow which increased the ozone transfer despite a shorter residence time (Table 11).

The Figure 30 represents the abatement of the targeted MP after each water run in the contactor. The calculation was based on the initial MP concentration at the inlet of the contactor before the first run. We can see that for all the MP studied, the removal was better after each recirculation. About 23% of abatement was achieved for the targeted MP after the first run. For the 2nd and the 3rd run, the SUL abatement was insignificantly higher than the CBZ abatement (i.e. in the standard deviations). After three runs, abatements of 46% and 51% were achieved respectively for the CBZ and the SUL. A higher residence time has therefore a positive impact on the MP removal. However, the evolution of the abatement was not proportional to the evolution of the residence time, due to slower reaction kinetics when the MP concentrations decreased. For instance, the removal of the CBZ was doubled when the residence time was tripled. This highlights the necessity to optimize the residence time in a membrane contactor in order to find a compromise between the treatment duration and the MP concentration at the outlet.

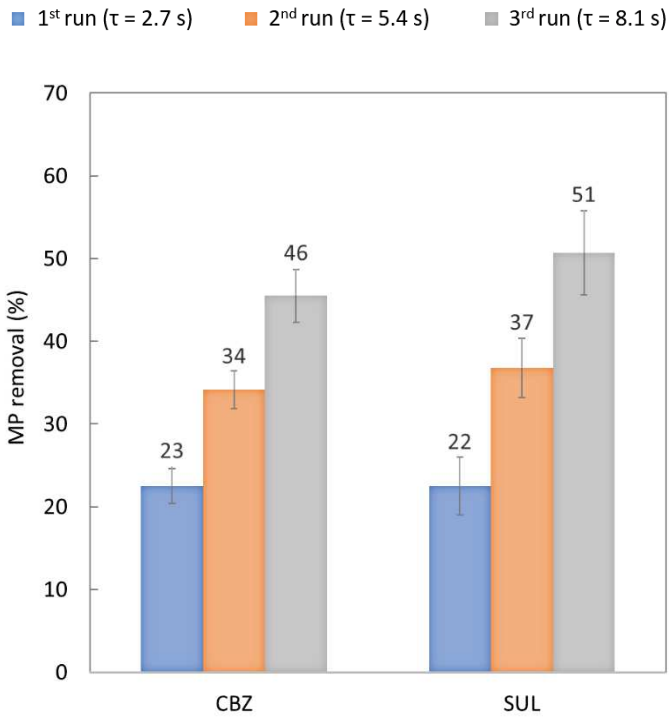

Figure 30. Percent removal of MP calculated from the inlet concentration before the 1st run during the experiments with recirculation of the water with an ozone concentration at the inlet of the gas phase of 15 $g.Nm^{-3}$, a liquid flowrate of 47.8 $L.h^{-1}$, a gas flowrate of 8 $L.h^{-1}$, at neutral pH.

The flux of MP removed per membrane surface during each run in the steady-state (in $mg.s^{-1}.m^{-2}$) was plotted on the Figure 31. Unlike the results presented on the Figure 30, the calculation was based on the inlet and outlet of each run. It can be observed that the fluxes of MP removed were significantly higher during the first run compared to the second and the third, where the fluxes were similar (i.e. in the standard deviations). However, the flux of ozone transferred, calculated from a mass balance on the gas phase, was approximately the same at each run, decreasing only slightly: 0.80 (+/- 0.05) $mgO_3.min^{-1}$ at the first run, 0.79 +/- 0.07 mg $O_3.min^{-1}$ during the second, and 0.74 +/- 0.06 mg $O_3.min^{-1}$ during the last run. Simultaneously, the concentration of residual ozone was about the same for each run (Table 12). Indeed, the difference between the first run and the following runs can be explained by a slower kinetics of reaction due to a lower concentration of MP.

The Figure 31 also represents the total flux of MP removed after three runs per membrane surface (in $mg.s^{-1}.m^{-2}$) which was calculated from the concentration at the inlet of the first run and gave similar results for the two MPs.

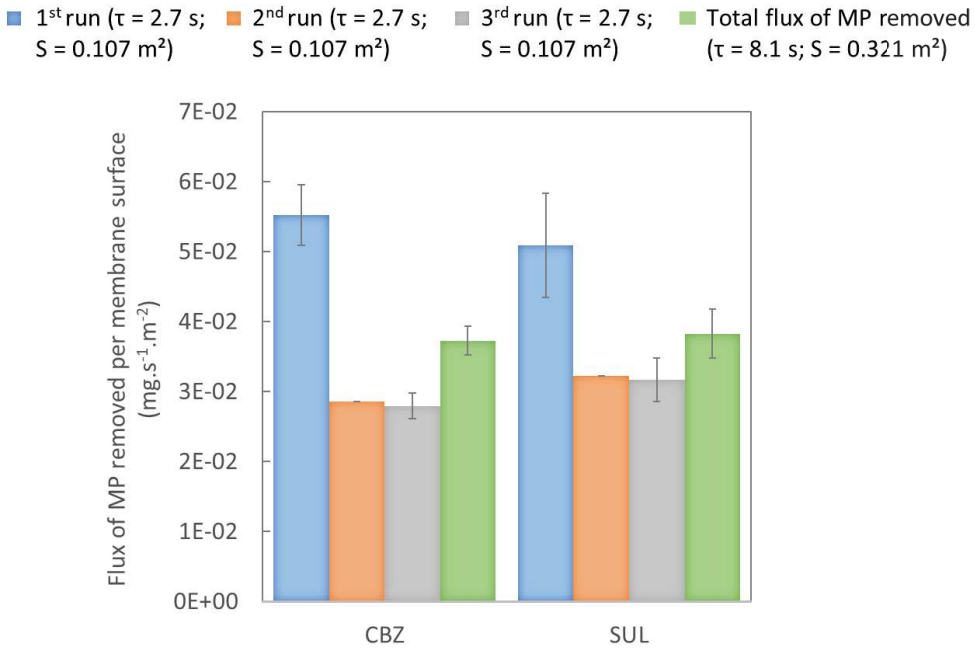

Figure 31. Flux of MP removed per membrane surface during each run and total after 3 runs ($mg.s^{-1}.m^{-2}$) during the experiments with recirculation of the water with an ozone concentration at the inlet of the gas phase of 15 $g.Nm^{-3}$, a liquid flowrate of 47.8 $L.h^{-1}$, a gas flowrate of 8 $L.h^{-1}$, at neutral pH.

During each run, similar fluxes of CBZ and SUL were removed. CBZ is almost as reactive with molecular ozone as SUL (3.0×10^5 $M^{-1}.s^{-1}$ and 4.2×10^5 $M^{-1}.s^{-1}$ respectively) and thus, as showed before, these results supports that the molecular mechanism was the main way of action for the targeted MP removal during the ozonation. In the case of MP less reactive to ozone, both molecular and radical

mechanism could occur simultaneously (for $10^2 < k_{O3} < 10^4$) or radical mechanisms could be predominant (for $k_{O3} < 10^2$) (Bourgin et al., 2017; Schmitt et al., 2020).

3.1.5. Residual ozone and bromate formation during the experiments on the removal of selected MPs

Table 12. Concentrations of bromides, bromates, and residual ozone before and after the different experiments.

Experiment	1	2	3	4	5	6	7
C_{Br^-} Before ozonation ($mg.L^{-1}$)	0.30 (0.01)	1.10 (0.02)	0.28 (0.01)	0.30 (0.01)		1.56 (0.03)	
C_{Br^-} After ozonation ($mg.L^{-1}$)	0.31 (0.01)	1.10 (0.03)	0.28 (0.01)	0.30 (0.01)	1.55 (0.03)	1.55 (0.03)	1.55 (0.03)
$C_{BrO_3^-}$ After ozonation ($mg.L^{-1}$)	< LOD	< LOD	< LOD	< LOD	< LOD	< LOD	< LOD
$C_{O_3,w}$ ($mg.L^{-1}$)	0.05 (0.01)	0.08 (0)	0.08 (0.01)	0.07 (0)	0.04 (0.03)	0.06 (0.03)	0.05 (0.03)

The Table 12 shows the concentration of bromide before and after each experiment of ozonation, as well as the concentrations of bromate and residual ozone (i.e. dissolved ozone) after ozonation. It can be observed that no bromate was detectable after the ozonation. It can be explained by the very low residual ozone concentration and the very short residence time, parameters leading to the limitation of bromate formation, as we will see in the next section. The LOD of the bromates was high (0.1 $mg.L^{-1}$), and thus it is interesting to analyze the evolution of the bromide concentration (whose the relative standard deviation is estimated at 2%). No reduction was noticed whatever the experiment, confirming that no (or very few) bromate was formed, even for the experiments with several runs in the membrane contactor (i.e. for the experiments with a longer residence time).

3.2. Minimization of bromates production with membrane contactor technology in comparison with bubble reactor

Bromates cannot be completely avoided as soon as the concentration of dissolved ozone increases, which is inevitable during the ozonation with a bubble reactor (von Gunten, 2003b). However, solutions may be considered to minimize their formation. In this section, the objective was to evaluate the production of bromates using the membrane contactor during the ozonation of real treated wastewater, having been spiked with 3 $mg.L^{-1}$ of bromides. This bromide concentration was particularly high compared to real waters and had been chosen to overcome the limits imposed by the detection and quantification of the analytical methods used (i.e. LOD and LOQ of ion chromatography).

Consequently, the experiments were made in very unfavorable conditions when the objective is to minimize the production of bromates.

The conditions of ozonation in the membrane contactor were the following: a gas flowrate of 30 $L.h^{-1}$, a liquid flowrate of 71.5 $L.h^{-1}$, and an ozone concentration at the inlet of the gas phase of about 10 $g.Nm^{-3}$. The initial volume of liquid flowing in the pilot was 1.5 L, decreasing over time due to the samples. The pH of the liquid has been measured at 8.2. A duplicate was made in order to estimate the standard deviation. In the graphs of this part, when no specification is provided, the results are those of the downstream.

In order to compare the results obtained to those of a conventional reactor, a bubble column was also used in semi-batch mode (i.e. gas was flowing in the form of bubbles from a porous diffusor, while liquid was not flowing). The conditions of ozonation in the bubble reactor were the following: a gas flowrate of 30 $L.h^{-1}$, and an ozone concentration at the inlet of the gas phase of about 9.2 $g.Nm^{-3}$. The initial volume of liquid flowing in the pilot was 3 L, decreasing over time due to the samples. The pH of the liquid has been adjusted then measured at 8.2. A duplicate was made in order to estimate the standard deviation.

3.2.1. Formation of bromates

The stoichiometric ratio between the bromates produced and the bromides consumed is plotted in the Annex I. The graph shows that one mole of bromate was formed for one mole of bromide consumed, whatever the process used (conventional with the bubble reactor, or with the membrane contactor). The difference noticeable between the results obtained according to the process used is explained by the initial concentration of bromide.

The matrix studied, providing from the outlet of the WWTP of La Grande-Motte and containing during winter about 0.3 $mg.L^{-1}$ of bromide (= 3.75 $mol.L^{-1}$) (and even higher during summer period), could therefore achieve a concentration of 3.75 $mol.L^{-1}$ of bromate (= 4.8 $mg.L^{-1}$) after ozonation. This concentration is significantly higher than that authorized in drinking waters (maximum of 10 $\mu g.L^{-1}$), but no regulation is defined about the bromates level in wastewater.

The Figure 32 plots the evolution of the bromide and bromate normalized concentrations as a function of the specific dose of ozone transferred ($mgO_3.mgDOC^{-1}$), which were calculated from a mass balance on the gas phase. It provides a comparison between the two processes used and thus is useful to evaluate the interest of the membrane contactor to minimize bromate formation. The parameters used for the two processes were the same, in particular the pH which has a significant impact in the reaction mechanism involving the transformation of bromides into bromates. Only the initial

concentration of bromide differed for the reason aforementioned, placing the experiments realized with the bubble reactor in disadvantageous conditions for the minimization of bromate formation.

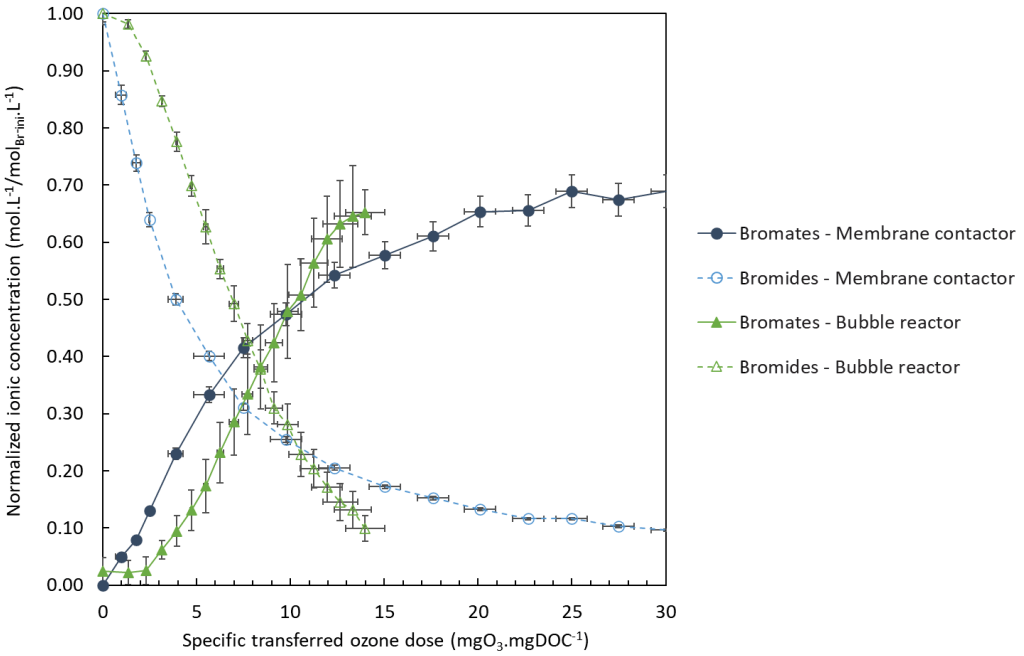

Figure 32. Normalized concentrations of bromate and bromide at pH 8.2 as a function of the specific dose of ozone transferred ($mgO_3.mgDOC^{-1}$).

On the Figure 32, we observe two different steps. First, for a specific dose of ozone transferred up to 9.9 $mgO_3.mgDOC^{-1}$, more bromates were produced using the membrane contactor despite a lower quantity of bromides. Once this dose was exceeded, less bromates were formed with the membrane contactor than with the conventional process. Moreover, during this last stage, we can note a sharp slowdown of the bromate formation which tended to stabilize, while bromides were still disposable. Therefore, the use of a membrane contactor to minimize the bromate formation appears worthwhile only under certain conditions, that are for a high specific dose of ozone transferred. However, this dose was achieved after a long time (i.e. about 3 hours) of experiment with the membrane contactor and thus a lot of recirculation of the water in the contactor and a high residence time. In practice, when the configuration of the pilot is in open-loop, the residence time in the membrane contactor would be of only a few seconds, corresponding to a dose of ozone transferred very low. It would appear then that the conventional reactor (i.e. the bubble reactor) is more appropriate to minimize the bromate formation during a long duration of ozonation than the membrane contactor. Nevertheless, the very short contact time (i.e. some seconds) offers by the membrane contactor and leading to good MP abatements, as seen in the section 3.1, could potentially lead to little or no bromate formation, as suggested in the results of the section 3.1.6 (althought the LOD was high). Indeed, a large part of the reactions involved in the bromate formation are slower than the reactions involved in the MP abatement. The mechanism of bromate formation is very complex, with a lot of reactions occurring

simultaneously between the compounds of the matrix, the ozone molecular, and the hydroxyl radicals (Von Gunten and Hoigne, 1994). The transformation of Br^- into BrO^- thanks to O_3, which initiates this this mechanism, is about 10^2 $M^{-1}.s^{-1}$, which is slower than the reaction rates between O_3 and the targeted MPs (Haag and Hoigné, 1983).

3.2.2. Production of hydroxyl radicals

The representation as a function of the dose of transferred ozone does not take into account the decomposition of the dissolved ozone into hydroxyl radicals. Hydroxyl radicals offer both a strong oxidizing power, useful to remove efficiently organic pollutants, and come into play in the mechanism of bromate formation to a lesser extent than the dissolved ozone. It is thus important to analyze the bromate formation according to the ozone exposure, parameter already highlighted by Pinkernell and Von Gunten as crucial for the bromate formation (Pinkernell and Von Gunten, 2001). The Figure 33 confirms this and shows that the bromate formation depends strongly on the ozone exposure.

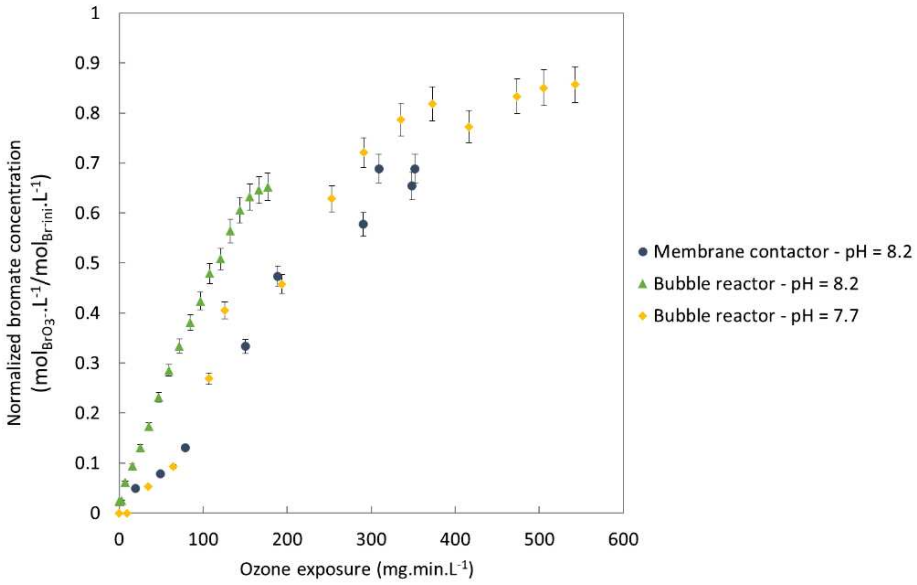

Figure 33. Normalized bromate concentration as a function of ozone exposure during the ozonation with: a membrane contactor at pH 8.2, a bubble reactor at pH 8.2, and a bubble reactor at pH 7.7.

Simultaneously, more bromates were produced with the semi-batch reactor than with the membrane contactor for a same ozone exposure. One assumption that might explain this result is the local concentration of the dissolved ozone in the reactors. The bubble reactor is considered as perfectly stirred, leading to a fast homogeneous distribution of the ozone. In the membrane contactor, the dissolved ozone is very concentrated close to the fibers but varies significantly according to the location, until becoming equal to zero in some areas (close to the shell wall). This concentration is then diluted and homogenized at the outlet. The local distribution of the dissolved ozone in a membrane contactor will be explored with more details in a future study.

Another important observation on the Figure 33 is the impact of the pH on the bromate formation. We can see that at higher pH values, more bromates are produced. For a pH at 7.7 instead of 8.2, approximately 44% less bromates are formed in average, depending on the ozone exposure. This coincides with the results presented by Pinkernell and Von Gunten: the decrease of the pH from 8 to 6 could lead to 60% less bromates with a river water at an ozone exposure of 10 $mg.L^{-1}.min^{-1}$ (Pinkernell and Von Gunten, 2001). In other study presented by Chao, the author concluded in that the pH was the parameter with the higher impact on the bromate formation, before the ozone exposure, the DOC, the bromides, or the ammonium (Chao, 2002). The control of the pH is therefore a good solution to minimize bromate formation, although not easy to put in place in WWTP.

In order to monitor the quantity of hydroxyl radicals produced during the ozonation, p-CBA had been added to the matrix. The Figure 34 shows that, for a same initial p-CBA concentration, the complete elimination of the p-CBA (and thus the same production of hydroxyl radicals) was achieved while 1.6 $mg.L^{-1}$ of bromates were produced with the membrane contactor and 3.5 $mg.L^{-1}$ with the traditional reactor. Moreover, the complete elimination of p-CBA was achieved for a specific dose of ozone transferred of 5.7 $mgO_3.mgDOC^{-1}$ and 11.3 $mgO_3.mgDOC^{-1}$ respectively with the membrane contactor and with the bubble reactor. A lower specific dose of ozone transferred was thus necessary with the membrane contactor to product the same quantity of hydroxyl radicals. This result brings out the possibility for the membrane contactor to produce a significant quantity of HO°, in order to efficiently remove micropollutants, while minimizing the bromate formation compared to a conventional reactor during the ozonation of WWTP effluents.

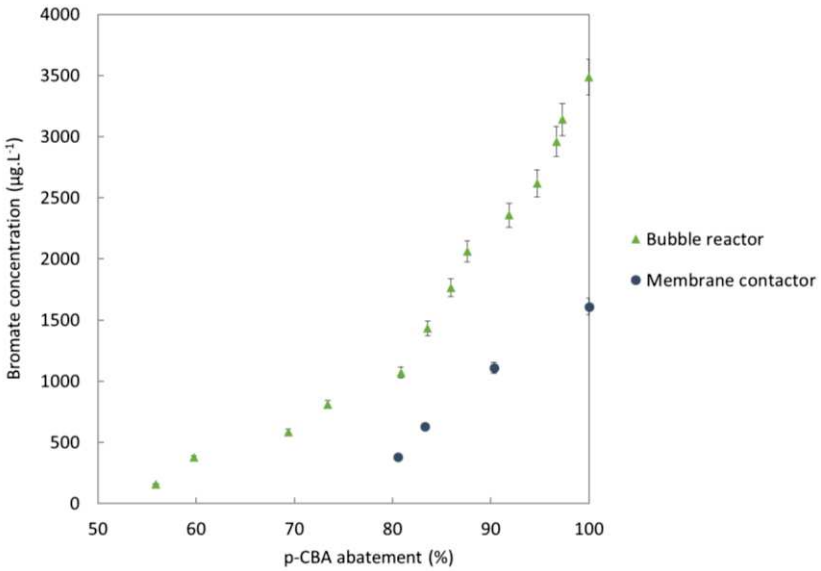

Figure 34. Evolution of bromate concentration as a function of p-CBA abatement according to the process of ozonation used, at pH 8.2.

The profile of the curves obtained on the Figure 34 is almost similar to that of the work of Merle et al., who also studied the ozonation via a membrane contactor (Merle et al., 2017). Our values cannot be compared to theirs values due to the very different initial concentrations of bromide and the use of peroxone in their case (i.e. not only ozone). The authors demonstrated the interest to decrease the ozone concentration in the gas phase to minimize the bromate production. They also proved that for a longer residence time in the contactor (i.e. a liquid flowrate lower), more bromates are produced, but also more hydroxyl radicals. Roustan had already highlighted the importance of the residence time in the contactor in the bromate formation (Roustan, 2003). In that sense, the membrane contactor presented in this work seems to be ideal thanks to its very short liquid residence time (< 2s for a liquid flowrate of 71.5 $L.h^{-1}$ in a single pass). Besides, no bromate was detected after the experiments with the liquid in open circuit. However, the limit of detection of the ion chromatography used is estimated at about 0.1 $mg.L^{-1}$, which is higher than the regulatory limit of 10 $\mu g.L^{-1}$ in drinking water.

Although the HO° production is very important for a good removal of the organic pollutants, HO° also contribute to bromate formation. Indeed, bromates are produced both by molecular and radical pathways. The ratio of each mechanism depends on the quality of the water and the parameters of the ozonation. Von Gunten et al. showed that the contribution of radical mechanism is higher than molecular mechanism in the case of short ozone exposure and small bromide concentration (Von Gunten et al., 1995).

4. Conclusions

Using the membrane contactor to treat carbamazepine and sulfamethoxazole in real wastewater for very short contact times, enables under certain conditions to achieve important removal yield depending on the micropollutant reactivity towards ozone and hydroxyl radicals with little or no bromate thanks to this short residence time.

Depending on the tested conditions and for a residence time lower than 3s, up to 59% and 50% of abatement have been achieved respectively for the carbamazepine and the sulfamethoxazole. When the contact time was lengthened to about 8s, the percent removal reached respectively 46% and 51% without the optimization of the process parameters. Therefore, a higher ozone concentration in the gas phase and a higher liquid flowrate, but also lower initial MP concentrations (the MP concentrations used in this work being not representative of the real concentration at the outlet of a WWTP), would certainly lead to better abatement.

In addition, the very short contact time in the membrane contactor may have a positive impact to prevent bromate formation thanks to the faster ozonation reactions with MPs than the reactions implied in the mechanism of bromate formation.

Nevertheless, it is difficult to conclude that less bromates are produced with a membrane contactor than with a bubble reactor under the experimental conditions used in this work. For a low dose of transferred ozone, the bubble reactor seems more suitable to minimize bromate formation despite experimental conditions promoting the production of bromates such as higher initial bromide concentration and higher DOC than during the experiments with the membrane contactor. Moreover, whatever the reactor used, the initial conditions of the experiments were very unfavorable for this minimization, with an initial bromide concentration very high compared to other studies and to the real concentration in a wastewater.

However, this study highlighted that less bromates were produced with the membrane contactor than with the bubble reactor for a same production of hydroxyl radicals and a same ozone exposure. Membrane contactors seems therefore to be a good alternative to bubble columns for simultaneous treatment of refractive pollutants in wastewater treatments and bromate minimization.

Conclusions et perspectives du Chapitre IV

L'objectif du chapitre IV était d'une part d'évaluer l'efficacité de l'ozonation par contacteur membranaire pour l'élimination de micropolluants organiques, et d'autre part d'évaluer la formation de bromates lors de l'ozonation par contacteur membranaire en comparaison avec un réacteur traditionnel à bulles.

Afin de prendre en compte l'impact de la matrice, les essais réalisés dans le cadre de ce chapitre ont été accomplis à partir d'eau réelle provenant de la sortie de la station d'épuration de la Grande-Motte, près de Montpellier. Cette matrice était ensuite dopée (soit avec les MPs ciblés, soit avec des bromures et du p-CBA) afin de s'affranchir des limites de détection et de quantification des appareils d'analyse utilisés.

Ce chapitre a confirmé l'efficacité du contacteur membranaire lors de l'ozonation de la carbamazépine et du sulfaméthoxazole, deux micropolluants organiques d'origine pharmaceutique sélectionnés comme composés modèles de par leur occurrence en sortie de station d'épuration et dans les eaux de surface du monde entier, leur très bonne réactivité aux mécanismes d'ozonation, et l'expertise d'analyse présente au sein de l'Institut Européen des Membranes.

- A l'échelle pilote, des abattements respectifs de 59% et 50% pour la carbamazépine et le sulfaméthoxazole ont été atteints pour des temps de séjour dans le contacteur particulièrement courts (< 3 s) et pour les conditions d'ozonation suivantes : une concentration en entrée dans la phase gaz de 31 $g.Nm^{-3}$, un débit de gaz de 8 $L.h^{-1}$, un débit de liquide de 46 $L.h^{-1}$, et un pH neutre. En comparaison, l'abattement de ces composés par des procédés d'ozonation conventionnels en traitement tertiaire (i.e. en sortie de station d'épuration) est de 100% pour la carbamazépine et entre 97 et 99% pour le sulfaméthoxazole, pour des temps de contact variant entre 10 et 15 min (Mathon et al., 2021; Penru et al., 2016). Toutefois, Mathon et al. avaient constaté au cours d'essais réalisés dans un réacteur à bulles un flux de carbamazépine éliminé inférieur à celui déterminé avec le contacteur membranaire dans ce chapitre, malgré une dose d'ozone spécifique transférée largement supérieure à celle utilisée dans notre étude.
- Dans ce chapitre, les abattements ont été atteints sans utiliser les paramètres optimisés du procédé définis à la suite du Chapitre III et pour une concentration initiale en MPs supérieure à la concentration réelle en sortie de station d'épuration. Le calcul du flux éliminé permet de palier partiellement cette différence de concentration dans un objectif de comparaison de l'efficacité de ce procédé par rapport à un procédé traditionnel d'ozonation. Cependant, une

plus grande concentration entraîne une cinétique d'élimination plus rapide et aura donc tout de même un impact sur le résultat final.

- Ce chapitre a confirmé l'impact positif et significatif de la concentration en ozone dans la phase gaz et du débit liquide sur le transfert d'ozone et donc l'élimination des MPs ciblés. Ces paramètres avaient d'ores-et-déjà été mis en évidence lors du Chapitre III.
- Il est important de souligner que les résultats présentés dans cette étude ont été obtenus avec un contacteur membranaire à fibres creuses présentant une surface d'échange de 0.107 m². Les procédés membranaires ont l'avantage d'être facilement modulables. Cette surface pourrait ainsi facilement être augmentée grâce à l'augmentation du nombre de fibres, une longueur de module plus élevée, ou encore la mise en place de plusieurs contacteurs en parallèle ou en série. Dans ce sens, le Chapitre V de cette thèse abordera le sujet de la géométrie du contacteur membranaire, et notamment de la longueur du module.

Ce chapitre ne permet cependant pas de conclure clairement au sujet de la minimisation de la formation de bromates en comparaison de réacteurs d'ozonation traditionnels.

Le réacteur à bulle produit moins de bromates que le contacteur membranaire dans les conditions suivantes :

- Pour une dose spécifique d'ozone transféré inférieure à 9.9 $mgO_3.mgDOC^{-1}$, le réacteur à bulles semble produire moins de bromates malgré des conditions expérimentales favorables à leur formation (concentration initiale en bromure supérieure à celle des essais avec le contacteur membranaire).
- Il est important de noter que ce résultat a été obtenu pour des doses spécifiques d'ozone transféré très élevées ainsi qu'un temps de séjour très élevé grâce à la recirculation du liquide. A l'échelle d'une station d'épuration, la limite viable économiquement pour un procédé d'ozonation est estimée autour de 1 $mgO_3.mgC^{-1}$ maximum (Choubert et al, 2017). Ainsi, la dose limite de 9.9 $mgO_3.mgDOC^{-1}$ citée précédemment ne sera jamais atteinte dans la réalité et le réacteur à bulles semblerait être la meilleure solution dans un objectif de minimisation des bromates.

L'utilisation du contacteur membranaire ne produit pas de bromates ou moins que le réacteur à bulle dans les conditions suivantes :

- Dans le cas des essais réalisés avec les deux micropolluants sélectionnés, où le temps de séjour n'excédait pas 9 s et où l'eau réelle n'avait pas été dopée en bromures, **aucun bromate n'a**

été détecté, et aucune diminution de la concentration en bromures n'a été mesurée. Si ces résultats sont à prendre avec précaution de par la limite de détection et la sensibilité de l'appareil d'analyse utilisé, ils sont néanmoins particulièrement encourageants dans un objectif de minimisation de la formation des bromates lors de l'ozonation des polluants ciblés. En conservant un temps de contact très court, le contacteur membranaire pourrait limiter la formation de bromates par rapport à un réacteur à bulles.

- Nos travaux ont montré que pour une même exposition à l'ozone dissous ou une même quantité de radicaux hydroxyles produits, moins de bromates étaient formés avec le contacteur membranaire qu'avec un réacteur à bulles. De plus, pour la formation d'une même quantité de radicaux hydroxyles, la dose spécifique d'ozone transférée nécessaire était beaucoup plus faible dans le cas du contacteur membranaire que dans celui du réacteur à bulles.

Ainsi, malgré des conclusions mitigées concernant la formation des bromates lors de l'ozonation par contacteur membranaire en lieu et place des réacteurs à bulles, ceux-ci restent donc une solution intéressante pour l'élimination de polluants émergents présents dans les eaux usées organiques tout en minimisant la formation de sous-produits dangereux issus des réactions d'oxydation, et notamment de bromates.

Bibliographie du Chapitre IV

AIDA, 1998. Directive n° 98/83/CE du 03/11/98 relative à la qualité des eaux destinées à la consommation humaine.

Ashton, D., Hilton, M., Thomas, K.V. V, 2004. Investigating the environmental transport of human pharmaceuticals to streams in the United Kingdom. Sci. Total Environ. 333, 167–184. https://doi.org/10.1016/J.SCITOTENV.2004.04.062

Bader, H., Hoigné, J., 1982. Determination of Ozone In Water By The Indigo Method: A Submitted Standard Method. Ozone Sci. Eng. J. Int. Ozone Assoc. 4, 169–176. https://doi.org/10.1080/01919510390481531

Bamperng, S., Suwannachart, T., Atchariyawut, S., Jiraratananon, R., 2010. Ozonation of dye wastewater by membrane contactor using PVDF and PTFE membranes. Sep. Purif. Technol. 72, 186–193. https://doi.org/10.1016/j.seppur.2010.02.006

Beltrán, F. J., Rey, A., 2018. Free Radical and Direct Ozone Reaction Competition to Remove Priority and Pharmaceutical Water Contaminants with Single and Hydrogen Peroxide Ozonation Systems. Ozone Sci. Eng. 40, 251–265. https://doi.org/10.1080/01919512.2018.1431521

Berry, M.J., Taylor, C.M., King, W., Chew, Y.M.J., Wenk, J., 2017. Modelling of Ozone Mass-Transfer through Non-Porous Membranes for Water Treatment. Water 9, 452. https://doi.org/10.3390/w9070452

Björlenius, B., Ripszám, M., Haglund, P., Lindberg, R.H., Tysklind, M., Fick, J., 2018. Pharmaceutical residues are widespread in Baltic Sea coastal and offshore waters – Screening for pharmaceuticals and modelling of environmental concentrations of carbamazepine. Sci. Total Environ. 633, 1496–1509. https://doi.org/10.1016/j.scitotenv.2018.03.276

Bolong, N., Ismail, A.F., Salim, M.R., Matsuura, T., 2009. A review of the effects of emerging contaminants in wastewater and options for their removal. Desalination 239, 229–246. https://doi.org/10.1016/j.desal.2008.03.020

Bourgin, M., Borowska, E., Helbing, J., Hollender, J., Kaiser, H.-P., Kienle, C., McArdell, C.S., Simon, E., von Gunten, U., 2017. Effect of operational and water quality parameters on conventional ozonation and the advanced oxidation process O3/H2O2: Kinetics of micropollutant abatement, transformation product and bromate formation in a surface water. Water Res. 122, 234–245. https://doi.org/10.1016/j.watres.2017.05.018

Cabeza, Y., Candela, L., Ronen, D., Teijon, G., 2012. Monitoring the occurrence of emerging contaminants in treated wastewater and groundwater between 2008 and 2010. The Baix Llobregat (Barcelona, Spain). J. Hazard. Mater. 239–240, 32–39. https://doi.org/10.1016/J.JHAZMAT.2012.07.032

Chao, P.F., 2002. Role of hydroxyl radicals and hypobromous acid reactions on bromate formation during ozonation. Thesis. Arizona State University.

Choubert, J.M., Penru, Y., Mathon, B., Guillon, A., Esperanza, M., Crétollier, C., Dherret, L., Daval, A., Masson, M., Lagarrigue, C., Miège, C., Coquery, M., 2017. Elimination de substances prioritaires et émergentes des eaux résiduaires urbaines par ozonation : évaluation technique, énergétique et environnementale. Rapport final du projet MICROPOLIS-PROCEDES 164.

Fent, K., Weston, A.A., Caminada, D., 2006. Ecotoxicology of human pharmaceuticals. Aquat. Toxicol. 76, 122–159. https://doi.org/10.1016/j.aquatox.2005.09.009

Gomes, J., Costa, R., Quinta-Ferreira, R.M., Martins, R.C., 2017. Application of ozonation for pharmaceuticals and personal care products removal from water. Sci. Total Environ. 586, 265–283. https://doi.org/10.1016/j.scitotenv.2017.01.216

Haag, W.R., Hoigné, J., 1983. Ozonation of Bromide-Containing Waters: Kinetics of Formation of Hypobromous Acid and Brómate. Environ. Sci. Technol. 17, 261–267. https://doi.org/10.1021/es00111a004

Hirsch, R., Ternes, T., Haberer, K., Kratz, K.L., 1999. Occurrence of antibiotics in the aquatic environment. Sci. Total Environ. 225, 109–118. https://doi.org/10.1016/S0048-9697(98)00337-4

Huber, M.M., Canonica, S., Park, G.-Y., von Gunten, U., 2003. Oxidation of Pharmaceuticals during Ozonation and Advanced Oxidation Processes. Environ. Sci. Technol. 37, 1016–1024. https://doi.org/10.1021/es025896h

Iversen, S.B., Bhatia, V.K., Dam-Johansen, K., Jonsson, G., 1997. Characterization of microporous membranes for use in membrane contactors. J. Memb. Sci. 130, 205–217. https://doi.org/10.1016/S0376-7388(97)00026-4

Khan, N.A., Khan, S.U., Ahmed, S., Farooqi, I.H., Yousefi, M., Mohammadi, A.A., Changani, F., 2020. Recent trends in disposal and treatment technologies of emerging-pollutants- A critical review. Trends Anal. Chem. 122. https://doi.org/10.1016/j.trac.2019.115744

Khayet, M., Matsuura, T., 2001. Preparation and Characterization of Polyvinylidene Fluoride Membranes for Membrane Distillation. Ind. Eng. Chem. Res. 40, 5710–5718. https://doi.org/10.1021/ie010553y

Kolpin, D.W., Furlong, E.T., Meyer, M.T., Thurman, E.M., Zaugg, S.D., Barber, L.B., Buxton, H.T., 2002. Pharmaceuticals, hormones, and other organic wastewater contaminants in U.S. streams, 1999-2000: a national reconnaissance. Environ. Sci. Technol. 36, 1202–1211. https://doi.org/10.1021/es0200903

Kråkström, M., Saeid, S., Tolvanen, P., Kumar, N., Salmi, T., Kronberg, L., Eklund, P., 2020. Ozonation of carbamazepine and its main transformation products: product determination and reaction mechanisms. Environ. Sci. Pollut. Res. 27, 23258–23269. https://doi.org/10.1007/s11356-020-08795-0

Lee, Y., Kovalova, L., McArdell, C.S., von Gunten, U., 2014. Prediction of micropollutant elimination during ozonation of a hospital wastewater effluent. Water Res. 64, 134–148. https://doi.org/10.1016/J.WATRES.2014.06.027

Lee, Y., von Gunten, U., 2016. Advances in predicting organic contaminant abatement during ozonation of municipal wastewater effluent: reaction kinetics, transformation products, and changes of biological effects. Environ. Sci. Water Res. Technol. 2, 421–442. https://doi.org/10.1039/C6EW00025H

Loos, R., Carvalho, R., António, D.C., Comero, S., Locoro, G., Tavazzi, S., Paracchini, B., Ghiani, M., Lettieri, T., Blaha, L., Jarosova, B., Voorspoels, S., Servaes, K., Haglund, P., Fick, J., Lindberg, R.H., Schwesig, D., Gawlik, B.M., 2013. EU-wide monitoring survey on emerging polar organic contaminants in wastewater treatment plant effluents. Water Res. 47, 6475–6487. https://doi.org/10.1016/j.watres.2013.08.024

Luo, Y., Guo, W., Ngo, H.H., Nghiem, L.D., Hai, F.I., Zhang, J., Liang, S., Wang, X.C., 2014. A review on the occurrence of micropollutants in the aquatic environment and their fate and removal during wastewater treatment. Sci. Total Environ. 473–474, 619–641.

https://doi.org/10.1016/j.scitotenv.2013.12.065

Luo, Y., Xu, L., Rysz, M., Wang, Y., Zhang, H., Alvarez, P.J.J., 2011. Occurrence and Transport of Tetracycline, Sulfonamide, Quinolone, and Macrolide Antibiotics in the Haihe River Basin, China. Environ. Sci. Technol. 45, 1827–1833. https://doi.org/10.1021/es104009s

Mathon, B., Coquery, M., Liu, Z., Penru, Y., Guillon, A., Esperanza, M., Miège, C., Choubert, J.M., 2021. Ozonation of 47 organic micropollutants in secondary treated municipal effluents: Direct and indirect kinetic reaction rates and modelling. Chemosphere 262. https://doi.org/10.1016/j.chemosphere.2020.127969

Merle, T., Pronk, W., Von Gunten, U., 2017. MEMBRO3X, a Novel Combination of a Membrane Contactor with Advanced Oxidation (O3/H2O2) for Simultaneous Micropollutant Abatement and Bromate Minimization. Environ. Sci. Technol. Lett. 4, 5, 180-185. https://doi.org/10.1021/acs.estlett.7b00061

Neta, P., Dorfman, L.M., 1968. Pulse radiolysis studies. XIII. Rate constants for the reaction of hydroxyl radicals with aromatic compounds in aqueous solutions. ACS Publications.

Penru, Y., Miege, C., Daval, A., Guillon, A., Esperanza, M., Crétollier, C., Masson, M., Le Goaziou, Y., Baig, S., Ruel, S.M., Coquery, M., Choubert, J.M., 2017. Traitement des micropolluants émergents par ozonation tertiaire. Performances de la station d'épuration des Bouillides, Sophia-Antipolis, France. Aqua & Gas 2017, 8. ⟨hal-02605912⟩

Petrie, B., Barden, R., Kasprzyk-Hordern, B., 2015. A review on emerging contaminants in wastewaters and the environment: current knowledge, understudied areas and recommendations for future monitoring. Water Res. 72, 3–27. https://doi.org/10.1016/j.watres.2014.08.053

Pi, Y., Schumacher, J., Jekel, M., 2005. The use of para-chlorobenzoic acid (pCBA) as an ozone/hydroxyl radical probe compound. Ozone Sci. Eng. 27, 431–436. https://doi.org/10.1080/01919510500349309

Pinkernell, U., Von Gunten, U., 2001. Bromate minimization during ozonation: Mechanistic considerations. Environ. Sci. Technol. 35, 2525–2531. https://doi.org/10.1021/es001502f

Reungoat, J., Macova, M., Escher, B.I.I., Carswell, S., Mueller, J.F.F., Keller, J., 2010. Removal of micropollutants and reduction of biological activity in a full scale reclamation plant using ozonation and activated carbon filtration. Water Res. 44, 625–637. https://doi.org/10.1016/J.WATRES.2009.09.048

Richardson, S.D., Plewa, M.J., Wagner, E.D., Schoeny, R., Demarini, D.M., 2007. Occurrence, genotoxicity, and carcinogenicity of regulated and emerging disinfection by-products in drinking water: a review and roadmap for research. Mutat. Res. 636, 178–242. https://doi.org/10.1016/j.mrrev.2007.09.001

Rosal, R., Rodríguez, A., Perdigón-Melón, J.A., Petre, A., García-Calvo, E., Gómez, M.J., Agüera, A., Fernández-Alba, A.R., 2010. Occurrence of emerging pollutants in urban wastewater and their removal through biological treatment followed by ozonation. Water Res. 44, 578–588. https://doi.org/10.1016/J.WATRES.2009.07.004

Roustan, M., 2003. Transferts gaz-liquide dans les procédés de traitement des eaux et des effluents gazeux. Éd. Tec & doc, Paris.

Schmitt, A., Mendret, J., Roustan, M., Brosillon, S., 2020. Ozonation using hollow fiber contactor technology and its perspectives for micropollutants removal in water: A review. Sci. Total Environ. 729, 138664. https://doi.org/10.1016/j.scitotenv.2020.138664

Shojaee Nasirabadi, P., Saljoughi, E., Mousavi, S.M., 2016. Membrane processes used for removal of pharmaceuticals, hormones, endocrine disruptors and their metabolites from wastewaters: a review. Desalin. Water Treat. 57, 24146–24175. https://doi.org/10.1080/19443994.2016.1140081

Soltermann, F., Abegglen, C., Tschui, M., Stahel, S., von Gunten, U., 2017. Options and limitations for bromate control during ozonation of wastewater. Water Res. 116, 76–85. https://doi.org/10.1016/j.watres.2017.02.026

Stylianou, S.K., Katsoyiannis, I.A., Ernst, M., Zouboulis, A.I., 2018. Impact of O3 or O3/H2O2 treatment via a membrane contacting system on the composition and characteristics of the natural organic matter of surface waters. Environ. Sci. Pollut. Res. 25, 12246–12255. https://doi.org/10.1007/s11356-017-9554-8

Stylianou, S.K., Katsoyiannis, I.A., Mitrakas, M., Zouboulis, A.I., 2018. Application of a ceramic membrane contacting process for ozone and peroxone treatment of micropollutant contaminated surface water. J. Hazard. Mater. 358, 129–135. https://doi.org/10.1016/j.jhazmat.2018.06.060

Ternes, T.A., 1998. Occurrence of drugs in German sewage treatment plants and rivers. Water Res. 32, 3245–3260. https://doi.org/10.1016/S0043-1354(98)00099-2

UNESCO and HELCOM, 2017. Pharmaceuticals in the aquatic environment of the Baltic Sea region - a status report UNESCO emerging pollutants in water series. Paris.

USEPA, 1998. Disinfectants and disinfection byproducts : proposed rule.

Valdés, M.E., Huerta, B., Wunderlin, D.A., Bistoni, M.A., Barceló, D., Rodriguez-Mozaz, S., 2016. Bioaccumulation and bioconcentration of carbamazepine and other pharmaceuticals in fish under field and controlled laboratory experiments. Evidences of carbamazepine metabolization by fish. Sci. Total Environ. 557–558, 58–67. https://doi.org/10.1016/j.scitotenv.2016.03.045

Vittenet, J., Aboussaoud, W., Mendret, J., Pic, J.S., Debellefontaine, H., Lesage, N., Faucher, K., Manero, M.H., Thibault-Starzyk, F., Leclerc, H., Galarneau, A., Brosillon, S., 2015. Catalytic ozonation with γ-Al2O3 to enhance the degradation of refractory organics in water. Appl. Catal. A Gen. 504, 519–532. https://doi.org/10.1016/j.apcata.2014.10.037

Von Gunten, U., 2003a. Ozonation of drinking water: Part I. Oxidation kinetics and product formation. Water Res. 37, 1443–1467. https://doi.org/10.1016/s0043-1354(02)00457-8

Von Gunten, U., 2003b. Ozonation of drinking water: Part II. Disinfection and by-product formation in presence of bromide, iodide or chlorine. Water Res. 37, 1469–1487. https://doi.org/10.1016/S0043-1354(02)00458-X

Von Gunten, U., Hoigne, J., 1994. Bromate Formation during Ozonation of Bromide-Containing Waters: Interaction of Ozone and Hydroxyl Radical Reactions. Environ. Sci. Technol. 28, 1234–1242.

Von Gunten, U., Hoigne, J., Bruchet, A., 1995. Bromate formation during ozonation of bromide-containing waters. Water Supply 13, 45–50.

Von Sonntag, C., Von Gunten, U., 2012. Chemistry of ozone in water and wastewater treatment. IWA publishing.

Wang, R., Shi, L., Tang, C.Y., Chou, S., Qiu, C., Fane, A.G., 2010. Characterization of novel forward osmosis hollow fiber membranes. J. Memb. Sci. 355, 158–167. https://doi.org/10.1016/j.memsci.2010.03.017

Weishaar, J.L., Aiken, G.R., Bergamaschi, B.A., Fram, M.S., Fujii, R., Mopper, K., 2003. Evaluation of Specific Ultraviolet Absorbance as an Indicator of the Chemical Composition and Reactivity of Dissolved Organic Carbon. Environ. Sci. Technol. 37, 20, 4702–4708.

Wenten, I.G., Julian, H., Panjaitan, N.T., 2012. Ozonation through ceramic membrane contactor for iodide oxidation during iodine recovery from brine water. Desalination 306, 29–34. https://doi.org/10.1016/j.desal.2012.08.032

Yang, Y., Ok, Y.S., Kim, K.H., Kwon, E.E., Tsang, Y.F., 2017. Occurrences and removal of pharmaceuticals and personal care products (PPCPs) in drinking water and water/sewage treatment plants: A review. Sci. Total Environ. 596, 303–320. https://doi.org/10.1016/j.scitotenv.2017.04.102

Yao, W., Rehman, S.W.U., Wang, H., Yang, H., Yu, G., Wang, Y., 2018. Pilot-scale evaluation of micropollutant abatements by conventional ozonation, UV/O3, and an electro-peroxone process. Water Res. 138, 106–117. https://doi.org/10.1016/J.WATRES.2018.03.044

Chapitre V

Computational fluid dynamics modeling of ozonation using a hollow fiber membrane contactor

Liste des symboles et abréviations du Chapitre V

ε_m	Membrane porosity	-
λ	Mean free path of the gas molecule which may collide the medium walls	m
η_g, η_w	Respectively the dynamic viscosity of the gas phase and of the liquid phase	Pa.s
ρ_g, ρ_w	Respectively the density of the gas phase and of the liquid phase	$kg.m^{-3}$
τ	Membrane tortuosity	-
2D, 3D	Respectively two dimensional and three dimensional	-
$\overrightarrow{v_g}$	Gas velocity vector	$m.s^{-1}$
$\overrightarrow{v_w}$	Liquid velocity vector	$m.s^{-1}$
$\bar{\bar{\tau}}$	Viscous stress tensor	Pa
BQM	By-product from the chemical reaction between molecular ozone and carbamazepine	-
$C_{O_3,0,g}, C_{O_3,0,w}$	Respectively the O_3 inlet concentration in the gas phase and in the liquid phase	$mg.L^{-1}$
$C_{O_3,g}$	Local concentration of O_3 in the gas phase	
$C_{O_3,m}$	Concentration of ozone at the interface between the membrane and the water	$mg.L^{-1}$
$C_{O_3,w}$	Local concentration of O_3 in the liquid phase	$mg.L^{-1}$
$C_{O_3,w,outlet}$	Concentration of dissolved ozone at the outlet of the liquid phase	$mg.L^{-1}$
$C_{CBZ,0,w}$	Concentration of carbamazepine at the inlet of the liquid phase	$\mu g.L^{-1}$
$C_{CBZ,w}$	Local concentration of carbamazepine in the liquid phase	$\mu g.L^{-1}$
CBZ	Carbamazepine	-

d_{pore}	Pore diameter of the membrane	m
$D_{CBZ,w}$	Diffusion coefficient of carbamazepine in the liquid phase	$m^2.s^{-1}$
$D_{O_3,m}^{eff}$	O_3 effective diffusion coefficient in the membrane	$m^2.s^{-1}$
$D_{O_3,g}$, $D_{O_3,w}$	Respectively the diffusion coefficient of O_3 in the gas phase and in the liquid phase	$m^2.s^{-1}$
$H_{O_3,w}$	Partition coefficient of O_3 in water	-
IQL, IDL	Respectively the instrument quantification limit and the instrument detection limit	$\mu g.L^{-1}$
k_b	Boltzmann constant	$m^2.kg.s^{-2}.K^{-1}$
κ_m	Permeability in the membrane	m^2
k_r	Reaction constant rate	$L.mol^{-1}.s^{-1}$
k_{O3}	Reaction constant rate between molecular ozone and carbamazepine	$L.mol^{-1}.s^{-1}$
K_n	Knudsen number	-
LC-MS/MS	Liquid chromatography-tandem mass spectrometry	-
$Q_{0,g}$, $Q_{0,w}$	Respectively the inlet gas flow rate and the inlet liquid flow rate	$L.h^{-1}$
p_g , p_w	Static pressure respectively in the gas and in the liquid	Pa
P_g	Gas pressure	Pa
R	Universal gas constant	$J.mol^{-1}.K^{-1}$
$R_{i,w}$	Reaction term of species i in water	-
RANS	Reynolds Averaged Navier–Stokes	-
T	Temperature	K
V_W	Local velocity in the water	$m.s^{-1}$

Objectifs et approche du Chapitre V

Les chapitres précédents ont permis de valider la technologie et d'évaluer l'effet de différents paramètres sur le transfert d'ozone, l'abattement de micropolluants et la quantité de bromates formés. La majeure partie des résultats obtenus dans ce manuscrit ont été validés jusqu'à présent en considérant une approche globale des mécanismes de transfert et de réaction au cours de l'ozonation. Néanmoins, certains résultats plus surprenants, notamment concernant la formation d'une quantité de bromates supérieure avec le contacteur membranaire qu'avec le réacteur à bulles pour une dose spécifique d'ozone transférée inférieure à 10 $gO_3.gC^{-1}$, ont soulevé de nouvelles questions concernant la distribution d'ozone au sein du contacteur membranaire ainsi que son évolution de la concentration en ozone le long du module.

Ainsi, la démarche suivie dans ce chapitre vise à mieux comprendre les phénomènes ayant lieu localement dans le contacteur membranaire lors du transfert du gaz vers le liquide via l'utilisation d'un outil numérique modélisant la configuration étudiée. A cet effet, la simulation du procédé a été réalisée grâce au logiciel de simulation numérique multiphysiques en dynamique des fluides Comsol Multiphysics®. En couplant hydrodynamique, transfert de matière, réactions multiples et géométrie complexe, la modélisation numérique apporte des informations sur les mécanismes de transfert à l'échelle locale. Contrairement aux études souvent réalisées en génie des procédés et basées sur les coefficients de transfert globaux, ce modèle expose les phénomènes se déroulant à l'intérieur de la « boîte noire » que représente le procédé lors d'une approche globale. Il est ainsi possible d'accéder à une meilleure compréhension des phénomènes mis en jeu lors de l'utilisation de ce type d'installation et ainsi d'optimiser la géométrie du contacteur utilisé (ex : longueur des fibres, nombre de fibres) ainsi que les paramètres du procédé d'ozonation (ex : débits de liquide et de gaz). A terme, le modèle créé pourrait servir de base dans l'élaboration et l'optimisation de procédés d'absorption gaz-liquide lors de l'utilisation de contacteur membranaire.

Dans un premier temps et en s'appuyant sur la littérature, un modèle 2D axisymétrique de contacteur possédant une unique fibre a été élaboré. L'écoulement et le maillage simplifiés de ce modèle apportaient des résultats immédiats. Dans le but de valider ce premier modèle, un contacteur spécifique à une fibre a été fabriqué dans le laboratoire afin de comparer les résultats obtenus expérimentalement. Afin de simplifier le modèle et de s'affranchir de la réaction de décomposition de l'ozone, les essais ont été réalisés dans de l'eau pure tamponnée à pH acide. Néanmoins, afin de comparer les résultats obtenus numériquement à ceux obtenus expérimentalement, il a été nécessaire de prendre en compte la géométrie réelle du contacteur membranaire utilisé, notamment la position des entrées et sorties de chaque fluide. En effet, le liquide entrait et sortait perpendiculairement à la

fibre, perturbant ainsi l'écoulement en créant des turbulences. A cet effet, un modèle 3D du contacteur membranaire, plus complexe, a été mis en place, ce qui était à notre connaissance une nouveauté pour une application d'ozonation. Ce modèle était toutefois plus lent à s'exécuter du fait du nombre de mailles important et de l'écoulement plus complexes qu'en 2D, et donnait un résultat après un long temps de calcul (plusieurs heures).

Une fois le modèle 3D validé expérimentalement sur le contacteur à une fibre, le travail a été poursuivi numériquement avec la simulation d'un contacteur multifibres afin d'étudier l'impact du nombre de fibres sur l'écoulement et sur l'efficacité du transfert localement. Le temps de calcul du logiciel utilisé pour la simulation était alors de plusieurs jours.

En parallèle, une réaction a été ajoutée au modèle créé afin de voir l'impact de celle-ci sur le transfert et d'estimer l'efficacité du procédé sur ce composé. Un micropolluant organique d'origine pharmaceutique, la carbamazépine (étudiée dans le Chapitre IV), a été choisie comme modèle. Les mécanismes réactionnels entre l'ozone, les radicaux hydroxyles, la carbamazépine mais aussi ses sous-produits de dégradation étant nombreux, il a été choisi de prendre en compte dans cette étude uniquement la réaction entre le produit mère (la carbamazépine) et l'ozone. Le temps de séjour dans le contacteur étant très court (< 3s) et la constante de réaction entre la carbamazépine et l'ozone moléculaire beaucoup plus élevée que celle de ses sous-produits (différence de 10^5 ordres de grandeur), nous avons considéré que les sous-produits d'oxydation ne réagissaient pas avec l'ozone. D'autre part, afin de pouvoir valider expérimentalement ce nouveau modèle qui ne prend pas en compte les réactions ayant lieu avec les radicaux hydroxyles, une solution tamponnée à pH acide a de nouveau été utilisée afin d'éviter toute décomposition de l'ozone moléculaire en radicaux hydroxyles.

Ce chapitre présente les principaux résultats obtenus via la simulation à partir du modèle élaboré ainsi que les résultats expérimentaux ayant permis la validation du modèle. L'approche numérique a été réalisée avec la collaboration de Denis Bouyer et Cyril Chevarin, de l'Institut Européen des Membranes, qui ont conçu le modèle numérique et effectué les différentes simulations. Ma contribution à cet article concerne la validation expérimentale du modèle, ainsi que l'interprétation des résultats obtenus grâce à la simulation numérique.

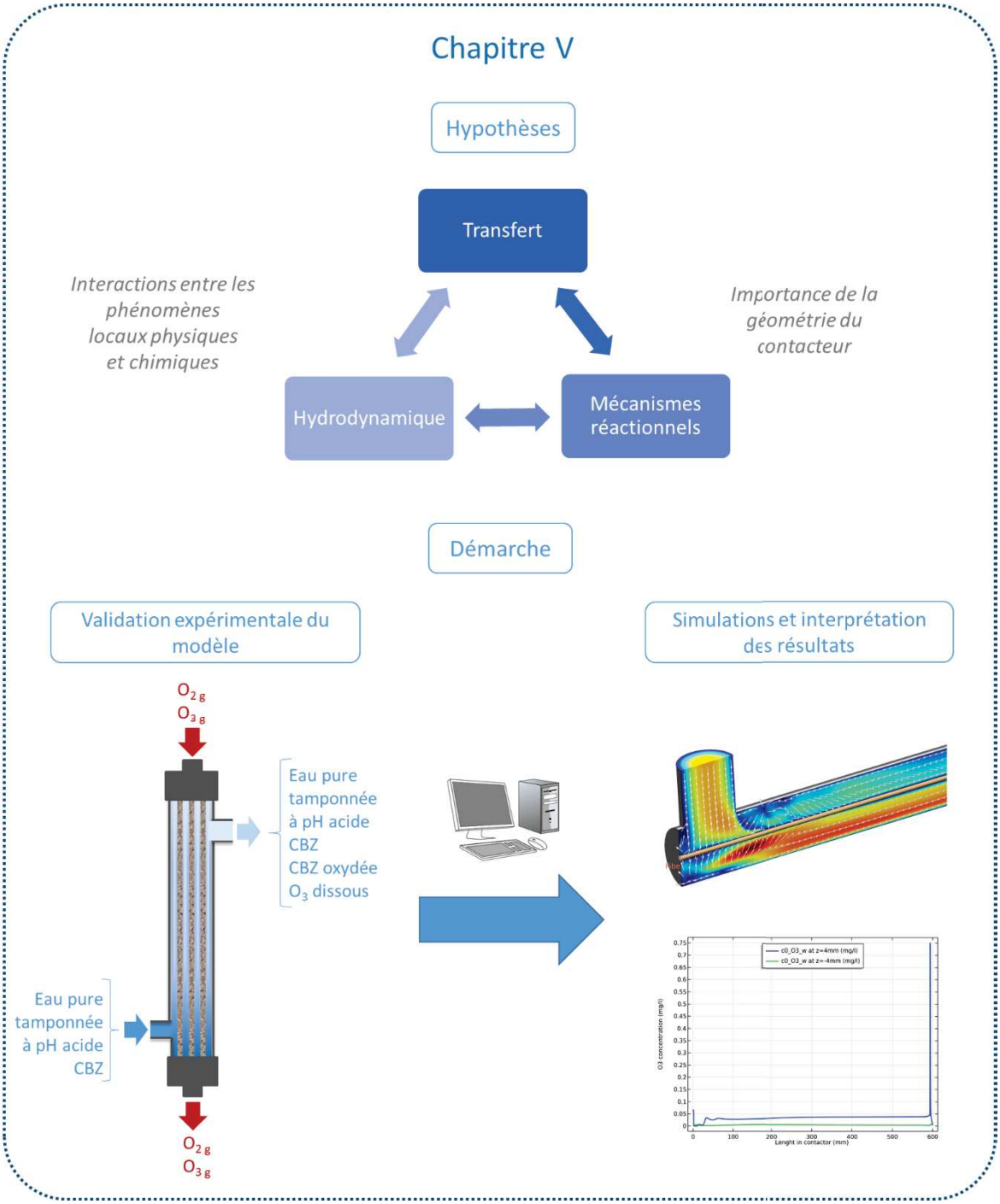
Chapitre V
Hypothèses
Transfert
Interactions entre les phénomènes locaux physiques et chimiques
Importance de la géométrie du contacteur
Hydrodynamique
Mécanismes réactionnels
Démarche
Validation expérimentale du modèle
Simulations et interprétation des résultats
$O_{2\,g}$
$O_{3\,g}$
Eau pure tamponnée à pH acide
CBZ
CBZ oxydée
O_3 dissous
Eau pure tamponnée à pH acide
CBZ
$O_{2\,g}$
$O_{3\,g}$

Computational fluid dynamics modeling of ozonation using a hollow fiber membrane contactor

Alice Schmitt[a], Julie Mendret[a], Cyril Chevarin[a], Denis Bouyer[a], Stephan Brosillon[a]

[a] IEM, University of Montpellier, CNRS, ENSCM, Montpellier, France

1. Introduction

Ozonation is applied for disinfection of drinking waters and wastewaters for a long time. In recent decades, ozonation processes have been successfully used to remove organic micropollutants, such as CBZ (Bourgin et al., 2017; Lee et al., 2014; Lee and von Gunten, 2016; Reungoat et al., 2010; Yao et al., 2018). Conventional ozonation processes (e.g. bubble columns and ozonation rooms) employ ozone dispersion in the form of bubbles, leading to several disadvantages such as foam generation, stripping of volatile organic compounds, high reactor footprint, high operational cost (due to in situ ozone production and destruction), and high energetic cost (due to mass transfer limitations). In addition, the ozone dosage is difficult to control and can result, in some cases, in an ozone over-consumption and in by-products production, which are sometimes even more dangerous than the original products (Gao et al., 2016; Gogoi et al., 2018; Schlüter-Vorberg et al., 2015). For instance, bromates are produced during the ozonation of waters containing bromides and are regulated in drinking water due to their carcinogenic potential (Soltermann et al., 2017; von Gunten, 2003). European Commission and US EPA defined this limit at 10 µg.L^{-1} in drinking water (AIDA, 1998; USEPA, 1998). Paraben ozonation by-products are another example. Indeed, Gao et al. showed that the paraben by-products were more toxic to green algae than the original compound itself, due to its reaction with hydroxyl radicals (Gao et al., 2016).

By using a bubbleless operation for transferring ozone, membrane contactors seem to be very promising devices to overcome these issues. The membrane acts as a barrier between the two phases and the mass transfer occurs by diffusion due to a concentration gradient. The process takes place under low pressure, hence limiting energy consumption. Moreover, hollow fibers membrane contactors offer the great advantage of a very high exchange surface (up to 10,000 $m^2.m^{-3}$) compared to conventional processes (between 3 and 600 $m^2.m^{-3}$) (Chabanon and Favre, 2017; Reed et al., 1995; Schmitt et al., 2020).

Usually, membrane contactors are used as separation method in two-phase contacting systems (Qatezadeh Deriss et al., 2021). For instance, these installations are frequently used for CO_2 absorption, where gaseous CO_2 is transferred through the membrane into the liquid phase (i.e. the absorbent)

thanks to a concentration gradient, and transformed in dissolved CO_2 at the gas/liquid interface (deMontigny et al., 2006; Li and Chen, 2005; Simons et al., 2009). Recently, membrane contactors have been pointed out for ozonation applications in wastewater treatment, leading potentially to efficient removal of micropollutants while limiting bromate formation (Merle et al., 2017; Schmitt et al., 2020; Stylianou et al., 2018).

In a previous study, we performed an experimental evaluation of an ozone diffusion process using a hollow fiber membrane contactor (Chapter III). However, it was pointed out that in order to better understand the mass transfer, to optimize the device design and to determine the most suitable process parameters, the development of a numerical model based on Computational Fluid Dynamics (CFD) can greatly assist (Qatezadeh Deriss et al., 2021). In addition, a literature review on ozone membrane contactors for water and wastewater treatment has pointed out that there is unused potential to optimize the geometry of membrane contactors (Bein et al., 2020).

A few studies have already been published on the modeling approach concerning membrane contactors for ozonation process. Two different approaches can be seen. Firstly, the model can be created from a global approach, where the membrane contactor acts like a “black box” (Gerun, 2006). In this case, the model provides the output data according to the input data by using overall material balances, without simulating the physical and chemical phenomena occurring inside the module. This model offers a global vision of the process and allows comparison of installations. However, it does not take into account velocity variations or concentration variations, and thus does not include diffusion and convection effects along the module, which can however have a substantial impact on the mass transfer. In order to improve the understanding of mass transfer and phenomena involved in the process, the model can also be established from a local approach. This type of model enables in particular an optimization of the contactor design.

Stylianou et al. worked on the modeling of ozonation in a ceramic membrane contactor with a global approach in order to provide fundamental basis for the design of bubbleless ozonation processes, in particular for micropollutants removal (Stylianou et al., 2016). Their model was based on both mass transfer and ozone decomposition reaction and was established from the exploitation of experimental data obtained in-situ with a hydrophobized α-Al_2O_3 ceramic membrane contactor. The aim was to allow the extrapolation of this model for different devices (scale-up) and experimental conditions, by adapting the values of major physical parameters (e.g. diffusivity or solubility) from literature or experiments. In this sense, they used Leveque equation, including dimensionless numbers such as the Sherwood and the Peclet numbers, and being valid in the case of a laminar regime. Berry et al. worked with a local approach and established a model by using Comsol Multiphysics® for the simulation of

ozone and oxygen transfer through a capillary non-porous membrane (Berry et al., 2017). The single fiber has been simulated with a two-dimensional axisymmetric domain. The model was validated for a laminar flow regime. However, based on experimental results found in literature, Berry et al. did not success validating their numerical model in transitional flow regime. Furthermore, no results were presented for turbulent flow regime. Focusing on experimental studies, Zoumpouli et al. worked on the ozone transfer through a non-porous tubular membrane. Using their experimental data obtained in absence of chemical reaction, they observed that the local model developed by Berry et al. slightly overestimated the mass transfer coefficients (Zoumpouli et al., 2018). They calculated molar fluxes of ozone and overall mass transfer coefficients for different ozone gas concentrations and liquid side velocities from their experimental data and they showed that membrane size (i.e. inner diameter) was an important parameter for the ozone transfer. They also experimentally studied the effect of the matrix on the removal of a model compound (i.e. the *para*-chlorobenzoic acid) but without including the chemical reaction in the model. According to Bein et al., one of the difficulties encountered for upscaling lab-scale results from mass transfer enhancement theory is the change in ozone concentration over fiber length (Bein et al., 2020). In the future, local approach should thus help to overcome this challenge.

In the aforementioned studies, only one fiber was simulated while multifiber contactors are much more interesting to promote the mass transfer thanks to higher exchange surface. Multifiber simulation allows to come closer to reality where the membrane contactors are often made of a lot of fibers within a cartridge, and therefore to take into account the liquid flow between the fibers and along the contactor. Qatezadeh Deriss et al. investigated the effect of the fibers number on the ibuprofen removal , another pharmaceutical, by using a hollow fiber membrane contactor with octanol (Qatezadeh Deriss et al., 2021). The simulation was made with a two-dimensional model, and the influence of the fibers number was studied using the method developed by Happel (Happel, 1959). Governing equations for the shell, membrane, and tube sides respectively were solved using Comsol Multiphysics®. In order to validate the model, their simulation results were compared with experimental data from the literature. Their results showed that the final concentration of ibuprofen was not proportional to the number of fibers, highlighting the need to consider the simulation of a multifiber system to predict the whole process efficiency.

The state of art thus exhibits that efforts should still be done on the modeling of ozonation process when using membrane contactors. To the best of our knowledge, no study on 3D multifiber simulation of ozonation process has already been achieved yet although the literature review has shown the need of such a modeling approach. Regardless of the applications, Zhao et al. had already highlighted that a

convection diffusion approach through a 3D grid would be a significant effort into module characterization of membrane contactor (Zhao et al., 2016). In a recent review, Ng et al. showed that only a very few studies concerning gas separation processes (and not ozonation processes) used a 3D approach (Bahlake et al., 2016; Cai et al., 2016; Kong et al., 2020; Ng et al., 2021). The authors concluded that previous models did not take into account non-ideal effects, such as a random fibers distribution, a random flow distribution, and the presence of channeling or dead zones (Ng et al., 2021). They underlined the necessity to include these effects in order to be closer to the reality of an industrial-scale installation. Although using much more computation time than other models due to additional directions and variables, 3-D modeling could overcome these challenges. Indeed, 3-D modeling could help to stick close to the reality of the experiments, which is crucial for a relevant model validation (Ng et al., 2021). Moreover, 2-D modeling is less relevant in the case of a turbulent flow regime and does not allow properly taking into account the local hydrodynamics effects caused by the presence of the fibers in the cartridge, although local turbulences provide higher ozone fluxes since the main transfer resistance is localized within the liquid boundary layer (Berry et al., 2017). A 3-D modeling enables also to study the impact of the hydrodynamics on the transfer according to the real contactor geometry. To this end, Cai et al. used 3-D modeling to model CO_2 absorption into water in a cross-flow hollow fiber membrane contactor in order to assess the design factors on the shell side flow distribution (Cai et al., 2016). Simultaneously, Bahlake et al. used 3-D modeling to model CO_2 and H_2S removal from water using nitrogen gas in a hollow fiber membrane contactor in order to take into account the variations of concentration from one fiber to another (Bahlake et al., 2016). More recently, Kong et al. (Kong et al., 2020) used 3-D modeling to model SO_2 absorption into a NaOH solution in a multichannel membrane contactor in order to assess the concentration and velocity in each channel individually.

Herein, this study aims at gaining better understanding of the ozone transfer through a hollow fiber membrane contactor using modeling approach. The effect of the contactor geometry (number of fibers and fibers length), the process conditions (ozone concentration in the gas phase and liquid flowrate), and hydrodynamics on the ozone transfer and carbamazepine removal efficiency were evaluated. In order to validate the numerical model properly before to go deeper in the extrapolation and interpretation of the results, the simulation results have been compared to experimental data obtained using a unique hollow fiber membrane contactor.

2. Material and methods

2.1. Experimental setup

2.1.1. Membrane contactor technology

The membrane contactor used in this work was home-made, designed and fabricated in the lab manufacturing work-shop. The membranes have been provided by the French company Polymem (Castanet Tolosan– France). The membrane characteristics are listed in Table 13. The potting of the fiber has been made with polyurethane resin, the hollow fiber was made of polytetrafluoroethylene (PTFE), known to be good ozone-resistant over time (Bamperng et al., 2010). The membrane has been treated with Fluoroetch® product (provided by Polyfluor) in order to improve the adhesion between the resin and the fiber. The hollow fiber form leads to a very compact process thanks to a large exchange surface.

Table 13. Membrane contactor technical specifications.

Fiber characteristics			
Number	1	Effective length (cm)	60
Inner diameter (mm) *	0.45	Effective outer surface (m^2)	1.64×10^{-3}
Outer diameter (mm) *	0.87	Material	PTFE
Porosity [a]	0.58		
Shell characteristics			
Inner diameter (mm) *	10	Material	Teflon (tube) Stainless steel (tee)

** Values specified by the manufacturer (Polymem, France)*

The membrane porosity ε_m ([a]) was determined by gravimetric method (Sartorius CPA 225D balance), by measuring the weight of isopropanol (IPA) inside the membrane pores (Wang et al., 2010). The porosity wad calculated such as:

$$\varepsilon_m = \frac{(w_{wet} - w_{dry})/D_{iso}}{\frac{w_{wet} - w_{dry}}{D_{iso}} + w_{dry}/D_{PTFE}}, \quad [45]$$

Where: w_{wet} is the weight of the wet membrane, w_{dry} is the weight of the dry membrane, D_{iso} is the IPA density, D_{PTFE} is the polymer density.

2.1.2. Ozonation pilot

The ozonation lab-scale pilot (Figure 35) consisted of a membrane contactor (see section 2.1.3) continuously feed by an ozone generator (BMT 803 N) from a lab-grade pure oxygen tank. Before circulating in the gas side of the membrane contactor, the ozone was diluted with the oxygen to achieve the desired gas flowrate. An ozone gas analyzer (BMT 964) was used to monitor both the ozone

concentration at the gas inlet and at the gas outlet, after dehumidification. Two electro valves connected to a computer were used to determine the desired concentration of the oxygen/ozone mix.

The liquid was flowing into the pilot thanks to a feed tank of 30L, which was stainless steel, stirred, and under thermostatic control (20°C). A peristaltic pump (Watson Marlow 323) was used for the liquid circulation. Two tapes (upstream and downstream of the membrane contactor) were used for sampling. The liquid was flowing in open circuit (i.e. the solution was circulating only once in the membrane contactor), and then recovered in a container with KI solution, in order to prevent the ozone degassing. Ozone was transferred from the gas phase of the membrane contactor to the liquid phase, thanks to a concentration gradient. Membrane in the contactor was acting as barrier. Gas was circulating inside the fiber and liquid in the shell via a counter-current flow.

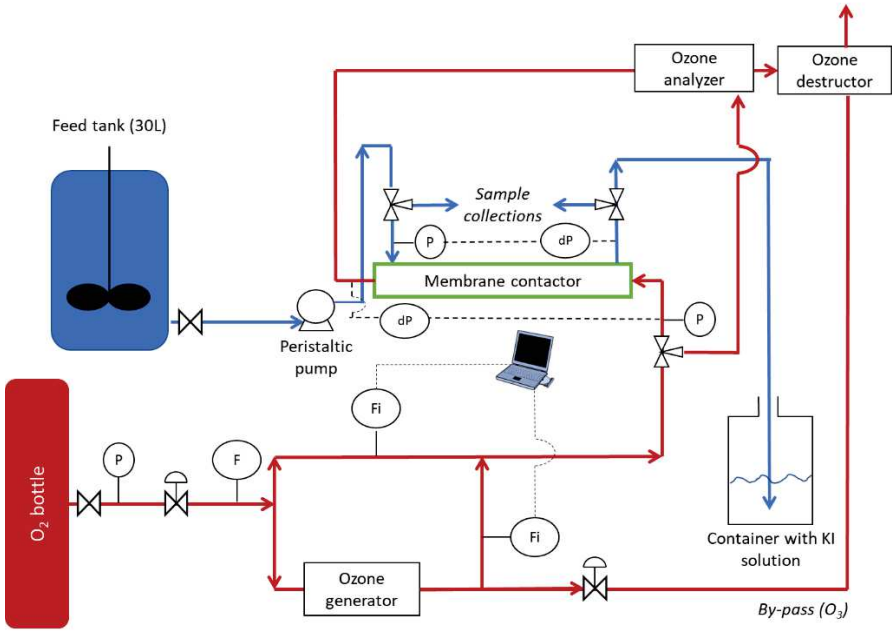

Figure 35. Flowsheet of the ozonation pilot.

2.1.3. Chemicals

Carbamazepine (CBZ) was chosen as a model compound due to its well-known reaction kinetics thanks to the numerous studies already made on this molecule. CBZ is an anti-epileptic drug used in many countries. This compound is only partially removed in conventional WWTP (Björlenius et al., 2018; UNESCO and HELCOM, 2017). As many other pharmaceuticals, CBZ is thus widespread in WWTP secondary effluent and has been widely reported in the literature (Cabeza et al., 2012; Luo et al., 2014; Rosal et al., 2010; Yang et al., 2017). Carbamazepine ($C_{15}H_{12}N_2O$) from Sigma was used (>99% purity). Pure potassium indigotrisulfonate from Sigma-Aldrich was used as ozone-scavenging reagent.

2.1.4. CBZ solution

Acid buffered CBZ solution was used. The solution was obtained by dissolving 2 ppm of CBZ in buffered water, which was produced by dissolving 1.2 $g.L^{-1}$ of sodium dihydrogen phosphate (NaH_2PO_4, Sigma-Aldrich) in deionized water (Total Organic Carbon < 30 ppb, Resistivity $\in [5\ M\Omega.cm; 15\ M\Omega.cm]$) and then by adjusting the pH with a few milliliters of phosphoric acid (H_3PO_4) concentrated at 84% (Sigma-Aldrich). The pH of the final matrix was 3.

After 24h stirring, the solution was injected in the feed tank. Then, the liquid was circulating in close-loop mode, with compressed air flowing in the fiber, for at least 12 h. This recirculation provided to achieve a balance between the system (i.e. the pilot materials) and the solution. The pilot was then put in open circuit, before starting the experiment of ozonation. In order to know the initial concentration of CBZ, 3 samples were collected both in the feed tank and through the upstream tap of the membrane contactor (see Figure 35).

2.1.5. Analytical methods

Indigo method (Bader and Hoigné, 1982) was used to determine the dissolved ozone concentration in the liquid phase. Liquid chromatography-tandem mass spectrometry (LC-MS/MS) was used to quantify CBZ and was performed with a Waters® device. A column with XSelect® HSS-T3-C18 resin (100 mm * 21 mm), 2.5 µm particles size was used as the stationary phase at room temperature, with eluent A (90 % HPLC grade water + 10 % HPLC grade acetonitrile (ACN) + 0.1% formic acid) and eluent B (ACN + 0.1% formic acid). The flow-rate was 0.25 $mL.min^{-1}$ and the gradient elution profile described in the Chapter II (Tableau 5) was applied. To achieve the best sensitivity, the MS was adjusted to facilitate the ionization process and the detection conditions were: capillary potential 3.5 kV, cone voltage 25 V, source temperature 120°C, desolvation temperature 450°C, cone gas flow 50 $NL.h^{-1}$, desolvation gas flow of 450 $NL.h^{-1}$, and collision energy of 20 V. Nitrogen was used as a nebulizer gas and argon as a collision gas. The calibration curves were made in the same matrix as the samples to avoid matrix effects on detection (i.e. calibration curves were made using buffered water with known concentrations of CBZ). Two calibration curves were made, by analyzing standard samples before and after analyte samples, to avoid instrumental drift. The instrument quantification limit (IQL) and the instrument detection limit (IDL) for the CBZ are respectively estimated about 10 $\mu g.L^{-1}$ and 3 $\mu g.L^{-1}$.

2.2. 3D Model development

Herein, we developed an original multi-physical model of the hollow fiber membrane contactor including a coupling between fluid flow within the membrane contactor, ozone mass transport though the membrane and mass transfer at the membrane/liquid flow interface and chemical reaction

involving ozone and carbamazepine in liquid phase. To ensure a reliable validation of the numerical model using the experimental data, a 3D model was necessary considering the geometry of the experimental pilot (Figure 35).

The experimental water and gas flow rate used in the ozonation lab-scale pilot (respectively 50 $L.h^{-1}$ and 1 $L.h^{-1}$) allowed to calculate in the case of the single fiber contactor Reynolds numbers of 55 and 1650 for gas flow and liquid flow, respectively. Laminar flow could therefore be considered in the hydrodynamic model and both flow patterns have been assessed numerically by solving the Reynolds Averaged Navier–Stokes (RANS) transport equations. Additional transport equations have to be solved to calculate the ozone concentration in the gas, within the membrane and in the water as well as the carbamazepine concentration in the water.

The numerical model was developed considering some assumptions described below:

i) 3D modelling with a YZ symmetry plan condition (

Figure 36.a); ii) steady-state and isothermal conditions; iii) Newtonian and incompressible fluids; iv) laminar flow for both phases in the contactor; v) membrane is gas-phase filled, i.e non-wetted membrane; vi) gravity effect is neglected; vii) thermodynamic equilibrium is reached at the membrane/water interface; viii) Ideal gas behavior is assumed; ix) Convective mass transfer in gas-filled membrane pores is neglected; x) isothermal model (298 K).

2.2.1. Monofiber 3D model

A first model was developed with only one fiber within the cartridge to properly validate the numerical results using our own experiment data. The 3D one hollow fiber membrane contactor geometry was built using Comsol Multiphysics® software (

Figure 36.a). The overall dimensions corresponding to the device are 600 mm length, a 10 mm diameter of the inlet water, the outlet water and the main axial tube containing the fiber. The inlet and the outlet are arranged perpendicular to the main tube and so to the fiber. The external fiber diameter is equal to 0.87mm. The model configuration is characterized by a longitudinal YZ symmetry plan leading to allow to consider a half-contactor geometry in our model (Figure 3).

The meshing of the 3D geometry has required to use hybrid hexahedral/tetrahedral meshes (Figure 36.b) to optimize the mesh quality and so to improve the numerical convergence of the model. Boundaries layers were built on the wall surfaces to properly simulate the flow in the vicinity of the walls, assuming no-slip condition. Despite the symmetry plan, 1.5 million meshes were necessary to obtain reliable convergence with RANS model.

a.

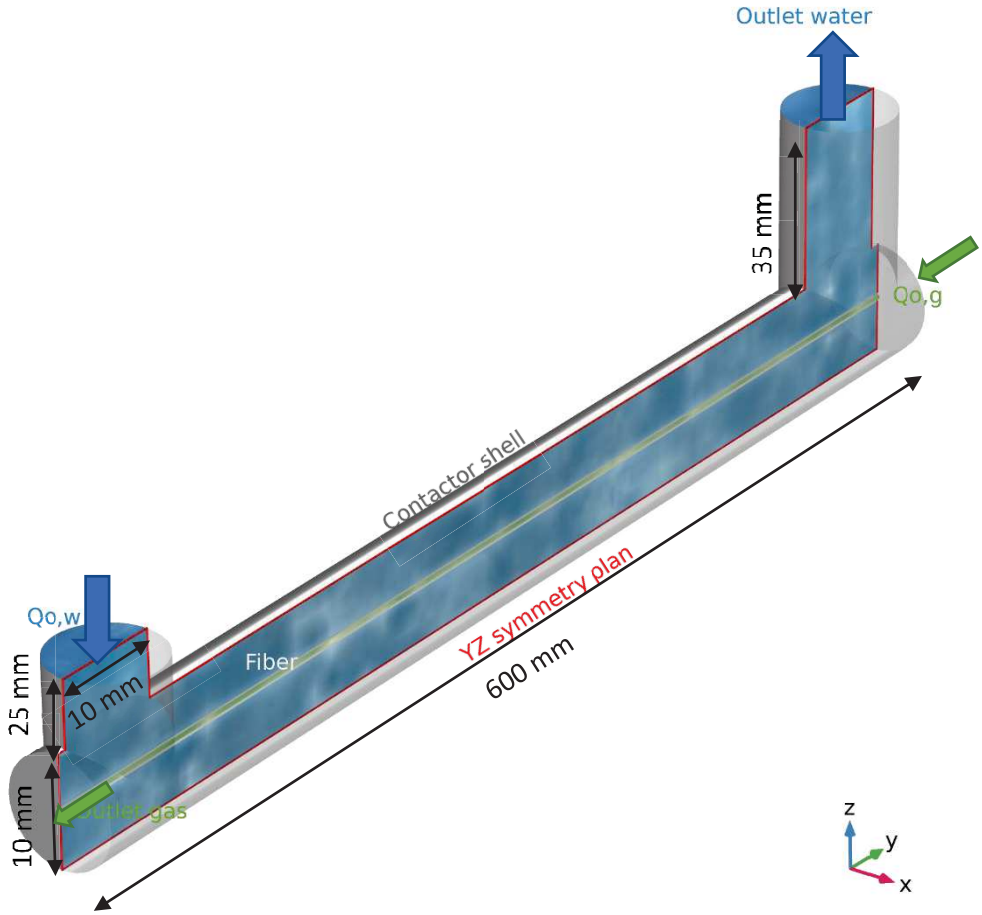

b.

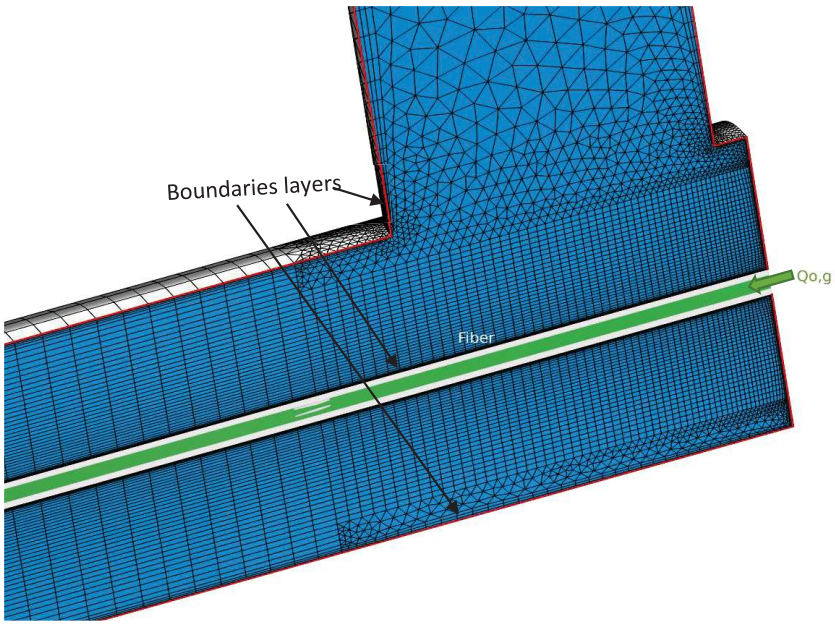

Figure 36. 3D Comsol® software views of a. the unique hollow fiber membrane contactor geometry and its dimensions; b. the hybrid hexaedral/tetrahedral mesh zoomed at the inlet gas in the half-contactor.

2.2.2. Gas phase

- **Fluid flow:**

According to the assumptions described in the previous section, the gas flow within the inner side of the membrane can be described using the following equation (Cussler, 1997):

$$\boldsymbol{\rho_g}(\boldsymbol{\nabla}.\vec{\mathbf{v}}_{\boldsymbol{g}})\vec{\mathbf{v}}_{\boldsymbol{g}} = -\boldsymbol{\nabla}\mathbf{p_g} + \boldsymbol{\nabla}.(\boldsymbol{\eta_g}\left[\left(\boldsymbol{\nabla}\,\vec{\mathbf{v}}_{\boldsymbol{g}} + \boldsymbol{\nabla}\,\overrightarrow{\mathbf{v}_{\boldsymbol{g}}}^{\boldsymbol{T}}\right)\right]), \quad [46]$$

where ρ_g denotes the density of the gas (in kg.m^{-3}), $\overrightarrow{v_g}$ is the gas velocity vector (in m.s^{-1}), p_g is the static pressure (in Pa), $\eta_g\left[\left(\nabla\overrightarrow{v_g} + \nabla\overrightarrow{v_g}^T\right)\right] = \bar{\bar{\tau}}$ is the viscous stress tensor, η_g is the dynamic viscosity of the gas (in Pa.s),

The fluid flow boundary conditions were:

- At the hollow fiber inlet, a fully developed flow is imposed with a constant gas flow rate $Q_{0,g}$ (l/h). Thus, the parabolic laminar flow profil was already established at this boundary.
- At the hollow fiber outlet, $p_g=p_{atm}$
- Inside the hollow fiber, at the gas/membrane interface, a no-slip wall condition was applied.
- At the plan symmetry, no flow crossing the boundary, i.e the normal velocity to the boundary is equal to zero $v_{n,g} = 0$

- **Mass transfer:**

The mass transfer of ozone requires to solve an additional convection-diffusion transport equation as follow (Cussler, 1997):

$$\boldsymbol{\nabla}.(-\boldsymbol{D_{O_3,g}}\,\boldsymbol{\nabla C_{O_3,g}} + \boldsymbol{C_{O_3,g}}\vec{\mathbf{v}}_{\boldsymbol{g}}) = \mathbf{0}, \quad [47]$$

where $C_{O_3,g}$ denotes the concentration of species i in the gas (in mol.m^{-3}), $\overrightarrow{v_g}$ is the gas velocity vector (in m.s^{-1}), $D_{O_3,g}$ is the diffusion coefficient of the ozone in the gas (in m².s^{-1}) and is assumed to be isotopic and constant.

The boundary conditions for gas transport within the hollow fiber is the following:

- Inlet: an inflow boundary condition (Danckwerts flux) with a constant concentration of the ozone in the gas was applied (Danckwerts, 1995):

$$\boldsymbol{n}.(-\boldsymbol{D_{O_3,g}}\boldsymbol{\nabla}\,\boldsymbol{C_{O_3,g}} + \vec{\mathbf{v}}_{\boldsymbol{g}} * \boldsymbol{C_{O_3,g}}) = \vec{\mathbf{v}}_{\boldsymbol{g}} * \boldsymbol{C_{O_3,0,g}}, \quad [48]$$

- Outlet: convective flux assuming no molecular diffusion ($n.D_{O_3,g}\nabla C_{O_3,g} = 0$) thus leading to $\frac{\partial C_{O_3,g}}{\partial y} = 0$.

2.2.3. Mass transfer within the porous membrane

Ozone transfers from the gas side of the hollow fiber through the porous membrane. It is assumed that ozone diffuses through the membrane pores and that no chemical reaction occurs in the membrane. Consequently, a stagnant gas phase was assumed within the membrane pores and ozone transport is driven by diffusion phenomena only, as described by the following equation:

$$\boldsymbol{\nabla}.(\boldsymbol{D}_{\boldsymbol{O_3,m}}^{\boldsymbol{eff}}\,\boldsymbol{\nabla C}_{\boldsymbol{O_3,m}}) = \mathbf{0}\ ,\ [49]$$

where $C_{O_3,m}$ denotes the ozone concentration in the membrane, $D_{O_3,m}^{eff}$ is the effective diffusion coefficient of ozone in the membrane.

In a porous media, both molecular and Knudsen diffusions occur and the Knudsen number indicates phenomenon dominates (Bird et al., 2002):

$$\mathbf{K}_{\boldsymbol{n}} = \frac{\boldsymbol{\lambda}}{\boldsymbol{d_p}}\ ,\ [50]$$

where d_p denotes the pore diameter and λ represents the mean free path of the gas molecule which may collide the medium walls, which is described as:

$$\boldsymbol{\lambda} = \frac{\boldsymbol{k_b T}}{\sqrt{2}\,\boldsymbol{\pi}\,\boldsymbol{d_p^2}\,\boldsymbol{P_g}}\ ,\ [51]$$

where k_b is the Boltzmann constant ($1.3806\times10^{-23}\ m^2.kg.s^{-2}.K^{-1}$), T is the temperature (K) and P_g the gas pressure (Pa).

According to the operating conditions of this study (T = 298.15 K, P_g = 1.2 bar, d_{pore} = 0.8 µm), the mean free path λ was equal to 1.21 x 10^{-2} pm and the Knudsen number K_n to 1.5×10^{-8}. So, regarding to the very low Knudsen number, the Knudsen diffusion was neglected in this work.

Thus, the effective diffusion coefficient was calculated following the equations (Gabelman and Hwang, 1999):

$$\boldsymbol{D}_{\boldsymbol{O_3,m}}^{\boldsymbol{eff}} = \mathbf{D}_{\boldsymbol{O_3,g}}\frac{\boldsymbol{\varepsilon_m}}{\boldsymbol{\tau}}\ ,\ [52]$$

$D_{O_3,g}$ $(\mathrm{in\ m^2.s^{-1}})$ is the ozone diffusion coefficient in the gas (Prasad and Sirkar, 1989), ε_m and τ are the membrane porosity and tortuosity , respectively. The tortuosity τ was estimated by the porosity-tortuosity relationship defined by (Iversen et al., 1997):

$$\boldsymbol{\tau} = \frac{(\mathbf{2}-\boldsymbol{\varepsilon_m})^2}{\boldsymbol{\varepsilon_m}}\ ,\ [53]$$

The boundary conditions were the following:

- At the membrane/water interface, Henry's law was used for gas/liquid transfer of ozone in water (Pines et al., 2005):

$$\boldsymbol{H_{O_3,w}} = \frac{\boldsymbol{C_{O_3,w}}}{\boldsymbol{C_{O_3,m}}}, \text{ [54]}$$

where $C_{O_3,m}$ and $C_{O_3,w}$ denote the concentration of the ozone in the membrane and in water, respectively. $H_{O_3,w}$ is the partition coefficient of ozone in water.

- At each side of the membrane in longitudinal axis, the normal total flux is equal to zero.

2.2.4. Liquid phase within the cartridge

- **Fluid flow:**

The water flow is described using the Navier-Stokes equation and the continuity equation as follow (Cussler, 1997):

$$\boldsymbol{\rho_w}(\boldsymbol{\nabla}.\vec{\mathbf{v}}_{\boldsymbol{w}})\vec{\mathbf{v}}_{\boldsymbol{w}} = -\boldsymbol{\nabla}\mathbf{p_w} + \boldsymbol{\nabla}.(\boldsymbol{\eta_w}\left[\left(\boldsymbol{\nabla}\,\vec{\mathbf{v}}_{\boldsymbol{w}} + \boldsymbol{\nabla}\,\overrightarrow{\mathbf{v}_{\boldsymbol{w}}}^{\boldsymbol{T}}\right)\right]), \text{ [55]}$$

$$\boldsymbol{\nabla}.(\overrightarrow{\mathbf{v}_{\boldsymbol{w}}}) = \mathbf{0}, \text{ [56]}$$

where ρ_w denotes the density of the water, $\overrightarrow{v_w}$ is the water velocity vector, p_w is the static pressure, η_w is the dynamic viscosity of the water.

The boundary conditions for fluid flow in the cartridge are:

- Inlet: a fully developed flow was imposed with a constant water flow rate $Q_{0,w}$, assuming a parabolic laminar flow profile.
- Outlet: $p_g = p_{atm}$.

At the membrane/water interface and at the wall of the contactor, a no-slip wall condition was imposed.

- **Mass transport in liquid phase**

Convection-diffusion equations were used to simulate the mass transport equations for ozone and carbamazepine while a coupling with chemical reaction between both aforementioned species as necessary as follows (Cussler, 1997):

$$\boldsymbol{\nabla}.(-\boldsymbol{D_{i,w}}\,\boldsymbol{\nabla C_{i,w}} + \boldsymbol{C_{i,w}}\vec{\mathbf{v}}_{\boldsymbol{w}}) = \boldsymbol{R_{i,w}}, \text{ [57]}$$

where $C_{i,w}$ denotes the concentration of species i in the water, $\overrightarrow{v_w}$ is the water velocity vector, $D_{i,w}$ is the diffusion coefficient of species i in the water and is assumed to be isotopic and constant, $R_{i,w}$ is the reaction term of species i in water.

The boundary conditions for ozone and carbamazepine in liquid phase:

- Inlet: an inflow boundary condition (Danckwerts flux) for carbamazepine in water was applied:

$$\boldsymbol{n}.(-\boldsymbol{D_{CBZ,w}}\boldsymbol{\nabla}\,\boldsymbol{C_{CBZ,w}} + \vec{\mathbf{v}}_{\boldsymbol{w}} * \boldsymbol{C_{CBZ,w}}) = \vec{\mathbf{v}}_{\mathbf{0},\boldsymbol{w}} * \boldsymbol{C_{CBZ,0,w}}, \quad [58]$$

  While a null flux was considered for ozone in the feeding water flux.

- Outlet: for all species i, the convective flux dominates the outgoing mass flux, so $\frac{\partial C_{i,w}}{\partial \mathrm{z}} = 0$.
- At the external cartridge wall, impermeable wall was considered, i.e. no flux for all species.

- **Chemical reactions:**

The chemical reaction between ozone and CBZ was taken into account in the model, while the other chemical reaction involved during ozone decomposition were not taken into account in this first study. This choice was motivated by the fact that the reaction between CBZ and molecular ozone is fast since ozone attacks the double bond of CBZ (Huber et al., 2003), leading to a high constant reaction term (k_{O3} = 3.0 x10^5 mol.L^{-1}.s^{-1}). This reaction yields to the formation of several by-products containing quinazoline-bases functional groups (McDowell et al., 2005). Reaction constants of the different by-products with O_3 are significantly lower comparing to CBZ (about five orders of magnitude) (McDowell et al., 2005). Moreover, the residence time of the liquid in the membrane contactor was very short (about 7 s for a liquid flow rate of 40 $L.h^{-1}$), and therefore it has been assumed that reactions between by-products and O_3 do not have the time to occur. Simultaneously, reaction of CBZ with hydroxyl radicals (generally present during ozonation processes because of the ozone decomposition) has not been taken into account in the model due to acidic conditions imposed herein (Alharbi et al., 2016; Roustan, 2003). So, the irreversible chemical reaction between ozone and carbamazepine was described as follows:

$$\boldsymbol{CBZ} + \boldsymbol{O_3} \rightarrow \boldsymbol{BQM}, \quad [59]$$

The rate of this second-order reaction was given by:

$$\boldsymbol{R_{i,w}} = \boldsymbol{k_r} * \boldsymbol{C_{O_3,w}} * \boldsymbol{C_{CBZ,w}}, \quad [60]$$

where k_r denotes the constant rate of the reaction.

Table 14. Model parameters.

Parameters	Values	Units	References
Gas phase			
Density : ρ_g	1.2	kg.m^{-3}	
Dynamic viscosity : η_g	1 × 10^{-5}	Pa.s	
Inlet Flow rate : $Q_{0,g}$	1	L.h^{-1}	
O_3 inlet concentration : $C_{O_3,0,g}$	50	mg.L^{-1}	
O_3 Diffusion coefficient : $D_{O_3,g}$	1.454 × 10^{-5}	m^2.s^{-1}	(Massman, 1998)
Universal gas constant : R	8.314	J.mol^{-1}.K^{-1}	
Fiber: microporous membrane			
Pore diameter : d_{pore}	0.8	µm	
Porosity : ε_m	0.58	[ ]	
Permeability : κ_m	3.932 × 10^{-15}	m²	Kozeny-Carman (Bear, 1972)
Tortuosity : τ	3.47	[ ]	
O_3 effective diffusion coefficient : $D_{O_3,m}^{eff}$	2.426 × 10^{-6}	m^2.s^{-1}	
Liquid phase : water			
Density : ρ_w	1000	kg.m^{-3}	
Dynamic viscosity : η_w	1.01 × 10^{-3}	Pa.s	
Inlet Flow rate : $Q_{0,w}$	50	L.h^{-1}	
O_3 inlet concentration : $C_{O_3,0,w}$	0	mg.L^{-1}	
O_3 Solubility in water : $H_{O_3,w}$	0.2479	[ ]	(Sander, 2015)
O_3 Diffusion coefficient : $D_{O_3,w}$	1.76 × 10^{-9}	m^2.s^{-1}	(Gottschalk et al., 2009)
CBZ inlet concentration : $C_{CBZ,0,w}$	0-1366	µg.L^{-1}	
CBZ Diffusion coefficient : $D_{CBZ,w}$	1 × 10^{-9}	m^2.s^{-1}	
Reaction constant rate : k_r	3 × 10^5	L.mol^{-1}.s^{-1}	(Huber et al., 2003)

3. Results and discussion

3.1. Model simplification

A first set of numerical simulations was launched in order to verify if the model could be simplified, especially concerning the gas flow within the inner fiber. Indeed, four contributions can be identified for characterizing the ozone transfer resistance from gas phase to liquid phase: (i) resistance in gas phase due to ozone diffusion, (ii) resistance within the porous membrane, (iii) resistance at the membrane/liquid interface due to phase change (Henry law) and (iv) resistance in liquid phase mainly due to molecular diffusion within the boundary layer. Among those four resistances, it can be reasonably expected that the resistance to ozone transfer in gas phase within the fiber can be neglected comparing to the others. Therefore, preliminary simulations were run to confirm this assumption: rather than computing gas flow within the fiber, a Dirichlet boundary condition was tested, assuming that ozone supply from the gas entrance was much higher than its transfer rate through the membrane, thus enabling to consider that the ozone concentration at the gas/membrane interface could be considered constant along the membrane length. In other words, a boundary condition of ozone concentration was considered at this interface instead of the gas flowrate, thus simplifying notably the numerical simulations. Table 15 shows results obtained during simulations with (complete model) and without (simplified model) circulation of the gas in the gas phases. When the gas was not flowing, the ozone concentration was supposed to be the same all along the fiber. We can see that the result obtained with the simplified model is the same than with the complete model. Therefore, the circulation of the gas inside the fiber and the evolution of the ozone concentration along the fiber were not taken into account in the following results.

Table 15. Comparative table of complete and simplified models.

Model	$Q_{0,w}$ ($L.h^{-1}$)	$Q_{0,g}$ ($L.h^{-1}$)	$C_{O_3,0,g}$ ($mg.L^{-1}$)	$C_{O_3,w,outlet}$ ($mg.L^{-1}$)
Complete	30	1	50	**0.071**
Simplified	30		50	**0.071**
Complete	40	1	50	**0.064**
Simplified	40		50	**0.064**
Complete	50	1	50	**0.061**
Simplified	50		50	**0.061**

Another comment concerns the graphical presentation of the main results obtained by the numerical simulation. Since the ratio between the membrane contactor length (600 mm) and the membrane thickness (10 mm) is very large (60), the main figures present a graphical representation of the result considering two specific regions of the contactor: the inlet region (80 mm length) and the outlet region (60 mm length).

3.2. One fiber contactor: 3D model without chemical reaction

The results presented in this section correspond to a liquid flowrate $Q_{0,w}$ of 50 L.h^{-1} at the inlet of the contactor and to an ozone concentration $C_{O_3,0,g}$ in the gas phase of $50\ \mathrm{mg}.L^{-1}$. This corresponds to an ozone concentration $C_{O_3,m}$ at the interface between the membrane and the water (i.e at the external surface of the fiber) of $12.4\ \mathrm{mg}.\mathrm{L}^{-1}$ according to the Henry's law (Equation [54], (Sander, 2015)). These conditions were chosen according to the experimental limits of the ozonation pilot.

3.2.1. Hydrodynamics

The Figure 37 shows the velocity field in the membrane contactor and clearly exhibits that the center of the membrane fiber cannot be considered as an axis of symmetry, thus justifying the choice of performing 3D simulations rather than 2D axi-symmetrical ones. Due to the geometry of the cartridge inlet, dead zone can be identified, especially in the vicinity of the cartridge extremities.

In the inlet zone, the velocity field exhibits that the velocity is much higher below the membrane that is due to the geometry of the inlet feed. More precisely, at the inlet the average velocity is equal to 0.18 m.s^{-1}, which corresponds to the flow rate of 50 L.h^{-1}. Below the fiber and along the Z axis, the flow velocity is ranged between 0.3 and 0.4 m.s^{-1}, while it is close to close to 0.15 m.s^{-1} below the fiber. Then, the flow becomes parallel to the fiber and the velocity magnitude tends towards a homogeneous average value on both sides of the fiber (around 0.25 m.s^{-1}). Finally, the flow pattern is strongly affected by the geometry of the contactor outlet, where counter-current flows promote the emergence of a high-speed area in the outlet canal (around 0.35 m.s^{-1}) and small recirculation zones characterized by low velocity magnitude.

Despite a Reynolds number indicating a laminar flow, the assumption of a laminar flow in the shell side seems not to be appropriated. This observation reflects that of previous works (Zheng et al., 2003, 2004). A 2-D modeling approach would not have provided this indication (Ng et al., 2021).

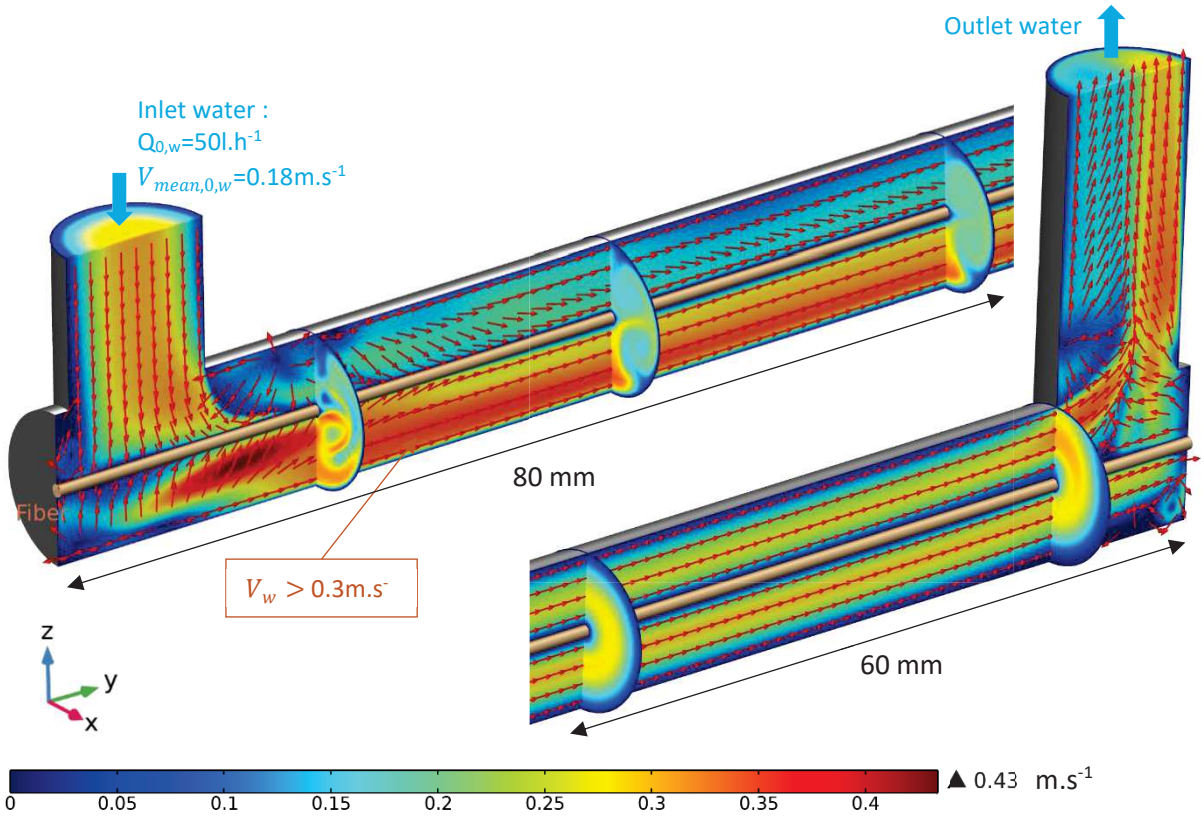

Figure 37. Velocity field (magnitude (m.s^{-1}) and direction) in the YZ symmetry plane in the single fiber contactor for $Q_{0,w}$ = 50 L.h^{-1} and $C_{O_3,0,g}$ = 50 $mg.L^{-1}$.

3.2.2. Ozone transfer

Figure 38 shows the ozone concentration distribution in the liquid phase on the YZ symmetry plan and on two ZX cross sections located in the inlet and the outlet region, respectively. The ozone concentration under the fiber along the Z axis is very low (<0.01 mg.L^{-1}) due to the high velocity magnitude (Figure 37). Conversely, the ozone concentration is high (up to 12.4 mg.L^{-1}) in a thin layer around the fiber all along the contactor. This underlines the very small effective volume of the contactor (i.e. the volume of liquid containing dissolved ozone), meaning that a large portion of the volume is not involved in the mass transfer. This layer can be interpreted as a boundary layer, where the transversal diffusion of ozone is the limiting parameter. In the vicinity at the outlet, a high ozone concentration area can be observed above the fiber, corresponding to dead zone of the flow because the main flow is directed upward while a recirculation zone is located at the end of the contactor. At the outlet of the contactor (cartridge side), the ozone concentration is homogenized and its value is ranged between 0.03 to 0.08 mg.L^{-1}, with a mean value of 0.064 mg.L^{-1}.

The previous results are noticeable since they exhibit that the ozone spatial distribution is heterogeneous along the membrane contactor with high concentrated zones near the membrane and a large fraction of the bulk that is characterized by a very low concentration of ozone. The numerical results therefore suggest that the diameter of the shell of the membrane contactor, with only one fiber, is oversized, meaning that the bulk volume containing the water could be significantly reduced. Obviously, an analytical model based on a global approach and dimensionless number could not allow to describing this ozone transfer and diffusion as precisely as the 3D model. However, even a 2D axi-symmetrical model would fail in describing the hydrodynamics within the membrane contactor and thus the ozone concentration in the bulk along the contactor, from the inlet to the outlet. This observation provides a better understanding of the phenomena limiting the transfer, and thus could lead to the optimization of the contactor geometry.

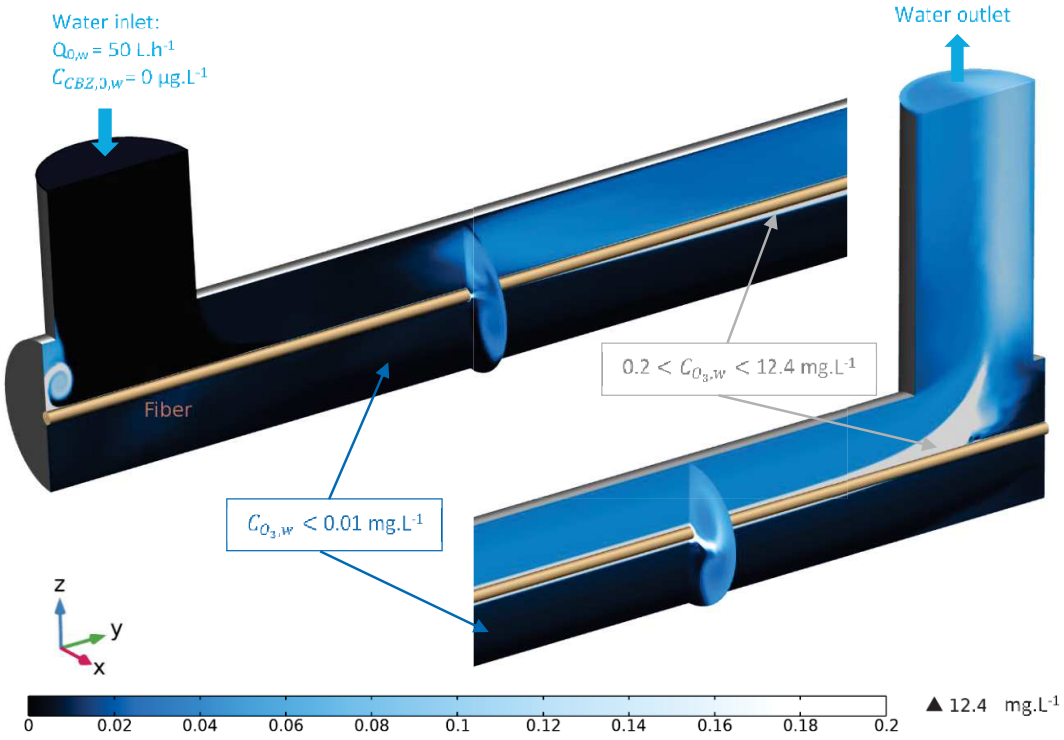

Figure 38. Ozone concentration in water (YZ symmetry plane and two ZX cross sections) (mg.L^{-1}) in the single fiber membrane contactor for $Q_{0,w}$ = 50 L.h^{-1} and $C_{O_3,0,g} = 50\ mg.L^{-1}$..

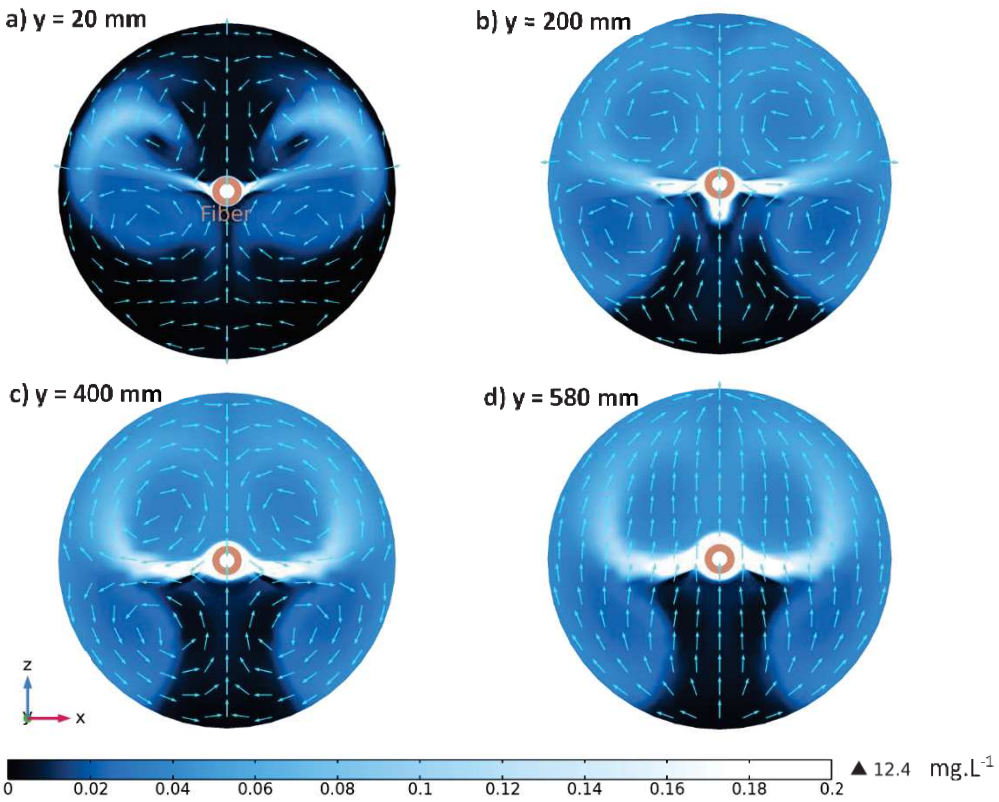

Figure 39. ZX cross sections of $C_{O_3,w}$ (mg.L^{-1}) and of normalized velocity vector in the single fiber contactor at: a) y=20mm ; b) y=200mm ; c) y=400mm and d) y=580mm, for $Q_{0,w}$ = 50 L.h^{-1} and $C_{O_3,0,g} = 50\ mg.L^{-1}$.

The Figure 39 represents the ozone concentration for cross sections of the membrane contactor at different distances from the water inlet. We can note that the concentration profile fits the water flow. This result suggests that the impact of the shell design on the transfer is significant, and is consistent with previous works (Cai et al., 2016; Wickramasinghe et al., 1992). In addition, the presence of vortexes with low velocities, due to the position of the fiber in the contactor disrupting the flow, promotes the mixing by convection.

As in the previous figure, a thin boundary layer can be observed around the fiber where the ozone concentration is high. Differences are noticeable according to the location of the cross section, indicating an evolution of the concentration profile and the thickness of this layer, depending on the contactor length. This result confirms the observation previously made by Bahlake et al. during the 3-D modeling of a hollow fiber contactor for an application of CO_2 and H_2S removal (Bahlake et al., 2016). The authors showed that the diffusion was lower at the inlet of the contactor than at the outlet, and thus that there was an evolution of the concentration gradient along the module.

The ozone dispersion around the fiber being not circular and uniform, and depending on the flow, Figure 38 and Figure 39 highlight the requirement of a 3D model, while a 2D axisymmetric model would not have been relevant.

3.2.3. Model validation: simulation VS experiment

Lots of studies still present numerical simulations without validating the results with experimental data obtained by the same authors in parallel. Herein, we decided to validate the simulation results by comparing the ozone concentration calculated by the model and this one determined experimentally using the lab-scale pilot especially designed for this purpose. Experimentally, the ozone concentration was calculated by using indigo method with samples collected at the outlet of the module, whereas that was calculated from the simulation by using the following equation:

$$C_{O_3,w,outlet} = \frac{\iint \overrightarrow{\varphi_{O_3}} . \vec{n} . dS_{outlet}}{\iint \vec{v}_w . \vec{n} . dS_{outlet}}, \quad [48]$$

where $C_{O_3,w,outlet}$ denotes the concentration of ozone at the outlet (in mg.L^{-1}) , $\overrightarrow{v_w}$ is the water velocity vector (in m.s^{-1}), $\vec{n}$ the normal vector to the outlet surface S_{outlet} and $\overrightarrow{\varphi_{O_3}}$ is the total normal density flux vector (diffusive and convective flux) (in mg.h^{-1}.m^{-2}) such as $\overrightarrow{\varphi_{O_3}} = -D_{O_3,w} \vec{\nabla} C_{O_3,w} + C_{O_3,w} \vec{v}_w$.

Table 16 shows the results obtained experimentally versus using simulation, for two different liquid flow rates and for an ozone concentration at the gas inlet around 50 g.Nm^{-3}. Results are consistent without PID regulator (i.e. no parameters were adjusted) and therefore support the model used.

Table 16. Results obtained with 3D model without chemical reaction versus experimentally.

Method	$Q_{0,w}$ (L.h^{-1})	$C_{O_3,0,g}$ (g.Nm^{-3})	$C_{O_3,w,outlet}$ (mg.L^{-1})
Simulation	40	47	0.060
Experiment	40.5	47.3	0.058 +/- 0.004
Simulation	50	52	0.064
Experiment	49.8	52.4	0.064 +/- 0.002

Once the model was validated, we did run simulations for quantifying the effect of some major operating parameters on the process efficiency.

3.2.4. Effect of the process conditions (liquid flow rate and ozone concentration in the gas phase) on the ozone transfer through the single fiber membrane contactor

In Figure 40, the residual ozone concentration calculated at the outlet is represented versus the liquid flow rate in the membrane contactor, for increasing ozone concentrations in the inlet gas flux. When the ozone concentration in gas phase doubles, the flux of transferred ozone also doubles. When the flow rate doubles, the ozone transfer is multiplied by 1.6 thanks to the diminution of the resistance on the liquid side. Therefore, both liquid flow rate and ozone concentration in the gas phase have a positive impact on the transfer. This result is consistent with previous studies (Bamperng et al., 2010; Stylianou et al., 2016)

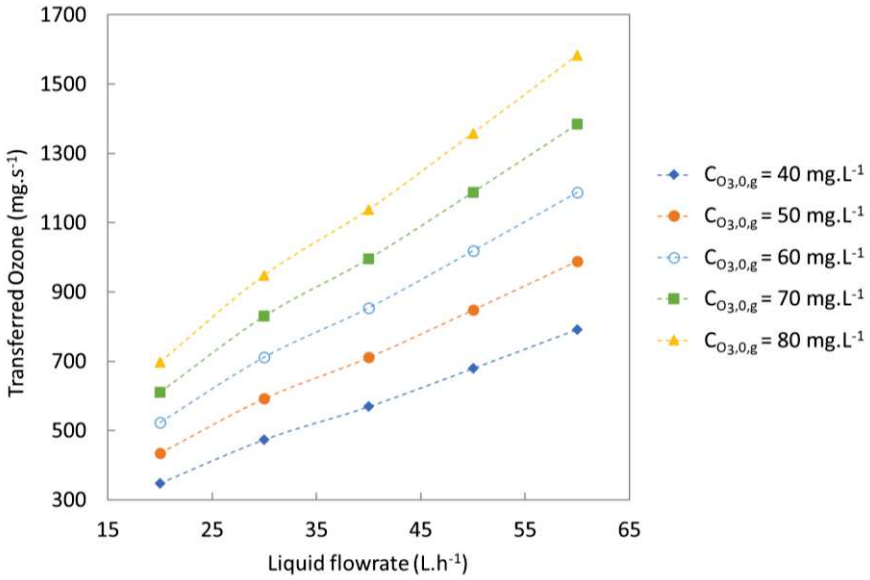

Figure 40. Effect of the liquid flow rate and the ozone concentration in the gas phase on the transferred ozone through the single fiber membrane contactor from the numerical simulation.

3.3. One fiber contactor: 3D model with reaction of ozone towards chemical reaction

In this part, the chemical reaction of ozone with carbamazepine has been added to the model. Results presented below correspond to a simulation with a water flow rate $Q_{0,w}$ at the inlet of 40 L.h^{-1}, an ozone concentration in the gas phase $C_{O_3,0,g}$ of $59\ \mathrm{mg.\,L^{-1}}$ (corresponding to a concentration on the fiber of $14.9\ \mathrm{mg.\,L^{-1}}$ according to the Henry's law) and an CBZ concentration at the water inlet $C_{CBZ,0,w}$ of $1366.5\ \mu\mathrm{g.\,L^{-1}}$. These conditions were chosen according to the experimental limits of the ozonation pilot.

3.3.1. Ozone transfer

Figure 41.a represents the ozone concentration in water and can be directly compared to Figure 38 where no chemical reaction was involved in the model. As expected, the ozone concentration is lower than in absence of CBZ in liquid phase because of its consumption by O_3 which is known to be non-limiting. The ozone concentration is close to zero in a wide part of the contactor, both above and under the fiber. In the vicinity of the fiber, a small effective volume with a thin layer of ozone is detected, which is thinner than in the Figure 38, where the ozone concentration is high (up to 14.9 mg.L^{-1}). From the results of the simulation, the mean boundary layer is estimated at 130 µm (but varying along the fiber) and thus the Hatta number is calculated to be 3.7, which corresponds to a fast reaction occurring in the liquid film (Roustan, 2003). This result confirms the previous observation made from the Figure 41: a large portion of the shell is not used for the reaction between O_3 and CBZ because this reaction takes place in the liquid film. At the outlet of the contactor, the values of ozone concentration range from 0.01 to 0.06 mg.L^{-1}, with an average of 0.02 mg.L^{-1}. The Figure 41.b can be

compared to Figure 42. A correlation between CBZ and O_3 concentration can be observed due to the consumption of CBZ by O_3.

a.

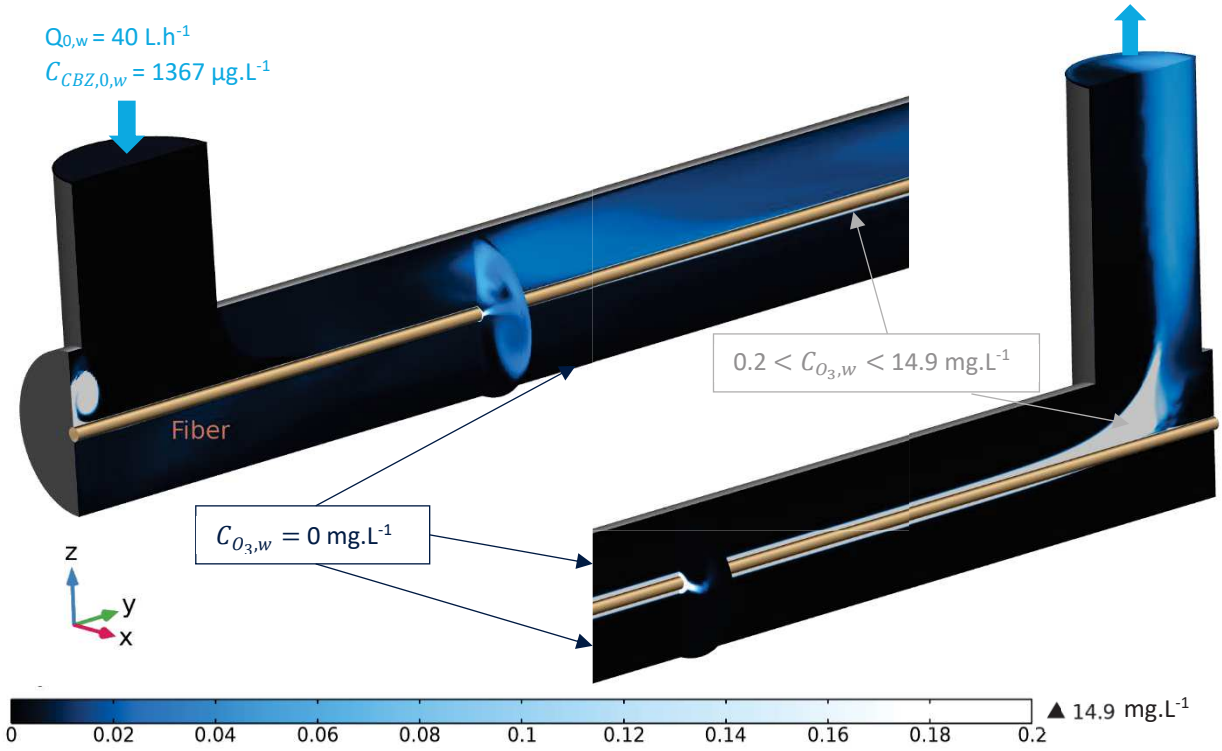

b.

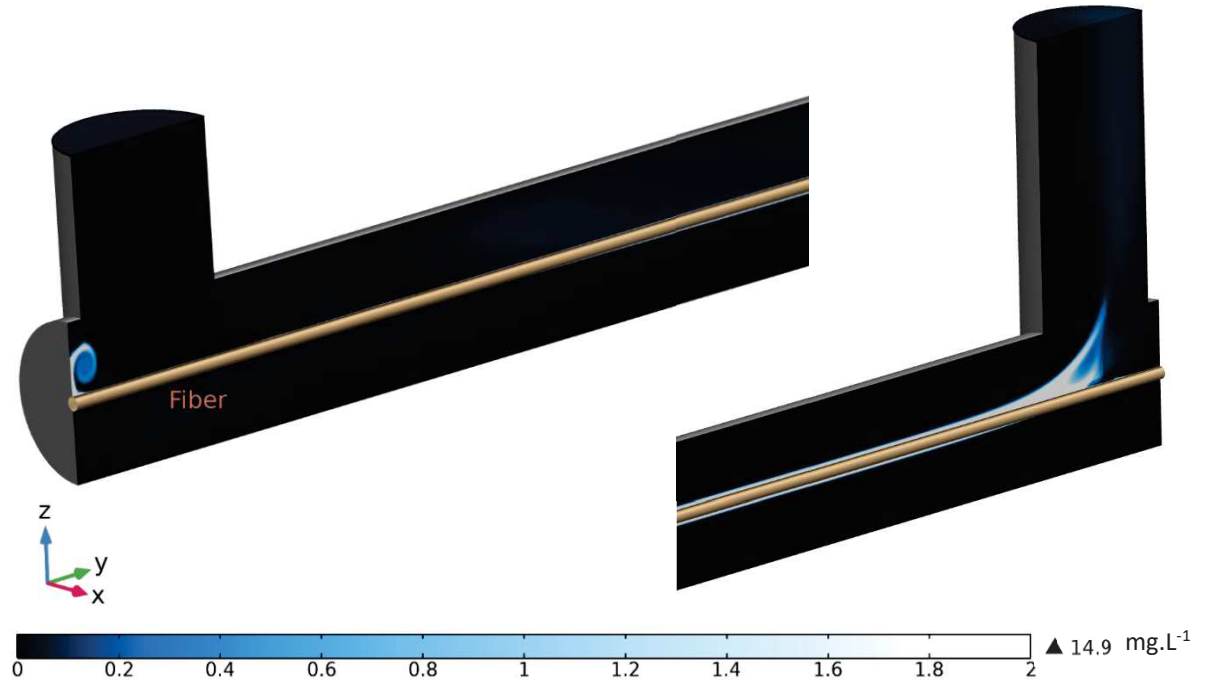

Figure 41. Ozone concentration in water (YZ symmetry cross section and two ZX cross sections) (mg.L^{-1}) in the single fiber contactor at two different scales: a. same scale than Figure 38, b. same scale than Figure 42, for $Q_{0,w}$ = 40 L.h^{-1} and $C_{O_3,0,g}$ = 59 $mg.L^{-1}$ and $C_{CBZ,0,w}$ = 1366.5 µg.L^{-1}.

3.3.2. CBZ degradation

Conversely to the spatial distribution of ozone, the CBZ is completely degraded in the vicinity of the fiber and in the dead zone close to the outlet, where the ozone concentration was shown to be the highest. Elsewhere, CBZ was partially transformed, with residual values ranged between 1070 and 1360 µg.L^{-1}. Above the fiber, the CBZ concentration was shown to be weakly lower than below because of higher liquid velocities in this region. The CBZ concentration was shown to be lower in the outlet zone corresponding to the zone where the concentration of dissolved ozone was higher. At the outlet, CBZ concentrations range from 1030 to 1160 µg.L^{-1}, with an average of 1078 µg.L^{-1}.

In order to better remove CBZ by ozone in the membrane contactor, the process parameters and the geometry of the contactor should be obviously optimized. For instance, one solution could be (i) to enhance contact time within the contactor ozone and CBZ, (ii) to increase the exchange surface between gas and liquid phases, (iii) to enhance the contactor length or finally (iv) to develop muti-fibers contactors. This last solution could also provide a better ozone distribution and hence a better CBZ removal. For these reasons, the second part of this paper will be devoted to the simulation of a multi-fiber contactor.

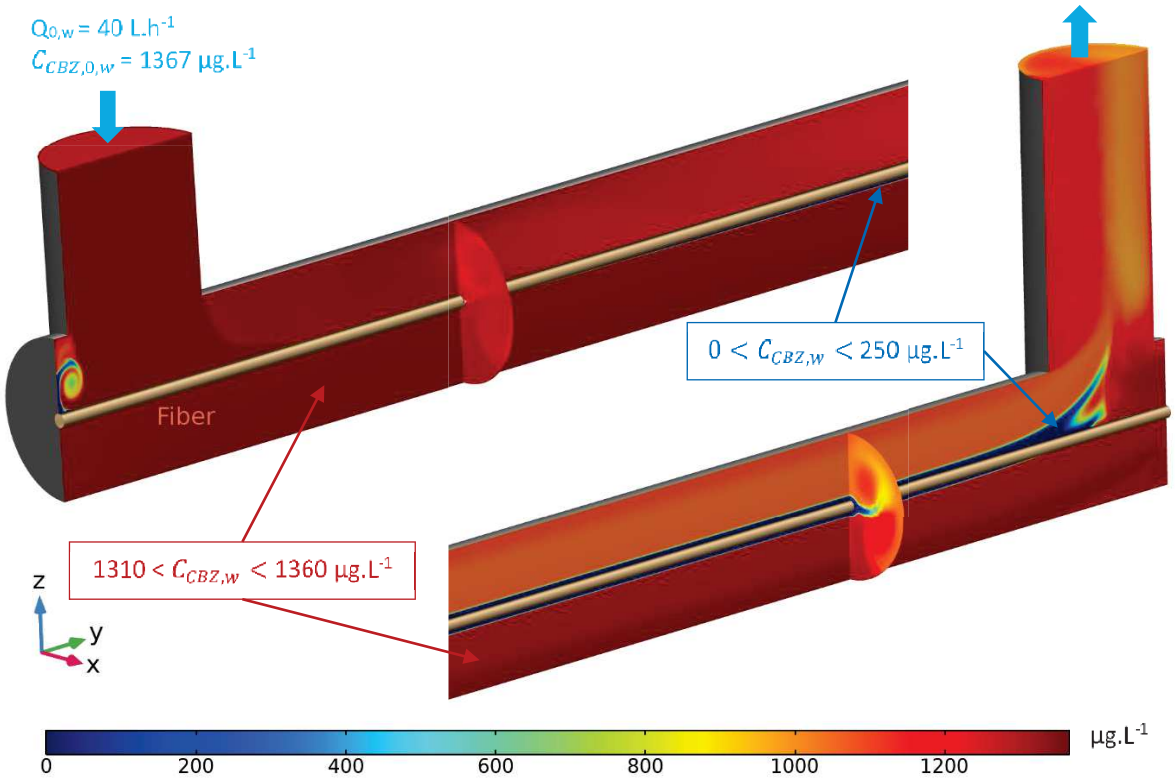

Figure 42. CBZ concentration in water (YZ symmetry cross section and two ZX cross sections) (µg.L^{-1}) in the single fiber contactor for $Q_{0,w}$ = 40 L.h^{-1} and $C_{O_3,0,g}$ = 59 $mg.L^{-1}$ and $C_{CBZ,0,w}$ = 1366.5 $\mu g.L^{-1}$.

3.3.3. Model validation: simulation VS experiment

In order to validate the reaction part of the model, an experiment was conducted at 20°C with a liquid flow rate of 40 $L.h^{-1}$, a gas flow rate of 1 $L.h^{-1}$, an ozone concentration at the gas inlet of 59.3 $g.Nm^{-3}$, and a CBZ concentration at the liquid inlet of 1366.5 +/- 32.5 $\mu g.L^{-1}$. Results are presented in Table 17. Results obtained with the simulation are consistent with those found experimentally without PID regulator (i.e. no parameters were adjusted), and therefore confirm the reliability of the reaction/transfer/transport model presented herein.

Table 17. Results obtained with 3D model with chemical reaction versus experimentally.

	$C_{CBZ,0,w}$ ($\mu g.L^{-1}$)	$C_{O_3,w,outlet}$ ($mg.L^{-1}$)	$C_{CBZ,w,outlet}$ ($\mu g.L^{-1}$)
Experiment	1367 +/- 33	0.03 +/- 0.02	1148 +/- 55
Simulation	1367	0.02	1078
	1399	0.02	1118

3.4. Multifiber contactor: 3D model without chemical reaction

In this section, the transfer of ozone in a membrane contactor (10 mm diameter) with 64 hollow fibers has been simulated. Fibers are evenly distributed and separated from each other with 0.18 mm of distance. For numerical reasons, the simulations were performed for a water flow rate $Q_{0,w}$ of 47.5 $L.h^{-1}$ at the inlet and an ozone concentration in the gas phase $C_{O_3,0,g}$ of $50\ \mathrm{mg.L^{-1}}$, corresponding to a concentration on the fiber $C_{O_3,m}$ of $12.4\ \mathrm{mg.L^{-1}}$ according to the Henry's law.

3.4.1. Hydrodynamics in the multifiber membrane contactor

Figure 43 shows the hydrodynamics simulated in the multi-fiber membrane contactor regarding the parameters previously described. More specifically, the velocity magnitude and direction located on the YZ symmetry plan and on the inlet and outlet section are plotted.

Although the velocity field is clearly more uniform compared to single-fiber configuration, preferential paths can be detected within the contactor, particularly at both sides of the shell. This result is consistent with the observation of Cai et al. in a previous study concerning the 3-D modeling of a hollow fiber membrane contactor for CO_2 absorption (Cai et al., 2016). The authors observed that modules with a high packing density led to more uniform flow distribution compared to sparsely packed modules. In our case, the packing density (i.e. the ratio between the exchange surface and the volume in the shell side) is higher for the multifiber contactor than for the single fiber contactor due to the higher number of fibers in shells of identical volume.

Like in the single fiber membrane contactor, hydrodynamics will affect the ozone distribution in the contactor. The preferential paths could potentially induce the formation of short-circuits, with low ozone supply in specific zones, where the CBZ removal could therefore be much less efficient. In order to limit these preferential paths, the contactor design could be improved for instance by adding baffles on the shell. However, this potential improvement has so far not been tested (Ng et al., 2021).

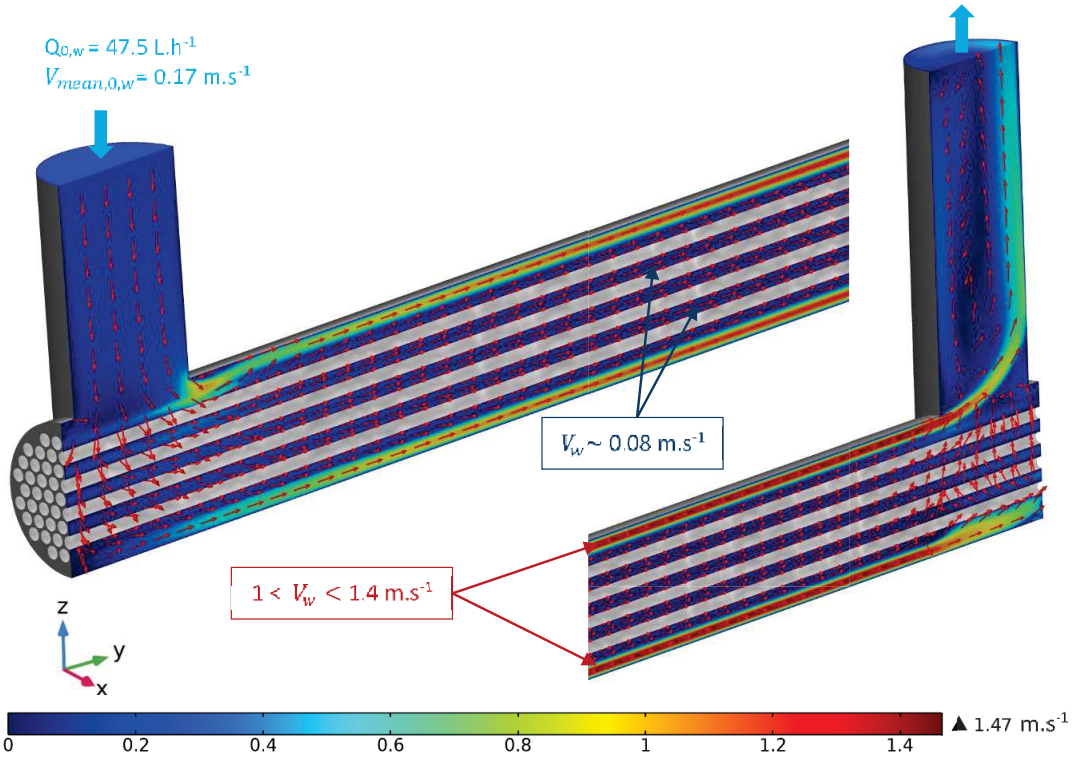

Figure 43. Velocity field (magnitude (m.s-1) and direction) in the YZ symmetry plane in the multifiber contactor for $Q_{0,w}$ = 47.5 L.h^{-1} and $C_{O_3,0,g}$ = 50 $mg.L^{-1}$.

3.4.2. Ozone transfer

The

Figure 44 shows the concentration distribution of dissolved ozone in the multifiber contactor. Between the fibers, the ozone concentration became more homogenized when approaching the outlet, and rises up to 12 mg.L^{-1}. Along the sides of shell, the ozone concentration was inferior to 0.2 mg.L^{-1} on the upper side and between 0.8 and 5 mg.L^{-1} on bottom side, due to the presence of short-circuits in these areas. The channeling effect provoking these short-circuits has already been observed in previous studies (Gebremariam, 2017; Keshavarz et al., 2008). This phenomenon leads to a lower mass transfer efficiency due to the by-pass of fluid around large amount of fibers (Ng et al., 2021).

At the outlet, the ozone concentration was homogeneous with a value of 3.3 mg.L^{-1}, which was significantly higher than with the single fiber contactor where the average value was 0.64 mg.L^{-1}. This

difference was explained by the hydrodynamics in the multifiber contactor, where the presence of the fibers leads to a better ozone distribution.

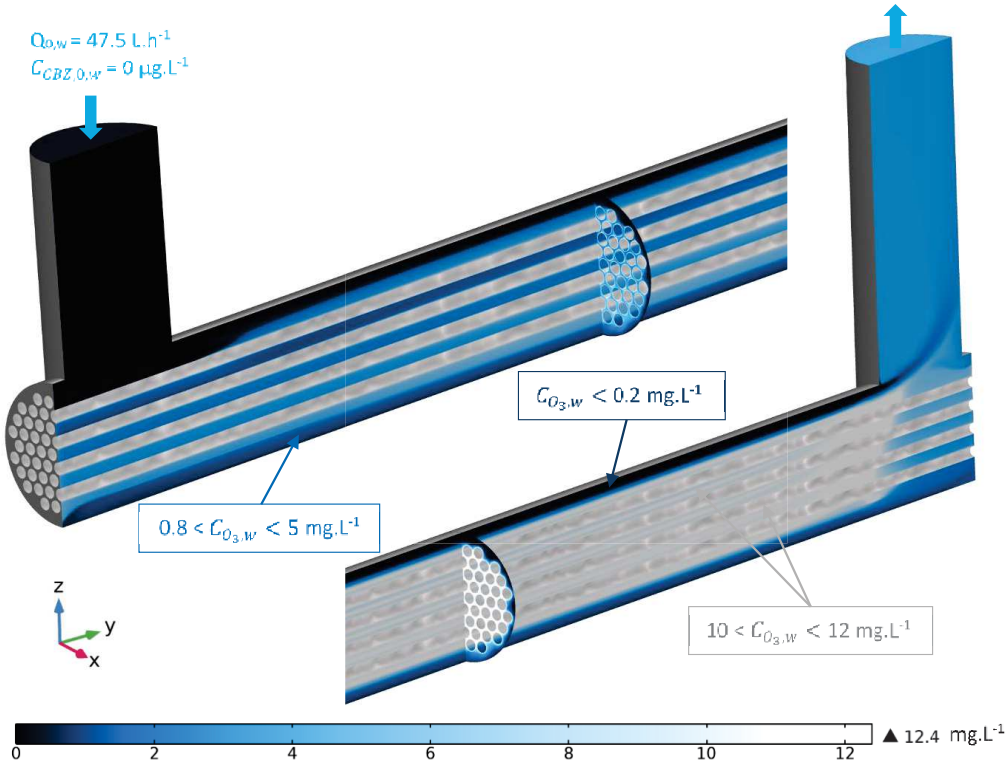

Figure 44. Ozone concentration in water in the multifiber contactor (YZ symmetry plane and two ZX cross sections) (mg.L^{-1}) for $Q_{0,w}$ = 47.5 L.h^{-1} and $C_{O_3,0,g}$ = 50 mg. L^{-1}.

3.4.3. Effect of the fiber length in multifiber membrane contactor

Table 18 shows the impact of the length of the membrane contactor (or the residence time) on the flux of ozone transferred calculated from the ozone concentration at the water inlet obtained from the model. For a length three times superior, the ozone transferred is only 19% higher, and thus the flux is not proportional to the length. This aspect highlights the interest of the model in order to optimize the length, and more generally the geometry, of the contactor. In a previous study concerning the ozonation of humic substances in a membrane contactor with a peroxone treatment (i.e. O_3 was injected with H_2O_2), Jansen had already suggested that the module length or the residence time may have a strong impact on OH° and ozone exposures (Bein et al., 2020; Jansen, 2005). This 3D modelling approach suggest that transferred ozone was not proportionally increased by increasing the membrane area because at the surface of the membrane the ozone concentration was at the equilibrium. This equilibrium corresponds to the maximum of dissolved ozone concentration achievable for a specified ozone concentration in the gas phase (according to the Henry's law). Only a better hydrodynamics favoring the mixture could improve the transfer. This result emphases the need to consider the geometry and hydrodynamics of the membrane contactor to improve the mass

transfer, which is not possible without using a 3D modelling approach. This model is thus a first proposition to overcome the unused potential highlighted recently by Bein et al. to optimize design of ozone membrane contactors as fiber diameters and module length impact on the mass transfer (Bein et al., 2020).

Table 18. Impact of the contactor length on the ozone transferred.

Length of the contactor (mm)	$Q_{0,w}$ ($L.h^{-1}$)	$C_{O_3,w,outlet}$ ($mg.L^{-1}$)	Transferred ozone ($mg.s^{-1}$)
600	41.5	3.14	3.62×10^{-2}
200	41.8	2.63	3.05×10^{-2}

3.5. Multifiber contactor: 3D model with reaction of ozone towards chemical reaction

In this section, simulations of ozone transfer in the same multifiber contactor as previously were performed for numerical reasons for a water flow rate $Q_{0,w}$ of 47.5 $L.h^{-1}$ at the inlet, an ozone concentration in the gas phase $C_{O_3,0,g}$ of $50\ mg.L^{-1}$, corresponding to a concentration on the fiber $C_{O_3,m}$ of $12.4\ mg.L^{-1}$ according to the Henry's law, and a CBZ concentration at the water inlet $C_{CBZ,0,w}$ of $1366.5\ \mu g.L^{-1}$ in order to compare with the single fiber contactor (Section 3.3). The Figure 45 shows the CBZ concentration in water in the multifiber contactor.

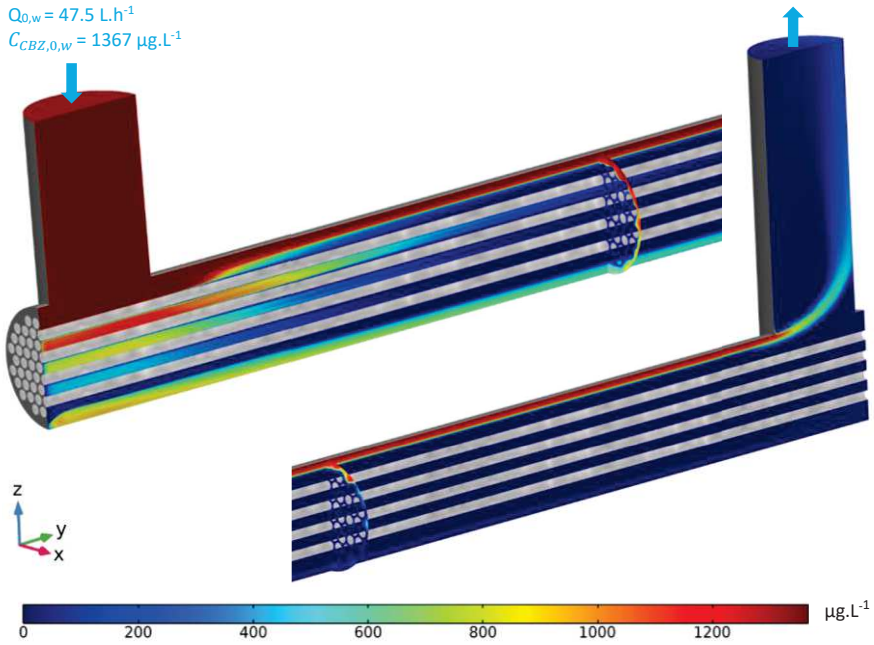

Figure 45. CBZ concentration in water in the multifiber contactor (YZ symmetry cross section and two ZX cross sections) ($\mu g.L^{-1}$) for $Q_{0,w}$ = 47.5 $L.h^{-1}$, $C_{O_3,0,g} = 50\ mg.L^{-1}$ and $C_{CBZ,0,w} = 1366.5\ \mu g.L^{-1}$.

Conversely to the spatial distribution of ozone without CBZ (Figure 44), the CBZ is completely degraded in the vicinity of the fibers, where the ozone concentration was shown to be the highest. Above the fibers, a short-circuit is noticeable where the CBZ is not degraded at all due to the absence of dissolved

ozone. This result highlights the potential impact of the design of the shell on the transfer and the necessity to create mixing along the sides of the shell, for instance with baffles.

A better CBZ removal is obtained than with the single fiber contactor due to a better ozone distribution (86 µg.L^{-1} of CBZ concentration at the outlet in average instead of 1078 µg.$L^{-1}$with the single fiber contactor), with slightly different conditions of ozonation *(*$Q_{0,w}$ = 40 L.h^{-1} and $C_{O_3,0,g}$ = $59\ mg.L^{-1}$ without CBZ and $Q_{0,w}$ = 47.5 L.h^{-1}, $C_{O_3,0,g}$ = $50\ \mathrm{mg.L^{-1}}$ with CBZ).

4. Conclusions

The transfer of ozone into water through a single fiber and a multifiber membrane contactor was studied with a local approach thanks to the establishment of a 3D model by using Comsol Multiphysics®. To the best of the author's knowledge, this model is the first combining both 3D and multifiber membrane contactor for an ozonation application.

The model established could serve as a basis for optimization of bubbleless processes and membrane contactor scale-up, including the ozonation of micropollutants. The model established has been validated with dedicated experiments. An excellent consistency was obtained between the simulation and experimental results. The main conclusions are as follows:

- The use of a 3-D modeling approach enables non-ideal effects that occurs in hollow fibers membrane contactor to be taken into account, such as random flow distribution, channeling, and dead zones (Ng et al., 2021).
- Hydrodynamics is very important, more specifically the flow, to ensure a good distribution of ozone and therefore a good treatment of the pollutants.
- A very small effective volume containing dissolved ozone appears around the single fiber.
- Using a multifiber contactor rather than a single fiber contactor leads to a better flow distribution (i.e. a better mixing), while offering a larger exchange surface.
- The transferred ozone is not proportionally increased with increasing membrane length or residence time.
- A compromise has to be found on the contactor length and on the number of fibers to optimize the geometry of the contactor and therefore make the process as effective as possible.

The model established could be improved by taking into account random distribution of fibers. Indeed, if uniform distribution of fiber may be considered acceptable for a lab-scale module due to fewer number of fibers, it is not the case for pilot and commercial modules with a higher number of fibers. In the future, such a model could be developed for industrial-scale module.

Conclusions et perspectives du Chapitre V

Dans ce dernier chapitre, le transfert d'ozone d'une phase gaz à une phase liquide à travers un contacteur membranaire à fibre creuse a été modélisé à l'aide du logiciel Comsol Multiphysics®. Un modèle en 3 dimensions a été conçu et validé expérimentalement pour un contacteur monofibre avec et sans présence de réaction chimique. Le modèle a ensuite été développé afin de simuler un contacteur multifibre.

- ***Intérêt d'une approche locale en 3 dimensions (3D)***

Cette étude a montré l'intérêt de modéliser les contacteurs membranaires avec une approche locale. Contrairement à une approche globale (basée sur le coefficient de transfert global et fonctionnant comme une « boîte noire »), cette méthode rend compte des phénomènes locaux de diffusion et de convection. Une meilleure compréhension des processus de transfert mis en jeu permet ainsi d'améliorer le design du contacteur et d'optimiser les paramètres du procédé afin d'augmenter l'efficacité du procédé, ici d'ozonation.

L'établissement d'un modèle 3D permet de prendre en compte l'évolution de la concentration le long de chaque fibre qui impacte localement le gradient de concentration et donc le transfert. De plus, le modèle 3D fournit un résultat bien plus proche de la réalité que celui établi en deux dimensions grâce à la prise en considération des effets non-idéaux (Ng et al., 2021). En particulier, cette étude a révélé la présence d'un écoulement dans l'enveloppe présentant des chemins préférentiels et zones mortes, ayant un fort impact sur la distribution d'ozone. D'autres effets n'ont pas été pris en compte dans ce modèle mais pourraient y être intégrés, notamment la disposition des fibres non optimisée (espacement entre les fibres inégal). En effet, si à l'échelle du laboratoire, une distribution uniforme des fibres au sein du module peut être considérée acceptable du fait du faible nombre de fibres, ce n'est pas le cas pour les modules commerciaux ou à plus grand échelle (Fu et al., 2020; Gebremariam, 2017; Keshavarz et al., 2008; Zheng et al., 2003). Ce constat est visible sur le module multifibre utilisé lors des premiers chapitres de cette thèse (Figure 46).

Figure 46. Photo du contacteur membranaire multifibre : répartition non égale des fibres

- ***Application à l'ozonation : Principales conclusions***

Le modèle conçu a révélé l'importance de l'hydrodynamique, plus particulièrement de l'écoulement, pour assurer une bonne distribution de l'ozone et ainsi un bon traitement des polluants ciblés lorsque le liquide circule dans l'enveloppe.

Dans le contacteur monofibre, il a également mis en avant la présence tout autour de la fibre d'un très petit volume utile contenant de l'ozone dissous.

Le contacteur multifibre présente un écoulement plus homogène grâce à un meilleur mélange dû à la présence des fibres, et permet ainsi une meilleure distribution de l'ozone dissous, tout en offrant une surface d'échange plus importante que celle du contacteur monofibre. Cependant, des courts-circuits persistent le long de la paroi de l'enveloppe malgré cette configuration. Une amélioration envisageable serait la mise en place de chicanes le long de la paroi du carter.

Enfin, cette étude a montré que l'augmentation de l'ozone transféré n'était pas proportionnelle à l'augmentation de la surface d'échange, ce qui souligne l'intérêt d'optimiser la géométrie du contacteur.

- ***Perspectives***

In fine, le modèle conçu pourrait ainsi servir à optimiser le design et le dimensionnement des contacteurs membranaires utilisés dans des applications d'ozonation, ou encore à optimiser les paramètres d'utilisation du procédé notamment le débit de liquide et la concentration en ozone dans la phase gaz qui sont des paramètres significatifs (voir Chapitre III). Ce modèle pourrait également être adapté pour le cas d'autres applications d'absorption gaz-liquide.

Pour une application d'ozonation, l'implémentation dans le modèle de mécanismes réactionnels complets se produisant lors du processus d'ozonation avec les micropolluants, les sous-produits mais aussi la matrice, pourrait permettre d'optimiser l'efficacité du procédé en limitant la formation de sous-produits dangereux (voir Chapitre IV). Ce type de modèle pourrait également servir de base pour la compréhension et la validation des réactions mises en jeu à partir de résultats obtenus expérimentalement.

- ***Verrous***

La principale limite du modèle conçu est la très grande durée de calcul nécessaire causée par l'utilisation de la géométrie 3D, qui multiplie le nombre de mailles et augmente les probabilités de divergence. Il semblerait donc difficile d'appliquer un tel modèle à une échelle industrielle où les contacteurs peuvent posséder des milliers de fibres (Ng et al., 2021).

Bibliographie du Chapitre V

AIDA, 1998. Directive n° 98/83/CE du 03/11/98 relative à la qualité des eaux destinées à la consommation humaine.

Alharbi, S.K., Price, W.E., Kang, J., Fujioka, T., Nghiem, L.D., 2016. Ozonation of carbamazepine, diclofenac, sulfamethoxazole and trimethoprim and formation of major oxidation products. Desalin. Water Treat. 57, 29340–29351. https://doi.org/10.1080/19443994.2016.1172986

Bader, H., Hoigné, J., 1982. Determination of Ozone In Water By The Indigo Method: A Submitted Standard Method. Ozone Sci. Eng. J. Int. Ozone Assoc. 4, 169–176. https://doi.org/10.1080/01919510390481531

Bahlake, A., Farivar, F., Dabir, B., 2016. New 3-dimensional CFD modeling of CO2 and H2S simultaneous stripping from water within PVDF hollow fiber membrane contactor. Heat Mass Transf. und Stoffuebertragung 52, 1295–1304. https://doi.org/10.1007/s00231-015-1635-y

Bamperng, S., Suwannachart, T., Atchariyawut, S., Jiraratananon, R., 2010. Ozonation of dye wastewater by membrane contactor using PVDF and PTFE membranes. Sep. Purif. Technol. 72, 186–193. https://doi.org/10.1016/j.seppur.2010.02.006

Bear, J., 1972. Dynamics of Fluids in Porous Media, Dynamics of Fluids in Porous Media. Elsevier Scientifique, 222-244.

Bein, E., Zucker, I., Drewes, J.E., Hübner, U., 2020. Ozone membrane contactors for water and wastewater treatment: A critical review on materials selection, mass transfer and process design. Chem. Eng. J. 413. https://doi.org/10.1016/j.cej.2020.127393

Berry, M.J., Taylor, C.M., King, W., Chew, Y.M.J., Wenk, J., 2017. Modelling of Ozone Mass-Transfer through Non-Porous Membranes for Water Treatment. Water 9, 452. https://doi.org/10.3390/w9070452

Bird, R.B., Stewai, W.E., Lightfoot, E.N., 2002. Transport Phenomena, Second Edi. ed. John Wiley & Sons, Inc., Wisconsin-Madison.

Björlenius, B., Ripszám, M., Haglund, P., Lindberg, R.H., Tysklind, M., Fick, J., 2018. Pharmaceutical residues are widespread in Baltic Sea coastal and offshore waters – Screening for pharmaceuticals and modelling of environmental concentrations of carbamazepine. Sci. Total Environ. 633, 1496–1509. https://doi.org/10.1016/j.scitotenv.2018.03.276

Bourgin, M., Borowska, E., Helbing, J., Hollender, J., Kaiser, H.-P., Kienle, C., McArdell, C.S., Simon, E., von Gunten, U., 2017. Effect of operational and water quality parameters on conventional ozonation and the advanced oxidation process O3/H2O2: Kinetics of micropollutant abatement, transformation product and bromate formation in a surface water. Water Res. 122, 234–245. https://doi.org/10.1016/j.watres.2017.05.018

Cabeza, Y., Candela, L., Ronen, D., Teijon, G., 2012. Monitoring the occurrence of emerging contaminants in treated wastewater and groundwater between 2008 and 2010. The Baix Llobregat (Barcelona, Spain). J. Hazard. Mater. 239–240, 32–39. https://doi.org/10.1016/J.JHAZMAT.2012.07.032

Cai, J.J., Hawboldt, K., Abdi, M.A., 2016. Analysis of the effect of module design on gas absorption in cross flow hollow membrane contactors via computational fluid dynamics (CFD) analysis. J. Memb. Sci. 520, 415–424. https://doi.org/10.1016/j.memsci.2016.07.054

Chabanon, E., Favre, E., 2017. 3.9 Membranes Contactors for Intensified Gas–Liquid Absorption Processes. Compr. Membr. Sci. Eng. https://doi.org/10.1016/B978-0-12-409547-2.12250-4

Cussler, E.L., 1997. Diffusion: Mass Transfer in Fluid Systems, Cambridge Series in Chemical Engineering. Cambridge University Press.

Danckwerts, P. V, 1995. Continuous flow systems. Distribution of residence times. Chem. Eng. Sci. 50, 3857–3866.

deMontigny, D., Tontiwachwuthikul, P., Chakma, A., 2006. Using polypropylene and polytetrafluoroethylene membranes in a membrane contactor for CO2 absorption. J. Memb. Sci. 277, 99–107. https://doi.org/https://doi.org/10.1016/j.memsci.2005.10.024

Gabelman, A., Hwang, S.T., 1999. Hollow fiber membrane contactors. J. Memb. Sci. 159, 61–106. https://doi.org/10.1016/S0376-7388(99)00040-X

Gao, Y., Ji, Y., Li, G., An, T., 2016. Theoretical investigation on the kinetics and mechanisms of hydroxyl radical-induced transformation of parabens and its consequences for toxicity: Influence of alkyl-chain length. Water Res. 91, 77–85. https://doi.org/10.1016/j.watres.2015.12.056

Gebremariam, S.K., 2017. Modelling a Membrane Contactor for CO2 Capture. Master's thesis. NTNU.

Gerun, L., 2006. Installation de traitement des déchets carbonés innovante, in: Techniques de l'ingénieur. pp. 0–8.

Gogoi, A., Mazumder, P., Tyagi, V.K., Tushara Chaminda, G.G., An, A.K., Kumar, M., 2018. Occurrence and fate of emerging contaminants in water environment: A review. Groundw. Sustain. Dev. 6, 169–180. https://doi.org/10.1016/j.gsd.2017.12.009

Gottschalk, C., Libra, J.A., Saupe, A., 2009. Ozonation of Water and Waste Water: A practical guide to understanding ozone and its applications. John Wiley & Sons.

Happel, J., 1959. Viscous Flow Relative to Arrays of Cylinders JOHN. AIChE J. 5, 174–177. https://doi.org/https://doi.org/10.1002/aic.690050211

Huber, M.M., Canonica, S., Park, G.-Y., von Gunten, U., 2003. Oxidation of Pharmaceuticals during Ozonation and Advanced Oxidation Processes. Environ. Sci. Technol. 37, 1016–1024. https://doi.org/10.1021/es025896h

Iversen, S.B., Bhatia, V.K., Dam-Johansen, K., Jonsson, G., 1997. Characterization of microporous membranes for use in membrane contactors. J. Memb. Sci. 130, 205–217. https://doi.org/10.1016/S0376-7388(97)00026-4

Jansen, R., 2005. Ozonation of humic substances in a membrane contactor: Mass transfer, product characterization and biodegradability. Thesis. University of Twente, The Netherlands.

Keshavarz, P., Ayatollahi, S., Fathikalajahi, J., 2008. Mathematical modeling of gas--liquid membrane

contactors using random distribution of fibers. J. Memb. Sci. 325, 98–108.

Kong, X., Gong, D., Ke, W., Qiu, M., Fu, K., Xu, P., Chen, X., Fan, Y., 2020. Investigation of Mass Transfer Characteristics of SO2Absorption into NaOH in a Multichannel Ceramic Membrane Contactor. Ind. Eng. Chem. Res. 59, 11054–11062. https://doi.org/10.1021/acs.iecr.0c01327

Lee, Y., Kovalova, L., McArdell, C.S., von Gunten, U., 2014. Prediction of micropollutant elimination during ozonation of a hospital wastewater effluent. Water Res. 64, 134–148. https://doi.org/10.1016/J.WATRES.2014.06.027

Lee, Y., von Gunten, U., 2016. Advances in predicting organic contaminant abatement during ozonation of municipal wastewater effluent: reaction kinetics, transformation products, and changes of biological effects. Environ. Sci. Water Res. Technol. 2, 421–442. https://doi.org/10.1039/C6EW00025H

Li, J.L., Chen, B.H., 2005. Review of CO2 absorption using chemical solvents in hollow fiber membrane contactors. Sep. Purif. Technol. 41, 109–122. https://doi.org/10.1016/j.seppur.2004.09.008

Luo, Y., Guo, W., Ngo, H.H., Nghiem, L.D., Hai, F.I., Zhang, J., Liang, S., Wang, X.C., 2014. A review on the occurrence of micropollutants in the aquatic environment and their fate and removal during wastewater treatment. Sci. Total Environ. 473–474, 619–641. https://doi.org/10.1016/j.scitotenv.2013.12.065

Massman, W.J., 1998. A review of the molecular diffusivities of H2O, CO2, CH4, CO, O3, SO2, NH3, N2O, NO, and NO2 in air, O2 and N2 near STP. Atmos. Environ. 32, 1111–1127.

McDowell, D.C., Huber, M.M., Wagner, M., Von Gunten, U., Ternes, T.A., 2005. Ozonation of carbamazepine in drinking water: Identification and kinetic study of major oxidation products. Environ. Sci. Technol. 39, 8014–8022. https://doi.org/10.1021/es050043l

Merle, T., Pronk, W., Von Gunten, U., Eawag, †, 2017. MEMBRO 3 X, a Novel Combination of a Membrane Contactor with Advanced Oxidation (O 3 /H 2 O 2) for Simultaneous Micropollutant Abatement and Bromate Minimization. Environ. Sci. Technol. Lett 4, 13. https://doi.org/10.1021/acs.estlett.7b00061

Ng, E.L.H., Lau, K.K., Lau, W.J., Ahmad, F., 2021. Holistic review on the recent development in mathematical modelling and process simulation of hollow fiber membrane contactor for gas separation process. J. Ind. Eng. Chem. https://doi.org/10.1016/j.jiec.2021.08.028

Pines, D., Min, K.-N., J. Ergas, S., Reckhow, D., 2005. Investigation of an Ozone Membrane Contactor System. https://doi.org/10.1080/01919510590945750

Prasad, R., Sirkar, K.K., 1989. Hollow fiber solvent extraction of pharmaceutical products: A case study. J. Memb. Sci. 47, 235–259. https://doi.org/10.1016/S0376-7388(00)83078-1

Qatezadeh Deriss, A., Langari, S., Taherian, M., 2021. Computational fluid dynamics modeling of ibuprofen removal using a hollow fiber membrane contactor. Environ. Prog. Sustain. Energy 40, 1–11. https://doi.org/10.1002/ep.13490

Reed, B.W., Semmens, M.J., Cussler, E.L., 1995. Chapter 10 Membrane contactors. Membr. Sci. Technol. 2, 467–498. https://doi.org/10.1016/S0927-5193(06)80012-4

Reungoat, J., Macova, M., Escher, B.I.I., Carswell, S., Mueller, J.F.F., Keller, J., 2010. Removal of micropollutants and reduction of biological activity in a full scale reclamation plant using ozonation and activated carbon filtration. Water Res. 44, 625–637. https://doi.org/10.1016/J.WATRES.2009.09.048

Rosal, R., Rodríguez, A., Perdigón-Melón, J.A., Petre, A., García-Calvo, E., Gómez, M.J., Agüera, A., Fernández-Alba, A.R., 2010. Occurrence of emerging pollutants in urban wastewater and their removal through biological treatment followed by ozonation. Water Res. 44, 578–588. https://doi.org/10.1016/J.WATRES.2009.07.004

Roustan, M., 2003. Transferts gaz-liquide dans les procédés de traitement des eaux et des effluents gazeux. Éd. Tec & doc, Paris.

Sander, R., 2015. Compilation of Henry's law constants (version 4.0) for water as solvent. Atmos. Chem. Phys. 15, 4399–4981.

Schlüter-Vorberg, L., Prasse, C., Ternes, T.A., Mückter, H., Coors, A., 2015. Toxification by transformation in conventional and advanced wastewater treatment: the antiviral drug acyclovir. Environ. Sci. Technol. Lett. 2, 342–346. https://doi.org/10.1021/acs.estlett.5b00291

Schmitt, A., Mendret, J., Roustan, M., Brosillon, S., 2020. Ozonation using hollow fiber contactor technology and its perspectives for micropollutants removal in water: A review. Sci. Total Environ. vol. 729, p. 138664. https://doi.org/10.1016/j.scitotenv.2020.138664

Simons, K., Nijmeijer, K., Wessling, M., 2009. Gas-liquid membrane contactors for CO2 removal. J. Memb. Sci. 340, 214–220. https://doi.org/10.1016/j.memsci.2009.05.035

Soltermann, F., Abegglen, C., Tschui, M., Stahel, S., von Gunten, U., 2017. Options and limitations for bromate control during ozonation of wastewater. Water Res. 116, 76–85. https://doi.org/10.1016/j.watres.2017.02.026

Stylianou, S.K., Katsoyiannis, I.A., Mitrakas, M., Zouboulis, A.I., 2018. Application of a ceramic membrane contacting process for ozone and peroxone treatment of micropollutant contaminated surface water. J. Hazard. Mater. 358, 129–135. https://doi.org/10.1016/j.jhazmat.2018.06.060

Stylianou, S.K., Kostoglou, M., Zouboulis, A.I., 2016. Ozone Mass Transfer Studies in a Hydrophobized Ceramic Membrane Contactor: Experiments and Analysis. Ind. Eng. Chem. Res. 55, 7587–7597. https://doi.org/10.1021/acs.iecr.6b01446

UNESCO and HELCOM, 2017. Pharmaceuticals in the aquatic environment of the Baltic Sea region - a status report UNESCO emerging pollutants in water series. Paris.

USEPA, 1998. Disinfectants and disinfection byproducts : proposed rule.

von Gunten, U., 2003. Ozonation of drinking water: Part II. Disinfection and by-product formation in presence of bromide, iodide or chlorine. Water Res. 37, 1469–1487. https://doi.org/10.1016/S0043-1354(02)00458-X

Wang, R., Shi, L., Tang, C.Y., Chou, S., Qiu, C., Fane, A.G., 2010. Characterization of novel forward osmosis hollow fiber membranes. J. Memb. Sci. 355, 158–167.

https://doi.org/10.1016/j.memsci.2010.03.017

Wickramasinghe, S.R., Semmens, M.J., Cussler, E.L., 1992. Mass transfer in various hollow fiber geometries. J. Memb. Sci. 69, 235–250.

Yang, Y., Ok, Y.S., Kim, K.H., Kwon, E.E., Tsang, Y.F., 2017. Occurrences and removal of pharmaceuticals and personal care products (PPCPs) in drinking water and water/sewage treatment plants: A review. Sci. Total Environ. 596–597, 303–320. https://doi.org/10.1016/j.scitotenv.2017.04.102

Yao, W., Rehman, S.W.U., Wang, H., Yang, H., Yu, G., Wang, Y., 2018. Pilot-scale evaluation of micropollutant abatements by conventional ozonation, UV/O3, and an electro-peroxone process. Water Res. 138, 106–117. https://doi.org/10.1016/J.WATRES.2018.03.044

Zhao, S., Feron, P.H.M., Deng, L., Favre, E., Chabanon, E., Yan, S., Hou, J., Chen, V., Qi, H., 2016. Status and progress of membrane contactors in post-combustion carbon capture: A state-of-the-art review of new developments. J. Memb. Sci. 511, 180–206. https://doi.org/https://doi.org/10.1016/j.memsci.2016.03.051

Zheng, J., Xu, Y., Xu, Z., 2003. Flow distribution in a randomly packed hollow fiber membrane module. J. Memb. Sci. 211, 263–269. https://doi.org/10.1016/S0376-7388(02)00426-X

Zheng, J.M., Xu, Z.K., Li, J.M., Wang, S.Y., Xu, Y.Y., 2004. Influence of random arrangement of hollow fiber membranes on shell side mass transfer performance: A novel model prediction. J. Memb. Sci. 236, 145–151. https://doi.org/10.1016/j.memsci.2004.02.016

Zoumpouli, G., Baker, R., Taylor, C., Chippendale, M., Smithers, C., Xian, S., Mattia, D., Chew, J., Wenk, J., 2018. A Single Tube Contactor for Testing Membrane Ozonation. https://doi.org/10.3390/w10101416

Conclusions générales et perspectives

L'objectif principal de cette thèse était d'étudier l'utilisation de contacteurs membranaires en lieu et place des réacteurs d'ozonation traditionnels, en traitement tertiaire d'affinage, pour la dégradation de molécules réfractaires lors du traitement des eaux usées. Afin d'y parvenir, il s'agissait d'effectuer une caractérisation complète du procédé et des phénomènes de transfert impliqués, puis d'étudier son application pour l'élimination de molécules organiques et la minimisation de la formation de bromates. A cet effet, deux micropolluants organiques d'origine pharmaceutique, la **carbamazépine** et le **sulfaméthoxazole**, ont été sélectionnés comme molécules modèles selon plusieurs critères : constante de réaction avec l'ozone élevée, forte occurrence dans les eaux de sortie de station d'épuration ainsi que dans la littérature et expertise d'analyse disponible au laboratoire.

En couplant une démarche expérimentale et numérique, ces travaux de thèse ont traité différents verrous scientifiques :

- Une analyse bibliographique des travaux publiés sur le sujet (Chapitre I) ainsi qu'un travail expérimental de caractérisation du transfert d'ozone à travers un contacteur membranaire (Chapitre III) ont montré que la **principale résistance au transfert d'ozone** par contacteur membranaire était située du **côté liquide**.
- Les Chapitres I et III ont mis en évidence les **principaux paramètres du procédé impactant le transfert** de l'ozone qui sont la **concentration en ozone dans la phase gaz** ainsi que le **débit de la phase liquide**. Le Chapitre IV, qui consistait en un travail expérimental d'évaluation de l'efficacité du procédé pour i) la dégradation des micropolluants sélectionnés et ii) la minimisation des bromates formés, a confirmé l'impact **significatif** de ces paramètres sur l'abattement des micropolluants ciblés dans cette thèse.
- Le Chapitre III a montré que la présence de réaction chimique dans la phase liquide augmentait faiblement la quantité d'ozone transféré, le facteur d'accélération E n'étant pas significatif.
- Comme supposé à partir de l'analyse bibliographique du Chapitre I, le procédé d'ozonation par contacteur membranaire s'est révélé **efficace pour l'abattement des micropolluants organiques sélectionnés** dans cette étude (la carbamazépine et le sulfaméthoxazole) avec des **temps de séjour de quelques secondes**, ce qui est particulièrement court en comparaison des procédés d'ozonation conventionnels (Chapitre IV).
- Malgré des **résultats mitigés** concernant la **minimisation des bromates formés** lors de l'ozonation par contacteur membranaire **en comparaison avec un réacteur à bulles**, le Chapitre IV a montré que, **sous certaines conditions**, le contacteur membranaire ne produisait **pas ou peu de bromates**. En outre, **une même production de radicaux hydroxyles** nécessitait une **dose spécifique d'ozone transféré** (mgO_3/mgC) **inférieure** dans le cas du contacteur membranaire que dans celui du réacteur à bulles et était accompagnée de **moins de bromates**

formés. **Ainsi, le procédé d'ozonation par contacteur membranaire semble être une solution intéressante pour limiter la formation de bromates tout en éliminant efficacement les micropolluants organiques.**

- Les **profils de concentration** de l'ozone dans un contacteur à géométrie fibre creuse ont été simulés à l'aide du logiciel **Comsol Multiphysics®** (Chapitre V). Un modèle en **trois dimensions** a été conçu et validé expérimentalement pour un contacteur **monofibre** avec et sans présence de **réaction chimique**. Le modèle a ensuite été développé afin de simuler un contacteur **multifibre**.
- Grâce au modèle conçu, le Chapitre V a mis en évidence **l'importance de l'écoulement du liquide** lorsque celui-ci circule dans l'enveloppe pour assurer une **bonne distribution de l'ozone** et ainsi un bon traitement des polluants ciblés.
- De la même façon, le Chapitre V a mis en lumière que le **transfert d'ozone** n'était **pas proportionnel à la surface de membrane**, notamment à la longueur du module.
- Les Chapitres I et III ont également soulevé le problème du **vieillissement** des contacteurs membranaires au contact de l'ozone. Celui-ci dépend des matériaux utilisés non seulement pour la **constitution des membranes** mais également pour leur **empotage**. Le Chapitre III a notamment montré une limite de résistance à l'ozonation au niveau de la résine polyuréthane utilisée pour l'empotage, ainsi que des modifications au niveau de la surface des fibres en **PTFE** (polytétrafluoroéthylène) qui avaient été en contact avec de l'ozone dissous, alors même qu'il s'agissait du matériau polymère identifié comme le plus résistant à l'ozonation d'après le Chapitre I.

Ainsi, les **temps de résidence très courts** couplés à la très **faible empreinte au sol** nécessaire grâce à la compacité des membranes rendent l'implémentation de ce procédé dans les stations d'épuration existantes en tant que traitement tertiaire envisageable. Les **perspectives** de travail afin de rendre ce procédé **applicable à l'échelle de la station d'épuration** sont nombreuses :

- Le modèle conçu dans le Chapitre V pourrait servir pour **optimiser** le **design** et le **dimensionnement** des contacteurs membranaires utilisés dans des applications d'ozonation, ou encore pour optimiser les **paramètres d'utilisation** du procédé notamment le débit de liquide et la concentration en ozone dans la phase gaz qui sont des paramètres significatifs (Chapitre III). Si la présence d'un nombre de fibres plus important dans le contacteur multifibre améliore le mélange et ainsi la distribution de l'ozone, des **courts-circuits** restent présents au niveau des parois du carter. Ainsi, il semble particulièrement important de **créer de la turbulence dans l'enveloppe** et notamment au niveau des parois afin d'augmenter l'efficacité du procédé. Une solution envisageable serait la mise en place de **chicanes** le long de ces parois.

- Une **étude économique** prenant en compte l'OPEX et le CAPEX, c'est-à-dire respectivement les coûts opérationnels et les dépenses d'investissement, permettrait de connaître la faisabilité de ce procédé en lieu et place des réacteurs d'ozonation traditionnels au niveau des stations d'épuration, les travaux effectués durant cette thèse ayant été concentrés sur les aspects scientifiques et techniques.
- Malgré un **investissement initial élevé** lié aux membranes, le **recyclage de l'ozone** non transféré permettrait l'économie de production d'une grande quantité d'ozone, qui est toujours effectuée in-situ et est particulièrement coûteuse. De plus, cela permettrait de fixer une concentration en ozone dans la phase gaz élevée à moindre coût afin de favoriser le transfert d'ozone et l'abattement des micropolluants (Chapitres III et IV). En parallèle, cela éviterait des coûts opératoires liés au destructeur d'ozone dans les stations d'épuration. Néanmoins, un verrou réside dans la **présence possible d'humidité** dans la phase gaz après le passage dans le contacteur membranaire qui ne pourrait donc pas être réutilisé tel quel.
- Une **membrane dense** (ou composite avec une couche dense) permettrait de palier ce verrou, ainsi que les problèmes de **pressions transmembranaires** pouvant être rencontrés et réduisant fortement le transfert, comme montré dans le Chapitre I. En effet, la pression transmembranaire ne doit pas dépasser la « **pression de Percée** » afin d'éviter que le liquide ne pénètre dans les pores (phénomène de **mouillage**) et ne freine le transfert. A l'inverse, la pression côté gaz ne doit pas non plus être trop importante afin de ne pas dépasser la « **pression de bulle** », où les avantages liés à un procédé sans dispersion d'une phase dans l'autre seraient perdus.
- **Que le matériau membranaire soit poreux, dense, ou composite, il est nécessaire qu'il résiste à l'oxydation à long-terme pour rendre ce procédé applicable à l'échelle de la station d'épuration et constitue donc un choix crucial. Le développement de matériaux membranaires adaptés représente ainsi un véritable enjeu.**
- Les **membranes céramiques** semblent être une solution intéressante grâce à leur stabilité chimique bien que leur fabrication en géométrie fibre creuse soit encore limitée. L'utilisation de contacteur membranaire tubulaire en céramique, dont le diamètre est légèrement supérieur à celui des fibres creuses, pourrait être envisagée. Cependant, les matériaux céramiques ont généralement un caractère plus hydrophile que les matériaux polymères, et seront donc plus facilement sujet aux problèmes de mouillage dans le cas de matériaux poreux. L'utilisation de membranes céramiques denses semblerait donc être actuellement la meilleure solution à condition que le transfert de masse reste suffisamment élevé.

Annexes

Annexe I

Evolution de la concentration en bromate en fonction de la concentration en bromure